INFORMATION TO USERS

The most advanced technology has been used to photograph and reproduce this manuscript from the microfilm master. UMI films the original text directly from the copy submitted. Thus, some dissertation copies are in typewriter face, while others may be from a computer printer.

In the unlikely event that the author did not send UMI a complete manuscript and there are missing pages, these will be noted. Also, if unauthorized copyrighted material had to be removed, a note will indicate the deletion.

Oversize materials (e.g., maps, drawings, charts) are reproduced by sectioning the original, beginning at the upper left-hand corner and continuing from left to right in equal sections with small overlaps. Each oversize page is available as one exposure on a standard 35 mm slide or as a 17" × 23" black and white photographic print for an additional charge.

Photographs included in the original manuscript have been reproduced xerographically in this copy. 35 mm slides or 6" × 9" black and white photographic prints are available for any photographs or illustrations appearing in this copy for an additional charge. Contact UMI directly to order.

Accessing the World's Information since 1938

300 North Zeeb Road, Ann Arbor, MI 48106-1346 USA

Order Number 8809987

The development of slaty cleavage at Ocoee Gorge, Tennessee

Sutton, Sally Jo, Ph.D.

University of Cincinnati, 1987

U·M·I
300 N. Zeeb Rd.
Ann Arbor, MI 48106

PLEASE NOTE:

In all cases this material has been filmed in the best possible way from the available copy. Problems encountered with this document have been identified here with a check mark __✓__.

1. Glossy photographs or pages __✓__
2. Colored illustrations, paper or print _____
3. Photographs with dark background __✓__
4. Illustrations are poor copy _____
5. Pages with black marks, not original copy _____
6. Print shows through as there is text on both sides of page _____
7. Indistinct, broken or small print on several pages __✓__
8. Print exceeds margin requirements _____
9. Tightly bound copy with print lost in spine _____
10. Computer printout pages with indistinct print _____
11. Page(s) _____ lacking when material received, and not available from school or author.
12. Page(s) _____ seem to be missing in numbering only as text follows.
13. Two pages numbered _____. Text follows.
14. Curling and wrinkled pages _____
15. Dissertation contains pages with print at a slant, filmed as received _____
16. Other _____

_____

_____

UMI

THE DEVELOPMENT OF SLATY CLEAVAGE AT OCOEE GORGE, TENNESSEE

A dissertation submitted to the

Division of Graduate Studies and Research
of the University of Cincinnati

in partial fulfillment of the
requirements for the degree of

DOCTOR OF PHILOSOPHY

in the Department of Geology
of the College of Arts and Sciences

1987

by

Sally Jo Sutton

B.S., University of Michigan, 1979

UNIVERSITY OF CINCINNATI

October 1 19 87

I hereby recommend that the thesis prepared under my supervision by Sally J. Sutton

entitled The Development of Slaty Cleavage at Ocoee Gorge, Tennessee

be accepted as fulfilling this part of the requirements for the degree of Doctor of Philosophy

Approved by:

Warren D. Huff

John E. Grover

Craig Dietsch

ABSTRACT

Slaty cleavage exposed in the fine-grained metasediments of western Ocoee Gorge, Tennessee is characterized by zones enriched in cleavage-parallel white mica (P domains), alternating with zones enriched in quartz and feldspar and in which phyllosilicates are bedding-parallel (Q domains). This domainal fabric appears to develop by growth of new mica from mica components carried in a moving fluid. Solid state recrystallization of clays and mica may also have contributed to the development of the fabric, but little, if any, mechanical rotation or passive concentration of mica grains occurred. Both P domain morphology and mineralogical differences between P and Q domain phyllosilicate populations suggest that nucleation and growth of P domains may involve the expulsion of fluids, during diagenesis and low-grade metamorphism.

P domain phyllosilicates, compared to Q domain phyllosilicates, have (1) higher K content in white micas, (2) greater illite crystallinity, (3) less compositional variability, (4) a smaller amount of chlorite interstratified with mica (limit of 1/3 in P domain, no limit in Q domain), and (5) a higher mica/chlorite ratio. These differences between P and Q domain phyllosilicates are typical of differences seen between low-grade

metamorphic and diagenetic phyllosilicates.

The higher mica/chlorite ratio parallel to cleavage suggests that the appearance of chlorite predated fabric development. As low-grade metamorphism proceeded, chlorite, particularly chlorite interstratified with mica, disappeared. Fe- and Mg-rich carbonates provided a sink for Fe and Mg lost from chlorite as chlorite was replaced by white mica. As chlorite began to disappear, P domains may have nucleated around favorably oriented mica grains within thin phyllite layers. Then as metamorphic fluids flowed from the phyllite layers and into overlying siltstone layers, P domains propagated into the siltstone layers, growing from mica components in the fluid. P domains continued to develop by growth of new mica grains and compositional re-equilibration of older grains as more fluid migrated upward, preferentially flowing along developing P domains. The mica components in the fluid may have been at least partly supplied by the dissolution of K feldspar. The complete disappearance of K feldspar may be the factor that limited fabric development.

ACKNOWLEDGEMENTS

I would like to acknowledge the advice and support of my advisor, Dr. Warren D. Huff, without whom this would have been a far more difficult task, and of my other dissertation committee members, Drs. John E. Grover and Craig Dietsch. I would particularly like to thank all of them and Dr. J. Barry Maynard for their editorial efforts.

In addition I thank Ms. Stephanie Erb for help with the field work, Mr. George Losonsky for help with sample preparation, Dr. Maynard for help with the probe work, Dr. Nancy J. McMillan for help with the photomicrographs, Dr. Robert P. Wintsch for helpful discussions, and everyone else whose efforts helped me complete this dissertation.

For financial support I thank the Department of Geology, the University Research Council, Yankee Oil and Gas, Sigma Xi, the taxpayers, and my parents.

TABLE OF CONTENTS

LIST OF FIGURES

LIST OF TABLES

CHAPTER I

INTRODUCTION

Development of Thought on the Origin of Slaty Cleavage

Slaty cleavage (Figs. 1, 2), a type of rock foliation, was described by Bakewell in 1815. Speculating about its origin, he noted that it appeared to be unrelated to bedding-plane fissility and concluded that it was a deformational feature. Since then numerous studies have been conducted on various aspects of slaty cleavage. The classic problem in cleavage studies has been deciphering the geometric relationship that exists between cleavage orientation and the orientation of the stress and strain ellipsoids. For more than a century, investigators of cleavage have tried to determine whether the orientation of cleavage is perpendicular to the maximum principal compression, perpendicular to the direction of greatest shortening, or in the plane of the maximum shear strain. Indeed, review of the literature suggests that cleavage orientation was considered to be the cleavage problem for many years (e.g. Phillips, 1844; Haughton, 1856; Fisher, 1884; Harker, 1885, 1886; Becker, 1893, 1896; Fairbairn, 1949; Siddans,1972; Borradaile and Johnson, 1973; Wood, 1974; Bayly, 1974).

This geometric problem has been addressed in many ways, some workers performing experiments; some, field

Figure 1. Outcrop of phyllite belonging to the Walden Creek Group Sandsuck Formation. This exposure is about 2 miles east of Ocoee No. 1 along Ocoee Gorge. It exhibits slaty cleavage typical of these fine grained rocks. Bedding is roughly horizontal.

Figure 2. Thin section of Sandsuck Formation phyllite. Foliation is defined by development of zones enriched in foliation-parallel mica grains alternating with zones enriched in quartz and albite. Scale = 50x.

measurements of finite strain, and some, theoretical analyses. There is, however, still no agreement on an answer to this problem (e.g. see reviews by Siddans, 1972 and Wood, 1974). Dieterich (1969), for example, addressed this question analytically by using finite-element methods to estimate stress and strain orientations in viscous multilayers folded to high amplitudes. He compared his results with orientations of cleavages in some folded rocks, and concluded that the orientations of the principal axes of finite strain in the folded multilayers correspond more closely to the orientations of the cleavages in folded rocks than do the orientations of the principal axes of stress.

It seems, however, that pursuing the geometric problem of cleavage orientation without first identifying the essential characteristics of cleavage, and considering what processes might lead to their development puts the cart before the horse. It is difficult to understand how a particular geometric relationship can be expected to prevail for all occurrences of slaty cleavage unless all cleavage develops by identical processes driven by identical forces. Further, preexisting fabric must be altered so completely that it exerts no lasting influence on the developing cleavage.

Another difficulty in relating cleavage orientation to stress or strain orientation is that the relationship is

often described in terms of fold geometry. The problem with this is that the temporal relationship between the development of cleavage and the development of the fold must be known. Nickelsen (1979) suggested that many of the "spaced cleavages" of central Pennsylvania pre-dated folding, and were rotated into their present orientation during folding. In any case, it is difficult to understand why cleavage should be expected to show a particular geometric relationship to either stress or strain unless the mechanisms by which it develops are clearly dependent on stress or strain orientations.

There are two characteristics of slaty cleavage that appear to be essential and that must be accounted for in any consideration of the mechanisms of cleavage formation. These characteristics are (1) the preferred orientation of platy minerals arranged parallel to cleavage, and (2) the development of domainal fabric or compositional layering which parallels the mesoscopic cleavage (Fig. 2). A question that has arisen in studies of these characteristics is what are the nature and relative importance of various chemical and mechanical processes in their development. In other words, do preferred orientation and compositional layering arise through primarily mechanical deformation mechanisms, such as rotation or grain boundary sliding, or is there significant rearrangement of mineral components by such processes as

dissolution, diffusion, recrystallization, or new grain growth.

The first characteristic, preferred orientation, has received the attention of hundreds of investigators since Bakewell (1815) attempted to generate preferred orientation of clay particles by exposing mud to an electrical current. It seems that by 1815 a controversy had already arisen as to the processes involved in cleavage development; Bakewell voiced his opinion, stating that "If geologists had not been induced, by an attachment to theory, pertinaciously to adhere to opinions once received, they could not have failed to recognize the effect of crystallization in the cleavage of slate" (p. 85). Since Bakewell's time little has changed. Many geologists believe they have recognized the effect of crystallization (e.g. Holeywell and Tullis, 1976; Knipe, 1979, Lee et al. 1986), whereas others hold the view that preferred orientation develops primarily as a result of rotation of pre-existing grains (e.g. Williams, 1972; Holcombe, 1973; Weaver, 1984).

The development of the second characteristic, domainal fabric, has historically received much less attention than has the development of preferred orientation. The development of the compositional zonation that parallels slaty cleavage was puzzled over briefly in the first half of the nineteenth century by Bakewell (1815) and Darwin (1846), among others, but was largely ignored from then

until 1972, when Williams drew attention to it with his finely detailed descriptions of cleavages found at Bermagui, Australia. Since then, electron microscopy studies (e.g. White and Knipe, 1978) have revealed that virtually all slates possess, at some scale, a degree of mineralogical differentiation in layers or zones that parallel cleavage.

The question that arises in connection with this second characteristic is that of which phases or components are redistributed during the development of domains. In rocks made up primarily of quartz and mica it has variously been suggested that 1) only quartz is mobile, 2) only mica is mobile, 3) only some components of mica are mobile, or 4) both quartz and mica are mobile. As with the questions concerning both the geometric relationship between cleavage and stress and strain and the origin of preferred orientation by mechanical reorientation or oriented growth, different workers have reported observations that support each of these four possibilities (e.g. Rast, 1965; Williams, 1972; White and Knipe, 1978; Swager, 1985). It may be that many processes contribute to the development of slaty cleavage and one answer does not apply to all occurrences or, as Means (1977) said, "there may prove to be slates and slates".

Purpose of This Study

Identifying and describing the processes by which slaty cleavage develops is obviously complex. I believe that a successful approach will entail careful, detailed observation at several scales of the textural and mineralogical characteristics of slates in a particular locality. The purpose of this study is to integrate mesoscopic and microscopic observations with various types of analytical data, including X-Ray diffraction and electron microprobe data, to produce a detailed description of slaty cleavage and an account of the processes involved in its development. I have chosen as my field area Ocoee Gorge, Tennessee (Fig. 3), where slaty cleavage is occurs in phyllites of the Ocoee Series.

Figure 3. Index map of study area. Ocoee Gorge extends roughly from the Ocoee No.1 dam to the Ocoee No.3 dam.

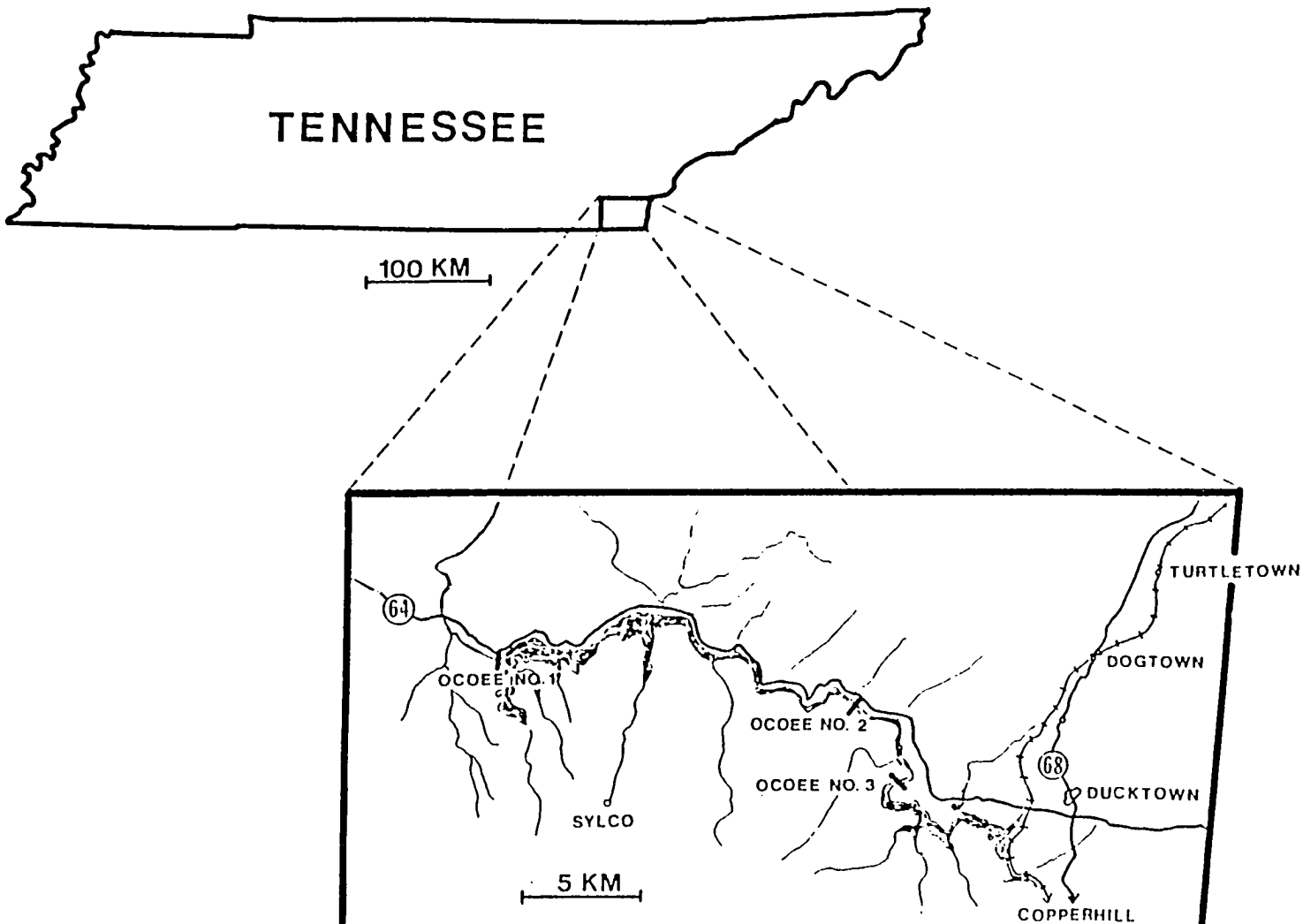

CHAPTER II

GEOLOGIC SETTING OF STUDY AREA

Ocoee Gorge is located in Polk County, Tennessee and lies within the Blue Ridge province of the southern Appalachians. The regional geology is shown in Figure 4, adapted from Magee (1970) and Nesbitt and Essene (1982). The rocks exposed along the gorge were first named by Safford (1856, 1869) as the Ocoee Conglomerate and Clay Slate. He described the exposures in the gorge as interstratified clay slates and coarse conglomerates, broadly folded and dipping to the southeast. About the Ocoee River, a tributary of the Tennessee River, he said that "for twelve or thirteen miles in its tortuous course [it] rolls along over the rocks, while high and grand cliffs of slate and conglomerate come down to the water's edge on both sides, scarcely affording, at any point, space enough for a garden spot. After leaving the narrows, the river flows for four or five miles through a more open valley, and then escapes entirely from the mountains into the great valley below." (Safford, 1856, p. 470).

Stratigraphy

Safford did not assign an age to the Ocoee rocks, but did place them between Precambrian basement of the Blue Ridge and the Chilhowee sediments of Cambrian age. Emmons and Laney (1926) classified rocks exposed in Ocoee Gorge as

Figure 4. Adapted from Magee (1970) and Nesbitt and Essene (1982). Ocoee Gorge runs from the Great Smoky Fault to about the biotite isograd. Most of the samples in this study were collected along 4 miles of the gorge that are bounded on the west by the Sylco Creek Fault.

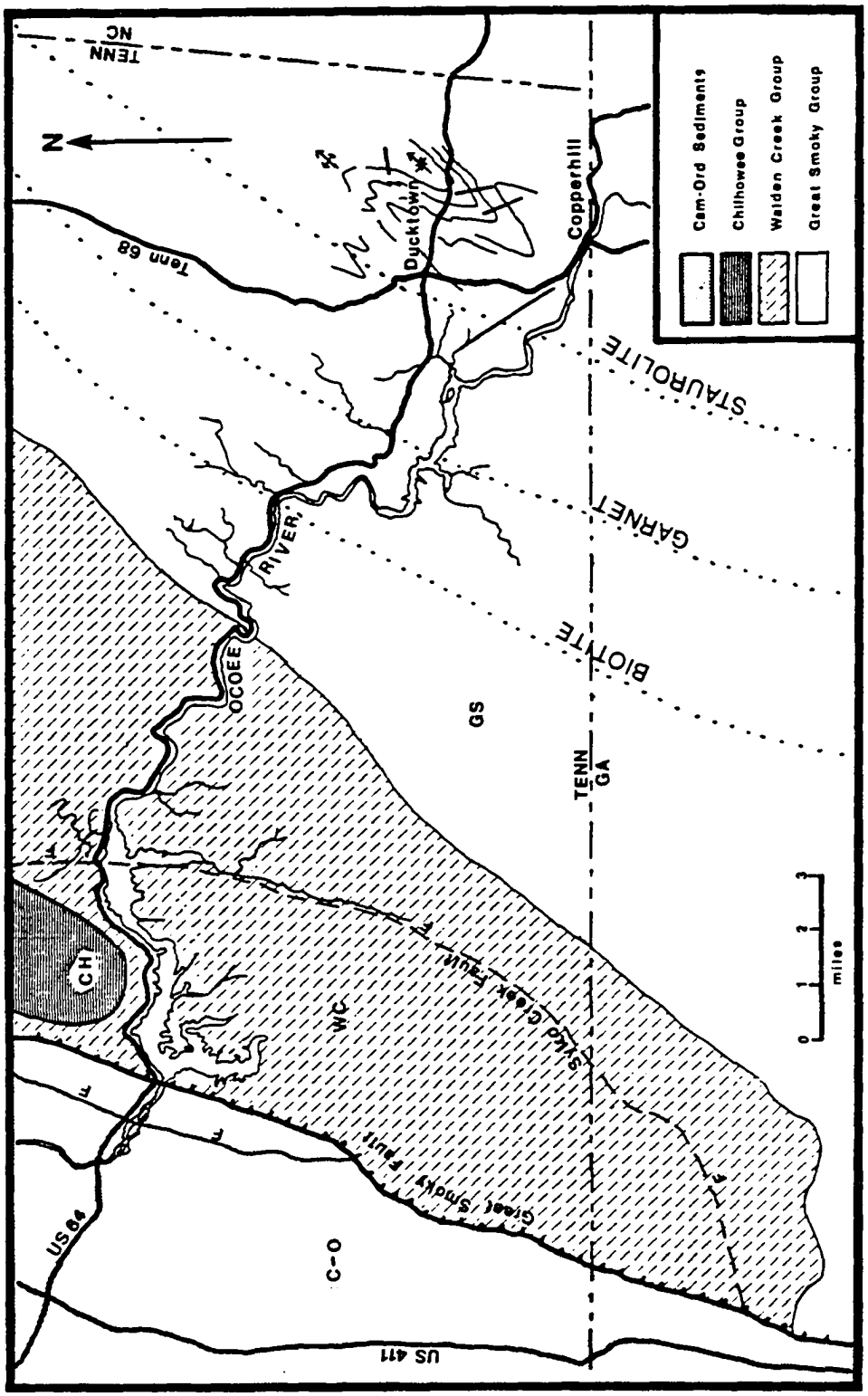

Cambrian, but since that time most workers have regarded them as Precambrian. Stose and Stose (1944, 1949) defined the Ocoee Series, and King et al. (1958) gave the Series a fairly detailed stratigraphy, including three groups, the Walden Creek, the Snowbird, and the Great Smoky. The Ocoee series is in excess of 12,000 m thick, with the Great Smoky Group being over 4500 m thick and the Walden Creek Group being about 3000 m thick (Hadley, 1970).

The repetitious nature of the sediments as well as the structural complexity of the area make stratigraphic correlation difficult. The region in which the Ocoee Series occurs is broken into at least six major thrust sheets (Hadley, 1970). It is therefore not surprising that the three groups of the Series are generally not found in conformable contact. An exception occurs in the Ocoee Gorge section, where the Great Smoky and Walden Creek Groups appear to be in conformable contact. Hurst and Schlee (1962), however, assigned all the exposures in Ocoee Gorge to the Great Smoky Group. Magee (1970) gave a stratigraphic sequence for the Ducktown area, including Ocoee Gorge, that indicates both groups are present in the gorge. Most recent work in the area (e.g. Holcombe, 1973; Granath, 1978; Nesbitt, 1979) has been based on the sequence he published (Table 1).

The Walden Creek Group is exposed in the western half of Ocoee Gorge and in this area is made up of one

Table 1. Stratigraphic sequence Northwest of the Ducktown region. From Magee (1970).

Age	Series	Group	Formations
Ordovician		Chickamauga	Athens Shale
		Knox	Undifferentiated
Cambrian		Chilhowee	Nebo Sandstone
			Nichols Shale
	?	?	?
	?	?	?
	?	?	?
	?	?	?
.....Disconformity.....			
Precambrian	Ocoee	Walden Creek	Sandsuck
		Great Smoky	Dean
			Hughes Gap
			Hothouse
			Copperhill

formation, the Sandsuck. In the eastern half of Ocoee Gorge the Dean and Hothouse Formations of the Great Smoky Group are exposed.

According to Hadley (1970), the source area for the Ocoee Series sediments is somewhere to the north. He speculated that the sediments were transported by turbidity currents, and then deposited in a low energy setting where sulfide and carbon-rich mud was also accumulating, probably in the hinge of a major downwarping of the continental margin during late Precambrian time. Rast and Kohles (1986) have suggested that the Ocoee Supergroup was shed off a northeast-southwest trending ridge, the Unaka Horst, and deposited in extensional basins on either side of the ridge. According to their model the turbidites of the Great Smoky Group were deposited northwest of the ridge, the shallow water clastics of the Snowbird Group to the southeast, and the shallow water clastics of the Walden Creek Group overstepped both of these.

The top of the section within Ocoee Gorge is the 450 m-thick Sandsuck Formation of the Walden Creek Group exposed along the western half of the gorge. It is comprised primarily of finely bedded, fine-grained grey-green phyllites thinly interbedded with arkosic and calcareous quartzites. The entire formation is rich in carbonates, containing ferroan dolomite and calcite. The phyllite beds are typically 1-5 cm thick, but range up to

15 cm thick. They consist of mica-rich layers referred to here as phyllite layers, quartz-mica-rich layers, referred to here as siltstone layers, and less common fine-grained carbonate-rich layers. The fine-grained quartzite beds are generally 2-10 cm thick and are abundant in a 15 m-thick zone, interbedded with phyllite.

At the bottom of the Walden Creek Group, near the middle of the gorge, is a dark, pyritic slate that has been assigned both to the Walden Creek Group and to the underlying Great Smoky Group, and is conformable with both. The slate unit is 175 m thick and is finely laminated, with 1 cm thick mica-rich layers alternating with somewhat lighter colored carbonate-rich layers, commonly packed with pyrite cubes.

Below the pyritic slate is the upper portion of the Great Smoky Group, the Dean Formation, which is comprised of thinly bedded quartzites and green phyllites. Below this zone are thick, interbedded metaconglomerates, metagraywackes, and phyllites. The base of the Ocoee gorge section, at the eastern end, is a monotonous sequence of metagraywacke and mica schist, apparently belonging to the Hothouse Formation.

Structure

Holcombe (1973) studied large scale structures and microstructures of both Ocoee Gorge and Ducktown. He performed statistical analyses of foliation, lineation, and

Figure 5. Structural domains and cross section of Ocoee Gorge. From Holcombe 1973.

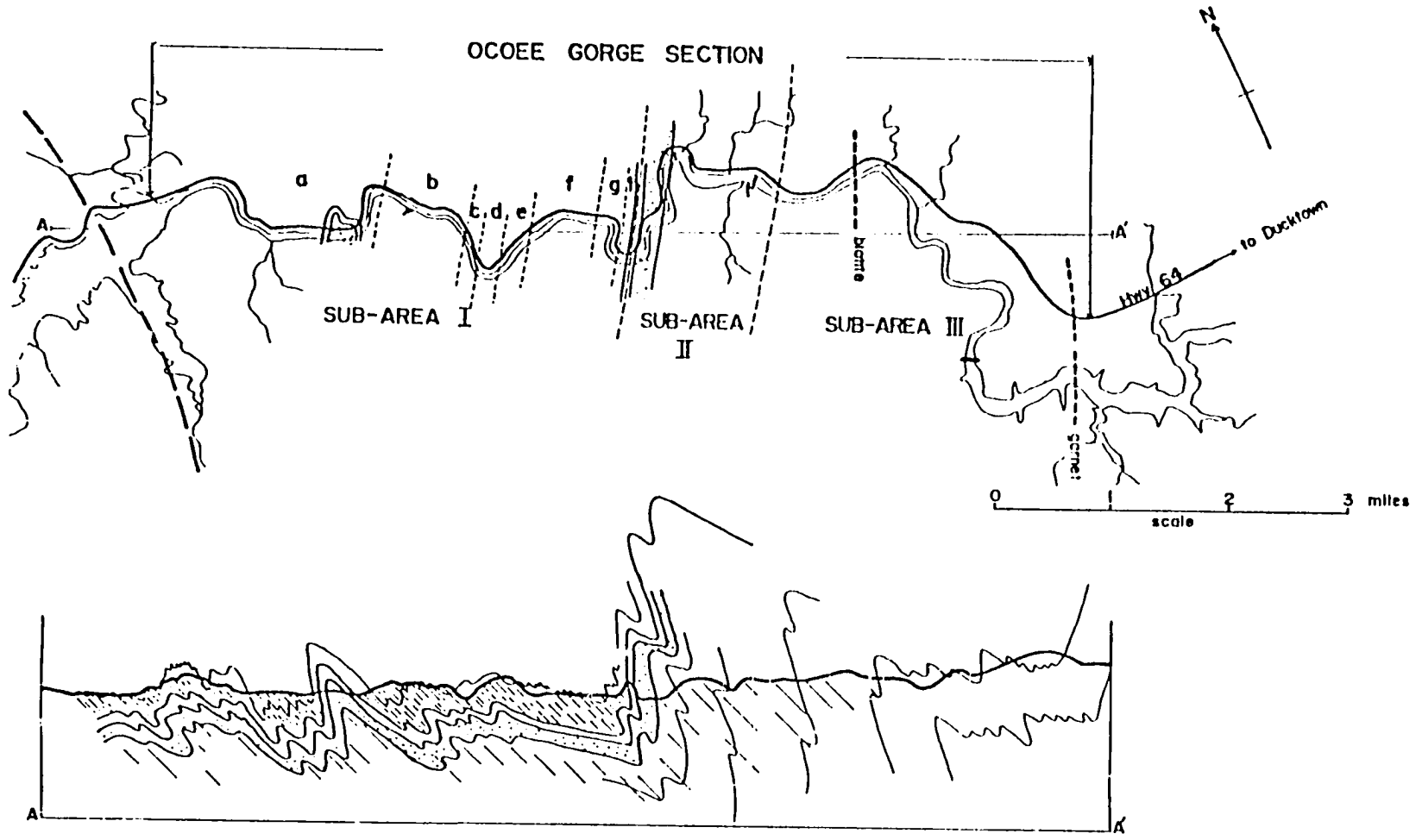

fold orientations, and defined temporal and geometric relationships among these fabric elements. Throughout the gorge he found evidence of two episodes of deformation and near the eastern end, three or more. On the basis of statistical analyses, he divided the gorge into three sub-areas, each exhibiting a different dominant orientation of fold axes (Fig. 5). Sub-area I, within the Walden Creek Group, is distinguished by horizontal fold axes and open, cylindrical folds. The microstructures here include well developed slaty cleavage, with subordinate mineral streaking lineations and kink bands. Sub-area II, within the Great Smoky Group, has more open and less cylindrical folds than sub-area I. Typically folds in sub-area II have steeply plunging axes, although there is considerable local variation. The axial plane orientation of macroscopic folds is about the same in both sub-areas I and II. The boundary between sub-areas I and II corresponds roughly to the contact between the Walden Creek Group and the Great Smoky Group. Holcombe speculated that the change in structural style across the contact is caused by differences in the mechanical properties of the rocks. Sub-area III, also within the Great Smoky Group, is characterized by statistically cylindrical folds plunging gently to the south, although individual fold axes vary considerably in orientation. In sub-area III there is a well-developed crenulation cleavage that becomes the most

prominent fabric element near the eastern end of the gorge.

Using his observations of the relationships among fabric elements as a basis, Holcombe summarized the tectonic history of the region as follows:

1. Deposition of the Great Smoky Group graywackes and conglomerate, followed by deposition of the finer grained Walden Creek Group.

2. The first deformation, F1, produced large, open folds and slaty cleavage throughout the area. Metamorphism reached garnet grade in Ducktown.

3. The second deformation, F2, produced isoclinal folds in Ducktown and crenulation cleavage in eastern Ocoee Gorge, but barely affected rocks in western Ocoee Gorge. Metamorphism reached staurolite grade in Ducktown, and kyanite grade to the southeast of Ducktown.

4. The third deformation, F3, produced relatively open folding and minor faulting. Metamorphism was retrograde to biotite or chlorite grade.

5. Minor deformations produced at least two sets of crenulations and small chevron folds that overprint older structures.

Metamorphism

The entire Ocoee Gorge-Ducktown region has been regionally metamorphosed, with the grade increasing from the western end of the gorge eastward to Ducktown. Carpenter (1970) established metamorphic isograds by

mapping index minerals in stream sediments, and Nesbitt and Essene refined the location of Carpenter's isograds (1982) by studying outcrop and, in the Ducktown area, core samples (Fig. 4). The Ocoee Gorge section is almost entirely within the chlorite zone; the biotite isograd cuts across the far eastern end of the gorge.

Granath (1978) studied a small outcrop of the Great Smoky Group in Ducktown, where metamorphism reaches staurolite grade. He found evidence for two separate metamorphic events. One of these has been dated at around 430 m.y.a. (Taconic) by Butler (1972) and the other around 350 m.y.a. (Appalachian) by Kinkel et al. (1965). Holcombe (1973) found evidence that both the Taconic and Appalachian metamorphic events affected rocks in the gorge. He cites the only available radiometric age as 434 m.y.a. for rocks near the biotite isograd at the eastern end of the gorge. At the western end of the gorge there is no evidence that more than one metamorphic event has occurred.

Within the chlorite zone, phyllites contain the assemblage quartz-albite-muscovite-chlorite-ferroan dolomite-calcite-rutile. Cubes of pyrite are abundant in the phyllites in the western half of the gorge, whereas in the eastern half of the gorge elongate blebs of pyrrhotite are found. As noted by Holcombe, the biotite isograd is difficult to locate exactly; he placed it 15.0 miles east of Parksville Dam along Highway U.S. 64, whereas Hurst and

Schlee (1962) placed it 15.7 miles east of the dam. I first found biotite at about mile 15.0, but could not find any in hand samples between miles 15.2 and 15.7. There are two difficulties in locating the isograd: first, it appears in slaty beds before metaconglomerate beds, which are predominant near mile 15.0; and second the first appearance of biotite is in a particular set of microstructural domains rather than throughout the rock.

No metamorphic temperatures or pressures have been reported for Ocoee Gorge rocks. Nesbitt and Essene (1982) calculated a temperature of 540 ± 50°C at a pressure of 6 ± 1 kilobar for the higher grade rocks of Ducktown.

Chemical Data

In addition to analyzing the structure in Ocoee Gorge, Holcombe performed qualitative microprobe analyses of the microstructural domains defined by the foliation. Areas fifty microns in diameter were analyzed, including both P and Q domains. He determined distributions of Si, Al, K, O, Na, Ca, Fe, Mg, Ti, Zr, C, S, Mn, P, and B, and reported that (1) K outlines the distribution of mica; (2) Na is associated only with albite; (3) Ti is present as rutile; (4) Mn distribution matches that of Ca and apparently is in carbonate; and (5) Zr, P, and S are present only in scattered grains of zircon, apatite, and sulfide, respectively.

Holcombe compared the chemical and mineralogical

constituents of P domains to those of Q domains, and found that P domains are enriched in K, Al, and Ti, but depleted in Si, Ca, Fe, Mn, and Na relative to Q domains. He reported that mica and rutile are concentrated in P domains, whereas quartz, albite, and carbonate are concentrated in Q domains.

CHAPTER III

PREVIOUS WORK ON CLEAVAGE

Terminology

Darwin (1846, p.424) defined rock cleavage as "those planes of division which render a rock, appearing to the eye quite or nearly homogeneous, fissile." His definition of cleavage is the traditional one, and is based on the ease with which rocks having cleavage split along parallel planes. This characteristic has generally been attributed to the preferred orientation of platy minerals parallel to cleavage. Preferred orientation is, however, one of two essential properties of rock cleavage.

The second essential property of rock cleavage is the presence of domainal fabric, a type of mineral segregation occurring in elongate domains that crosscut sedimentary layering. In pelitic rocks, this property is characterized by anastomosing zones that have been enriched in phyllosilicates relative to quartz, feldspar, and carbonate (e.g. Williams, 1972; Holcombe, 1973). In this study these phyllosilicate-rich zones and the intervening areas are called P domains and Q domains, respectively. The existence of domainal fabric associated with slaty cleavage was recognized by some of the earliest students of cleavage (e.g. Sedgewick, 1835; Darwin, 1846), but has been neglected by most until quite recently, with much attention

paid it only since it was described in detail by Williams (1972).

The fabric defined by both preferred orientation of platy mineral grains and domainal fabric is slaty cleavage. Crenulation cleavage (Fig. 6) is a closely related fabric distinguished by a non-penetrative foliation superposed either on a pre-existing penetrative foliation or on bedding. Typically this non-penetrative foliation takes the form of either rotated limbs of microfolds or slip surfaces of microfaults. The distinction between slaty cleavage and crenulation cleavage seems to be morphologic rather than genetic; the differences may be due to differences in the pre-existing fabric of the rock. Crenulation cleavage that undergoes enough metamorphic differentiation between hinges and limbs of microfolds is not distinguishable from slaty cleavage. It seems artificial to consider slaty and crenulation cleavage as two distinct fabric types. Both are present in the rocks of Ocoee Gorge and, because they cannot always be distinguished from one another, both are analyzed in this study.

Terminology used to characterize cleavage has become confusing both because terms are not used consistently, and because workers have a tendency to coin terms that carry genetic implications. So many terms have been used to describe cleavage, that for clarity it seems necessary to

Figure 6. Negative print of a thin section of Great Smoky Group schist from Ducktown. The well-developed domainal fabric is overprinted by the development of crenulation cleavage. Scale = 40x.

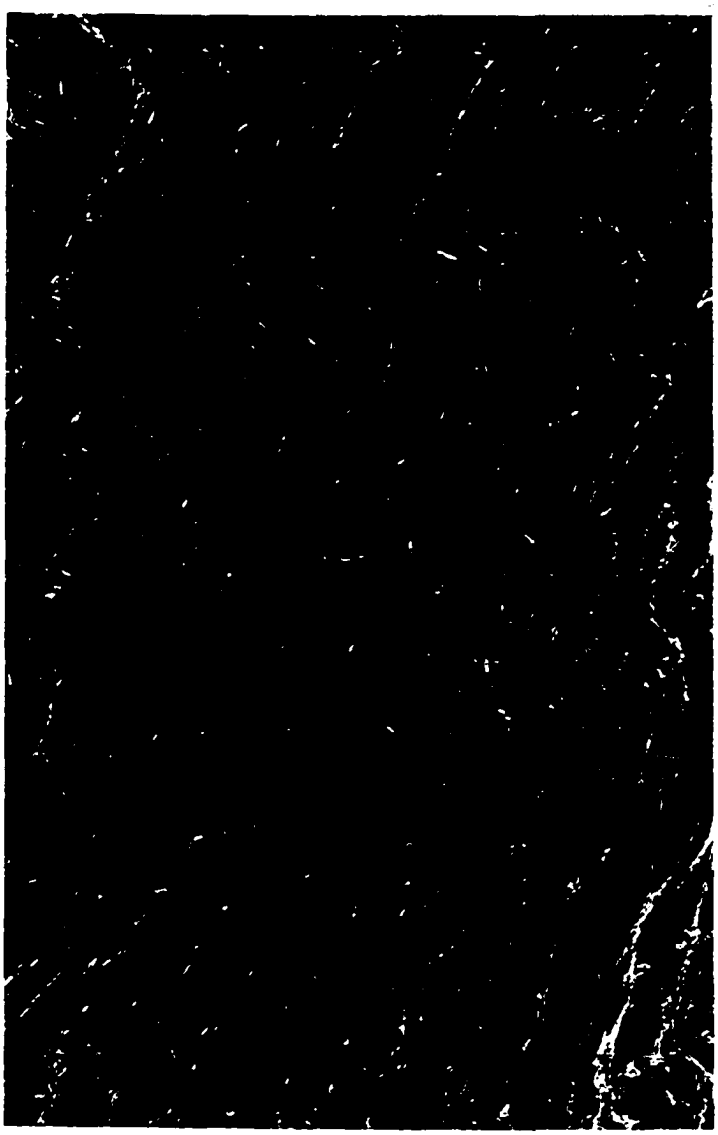

briefly review them.

Leith (1905) divided rock cleavage into original and secondary cleavage. Original cleavage refers to bedding and igneous foliations, whereas secondary cleavage includes all types of metamorphic foliations. He further subdivided secondary cleavage into flow cleavage and fracture cleavage. He defined flow cleavage to be secondary cleavage possessing a parallel arrangement of mineral constituents, in other words, penetrative slaty cleavage. Fracture cleavage, in contrast, is non-penetrative and has spaced parting surfaces that are, according to Leith, unrelated to preferred orientation of minerals. His illustrations, however, show that fracture cleavage may be synonymous with crenulation cleavage, i.e. his fracture cleavage does possess spaced zones of mica grains oriented parallel to the cleavage. Leith's flow cleavage and fracture cleavage seem to be equivalent to Van Hise's (1896) cleavage and fissility, respectively. Other terms Leith noted used for fracture cleavage include false cleavage, grain cleavage, bate cleavage, and close joints cleavage.

Several other schemes for naming and classifying cleavages have been published (e.g. Gray, 1977a, 1979; Powell, 1979), but all are based on whether or not a cleavage is penetrative at a particular scale of observation, usually the mesoscopic scale, and on the

morphology of the cleavage surfaces. The complexity of the terminology is somewhat difficult to understand; all these types of cleavage seem to be rather poorly delimited members of a continuum. Therefore I will restrict myself to two specific terms, slaty and crenulation cleavage, for penetrative and non-penetrative cleavage, respectively, and, for more general cases I will use rock cleavage. In fine-grained pelitic rocks, such as those found in the western end of Ocoee Gorge, the terms slaty and crenulation cleavage adequately describe the cleavages, and in this work are intended as strictly descriptive terms.

Previous Descriptions of Cleavage Fabric

The ability of slates to cleave has generally been attributed to the parallel arrangement of platy minerals. Sorby (1853) noted that in thin sections cut perpendicular to slaty cleavage and in the line of dip, most mica grains are within twenty degrees of being parallel to cleavage. In thin sections cut perpendicular to slaty cleavage and in the line of strike, the preferred orientation is less pronounced. According to Sorby (1856) cleavage is best developed where constituent grains show the highest aspect ratios.

Leith (1905) described the arrangement of mica flakes in slaty cleavage as roughly parallel to the cleavage, but with some irregularities. Mica grains may be bent or broken, in some places to such an extent that the cleavage is a linear rather than a planar feature (pencil or pumpkinseed cleavage). Cleavage may wrap around refractory grains, changing orientation as it does so, but returning to its average orientation between refractory grains. Undeformed mica flakes, he found, may be arranged irregularly, abutting against one another, particularly where biotite and muscovite constitute neighboring grains. Biotite, but not muscovite, Leith stated, may occur as stumpy grains not aligned with cleavage. Aligned micas show a uniform orientation of only their shortest dimensions (perpendicular to cleavage).

Domainal fabric in slates was first described in detail by Williams (1972). He examined cleavage in a sequence of alternating graywackes and pelites, and reported mineralogically segregated layering parallel to axial planar cleavage in both rock types. He noted that the domains alternately enriched in quartz or mica are discontinuous across pelite-graywacke contacts, and are more closely spaced in the pelite. More recently, descriptions of both preferred orientation and domainal fabric, have been extended to a finer scale by the work of White and Knipe (1978), White and Johnston (1981), and Lee et al. (1984, 1986).

Review of Studies on the Composition of P and Q Domains

Two previous studies have compared bulk compositions of P and Q domains. One is a qualitative electron microprobe study by Holcombe (1973) on the Ocoee Gorge rocks in which he found K, Al, and Ti to be concentrated in P domains, and Si, Ca, Mn, Mg, and Fe to be concentrated in Q domains. The other is a study by Stephens et al. (1979) on metamorphic layering in slates from near Clunes, Australia. This study was made by separating samples of P and Q domain material found in sandstones and siltstones associated with the slates, and analyzing them by X-Ray Fluorescence(XRF) spectrometry. Material from P and Q domains in the slates was not analyzed. P domains were most enriched relative to Q domains in K, and were also significantly enriched in Ti, Y, Zr, and Al. P domains were also enriched to a smaller extent in Mg, Fe, P, and Ca. Relative depletion was noted for Si, Na, and possibly for Mn. In analyzing these data, they assumed that Ti is immobile, and then calculated enrichment and depletion of other elements in terms of volume change relative to volume change for Ti. With this method, they concluded that as the domainal fabric evolved, K enrichment occurred in the P domains, Ti, Y and Zr did not change, and all other elements were depleted in P domains relative to Q domains.

Stephens et al. also presented infrared modal analyses of major constituents of P and Q domains. Again, they only

presented data for the relatively coarse-grained sandstone and siltstone beds. They found P domains to be enriched in mica and chlorite and depleted in quartz and albite relative to Q domains. They also found siltstone to have more phyllosilicates and less quartz and albite relative to sandstone. In comparing the domains in both rock types, they found that the modal composition of sandstone P domains is quite similar to that of siltstone Q domains.

Mechanisms for Development of Preferred Orientation

Since cleavage was first recognized as a distinct type of rock fabric, a variety of chemical and mechanical mechanisms for its development have been proposed, particularly mechanisms for the evolution of preferred orientation. For over 150 years there has been an ongoing debate as to whether chemical or mechanical processes dominate during the development of preferred orientation associated with rock cleavage. Dale (1914, p.20) summed up the then current status of the debate when he said, "While there has been substantial agreement as to the general microscopic and chemical character of roofing slates, there have been questions as to the origin of some of their constituents. Is the muscovite which makes up from a third to a half of the mica slates the product of the metamorphism of argillaceous material, or are these shredlike scales the result of the disintegration of some micaceous rocks, the effect of pressure having been simply to bring the shreds into parallelism and to mat them together?" From a review of more recent literature (for example see Weaver, et al., 1984), it is not clear that the nature of the debate has changed very much since 1914.

Two of the earliest students of cleavage, Bakewell (1815) and Sedgewick (1835), suggested that it formed as a result of recrystallization during metamorphism, whereas Phillips (1844) recognized that its development is related

to deformation. Sharpe (1847, 1849) reported that the particles in slates are individually flattened and elongated in the orientation of the cleavage planes, but he recognized no evidence of crystallization or recrystallization. He noted, after studying strained fossils in slates, that shortening appeared to have taken place perpendicular to cleavage and lengthening in the dip direction of the cleavage. In the strike direction of the cleavage, Sharpe noted neither shortening nor stretching of fossils. Regarding the cause of cleavage, he stated, "... all our observations and deductions ultimately converge to the conclusion that the cleavage must be attributed to pressure caused by the elevation of great masses of rock under conditions of which we are ignorant. And if to this conclusion it should be objected that no similar results can be produced by experiment, I reply that we have never tried the experiment with a power at all to be compared to that employed; and that this may be one of many cases where attempts to imitate the operations of nature fail, owing to the feebleness of our means, and the shortness of the period during which we can employ them."

Important Studies of Sorby, Van Hise, and Leith

Sorby (1853) also noted finite strain associated with rock cleavage. He reported that reduction spots in shale are spheroidal or elongate parallel to bedding, whereas reduction spots in slates are elongate parallel to cleavage

and concluded that slates have been mechanically flattened perpendicular to the plane of the cleavage. Sorby suggested that chemical processes not only do not contribute to cleavage development, but that recrystallization would obliterate cleavage (1856). He wrote (1853) that mineral grains in slates change position and rotate as rigid bodies, but do not distort. The total rock, however, distorts, and Sorby assumed that it underwent significant volume reduction. Harker (1885) agreed that rocks with slaty cleavage have lost volume, and suggested that this loss is caused by closer packing of grains and expulsion of interstitial water.

Van Hise (1896) speculated that during cleavage development large, detrital mineral grains dissolve, while new grains, particularly mica, grow with their long dimensions parallel to cleavage, and that none of the mica or chlorite parallel to cleavage is detrital. He stated (p. 638) that, "....it is easy to discriminate the large, comparatively sparse fragmental mica plates, if any are present, from those which are autogenic. As soon as a new mineral particle has developed it is subjected to flattening and rotation precisely as is an original mineral particle. This parallel arrangement of minerals developed in situ is probably the most important single cause of cleavage."

Leith (1905) wrote that much of the confusion over the

origin of cleavage was due to attempts to find one cause for all types of cleavage. For the development of preferred orientation he recognized four possible mechanisms which might act alone or in combination. The mechanisms Leith recognized were: (1) crystallization and recrystallization, terms he used synonymously, (2) gliding within mineral grains, causing flattening, (3) rotation of old grains, and (4) granulation or breaking of grains into parallel slices. As evidence against strictly physical mechanisms of reorientation, he listed the following: (1) presence of new phases, (2) minerals grains oriented at right angles to bedding where there is insufficient strain preserved to make rotation credible, (3) shape of grains differing from that in the original rock, (4) contacts between grains that could not be produced mechanically, e.g. mica grains dovetailing into one another, (5) an increase in grain size relative to that of the original rock, (6) lack of strain within grains, (7) complete parallelism of grains without bending or breaking, and (8) metamorphic differentiation.

Leith (1905) favored recrystallization as the most important process in the development of slaty cleavage. He said that where there is no clear evidence of recrystallization, generally there is little or no development of preferred orientation. Rarely, however, "granulation and slicing" may produce a well-developed

preferred orientation, sometimes among grains that are later recrystallized and therefore are mistakenly thought to have been reoriented by recrystallization. In rocks showing evidence of rotation, but not evidence of recrystallization, Leith reported that some degree of preferred orientation may develop, but not enough to produce a good cleavage. Recrystallization, he suggested, could be brought about by solution of non-aligned mineral grains in interstitial water, followed by redeposition of grains in the preferred orientation. Minerals in certain orientations may grow in preference to those in other orientations, and strained minerals will dissolve more rapidly than unstrained ones. Hence, detrital minerals in certain preferred orientations are apt to survive and new minerals are more apt to grow in these same orientations.

Leith suggested that rotation may be accompanied by recrystallization or may operate alone. In either case rotation requires that particles have sufficient freedom to move toward a parallel position when stressed, that is, the rotating grains must not be constrained by their matrix or by one another. He concluded, however, that it is unlikely that inequant grains defining a well-developed foliation could freely rotate past one another without developing greater strain than that typically observed.

Review of the mechanisms for producing preferred orientation of platy minerals suggested by Sorby (1853),

Van Hise (1896), and Leith (1905), indicates that mechanisms fall into one of two fundamental categories: (1) growth of crystals oriented in a preferred orientation, including both crystallization and recrystallization, and (2) mechanical reorientation of grains during deformation to produce preferred orientation. All explanations of preferred orientation involve these two mechanisms singly or in combination.

Two Models for Mechanical Reorientation

Two models have been proposed for the mechanical reorientation of platy minerals: (1) rotation of rigid particles in a deforming medium (Jeffrey, 1922; Bilby, Eshelby, and Kundu, 1975; Bilby and others, 1976; Dixon, 1976; Ghosh and Ramberg, 1978; Ferguson, 1979) and (2) reorientation of passive markers in a deforming medium (March, 1932; Oertel, 1970; Owens, 1973; Lipshie et al., 1975; Tullis, 1976). The difference between these is that in the first model, the particles are stiffer than the medium in which they are rotating, whereas in the second model the passive markers are mechanically identical to the medium; they are merely a device for recording the rotation of regions within the medium. Jeffrey (1922) modelled the behavior of widely spaced, rigid ellipsoidal particles in a viscous medium and obtained an expression relating degree of development of preferred orientation to deviatoric strain and a shape parameter. In March's model (1932),

randomly distributed plates and rods act as passive markers in a medium subjected to homogeneous deformation. This model yields a quantitative relationship between development of preferred orientation and deviatoric strain. Both models predict a consistent relationship between degree of development of preferred orientation and the magnitudes of the strains.

Oertel (1970) and Lipshie et al. (1976) recognized that the March model is an inadequate theoretical basis for understanding the development of preferred orientation in slates; it is unclear what would play the role of the medium within which the micas were supposed to rotate passively. Oertel and Phakey (1972), however, suggested that the matrix might be a soluble phase in some slates. Tullis (1971, 1976) compared these models by performing a series of room-temperature experiments with mica grains, to determine the degree of preferred orientation as a function of gross deformation. He found that if the grains were loosely packed and the strains were small, the results agreed with those predicted by both the March and Jeffrey models. If, however, the grains were packed tightly, or strains were large, the degree of preferred orientation was lower than that predicted by either model. Presumably grain boundary sliding is the principle deformation mechanism in the experiments by Tullis. Several investigators (Spry, 1969; Vernon, 1975; Williams, 1976;

Borradaile, 1979, 1981) have suggested that grain boundary sliding, with or without intragranular deformation, might contribute to the development of slaty cleavage.

Pressure Solution During Reorientation

Removal of one or more soluble phases from between phyllosilicate grains by pressure solution has been suggested to explain mechanical reorientation. Material undergoing pressure solution dissolves in highly stressed regions at and around grain contacts (Weyl, 1959; Voll, 1960; Durney, 1972; De Boer, 1977; Robin, 1978, 1979). Presumably points of collision between rotating phyllosilicate grains would be likely points for dissolution. An increase in mean stress at grain-to-grain contacts increases the local chemical potential of dissolved mineral components (Kamb, 1959, 1961; Fletcher, 1961). A chemical potential gradient is thus established that drives diffusion of these dissolved components toward regions of lower mean stress, where they may precipitate. Several investigators have suggested pressure solution as a process contributing to the development of preferred orientation associated with rock cleavage (Williams, 1972; Oertel and Phakey, 1972; Cosgrove, 1976; Groshong, 1976; Morris, 1981).

Pressure solution could augment the development of preferred orientation by mechanical rotation in at least two ways: (1) by removing those portions of rotating

phyllosilicate grains that would otherwise interlock and block further rotation, and (2) by removing quartz or other soluble phases from domains rich in phyllosilicates, forcing the platy minerals to be pushed together into a subparallel arrangement.

Sedimentary Dewatering During Reorientation

Mechanical rotation of platy minerals during dewatering of sediments was suggested as a process of reorientation by Harker (1885) and later by Maxwell (1962), and has been endorsed by several investigators (Moench, 1966; Powell, 1969, 1972; Braddock, 1970; Clark, 1970a). Maxwell studied slaty cleavage in the Martinsburg Formation near the Delaware Water Gap, and suggested that the cleavage formed rapidly in a thick, unmetamorphosed, water-bearing pelitic sequence, probably during dewatering under high pore water pressure which reduced friction among grains, enabling them to rotate easily.

Clark (1970a, 1970b) investigated Maxwell's hypothesis by conducting experiments on mixtures of kaolin and water to verify the role of rotation in the development of preferred orientation of platy minerals. In experiments where the mixtures were subjected to uniaxial compression, the degree of preferred orientation that developed was high only for compactions greater than 50 per cent. Clark concluded that for compaction of sediments to cause preferred orientation, the initial presence of at least 50

per cent water by volume was required. In other experiments, kaolin-water mixtures were subjected to pure shear, i.e. volume was held constant. The preferred orientation was consistently normal to the direction of greatest shortening.

Epstein and Epstein (1969) reviewed the evidence for dewatering in the Martinsburg Formation and made some observations that are not compatible with a sedimentary dewatering origin for cleavage. Their thin sections show evidence both of low-grade metamorphism accompanying cleavage development, and of bedding-plane slickensides deformed by cleavage, indicating that cleavage did not form in unconsolidated sediments. Holeywell and Tullis (1975) found evidence in the Martinsburg at Lehigh Water Gap against mechanical reorientation of platy minerals either during or after dewatering. They observed that in this outcrop, where slaty cleavage is well developed at one end and undeveloped at the other end, the mica and detrital chlorite do not change from the bedding plane orientation to the cleavage orientation at the same place, as would be expected if their reorientation were mechanically controlled. Their observations suggest that the preferred orientation is largely due to dissolution and growth of crystals rather than rotation, as the latter should have affected both mica and chlorite equally.

Summary of Previous Works on Reorientation

In summary, mechanisms for the development of preferred orientation of minerals parallel to rock cleavage are all described by one or more of the following: (1) mechanical rotation, (2) new grain growth, and (3) recrystallization of detrital grains. The end members of the first, mechanical rotation, are represented by the March model, rotation of passive markers during deformation, and the Jeffrey model, rotation of rigid particles imbedded in a deforming viscous medium. A more specific mechanism proposed by some workers is the rotation of mica grains during dewatering of unlithified sediments; mica grains are rotated by the escaping water until parallel with the path the water is taking.

The second mechanism, new grain growth, involves growth of new mica grains in an anisotropic stress field. In this case mica grains grow in a thermodynamically favorable orientation, from the components available in pore fluid. Mica components may be supplied by the concurrent dissolution of less favorably oriented grains or by the dissolution of internally deformed grains having high strain energy. The third mechanism, recrystallization of solid grains, is also driven by a need to achieve a more thermodynamically favorable orientation or a lower strain energy.

A Model for Reorientation

The development of preferred orientation may involve some degree of initial rotation followed either by dissolution and redeposition of mica components, or by solid state recrystallization. Rotation might cause internal deformation of the mica grains, increasing their strain energy and making them more susceptible to dissolution or recrystallization. Strained grains would dissolve and their components would precipitate as new, unstrained grains, or as overgrowths on less strained or more favorably oriented grains. Alternatively, grains not aligned in the bedding plane orientation during lithification may become strained during burial and compaction, evolving into favorable sites for dissolution and recrystallization.

Rotation might also lead to dissolution of just those specific portions of grains that are rotated into contact with other grains, blocking further rotation. Stress concentrations at these contact points would make them particularly susceptible to dissolution.

There are at least two other ways in which rotation might work in combination with either new grain growth or recrystallization. One of these is the development of kink bands during deformation, followed by new grain growth parallel to pre-existing grains that rotated within the kink bands. The other is the bending of individual mica

grains during deformation, leading to high strain energy in the hinge of the bent grain. The highly strained hinge may then become a favored site for dissolution or recrystallization.

Mechanisms for Delvelopment of Domainal Fabric

The second basic element of cleavage fabric, domainal fabric, has received far less attention than preferred orientation and far less work has been published on possible mechanisms and processes responsible for its development. Leith (1905) suggested that the development of domains might be caused by crystallization or recrystallization along spaced planes associated with cleavages, but offered no insight into a driving force for such a process. Earlier, Van Hise (1896) hypothesized that domains might be formed by the injection of new material along pre-existing planes of fissility. Only in recent years have many processes or mechanisms for the development of domainal fabric been proposed. As a group, the mechanisms are, with one exception, chemical and they generally differ only in the identification of the mineral components mobilized, and whether the minerals are redeposited locally or are entirely removed from the system.

Transposition of Layering

The one mechanical mechanism that has been proposed for the development of domainal fabric is the mechanical transposition of pre-existing layering during repeated episodes of isoclinal folding (see for example Turner and Weiss, 1963). Several objections can be raised to mechanical transposition as a viable mechanism for the

development of domainal fabric, but perhaps the most serious is that in low-grade metamorphic rocks such as slates, domainal layering clearly overprints sedimentary layering (see, for example, Talbot and Hobbs, 1968).

Chemical Mechanisms

The chemical mechanisms that have been proposed for the development of domainal fabric generally rely on dissolution of thermodynamically unstable grains. Unstable grains may be grains that are highly stressed, highly strained, not compositionally stable under the given metamorphic conditions, or are highly anisotropic in their mechanical properties and are oriented at an unfavorable angle to the applied stress field. Once unstable grains have dissolved, their components are assumed to migrate through an intergranular fluid phase, and ultimately either exit from the system or be redeposited as new grains or as overgrowths on unstrained grains in stable orientations and with stable compositions.

The formation of mica-rich P domains could be caused either by migration and subsequent concentration of components of mica (e.g. Rast, 1965) or by dissolution and subsequent depletion of quartz (e.g. Gonzales-Bonorino, 1960; Dewey, 1965; Nicholson, 1966; Durney, 1972; Durney and Ramsey, 1973; Holcombe, 1973; Gray, 1978). Conversely, if Q domains are enriched in quartz relative to the parent rock, this enrichment could occur either by addition of

quartz or removal of other material. Several investigators of pressure solution have noted that the presence of clay minerals may enhance pressure solution between quartz grains (Heald, 1956; Weyl, 1959; Sibley and Blatt, 1976), and others have suggested that the surfaces of mica and clay particles serve as diffusion paths (Weyl, 1959; Durney, 1972; Elliot, 1973).

Robin (1979) suggested that in the development of domainal fabric in a bimineralic quartz-mica rock, an increase in mica content causes an increase in silica diffusion under a given stress. He considered a stressed multilayer composed of two kinds of alternating layers, one richer in mica than the other. He argued that if maximum compression is normal to the layers, two types of diffusive mass transfer occur: (1) intralayer diffusion, in which material is removed from grain boundaries normal to the maximum compression and is redeposited on grain boundaries parallel to the maximum compression, and (2) interlayer diffusion, which removes quartz from mica-rich layers and redeposits it in mica-poor layers, hence enhancing the compositional layering. Robin suggested that intralayer diffusion might be expected to dominate because of the shorter diffusion paths, but if mica does enhance diffusion of silica, interlayer diffusion could be important. If micas are oriented parallel to the diffusion direction, interlayer diffusion could dominate.

CHAPTER IV

PREVIOUS WORK ON DIAGENETIC AND METAMORPHIC PHYLLOSILICATES

Numerous works have been published on the composition of phyllosilicates found in diagenetic and low-grade metamorphic rocks. Some of these studies have traced the changes in composition and structure undergone by the clays, micas, and chlorites in fine-grained sedimentary rocks during regional diagenesis and greenschist facies metamorphism (e.g. Dunoyer de Segonzac, 1970; Hayes, 1970; Weaver et al., 1984; Curtis et al., 1985, White et al., 1985; Hunziker et al., 1986). Other studies have specifically related the composition and structure of these minerals to the microstructure of the rocks (e.g. Knipe, 1979; Stephens et al., 1979; White and Johnston, 1981; Lee et al., 1984, 1986). In both types of study, the interesting variations in the white micas appear to be the substitution of Mg and/or Fe for Al^{VI} (octahedral aluminum) accompanied by the substitution of Si for Al^{IV} (tetrahedral aluminum), the degree to which interlayer cation sites are filled, and changes in polytype. In chlorites variations in polytype and possibly in Fe to Mg ratios appear to be related to diagenesis and lowgrade metamorphism.

Review of Selected Studies Characterizing Diagenetic and Low-grade Metamorphic Phyllosilicates

Weaver (1979) summarized the findings of many other workers on diagenetic and low-grade metamorphic alteration of clay minerals in shales and slates. Among the changes with increasing grade that he noted are increases in both Al^{IV} and total Al (the sequence smectite to mixed-layer illite/smectite to illite to phengite). As clays evolve toward phengite, tetrahedral layers should increase in size relative to octahedral layers, a structural change that favors the introduction of K into the crystal and hence the development of mica. This increase in total Al can be accomplished either by adding Al or removing Si. He suggested that, on the basis of laboratory experiments, the removal of Si may be more important than the addition of Al.

Another of the trends noted in Weaver's review is a change in water content between illite and phengite or muscovite. Illites have been found to contain 4.6 to 8.0 weight percent H_2O, with an average of 7 percent, whereas phengites and muscovites range between 4.4 and 4.7 percent. The higher water content of illite has been attributed to either excess water trapped in nonexpanded layers, or the presence of some interstratified smectite, vermiculite, or chlorite layers.

Weaver noted other trends during clay evolution

towards mica include an increase in "crystallinity" or sharpness, a transition from the $1M_d$ to the 2M polymorph, a decrease in expandable layers, an increase in negative layer charge (mainly due to increase in tetrahedral charge), an increase in K content, and a related increase in the ratio of the 5 A peak intensity to the 10 A peak intensity. The (Mg + Fe) content may increase or decrease. He notes that the metamorphism of assemblages containing smectite and K-feldspar can follow two routes, depending on pressure. If pressure is high phengite and quartz will be formed, whereas if pressure is low muscovite and chlorite will be formed. In the first case, Al^{VI} is low, whereas in the second case some of the octahedral Fe and Mg have been replaced by Al.

Weaver et al. (1984) described textural and mineralogical changes in the shale to slate transition seen in the Cambrian Conasauga shale, exposed in the southern part of the Appalachian Valley and Ridge Province. They describe in detail the trends in the petrology and texture of the diagenetic zone, the anchizone[1], and the epizone[2]. This study is of particular interest because of both the geographic proximity of their study area to Ocoee Gorge and the similarity in the age of the rocks (Cambrian versus

---

[1] The zone of very low-grade metamorphism.

[2] The zone of low-grade (greenschist facies) metamorphism.

late Precambrian). The highest grade part of the Conasauga study area may have experienced conditions very similar to those experienced in the Walden Creek Group rocks exposed in Ocoee Gorge.

Near the low-grade edge of the diagenetic zone the phyllosilicates are reported to be predominantly illite and mixed-layer illite/smectite, with smaller amounts of chlorite, kaolinite, and detrital muscovite and biotite. As the degree of diagenesis increases, phengite, apparently formed from detrital biotite, and diagenetic white mica[a] appear. Near the boundary between the diagenetic zone and the anchizone, chlorite porphyroblasts appear, some containing intergrowths of biotite. An incipient mesoscopic cleavage also appears near the this same boundary. As metamorphic grade rises, these porphyroblasts are gradually replaced by fine-grained phengite and muscovite.

Weaver et al. noted that within the anchizone, the phyllosilicates are mostly illite, phengite, and white mica, with lesser chlorite and minor mixed-layer illite/smectite, comprising about 5 percent smectite. Detrital biotite and paragonite are common near the lower grade boundary of the anchizone, but appear to be gradually

---

[a] The distinction Weaver et al. (1984) make between phengite and white mica in the diagenetic zone and anchizone is apparently based on color rather than chemical analyses. They report that the phengite in the diagenetic zone is green.

replaced at higher grade by phengite and/or white mica. Porphyroblasts of pure chlorite or of chlorite intergrown with phengite or white mica are common throughout the anchizone.

Near the boundary between the anchizone and the epizone, well-developed slaty cleavage appears and white mica becomes more common than green phengite. Weaver et al. noted that this white mica may be a phengite with less iron or a different ferric/ferrous ratio than the green phengite. At the anchizone/epizone boundary, they observed closely spaced P domains that they suggested form by the recrystallization of dissolved material that has migrated from neighboring Q domains. This is an interesting idea that is the inverse of that suggested by many slaty cleavage workers, the idea that P domains form by passive concentration as soluble material in them dissolves and moves into Q domains.

Within the epizone, chlorite decreases in abundance, whereas phengite increases. The chlorite that is present in the epizone tends to be Mg-rich, and is thought to have replaced quartz and calcite. Chlorite porphyroblasts, as well as porphyroblasts of mixed phyllosilicate mineralogy, have nearly disappeared in this zone, apparently replaced by phengite.

Weaver et al. (1984) have, in addition to describing the above petrographic trends, systematically measured

several parameters derived from X-Ray diffraction (XRD) patterns and related to the crystal chemical evolution of illite to mica. They found that both the Kubler and the Weaver Indices[4] show increasing "illite crystallinity" toward higher metamorphic grade. They noted, however, that values obtained for both indices are strongly influenced by the grain-size fraction used for measurement. The Kubler Index values given for the boundaries between the diagenetic zone and the anchizone and between the anchizone and the epizone are 0.42 and 0.25 °2θ CuK_{α}, respectively.

Using XRD peak-height ratios 3.74 A/2.58 A and 2.80 A/ 2.58 Å to estimate the relative amounts of 2 M and 1 M_d mica polytypes, Weaver et al. found that the conversion of 1 M_d to 2 M takes place almost entirely within the anchizone, and that conversion illite/smectite does not begin until fewer than 10 percent expanded layers are present. The position of the illite (060) peak in °2θ CuK_{α}, and the ratio of (002)/(001), both of which may both be related to Fe or (Fe + Mg) content, were found to

---

[4] The Kubler or crystallinity index is a measurement made on X-Ray diffraction patterns of oriented samples of illite or white mica. It is the FWHM, or the full width at half maximum height of the 10 Å peak, and has traditionally been recorded in mm. Kubler has suggested that 2θ is a more reproducible measurement, the mm measurement being more easily affected by such measuring system variables as chart speed.

The Weaver Index or sharpness ratio is the height of the (001) illite peak at 10.5 Å compared to the height of same peak at its apex near 10 Å. For a review of various crystallinity indices see Weaver et al. (1984).

generally increase through the anchizone, but then decrease slightly in the epizone. The presence of detrital micas in the diagenetic zone and anchizone increases the variability of these measurements and makes the interpretation of these parameters somewhat difficult.

Studying the distribution of chlorite within the Conasauga Weaver et al. found that chlorite content is at a maximum near the middle of the study area. They first saw abundant chlorite near the boundary of the diagenetic zone and the anchizone. Chlorite's appearance is very abrupt, but its disappearance is gradual as grade increases. Apparently as the degree of metamorphism increases chlorite is replaced by (green) phengite and white mica.

Weaver et al. further noted that in XRD patterns, chlorite exhibits a trend in the width at half maximum height (FWHM) for the 7 Å peak (chlorite (002)). This parameter decreases from the point where chlorite first appears in the diagenetic zone, through the anchizone, to the anchizone-epizone boundary; within the higher grade epizone the trend apparently reverses. They noted, however, that most of the chlorite in the epizone samples was somewhat weathered, suggesting that peak width for these grains may be a function of weathering rather than of metamorphism.

Chlorite composition is reported to be strongly dependent on bulk composition of the rock. Using

measurements of (060) peak position and wet chemical analyses they did, however, find a slight trend in chlorite composition with increasing grade. Both Fe and Mg increased up to about the beginning of the epizone. Concurrently, the ratio Fe/(Fe + Mg) decreased. Qualitative energy dispersive X-Ray analyses (EDXA) also indicate a steady decrease in Fe to Mg ratios in chlorite from the first appearance of chlorite in the diagenetic zone into the epizone. They suggest that this trend may be due to preferential dissolution of Fe-rich chlorite to form phengite and pyrite. They also noted that in the anchizone there was some evidence of two different chlorite populations, one being the Fe-rich chlorite undergoing dissolution and the other the Mg-rich "tectonic" chlorite found as vein fillings and overgrowths.

Based on the various types of information Weaver et al. collected on the changes undergone by phyllosilicates during the shale-slate transition, they plotted stability ranges for the phyllosilicates found in the Conasauga shale (Fig. 7). Some of the specific changes they noted in white micas and chlorites are summarized in Table 2.

In a study of phyllosilicate intergrowths using backscattered electron microscopy, White et al. (1985) analyzed grains from a variety of clastic sedimentary and metasedimentary rocks. Unlike most of the other studies reviewed here White et al. did not study rocks from one

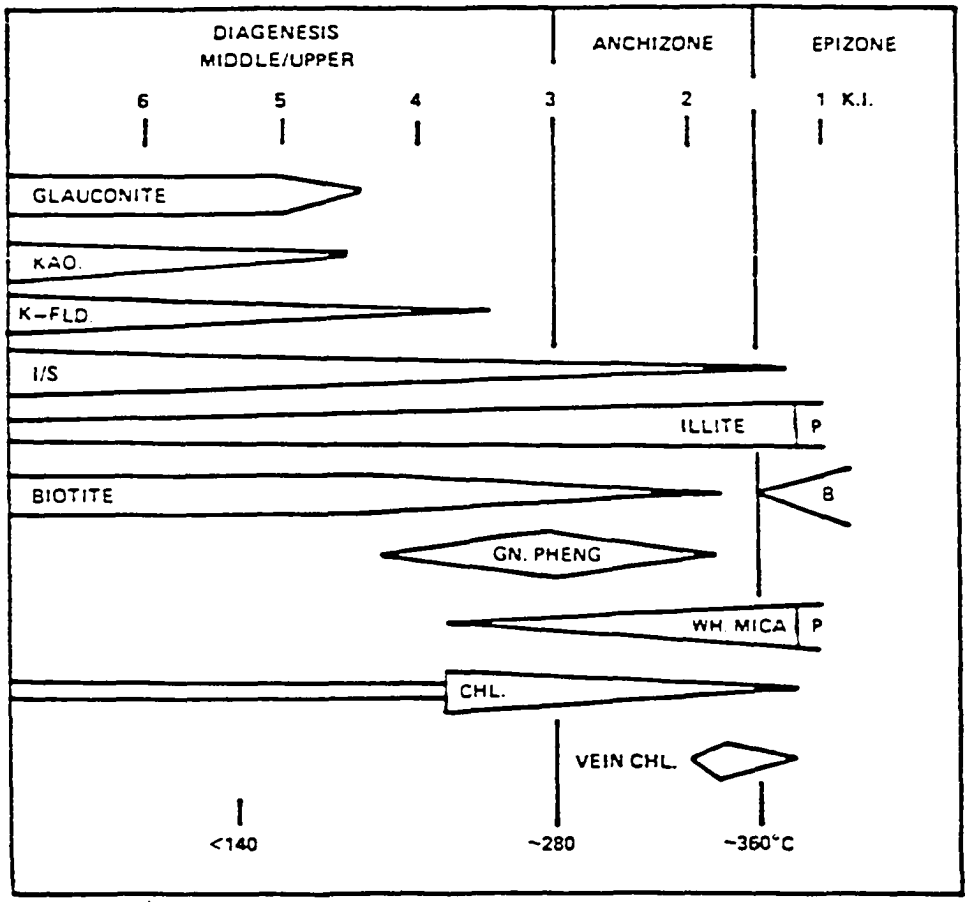

Figure 7. Stability ranges for phyllosilicates found in the Conasauga shale (from Weaver et al., 1984).

Table 2. Summary of some changes in white mica and chlorite reported by Weaver et al. (1984).

	Diagenesis		Anchizone		Epizone	
Kubler Index ($°2\theta CuK_\alpha$)		0.42			0.25	
(002)/(001) mica	0.2	0.34		0.47		0.42
2M/(2M+1Md)		0.0			1.0	
(060) value mica		1.499			1.499-1.510	
7A FWHM (mm)		1.4			1.2	
Fe/Mg ratio chlorite	1.4	1.4			0.7	0.5
Al^{IV} chlorite	0.60	0.85		1.05		

particular prograde sequence, but instead compared rocks of various grades and grain-sizes from a variety of locales. The non-metamorphic rocks typically contained intergrowths of illite and chlorite, with or without kaolinite, and metamorphic rocks had intergrowths of phengite and chlorite. In general, the higher grade the rock, the more likely the intergrowths are coherent. Increase in coherency is accompanied by an increase in crystallinity index. White et al. also observed a clear trend in white mica composition with increasing metamorphic grade. As grade increased white mica trended toward phengite, showing increasing K/Si. The compositions of individual mica grains within anchizone samples, however, varied considerably. White et al. found that chlorites do not display well defined compositional trends related to metamorphic grade, but in general range from Mg-rich to Fe-rich ripidolite in graywacke, and cluster in the Fe-rich ripidolite range in schist.

Hunziker et al. (1986) studied the crystal chemical evolution of illite to muscovite in the diagenetic to epimetamorphic transition that occurs in fine-grained sedimentary rocks between the Alpine foreland and the Helvetic Zone of the Central Alps. They used a variety of analytical techniques to characterize this evolution, including X-Ray diffraction, electron microprobe, and wet chemistry. Changes they noted include (1) transformation

of the low temperature $1M_d$ polytype to the high temperature $2M_1$ polytype (completed by the upper anchizone), (2) increases in K_2O from 6-8 weight percent in the diagenetic zone to 8.5-10 weight percent in the anchizone to 10-11.5 weight percent in the epizone, (3) an increase in the total layer negative charge form about 1.2 to about 2.0, (4) an increase in illite crystallinity, and (5) a decrease in chemical variation within the mica population, ascribed to the failure of detrital muscovite to survive above the anchizone/epizone boundary. Stable isotope data showed no differences in $\delta^{18}O$ and δD values for the diagenetic and metamorphic grains. From all of these data Hunziker et al. concluded that the transformation from illite to muscovite involves a restructuring of the lattice without breaking tetrahedral or octahedral bonds or changing hydroxyl radicals.

The diagenetic and metamorphic changes in chlorite have been studied by Hayes (1970) and Curtis et al. (1984, 1985). Hayes (1970) used XRD studies to characterize chlorite polytypes in a variety of environments. He found the diagenetic to low-grade metamorphic sequence of polytypes to be I_{bd} --> Ib(β=97°) --> Ib(β=90°). During low-grade metamorphism (around 150-200°C) the polytype is then converted to the IIb polytype. He noted, however, that the presence of mica makes it difficult to distinguish the chlorite polytype.

Curtis et al. (1984, 1985) conducted analytical transmission electron microscopy on authigenic chlorites in a sandstone. They found the Ib(β=90°) polytype to be stable during deep burial. Further, they noted that the composition of these diagenetic grains tends toward the Fe-rich end of the Fe-Mg substitutional range. The differences between these grains and metamorphic grains are reported to be in polytype (they confirmed Hayes' polytype sequence) and composition. Metamorphic grains were found to be richer in Mg and Al^{IV}.

In summary, crystal chemical changes reported to occur in phyllosilicates during diagenesis and metamorphism are more clearly established for the illite to muscovite or illite to phengite transition than for transitions that occur in chlorites. The changes that occur during the development of metamorphic micas include increases in K, total Al, Al^{IV}, total negative layer charge, illite "crystallinity", and the ratio (002)/(001) in XRD analyses. In addition, both water content and evidence of interlayering with other species decrease, while the stable polytype changes from $1M_d$ to 2M. The changes reported for chlorite include a change in polytype from Ib to IIb, increasing Mg/Fe, and increasing Al^{IV}.

Review of Selected Studies on the Relationship of Metamorphic Micas to Fabric

In addition to studies that relate compositional and structural changes in phyllosilicates to regional scale diagenesis and/or metamorphism, several studies have examined phyllosilicates in particular microstructural sites or orientations within a low-grade metamorphic fabric. These studies suggest that the metamorphic evolution of phyllosilicates is related not only to regional scale metamorphic (or diagenetic) conditions, but to other factors that allow different populations of grains to exist within microns of one another.

Knipe (1979), in an analytical electron microscopy study of phyllosilicates in a slate from Rhosneigr, North Wales, characterized the chemical composition of phyllosilicate grains found in each of three microstructural sites: (1) in P domains, (2) in Q domains, and (3) along domain boundaries (Fig. 8). In general he found illite (low K content for muscovite) in Q domains, phengite in P domains, and illite and phengite along the domain boundaries. Along domain boundaries, Knipe also found some very low K grains that he interpreted to be sites of preferential weathering. The Q domain mica grains he analyzed are more variable in composition than his P domain mica grains. Large, bent grains oriented so that one limb is in a P domain and one limb is in a Q domain he

Figure 8. (1) a-d illustrate the range in Knipe's (1979) analyses of individual, undeformed grains within the Rhosneigr Slate. I is illite, M is muscovite, and P is phengite; all three compositions are from Bailey (1984). R is a ripidolite from the intermediate part of the ripidolite range given by Deer et al. (1975) (see Fig. 26). (2) Knipe's analyses of 67 Q domain grains. (3) Knipe's analyses of 75 P domain grains. (4) Knipe's analyses of 39 grains from along domain boundaries.
A = Al_2O_3/SiO_2, F = $(FeO+MgO)/SiO_2$, K = K_2O/SiO_2, N = Na_2O/SiO_2. A + F + (K or N) = 100.
Total iron was calculated as FeO.

1.

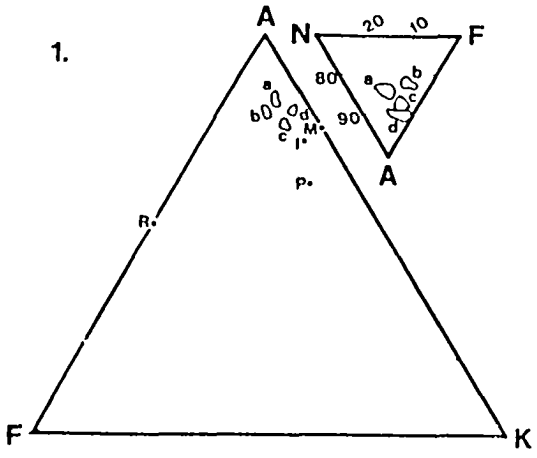

2.

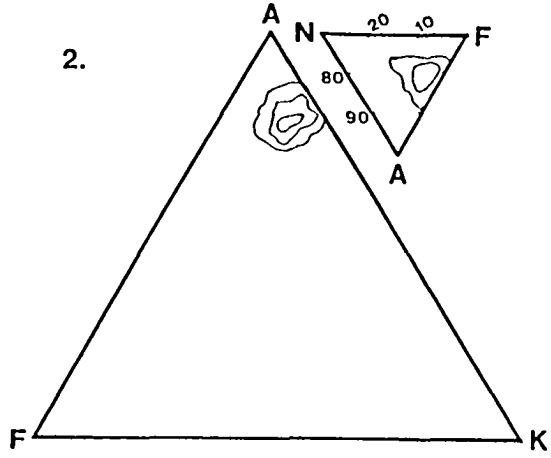

3.

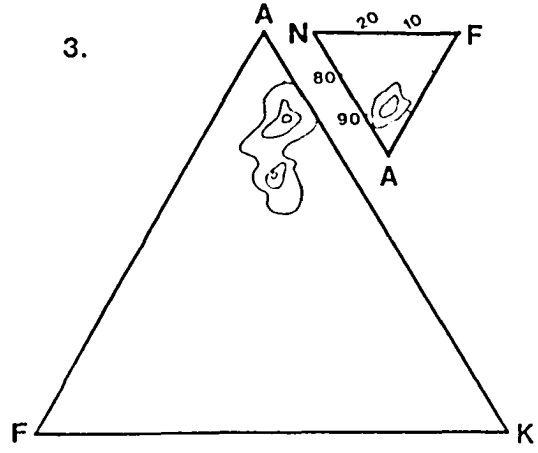

4.

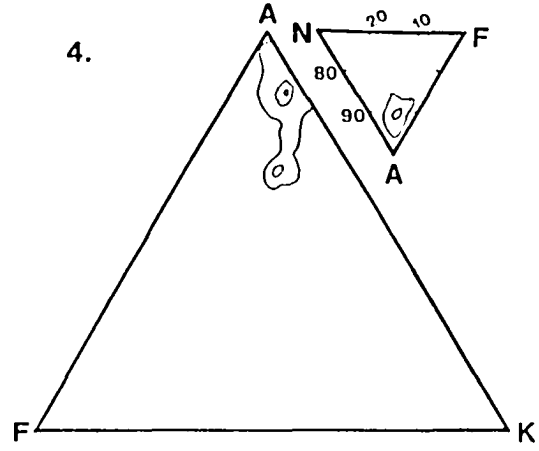

found actually change in composition from one domain to the other; they increase in K from outside the P domain to inside it. The composition of chlorite found in all three structural sites was less variable than that of mica, but did show a slightly higher Fe content in Q domains than in P domains. Compared to regional studies such as Hunziker et al. (1985) and Weaver et al. (1984), Knipe's P domain grains have crystal chemical characteristics of a higher metamorphic grade than his Q domain grains have.

In a study of the development of metamorphic layering in Ordovician metasediments from Clunes, Australia, Stephens et al. (1979) also compared mica compositions for grains found in P and Q domains. They found more distinctive differences in mica compositions when they compared detrital to metamorphic micas than when they compared P domain to Q domain micas. Detrital micas were identified as being coarser-grained, more likely to exhibit undulose extinction, and having smaller aspect ratios than the grains identified as metamorphic. In general, detrital micas were higher in K and Al, but lower in Si, Fe, and Mg than the metamorphic micas: the detrital micas tend to be muscovite and the metamorphic micas tend to be K-poor phengite. Stephens et al. found few differences between the P and Q domain metamorphic micas, but did find that P domains micas are more variable chemically and have a tendency to be slightly more phengitic than Q domain micas.

In comparing chlorites of the P and Q domains, Stephens et al. found clearer differences than were reported by Knipe (1979). In general, they found that P domain chlorite is more variable in composition and has a higher $Al^{VI}/(Fe + Mg)$ ratio than Q domain chlorites. These assessments of both mica and chlorite compositions appear to be based on only a few analyses.

White and Johnston (1981), in an high voltage electron microscopy (HVEM) and scanning transmission electron microscopy (STEM) study of an Ordovician slate from the S.E. Australian slate belt (near the Clunes study area of Stephens et al.), determined that mica within P domains is more phengitic than mica in Q domains. P domain chlorite was found to be richer in Al and poorer in Fe than chlorite in Q domains. They also noted that chlorite was more common in Q domains than in P domains and that the differences between P and Q domain phyllosilicates do not correlate with the size or spacing of P domains. Use of the STEM permitted analysis of P domains too narrow to be resolved with other techniques, P domains that might otherwise have been incorporated into Q domain analyses.

Lee et al. (1984, 1986) examined phyllosilicates from an outcrop at Lehigh Gap, Pennsylvania, where mudstone grades into slate over a distance of about 100 meters. Slaty cleavage develops gradually over this interval and is well-developed in the slate. Most phyllosilicates are

oriented parallel to bedding in the mudstone and parallel to cleavage in the slate. At some intermediate point along the outcrop they undergo an abrupt and apparently discontinuous reorientation. In other words, most grains are either parallel to bedding or to cleavage; few grains are in intermediate orientations, even near the point where reorientation takes place. Lee et al. found, as did Holeywell and Tullis (1976), who studied the same outcrop, that the point along the outcrop where this change in orientation occurs is different for illite than for chlorite; illite becomes reoriented a little closer to the mudstone end of the outcrop.

Lee et al. used transmission electron microscopy (TEM) and analytical electron microscopy (AEM) to obtain lattice fringe images, selected area diffraction patterns, and high resolution energy dispersive X-Ray analyses. AEM analyses of illites from mudstone, slate, and intermediate samples all showed considerable Mg and Fe, but unlike other studies, no systematic trend was found in the concentrations of these elements. Lee et al. did find large increases in the K and Al content of illites from mudstone to intermediate samples to slate. They also noted that in intermediate samples (where there were many grains in each of the two common orientations, parallel to cleavage and parallel to bedding) there was a tendency for the grains oriented parallel to cleavage to have higher K

and Al contents than those of grains oriented parallel to bedding.

Lee et al. found interlayering of 10 A mica and 14 A chlorite to be common in mudstone, but virtually absent in slate. The slate instead shows semicoherent intergrowths of packets of pure chlorite and illite, each thousands of angstroms thick. Interlayering of mica with kaolinite is also present, if uncommon, throughout the outcrop, but is much rarer in slate than in mudstone. Other transitions they noted include the replacement of the 1M polytype of illite in the mudstone by the 2M polytype in the slate. Lee et al. used the sharpness ratio to evaluate the crystallinity of illite, but found no systematic trend in this parameter. There were marked changes in the degree of crystal perfection from one end of the outcrop to the other. In general, grains from the slate samples showed fewer imperfections, and were more likely to have coherent or semi-coherent grain boundaries than grains from the mudstone.

CHAPTER V

SLATY CLEAVAGE IN THE SANDSUCK FORMATION

The slaty cleavage seen in the Walden Creek Group's Sandsuck Formation in western Ocoee Gorge can be described on two scales, the mesoscopic and microscopic, and in this chapter those observations are organized in terms of those two.

Mesoscopic Description

The best exposures of well-developed slaty cleavage in Ocoee Gorge are present along a 1000 m-long stretch between Greasy Creek and Madden's Branch, near the western end of the gorge. Here a 130 m-thick section of chlorite-grade interbedded phyllites and metasiltstones of the Walden Creek Group's Sandsuck Formation is folded on a mesoscopic scale into upright, asymmetrical, open folds with a westward vergence. An axial planar foliation accompanies these folds throughout the region, and in the phyllite layers takes the form of a well-developed slaty cleavage (Fig. 9).

Lithologically the outcrop is dominated by interbedded gray-green phyllites and siltstones (Fig. 10), interrupted by isolated layers of silty dolomite or calcareous quartzite. Typically these isolated dolomite or quartzite layers are unfoliated (Fig. 11). They may, however, be interrupted by foliation-parallel fingers of phyllite and

Figure 9. Outcrop of Sandsuck Formation approximately 3 miles east of Sylco Creek Fault along Ocoee Gorge. Axial planar slaty cleavage is slightly refracted as it passes between phyllite and siltstone. Tension gashes near the center of the photograph are filled with calcite.

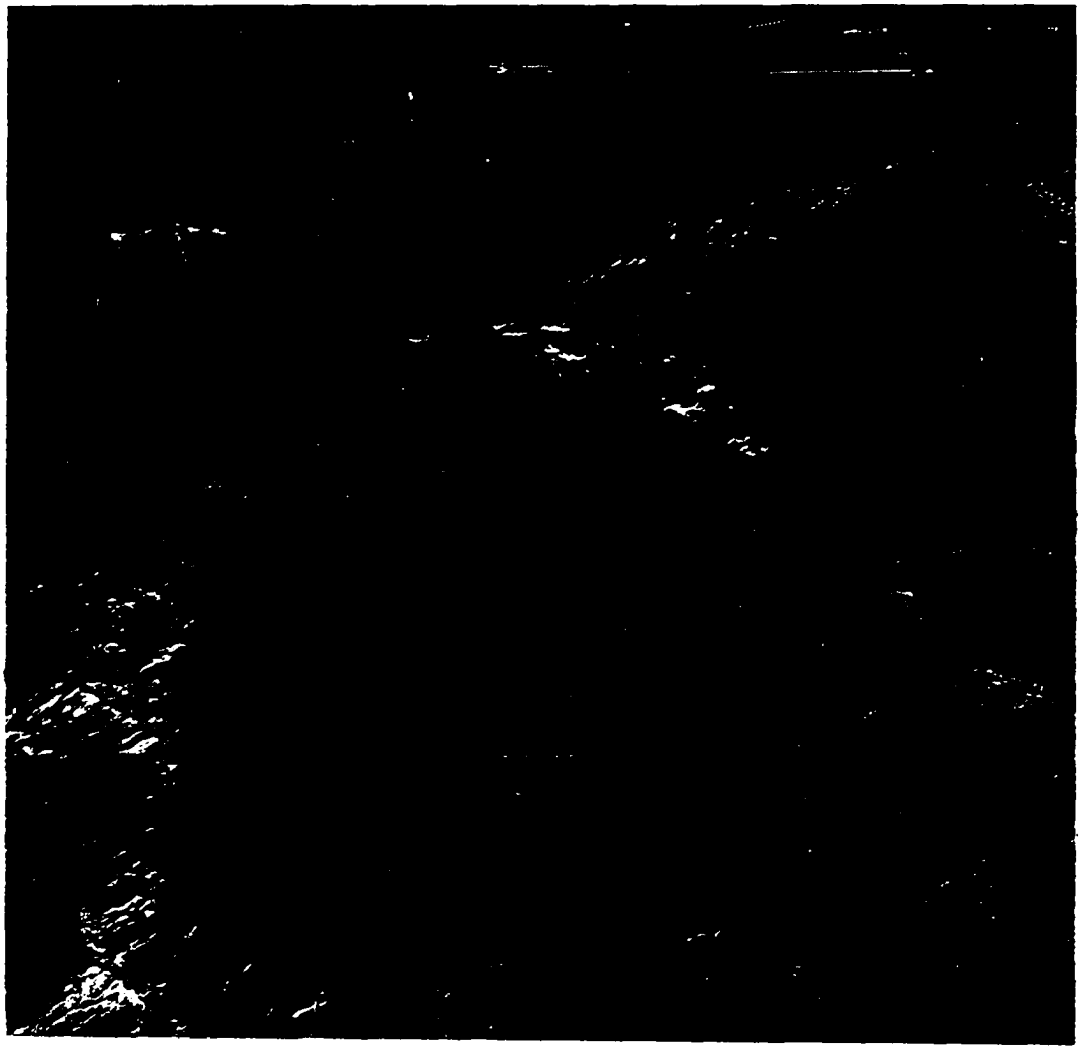

Figure 10. Interbedded phyllite and siltstone layers in Sandsuck Formation. Coin is 1.8 cm in diameter.

Figure 11. Carbonate-rich beds disrupting slaty cleavage in the Sandsuck Formation. Outcrop is immediately east of Sylco Creek Fault. Pencil is 14 cm long.

in places have formed boudinage in which well-foliated phyllite separates the segments of a dolomite or quartzite layer (Fig. 12).

The phyllite layers are typically between 0.5 and 15 cm thick, whereas the metasiltstone layers are between 0.5 and 5 cm thick. In general the siltstone layers are buff, and phyllite layers are gray-green, weathering red. Within the phyllite and siltstone interbeds, compositional layering, or domainal fabric, exists on a scale finer than that of bedding. This secondary layering crosscuts bedding and is parallel to the mesoscopic axial planar foliation. On weathered surfaces it has a topographic expression, "ridges" and "valleys", corresponding to the weathering resistance of the layers (Figs. 9, 10, 11, 12). The secondary layering varies considerably in continuity, and individual layers may be traced lengthwise for distances varying from less than a millimeter to tens of centimeters. In general, the secondary layering is better developed in phyllite layers than in siltstone layers.

Figure 12. Boudinage of dolomitic siltstone. Intervening phyllite displays well-developed slaty cleavage. Outcrop is about 2 miles east of Sylco Creek Fault along Ocoee Gorge.

Microscopic Description

In thin section, the phyllite layers are seen to contain fine-grained mica, chlorite, quartz, and albite, and in some layers, carbonate. In addition, pyrite and hematite are present as scattered blebs and fracture fillings. The mineralogy of the siltstone layers is similar to that of the phyllite layers, but they contain more quartz, carbonate, and albite and less mica and chlorite than do the phyllite layers. In both phyllite and siltstone layers, the small size of most of the phyllosilicate grains makes it difficult to identify them optically. The smaller grains appear to be either chlorite or muscovite, whereas larger grains appear to be nearly all muscovite. There are, however, a few large chlorite porphyroblasts (Fig. 13). Labotka (1971) reported that XRD analysis of the less than 2-micron fraction in the phyllite layers revealed illite, chlorite, and quartz. Holcombe (1973) reported that two varieties of chlorite are present: a fine-grained chlorite, probably prochlorite (ripidolite), and larger, isolated grains of penninite.

Mineralogically, the secondary layering is defined by thin zones enriched in phyllosilicates, particularly white mica, relative to surrounding material. These phyllosilicate-rich zones, or P domains, are an integral part of the cleavage fabric. Intervening Q domains are relatively rich in quartz and albite.

Figure 13. Chlorite porphyroblast in a siltstone layer. The porphyroblast is about 1 mm across.

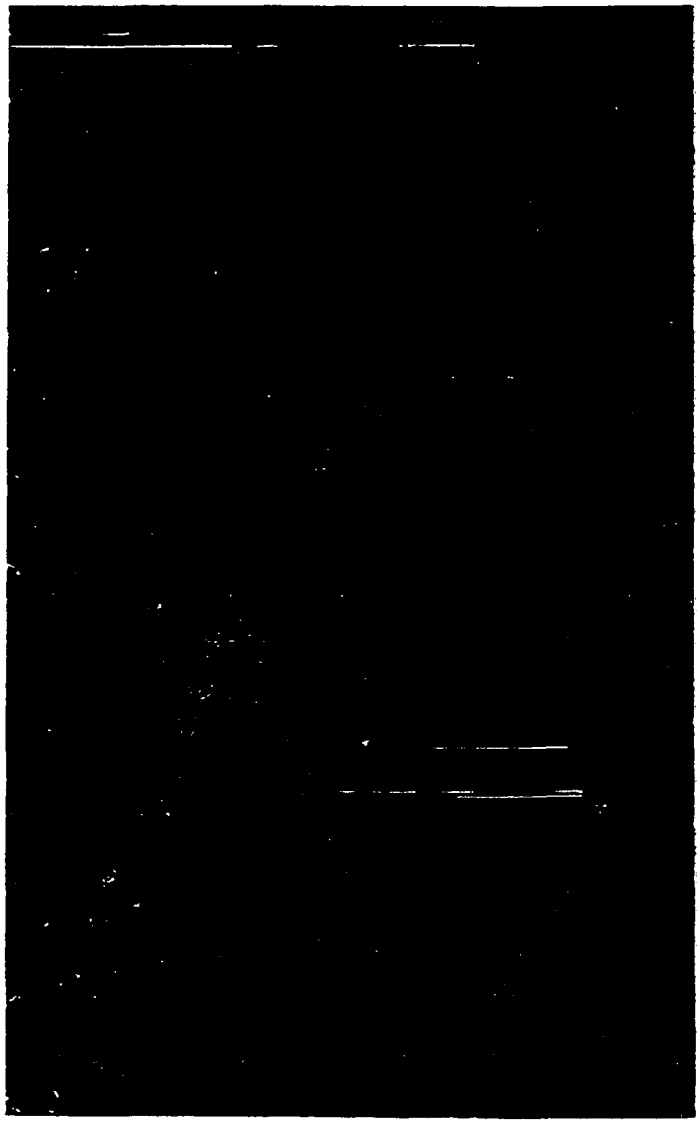

P domains are less continuous than Q domains and are better developed in phyllite than in siltstone. In many places P domains fade and disappear part way across a siltstone layer, commonly tapering or branching first. P domains tend to be best developed near the hinges of small-scale folds (five to ten centimeters in wavelength). In general, P domains do not penetrate dolomite or quartzite layers. Well-developed P domains are typically less than one millimeter thick and have an average spacing of about one to two mm, although there is considerable variation in both width and spacing from bed to bed.

P and Q domains crosscutting the interbedded primary layers sub-divide the rock into four types of microstructural sub-domains (Figs. 14a and 14b):

1. Within a phyllite layer and a P domain.
2. Within a phyllite layer and a Q domain.
3. Within a siltstone layer and a P domain.
4. Within a siltstone layer and a Q domain.

In some places the distinctions between these four sub-domain types become rather arbitrary, as the sub-domains grade into one another. In other places there are well defined narrow boundaries separating sub-domains.

Each of these sub-domains may be characterized in terms of mineralogy, composition, grainsize, grainshape of particular phases, preferred orientation of phyllosilicates, preferred dimensional orientation of

Figure 14. Negative prints of a thin section. Figure a. was printed with the thin section enclosed in a "pocket polarizer". Sub-domain types are labelled in with white numbers in Figure a. Scale = 3x.

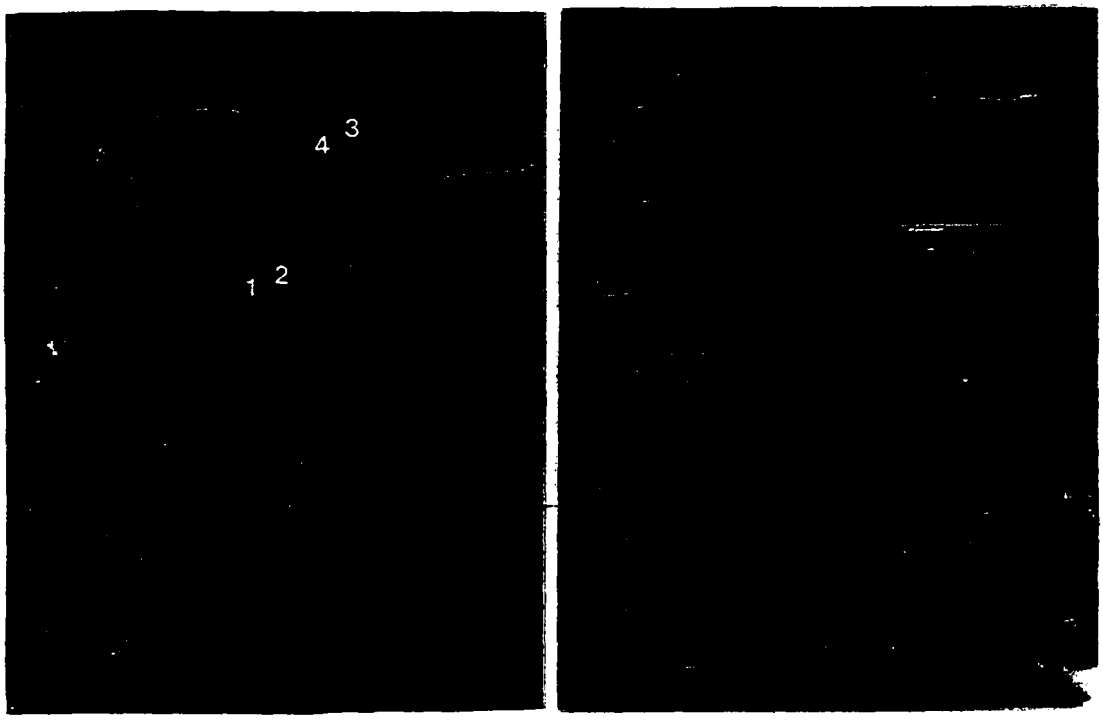

inequant quartz and albite grains, concentrations of opaque minerals, evidence of grainscale deformation, evidence of grain boundary corrosion or overgrowths, size and shape of the sub-domain, and lengthwise continuity and termination of the sub-domain.

Sub-Domain Type 1: phyllite layer, P domain

In sub-domain type 1 (within a phyllite layer and a P domain) white mica is the most abundant mineral, although there may also be quartz, albite, chlorite, carbonates, and opaques present. The mica grains are typically very elongate in cross-sections perpendicular to (001), roughly uniform in size, and exhibit a strong preferred orientation. Most grains cluster in orientations in which their basal cleavage is roughly parallel to the domain boundaries, and hence to the mesoscopic foliation of the rock. Within phyllite layers and at the boundaries between P domains and Q domains the preferred orientation of the mica shifts abruptly from the cleavage-parallel orientation of the P domain to the bedding-plane parallel orientation of the Q domain.

The phyllosilicates in type 1 sub-domains are commonly 100 percent or more longer than, but no wider than those in Q domains. The elongate white mica grains of sub-domain 1 show no signs of internal deformation and have smooth grain boundaries. The rare, larger mica grains present in type 1 sub-domains tend have lower aspect ratios than the finer

grained micas, typically between 1:1 and 1:4, as compared to 1:10 or higher for the smaller grains. These larger grains may show undulose extinction, kinking, and ragged grain boundaries, and are typically oriented at a high angle to domain boundaries.

A few isolated quartz and albite grains are found in type 1 sub-domains, but they are smaller than quartz and albite grains in neighboring Q domains and show little evidence of internal deformation. Many of these quartz and albite grains are equant, and those that are not show no obvious dimensional preferred orientation. Some non-equant quartz and albite grains may be aligned parallel to the basal cleavages of the aligned mica grains, although quartz and albite grains lying perpendicular to the aligned mica grains are more common. Some quartz and albite grains have smooth, planar grain boundaries on one or two sides, where the grain abuts a train of mica grains. Other quartz and albite grains have irregular grain boundaries that appear to be intergrown with clots of fine-grained mica. Type 1 sub-domains may contain thin, discontinuous foliation-parallel lenses of quartz and albite (Fig. 15). The grains in these lenses resemble in size and shape those found in Q domains. Typically these quartz and albite grains are rimmed with fine-grained mica. The mica grains in these rims tend to parallel the grain boundaries of the coarser quartz and albite.

Figure 15. Photomicrograph of quartz lens in a P domain. Scale = 40x.

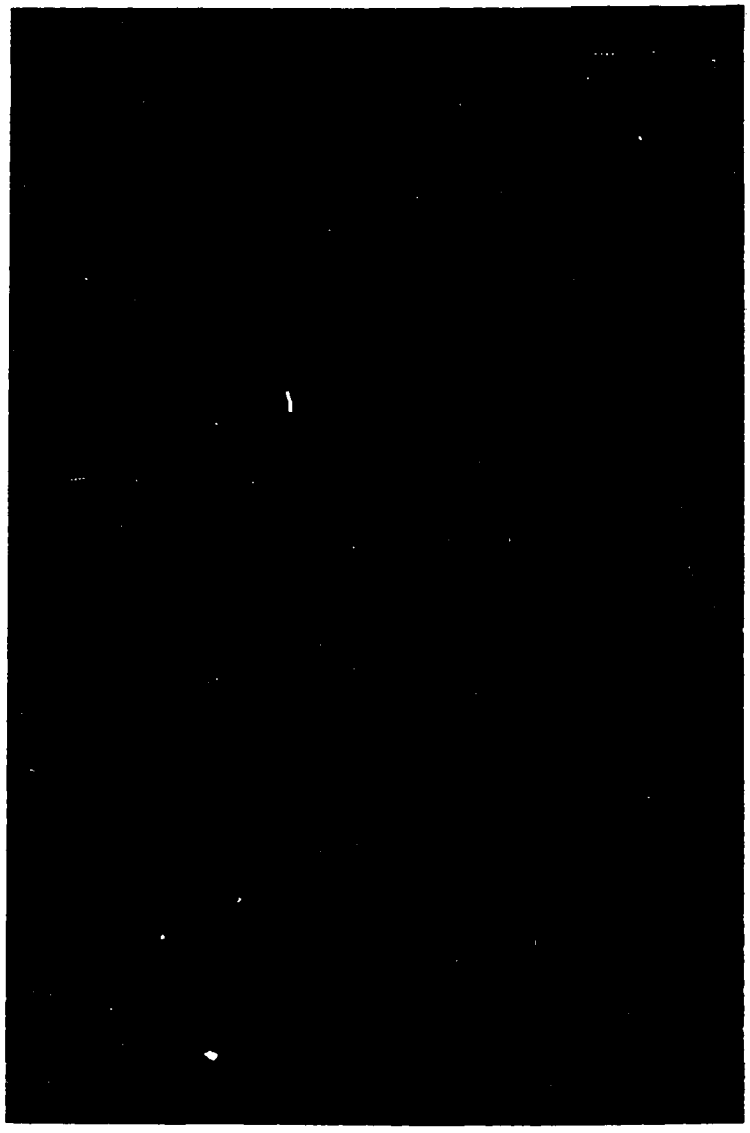

Optically, two types of chlorite grains can be distinguished in type 1 sub-domains, fine-grained chlorite mingled with the fine-grained white mica, and rare, deformed porphyroblasts (Fig. 13) that are much larger than domains are thick. The fine-grained chlorite is typically finer than the mica and to the eye seems somewhat less likely to be in the cleavage-parallel preferred orientation.

Type 1 sub-domains are usually tabular, although some change in width or course may occur, apparently affected by the position of the sub-domain relative to very small folds. These sub-domains may be parallel to one another or may fan slightly around the small folds. Moreover they are persistant, i.e. P domains do not normally die out within phyllite layers (Fig. 16).

Sub-Domain Type 2: phyllite layer, Q domain

Type 2 Sub-domains (within a phyllite layer and a Q domain) differ from type 1 in both size and orientation of phyllosilicate grains, as well as in mineralogy. Here most phyllosilicate grains are roughly bedding-parallel, but there is greater variation in orientation than in type 1 sub-domains. There is also a second, less prominent preferred orientation parallel to the mesoscopic foliation. The small, isolated, grains found in this second preferred orientation display needle-shaped cross-sections in thin sections cut normal to both bedding and the mesoscopic

Figure 16. Negative prints of a thin section. Figure a. was printed with the thin section enclosed in a "pocket polarizer". The domainal fabric seen here is more pervasive than that in Figure 14. Sub-domain types are labelled with white numbers. Scale = 3x.

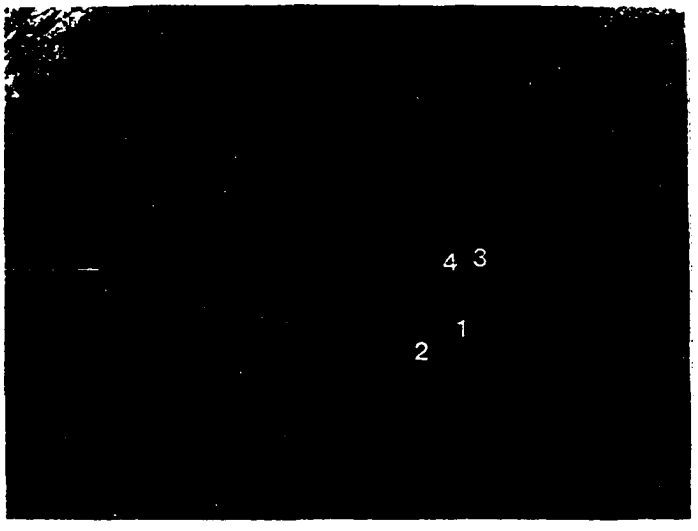

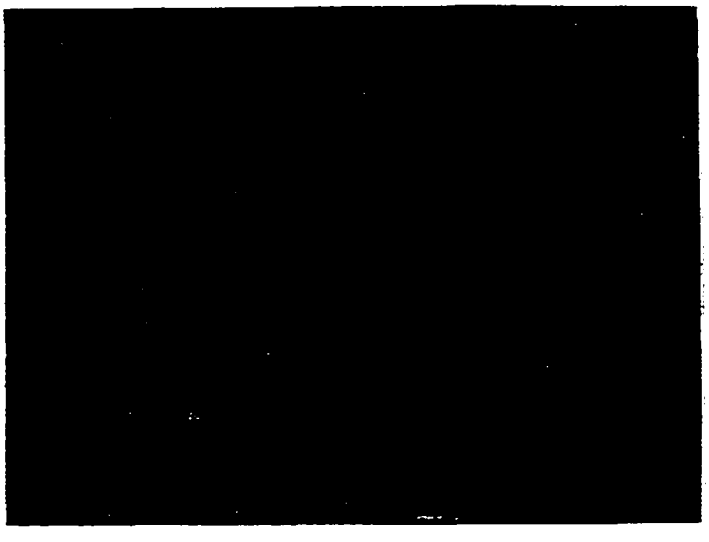

foliation.

Grain-size is much more variable for phyllosilicate grains in type 2 sub-domains than for those in type 1 sub-domains. Some grains are too small to be optically resolved as individuals, except under an oil immersion objective. The number of large, detrital mica grains is greater here than in type 1 sub-domains. They are likely to be deformed or have corroded boundaries and tend to be larger than the largest grains in type 1 sub-domains, but like the large type 1 grains, they have relatively small cross-sectional aspect ratios, typically between 1:1 and 4:1.

Chlorite makes up a greater proportion of the phyllosilicates in type 2 sub-domains than in type 1 sub-domains. Typically much of the chlorite occupies an ill-defined, bedding-parallel preferred orientation. In thin sections cut perpendicular both to the mesoscopic foliation and to bedding, most type 2 sub-domain micas are seen in cross-sections perpendicular to their basal cleavage, and are generally parallel to either bedding or foliation. In contrast, chlorite is much more likely to appear in other orientations, including (001) parallel to the cut surface (normal to foliation and bedding).

Quartz and albite are more abundant in type 2 sub-domains than in type 1, and the grains are typically slightly larger than type 1 grains. In general, they show

neither internal deformation nor corroded grain boundaries, although some large grains have both undulose extinction and ragged grain boundaries. As in type 1 sub-domains, but less commonly, quartz and albite grain boundaries may be smeared with very fine-grained mica (Fig. 17). Near, but within or partially within, the boundaries of some quartz grains, very small, isolated mica grains appear to have been imbedded in the quartz. Where quartz grain boundaries are cleanly defined, grain shape may be irregular, with oddly-shaped protuberances. In general there is no easily discerned geometric relationship between the orientation of these protuberances and either the foliation-parallel or bedding-parallel orientations.

The shapes of the type 2 sub-domains (Figs. 14, 16) reflect the shapes of the neighboring type 1 sub-domains; in layers where the type 1 sub-domains are tabular, the type 2 sub-domains occupy the tabular regions between them, and where the type 1 sub-domains widen, taper, or curve, the intervening type 2 sub-domains mirror them. Type 2 sub-domains may be thinner than neighboring type 1 sub-domains, but the thickest type 2 are considerably thicker than the thickest type 1.

Sub-Domain Type 3: siltstone layer, P domain

Type 3 sub-domains (within a siltstone layer and a P domain) are similar in mineralogy, but dissimilar in morphology to type 1 sub-domains. Sub-domain type 3 white

Figure 17. Photomicrograph showing fine-grained mica obscuring quartz and albite grain boundaries in a type 2 sub-domain. Scale = 50x

mica grains resemble those of sub-domain type 1; their (001) perpendicular cross-sections are elongate and roughly uniform in size. The preferred orientation of these mica grains is well-developed and usually parallel to the domain boundaries.

Within some type 3 sub-domains mica grains cluster in two preferred orientations. If the sub-domain contains little or no quartz, the two orientations are 10 to 15 degrees apart, but if much quartz is present the angle between them may increase to 60 degrees. Where quartz content is high, mica orientations become more diverse, with grains in anomalous orientations more common than elsewhere in type 3 sub-domains. In general, the mica grains that parallel domain boundaries have higher aspect ratios than grains in other orientations.

Where the siltstone layer hosting the sub-domain is thin, type 3 sub-domains are commonly refracted slightly, but return to the orientation of the mesoscopic foliation as they re-enter phyllite (Figs. 9 and 18). Where the host layer is relatively thick, type 3 sub-domains may fail to completely cross the siltstone layer, some penetrating only a short distance into the siltstone before disappearing (Fig. 19). Typically, type 3 sub-domains are thinner than the type 1 sub-domains to which they are connected (Fig. 16b). For a short distance (1 or 2 mm) after emerging from a phyllite layer type 3 sub-domains may be nearly as thick

Figure 18. Negative print of a thin section. Domainal fabric crosscuts bedding. Scale = 4x.

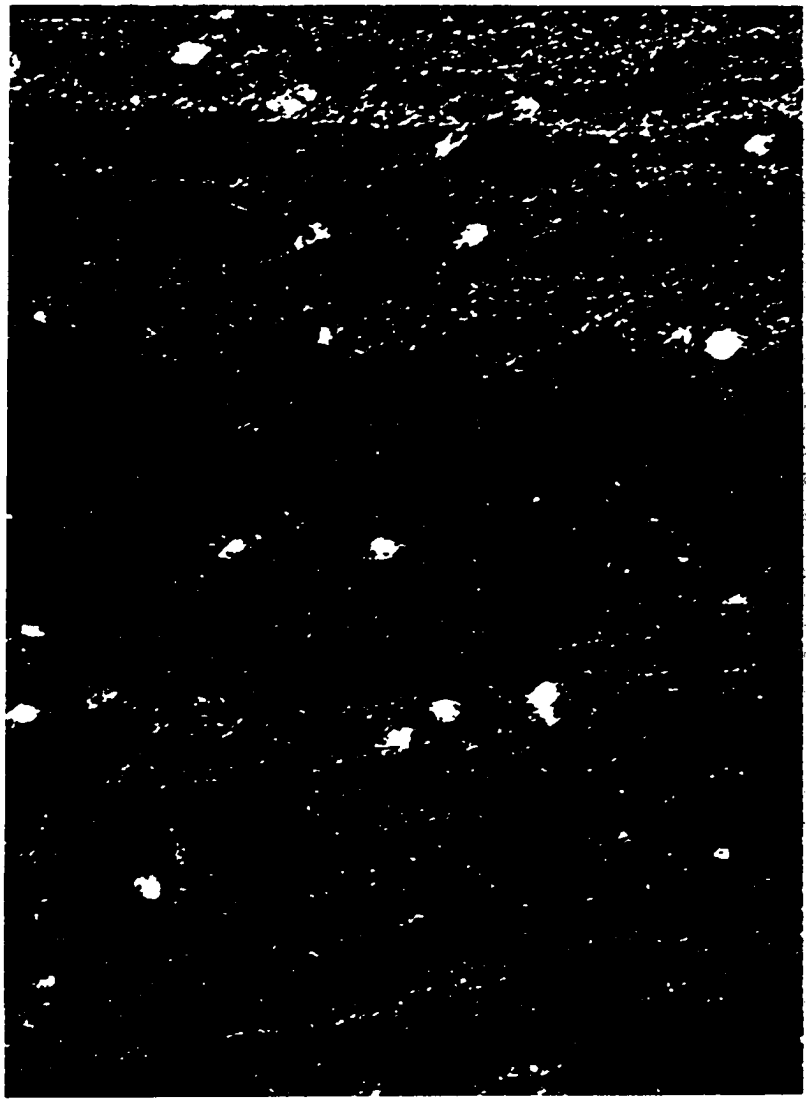

Figure 19. Negative print of a thin section. P domain failing to cross siltstone layer. Scale = 12x.

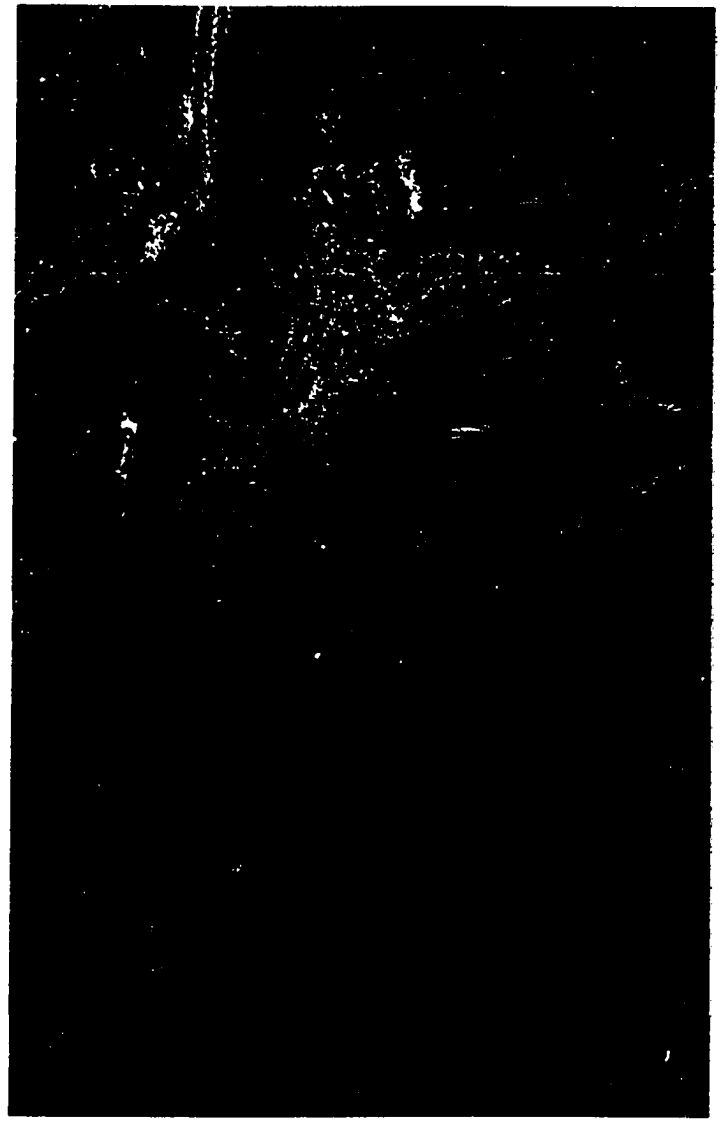

as the type 1 sub-domain to which they are connected, but they taper rapidly to a thickness about one quarter to one half that of the type 1 sub-domains to which they are connected. They then taper more gradually as they cross the siltstone layer, some succeeding in crossing the layer, and others branching and gradually fading away as the grains in them spread further apart.

A peculiarity of many type 3 sub-domains is that they bifurcate as they emerge from type 1 sub-domains, with two or more branches extending into a siltstone layer from the adjacent phyllite layer. One branch stays roughly parallel to the mesoscopic orientation of the foliation, whereas the other branch(es) may bend into an orientation as much as 60 degrees closer to the bedding-plane orientation than to the orientation of the mesoscopic foliation. Generally the bent branch becomes dendritic and fades within a few mm.

In many places, type 3 sub-domains that are continuous across siltstone layers make a sharp sideways step, near the middle of the siltstone layer, where they are thinnest (Fig. 20). Not uncommonly, a cluster of several type 3 sub-domains in a single siltstone layer will all show this morphology. Where several P domains show this morphology, the spacing between them on either side of the step tends to be about the same, but the domains on either side are not coplanar.

In some type 3 sub-domains, quartz and albite grains

Figure 20. Negative print of a thin section. This phyllite from near the contact between the Walden Creek Group and the Great Smoky Group around the middle of Ocoee Gorge has a second generation foliation overprinting an earlier domainal fabric. Scale = 5x.

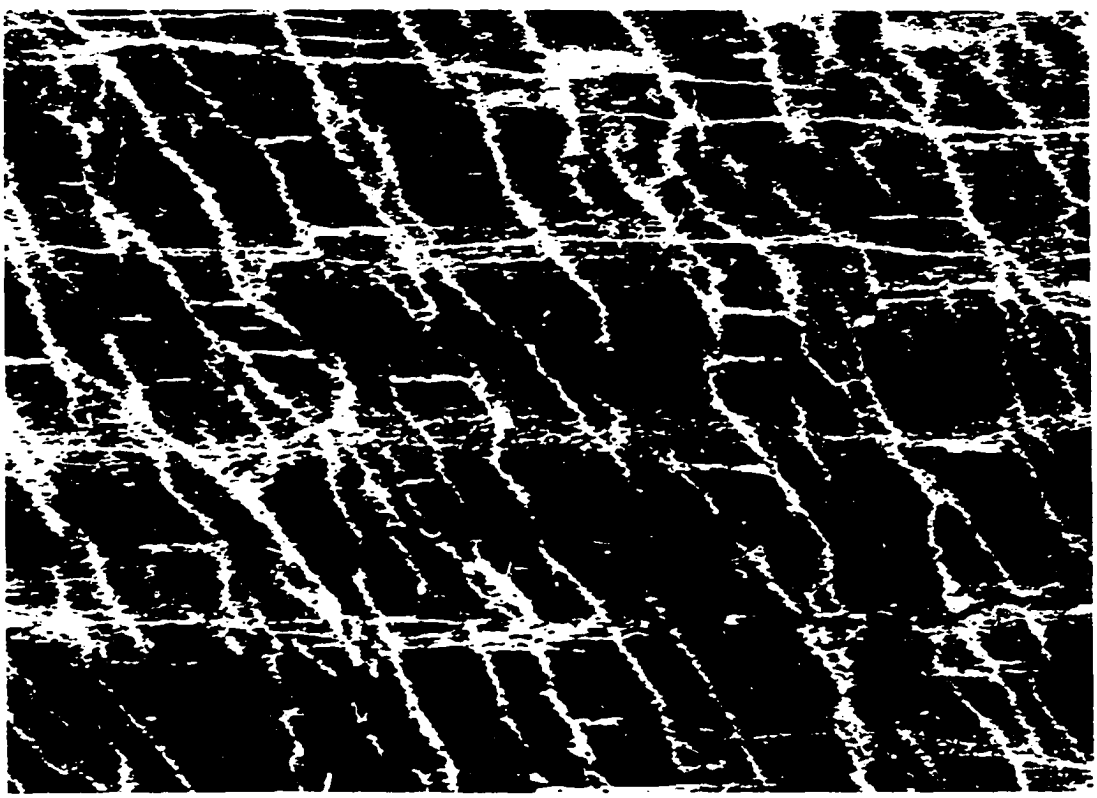

are fairly common and in others rare. Their abundance appears to be dependent on how diffuse the mica concentration is. Some P domains separate into many sub-parallel ramifications that fade out among the relatively coarse quartz and albite of the siltstone layer. When this is the case, quartz often has ragged grain boundaries, particularly perpendicular to foliation, that may be obscured by beards of very fine-grained mica. Commonly the quartz occurs in clusters of several grains or as thin, bedding-parallel lenses, through which the mica grains follow a fragmented, anastomosing route. These quartz grains may be somewhat elongated parallel to the cleavage orientation and typically are diamond-shaped, with mica grains flush against the flat sides of the diamonds. Where there are many of these diamond-shaped grains close together, mica is be present in two preferred orientations, orientations that are controlled by the parallel alignment of the sides of the diamond-shaped grains. In those parts of type 3 sub-domains where quartz and albite are relatively common, the distinction between type 3 and type 4 may become blurred and arbitrary (Fig. 21).

Sub-Domain Type 4: siltstone layer, Q domain

In type 4 sub-domains (within a siltstone layer and a Q domain) quartz, albite, carbonates, large mica and chlorite grains, and chlorite porphyroblasts are more common than in any of the other sub-domains. The mica

Figure 21. Photomicrograph. Scale = 40x.

grains are quite variable in size, shape, evidence of deformation, and orientation. They generally lie in one of three preferred orientations, one of these being bedding-parallel. The more common of the other two orientations, particularly for isolated mica grains far from P domains, is foliation-parallel. The third and least common preferred orientation is 30 to 60 degrees away from the mesoscopic foliation. Mica grains in this third orientation are usually present in strings or thin layers sandwiched between larger quartz grains. The orientation of these strings changes as they wind between individual quartz grains, following the curvature of the quartz grain boundaries. Where several mica grains are together in a type 4 sub-domain, they are usually bedding-parallel. Isolated mica grains that are fairly close to P domains are commonly in the same orientation as mica grains in those domains. In general, the type 4 sub-domain mica grains that lie near type 3 sub-domains are larger and have greater aspect ratios than mica grains further away from type 3 sub-domains, or than mica grains in other, anomalous orientations.

Quartz grains in type 4 sub-domains generally are larger than those found in any of the other sub-domains, and are commonly equant, or shaped like slightly elongated diamonds, although some are very irregularly shaped. Quartz grain boundaries may be either smooth or jagged.

Jagged grain boundaries border fine-grained phyllosilicates, whereas smooth grain boundaries may border phyllosilicates, quartz, or albite grains. As in other sub-domains, fine-grained phyllosilicates bordering large quartz grains may appear to violate the quartz grain boundaries. Jagged quartz grain boundaries are commonly, but not exclusively, oriented at high angles to mesoscopic foliation. Inequant grains with jagged boundaries are commonly oriented with their long axes perpendicular to the foliation. Another type of quartz grain boundary is common in these sub-domains. These grain boundaries are between pairs of quartz grains that appear to have been one grain originally, i.e. they are in optical continuity and have matching "coastlines", but are now separated by a thin layer of mica.

Large, rhombohedral carbonate grains are present in some type 4 sub-domains, and are more common than in any other sub-domain types. These isolated carbonate grains tend to be much larger than the surrounding grains of mica and quartz. Many of them have ragged grain boundaries and are infested with small mica grains both along grain boundaries and within the grain. Mica is somewhat more concentrated along boundaries oriented at a high angle to the foliation than along foliation-parallel boundaries, where it is commonly oriented parallel to the foliation (Fig. 22).

Figure 22. Photomicrograph. Three carbonate grains in poorly developed domainal fabric. Scale = 20x.

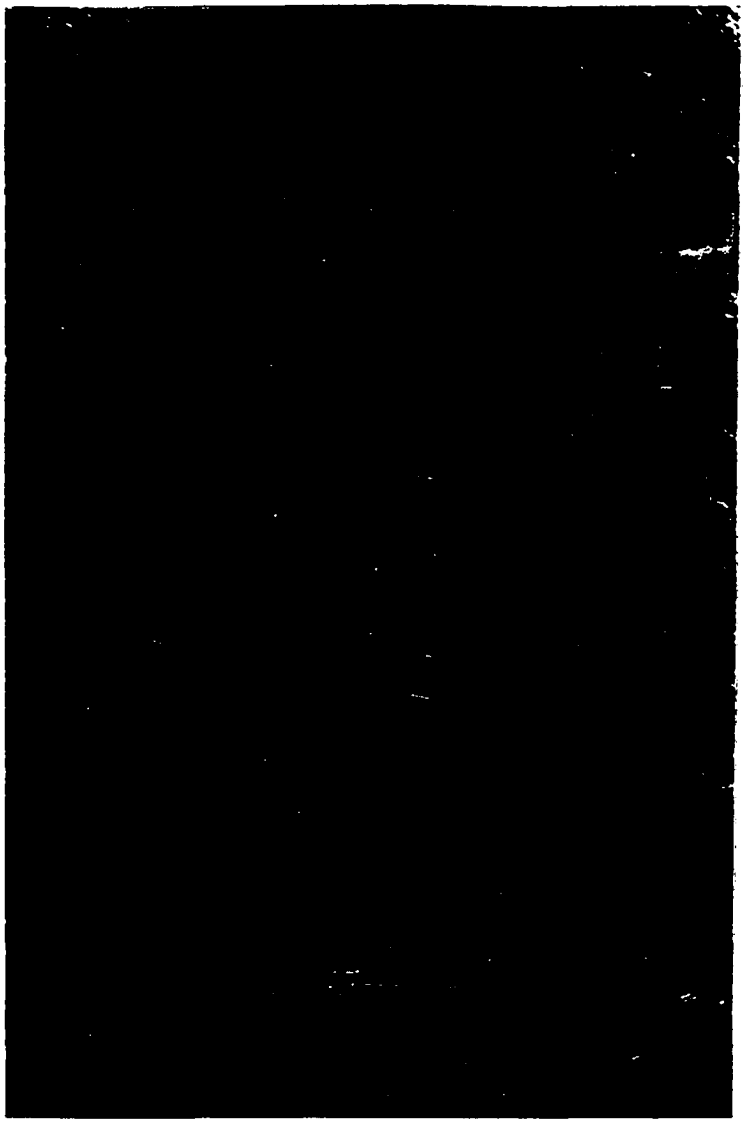

Summary of Small-scale Observations in Sandsuck Rocks

Small-scale observations are summarized in Table 3 (page 126) and by topic as follows.

1. Mica

The orientation, size, shape, composition, and probability of internal deformation of mica grains are all dependent on the microstructural sub-domain in which the grains are found. Mica grains within P domains are generally very uniform, while those in Q domains are more heterogeneous.

Within P domains (sub-domains 1 and 3) the average mica grain orientation is approximately parallel to the domain boundaries. In some cases, particularly in type 1 sub-domains, virtually all mica grains are within a few degrees of this orientation. In others, particularly the type 3 sub-domains, there may be two distinct preferred orientations, 10-15 degrees apart if little quartz is present, or up to 50 or 60 degrees apart if much quartz is present. Within Q domains (sub-domains 2 and 4), on the other hand, mica grains are generally parallel to bedding; this bedding-parallel preferred orientation is less uniformly developed than the foliation-parallel preferred orientation seen in the P domains.

Some mica grains encroach on or straddle domain boundaries. These micas, particularly if larger than average, may have orientations midway between that of the

bedding plane and that of the domain boundary, or they may be bent so that they have a limb in each orientation. Mica grains with small aspect ratios are more likely to be in anomalous orientations than are more elongate grains, regardless of the sub-domain in which they are found. Short, stumpy grains are rare within P domains, but the ones found there are commonly not parallel to, and may even be perpendicular to, the average mica grain orientation within the particular sub-domain.

Mica grains in P domains are generally more uniform and less apt to show signs of internal deformation or grain boundary corrosion than are mica grains in Q domains. These grains are white mica, and are all about the same size and shape. In contrast, mica grains in Q domains show great variability in size and shape. In Q domains there appear to be at least two distinct mica populations: the more common, bedding-parallel grains are on average somewhat smaller than the P domain mica grains, but include some significantly larger grains. These larger grains are more common in sub-domain type 4 than in sub-domain type 2, may be kinked or bent, and may have ragged grain boundaries. These larger grains are nearly all white mica, with very rare biotite grains. Because metamorphism in these rocks only reached chlorite grade, the biotite grains are assumed to be detrital. The smaller, bedding-parallel grains are a mixture of chlorite and white mica. The

second mica group present in the Q domains consists of very small, isolated, foliation-parallel, grains of white mica displaying a needle-shaped cross section. Except for their somewhat smaller size, the grains in this second group resemble the mica grains found in the P domains.

Mica grain shape is dependent not only on the type of sub-domain a grain is found in, but also on the orientation of the individual grain. The closer a grain lies to the orientation of the mesoscopic foliation, the greater its aspect ratio is likely to be, whether it is in a P domain or a Q domain. Grains oriented with their longest dimension perpendicular to foliation are not only much shorter, on average, than the foliation parallel grains, but also tend to be somewhat thicker. This is particularly easy to see in the cases of isolated mica grains found in type 4 sub-domains, but is also true for most mica grains elsewhere in the fabric.

2. Chlorite

The size, shape, and preferred orientation of chlorite grains are not as strongly dependent on the domain in which they are found as are those of the mica grains. They are in general very fine-grained, with highly variable aspect ratios, and no strongly developed preferred orientations. Within Q domains they have a poorly developed bedding-parallel preferred orientation. They are more common in some domains than in others, and generally make up a

greater part of the phyllosilicate population in Q domains than in P domains.

3. Chlorite Porphyroblasts

Large porphyroblasts of chlorite (Fig. 13) are found sporadically throughout both the phyllite and siltstone layers. They are several times larger than all other grains in the rock except the carbonates, and are quite rare. They are generally several times wider than a typical P domain, and are most common in phyllite layers. They do not show a discernible preferred orientation. Internally, they are nearly all deformed, with stacks of bent layers that are only roughly parallel to one another.

4. Quartz

The size, shape, and grain boundary definition of quartz grains are dependent on the sub-domain in which the grains are found. Quartz grains found within Q domains are larger than grains found in P domains, with the largest grains found in type 4 sub-domains. In Q domains, quartz grains are more apt to have ragged grain boundaries and undulose extinction than in P domains. The small grains found in P domains are commonly equant and have smooth grain boundaries, but some have ragged boundaries or may be elongate with smooth planar boundaries. Overgrowths on quartz grains have not been recognized in P domains, but are found on some grains in Q domains.

Nowhere in this fabric do quartz grains possess a

recognizable crystallographic preferred orientation. Whether they possess a dimensional preferred orientation is dependent, at least in part, on the sub-domain in which they are found. Quartz grains found in Q domains may be equant or elongate, and if elongate may lie parallel, perpendicular, or at an intermediate angle to foliation. It is therefore difficult to generalize about a dimensional preferred orientation for these grains. In P domains most quartz grains are equant, but some are elongate, with smooth planar boundaries along their long dimension. The boundaries present along the tips of these grains, on the other hand may be quite ragged with finer mica grains nestled along their irregular edges.

5. Feldspar

The only feldspar commonly found in the Walden Creek Group rocks is end-member albite (see probe data in Appendix 3). There is no K feldspar present in these fine-grained rocks, and only rare occurrences of Ca-bearing plagioclase. Grains possessing an anorthite component are only found adjacent to carbonate grains, and even there the common feldspar is pure albite. Within coarse-grained quartzite layers, however, a variety of detrital feldspars is found. Here there are large microcline grains, as well as a variety of plagioclase compositions.

6. Carbonates

Large, ragged carbonate grains (Fig. 22) are common in

some samples and seem to be more common in siltstone layers than in phyllite layers. The common carbonates are ferroan dolomite and calcite (see Appendix 3). All three phases may be present in a given sample, typically as elongate rhombohedral grains aligned with the foliation. They tend to be much larger than the grains around them and have numerous chlorite and quartz inclusions. Some have mica beards extending parallel to cleavage. Calcite is also found as a vein-filling.

7. Opaques

Along some interfaces between phyllite and siltstone there is a thin bedding-parallel layer of small, equant opaque grains, (Figs. 23). The fact that these opaque grains are found exclusively along the base of graded silt beds suggests that they are detrital. These opaque layers, although no more than 2 to 3 grains thick, are quite persistent and are commonly as continuous as the phyllite and siltstone layers they separate. The opaque layers are broken only where they are cross-cut by P domains. Where P domains are closely spaced, the opaque layers are broken into a series of detached, synformal arcs.

8. Domain Size and Shape

All of the material in siltstone and phyllite layers can be viewed as belonging either to a P domain or a Q domain. Volumetrically, a somewhat greater portion of the

Figure 23a. Photomicrograph showing 3 P domains crossing the boundary between a phyllite layer (lower left) and a siltstone layer (upper right). Cross-polarized. Scale = 35x.

Figure 23b. Plane polarized photomicrograph of 20a. Note the thin layer of opaque grains along the base of the siltstone layer. Scale = 35x.

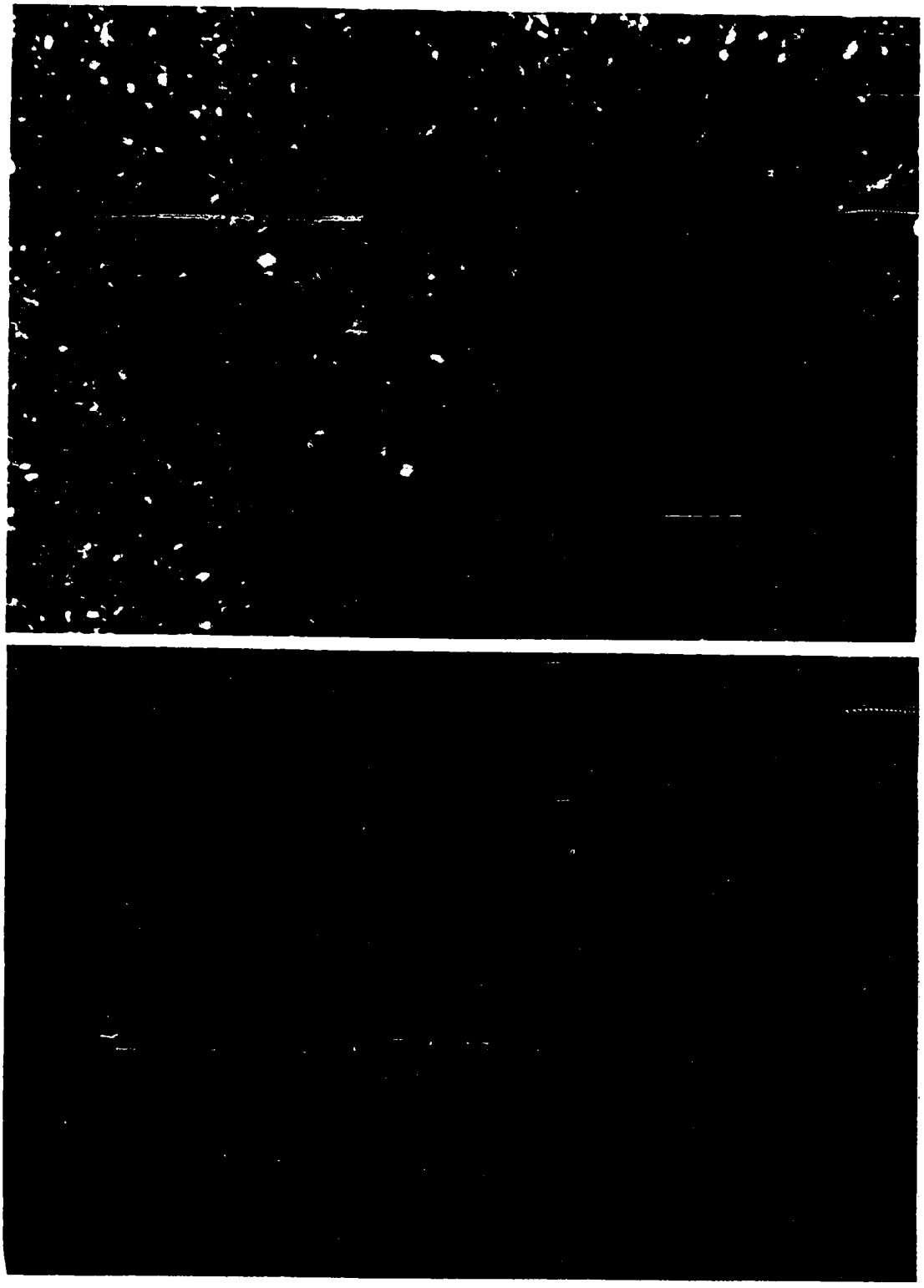

rock is occupied by Q domains than is occupied by P domains. Q domains are generally more continuous than P domains, with individual ones rarely terminating except at an intersection with another Q domain. P domains, however, are commonly discontinuous, with many failing to cross siltstone layers and a few terminating within phyllite layers. Commonly, P domains barely penetrate siltstone layers before dying out (Figs. 14, 19). P domains that terminate within phyllite layers tend to be very thin and may be as short as 1 millimeter. Possibly there are even thinner, shorter P domains that have not been recognized. In general, among the very short P domains, there is a strong correlation between length and thickness.

The P and Q domains within phyllite layers usually maintain a constant thickness as they cross the layer. Even the very short P domains that start and end within a single phyllite layer do not change much in thickness; they are never more than a few grains thick. Within siltstone layers, on the other hand, even continuous P domains are likely to be thinner near the middle, of the layer than they are near the bottom.

P domains crossing phyllite layers generally follow a straight or slightly curving course. Among the P domains that fail to cross siltstone layers, most terminate by branching out along so many courses that the domain loses its identity. More rarely, P domains branch and then

reconsolidate. In general, even where P domains exhibit irregular morphologies, the ratio of their volume to the volume of Q domains is smaller near the middle and top of a siltstone layer than it is near the bottom. Because siltstone layers are made up entirely of alternating P and Q domains, the morphologies of the Q domains within the siltstone layers mirror those of the P domains; they occupy all the space between the P domains.

Brief Summary of Petrographic Observations

In general the significant differences in P and Q domains can be summed up in terms of morphology, mineralogy, average orientations of different types of mineral grains, and grainscale deformation. The properties of sub-domains are summarized in Table 3.

P domains tend to be broader and more tabular in phyllite layers than in siltstone layers. In siltstone layers they are commonly discontinuous, and typically branch into many thinner mica trails that wind around the larger quartz and feldspar grains. P domains contain more mica than chlorite, and much more mica than quartz or feldspar. The mica grains are small, elongate, and oriented parallel to foliation. Chlorite grains in P domains tend to parallel foliation, but are highly variable in orientation. Quartz and albite do not display a discernible preferred orientation. Evidence of grainscale deformation is rare, although quartz may have undulose

extinction or ragged grain boundaries.

In contrast, Q domains are continuous in both phyllite and siltstone layers. They contain much quartz and albite and more chlorite than mica. Both mica and chlorite are more variable in size and shape than they are in P domains. Most phyllosilicates are oriented roughly parallel to bedding, although there is considerable variation. Undulose extinction and ragged grain boundaries are more common than in P domains, as are bent mica grains.

Table 3. Properties of Sub-domains

Type	Position	Shape	Mineralogy	Mica Grains	Quartz Grains
1.	phyllite, P domain	tabular, broad, may taper	mica, chl., qtz., alb., carb., opaques	small, uniform, elongate, parallel to foliation, undeformed	small, equant, no preferred orientation, deformation rare
2.	phyllite, Q domain	same as 1., but broader	qtz., alb., chl., mica, carb., opaques	variable size and shape, parallel to bedding, some bent	variable size, mostly equant some ragged boundaries
3.	siltstone P domain	may taper or ramify, discon-tinuous	mica, chl., qtz., alb., carb., opaques	same as 1.	equant or elongate, some large, some ragged, some undulose
4.	siltstone Q domain	broad, variable	qtz., alb carb., chl., mica, opaques	same as 2.	same as 3.

CHAPTER VI

X-RAY DIFFRACTION AND ELECTRON MICROPROBE ANALYSES

Several analytical techniques were used to characterize the mineralogy and bulk composition of the P and Q domains. Two types of microprobe analyses were performed, analyses of areas within individual phyllosilicate grains and analyses of areas made up of many grains. X-Ray diffraction (XRD) analyses were made of polished rock chips cut in several orientations and scanned over two ranges of 2θ. Details of the analytical methods are found in the sections on X-Ray diffraction analyses, phyllosilicate analyses, and microprobe traverses. X-Ray diffraction patterns, and tables of microprobe standards and microprobe data are in the appendix. All analytical work was performed using equipment in the University of Cincinnati Geology Department.

X-Ray Diffraction Analyses

Brief Review of Previous Studies

Many previous studies have used X-Ray diffraction to characterize phyllosilicates and the changes they undergo during diagenesis and low-grade metamorphism. Two of the more comprehensive are regional studies by Weaver et al. (1984) and Hunziker et al. (1985). A significant difference between the XRD analyses in these studies and those in the current study is the nature of the samples analyzed; the other studies employed samples of discrete grains segregated by grainsize, whereas this study used whole rock chips. In general, Weaver et al. and Hunziker et al. found that with increasing grade from diagenesis to epimetamorphism white micas show an increase in crystallinity, a change in polymorph from $1M_d$ to 2M, an increase in K, an increase in both total Al and Al^{IV}, a decrease in water content, a decrease in chemical variability, and an increase in total layer negative charge.

Weaver et al. (1984) also studied the changes in chlorite, and noted that in the anchizone and epizone Fe-rich chlorite is gradually replaced by phengite, whereas there is more Mg-rich chlorite in epizone rocks than in lower grade rocks. Hayes (1970) and Curtis et al. (1984, 1985) studied the diagenetic to epimetamorphic evolution of chlorite and found the polytype and the composition to

change. The stable polytype changes from I_b to II_b and the composition changes as both Mg/Fe and Al^{IV} increase.

Analytical Methods

All X-Ray diffraction analyses were performed on an automated Siemens D 500 diffractometer using Diffrac 11 software. The X-Ray samples were polished rock chips cut in one of four orientations, two orientations to emphasize the (001) reflections of phyllosilicates in P domains or Q domains (chips cut parallel to cleavage or parallel to bedding, respectively), and two additional orientations to display the (060) reflections for phyllosilicates in the two domains (perpendicular to cleavage or perpendicular to bedding). Because there are not unique planes that are perpendicular to cleavage and bedding, a further condition was put on each of these cuts. Cleavage-perpendicular cuts were made roughly 45 degrees off bedding, and bedding-perpendicular cuts were made roughly 45 degrees off cleavage. These particular cuts were selected to avoid producing strong (331) reflections from the cleavage- or bedding-parallel grains. If such reflections were present in the patterns they would obscure the (060) reflections. This is an adaptation of a technique developed by Sassi and Scolari (1974) for measuring the b_o of mica in foliated rocks. Standard sample preparation techniques for preparing oriented XRD mounts from the less than 2 micron size fraction were not used because it was not possible to

separate samples of P domain and Q domain material.

The samples were each scanned over one of two ranges. The samples cut parallel to either cleavage or bedding were scanned from $_2$° to 42° 2θ CuK_α and the samples cut perpendicular to cleavage or bedding from 55° to 65° 2θ CuK_α. All analyses were done in step-scan mode, with a step size of 0.020°2θ CuK_α, and a measuring time of 1 second.

Data

In order to examine and compare the (001) reflections of phyllosilicates in the two domains, pairs of chips were cut parallel to cleavage and parallel to bedding. These two cuts give patterns that are dominated by the (001) reflections of the P domain and Q domain grains, respectively. Figures 24 and 25 show representative patterns run on a pair of cleavage- and bedding-parallel chips cut from the same hand sample. These pairs of chips were each scanned over a 2θ range of 2 to 42 degrees. In general each pair of chips cut from the same hand sample produces patterns that have nearly identical peaks for quartz, albite, carbonates, and pyrite. The phyllosilicate peaks, however, show some variation in their intensities and "crystallinity" (peak width at half height), that is related to whether the chip is cleavage-parallel or bedding-parallel.

The 10 Å mica peak tends to show greater crystallinity

Figure 24. X-Ray diffraction patterns run on polished rock chips cut parallel to bedding (upper pattern) and parallel to cleavage (lower pattern). Sample WC22.

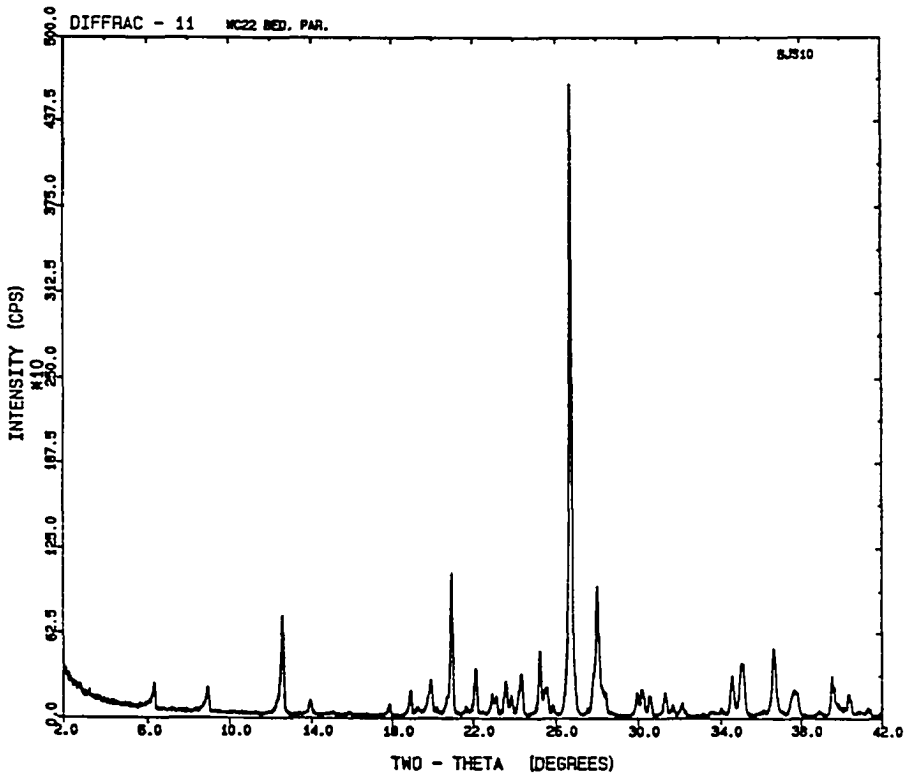

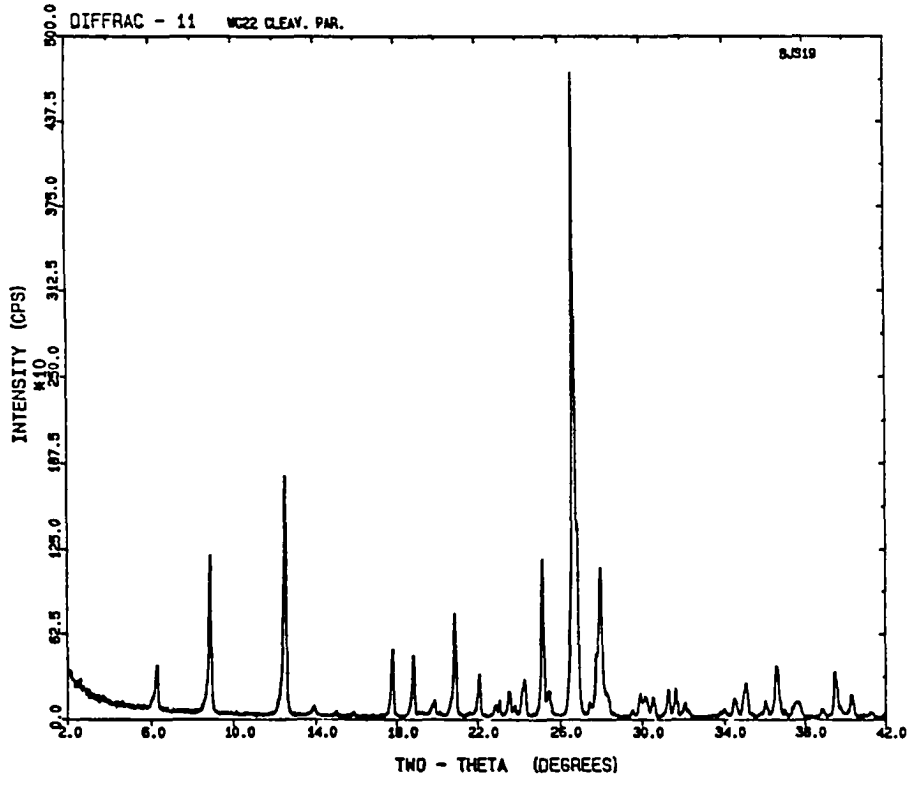

Figure 25. X-Ray diffraction patterns run on polished rock chips cut parallel to bedding (upper pattern) and parallel to cleavage (lower pattern). Sample WC33.

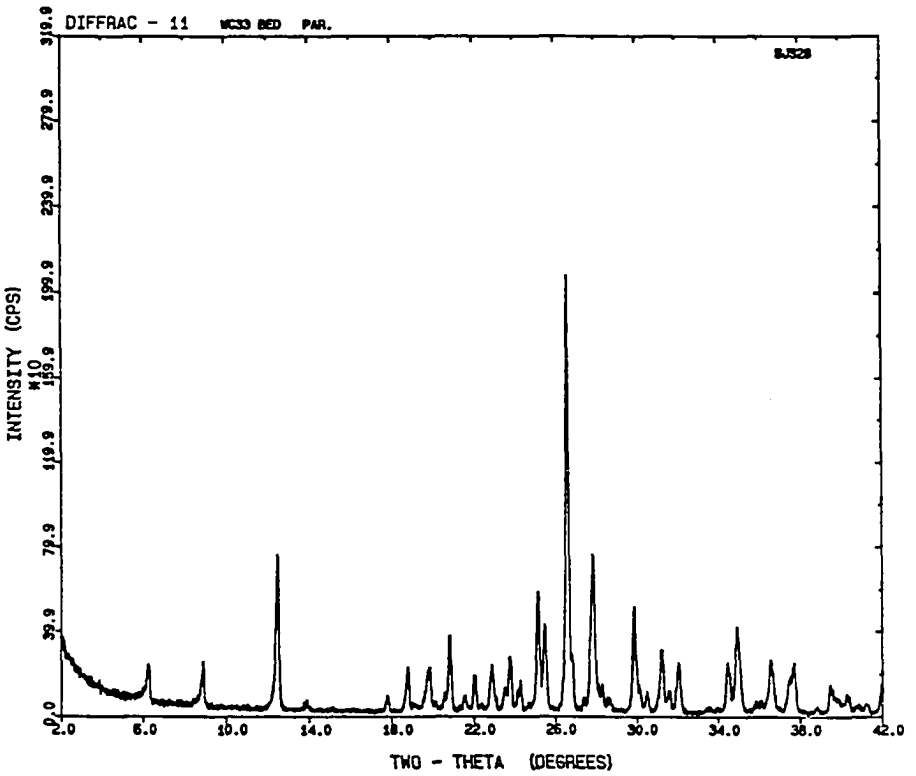

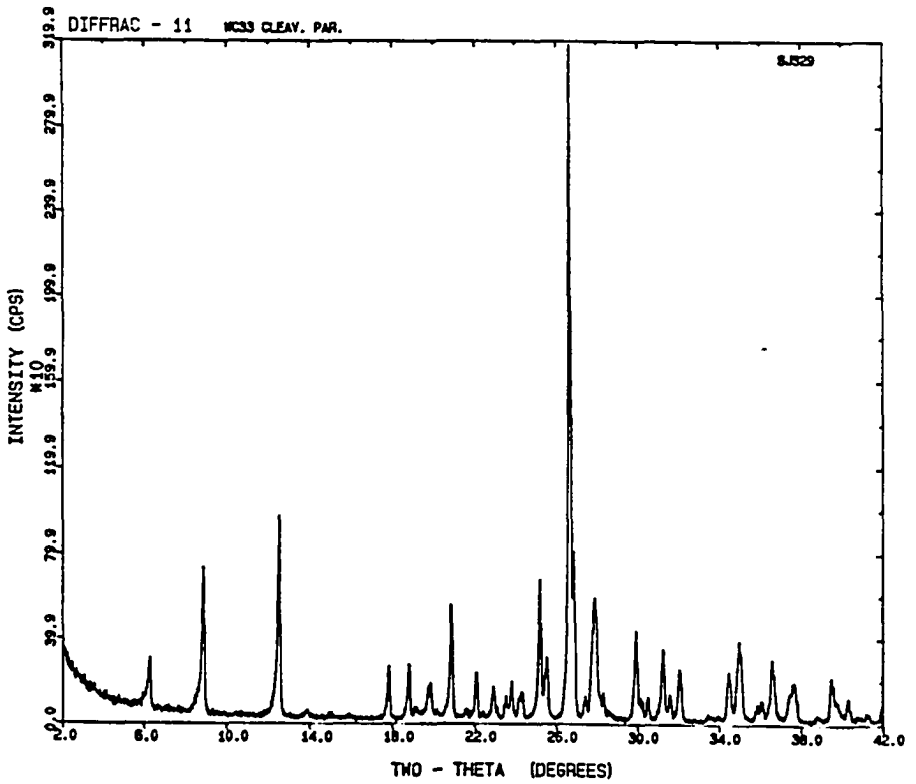

Figure 26. Bar graph comparing Kubler Index or K.I. for pairs of bedding-parallel and cleavage-parallel chips cut from the same sample. K.I. measures "crystallinity" of the 10 Å peak (illite (001)) as FWHM, or the peak width in °2θ at half maximum height.

(be narrower at half its maximum height) in the patterns produced from cleavage-parallel samples than in the patterns produced from bedding-parallel samples (Fig. 26). This is the peak traditionally used in illite crystallinity measurements, and several methods have been used by various workers to evaluate it (e.g. Weaver, et al., 1984). The measure of peak width used here is the Kubler index (K.I.), or the 2θ CuK_{α} width of the peak at half height (Weaver et al., 1984). The average K.I. value for cleavage-parallel samples is 0.14°2θ with a standard deviation of 0.06, whereas for bedding-parallel samples it is about 0.18°2θ with a standard deviation of 0.03.

An additional measurement made on XRD patterns run on cleavage- and bedding-parallel samples is the ratio of the intensity of the 7 Å (chlorite (002)) to the 10 Å (mica (001)) peaks. This intensity ratio is greater in bedding-parallel samples than in cleavage-parallel samples for all but one sample pair. For that pair the ratios are nearly equal. The average 7 Å to 10 Å intensity ratio of bedding-parallel samples is more than twice that of cleavage-parallel samples. Figure 27 summarizes these intensity ratios.

Intensity ratios have also been calculated for the ratio of 5 Å to 10 Å peaks (Fig. 28). These are the (002) and (001) mica reflections, respectively, and their relative intensities have been reported to depend variously

Figure 27. Bar graph of the ratio of the 7 Å peak height (chlorite (002)) to the 10 Å peak height (illite or mica (001)) for pairs of chips cut parallel to bedding and parallel to cleavage.

Figure 28. Bar graph of the ratio of the 5 Å peak height (mica (002)) to the 10 Å peak height (mica (001)) for pairs of chips cut parallel to bedding and parallel to cleavage.

on compositional parameters, including K, Fe, and Al/(Fe+Mg) (e.g. Weaver and Pollard, 1973) or on degree of metamorphism. No consistent difference was seen for measurements of samples in the two orientations. There is a slight difference seen in the average 5 Å/10 Å measurements for the two orientations, the average ratio for the bedding-parallel samples being about 0.51, whereas that for the cleavage-parallel samples is about 0.43.

Intensity ratios for the 2.80 Å and 2.58 Å peaks were also calculated and compared for each pair of samples. These data are given in Figure 29, and show that there is considerable variation in how the ratios compare for different pairs of samples. The average value of this ratio is about 0.7 for cleavage-parallel samples, as compared to about 0.5 for bedding-parallel samples. This ratio was determined because it may be useful in determining the proportions in which the 1Md and 2M mica polytypes are present in the two domains. According to Maxwell and Hower (1967) there is a positive, linear correlation between this ratio and the proportion of 2M mica to total 2M plus 1Md mica. Examining the less than 2 micron size fraction of argillaceous rocks from the Belt Series, they found that this ratio reaches about 0.25 at the degree of metamorphism where the 1Md polytype has disappeared. Of the patterns examined in this study, all but 3 bedding-parallel samples have 2.80 Å/2.58 Å ratios

Figure 29. Bar graph of the ratio of the 2.80 Å peak height to the 2.58 Å peak height for pairs of chips cut parallel to bedding and parallel to cleavage.

below 0.25.

For several samples, a second pair of chips was cut in two additional orientations, perpendicular to cleavage and perpendicular to bedding. The purpose in X-Raying chips cut in the cleavage- and bedding-perpendicular orientations was to produce diffraction patterns with strong (060) reflections. The position of this particular reflection is influenced by the Fe and Mg content of the grains and by whether the grains are closer to dioctahedral or trioctahedral in occupancy. In addition, asymmetry in the mica (060) peak is an indication of interstratified chlorite and mica.

Figure 30 shows a pair of typical XRD patterns run on chips cut in these two orientations. These pairs of chips were each scanned over a 2θ range of 55 to 65 degrees. Each pair of chips produced nearly identical peaks for the non-phyllosilicate minerals. As in the bedding-parallel and cleavage-parallel samples there are some systematic differences in phyllosilicate peaks seen in the bedding-perpendicular and cleavage-perpendicular samples. In Figure 30, there is an asymmetric shoulder on the low angle side of the mica (060) peak (the peak between 61° and 62° 2θ) in the cleavage-perpendicular pattern. In comparison, the bedding-perpendicular pattern has a small mica peak in virtually the same position as the larger cleavage-perpendicular mica peak. The asymmetric shoulder, however,

Figure 30. X-Ray diffraction patterns run on polished rock chips cut perpendicular to bedding (upper pattern) and parallel to cleavage (lower pattern). The bedding-perpendicular pattern is offset above the cleavage-perpendicular pattern. The counts per second scale is for the cleavage-perpendicular pattern.

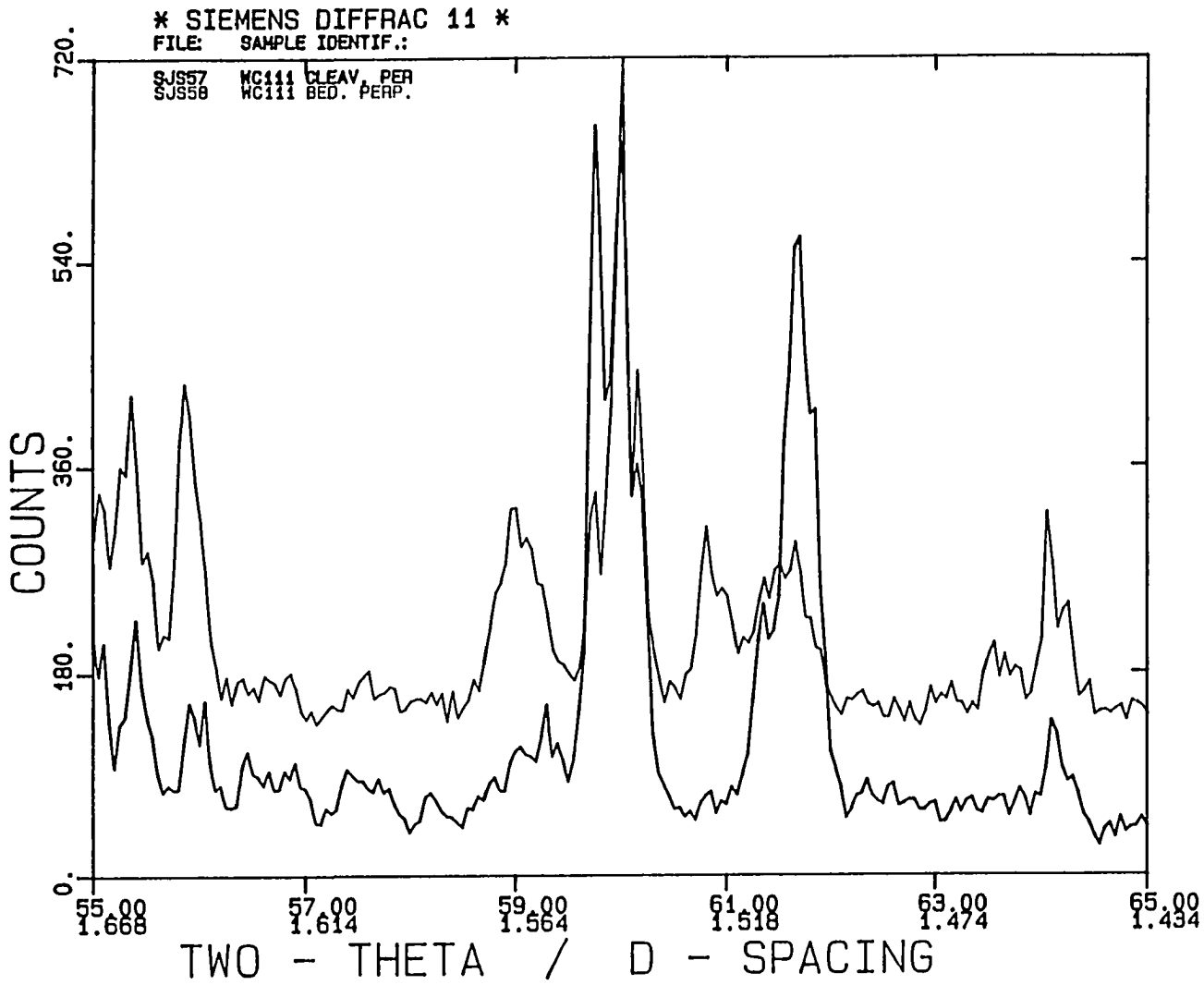

has been replaced by a separate, more intense peak at a slightly lower angle.

Figure 31 shows the intensity ratio of the mica (060) reflection to its lower angle shoulder or neighboring peak for each of the pairs of samples. In the cleavage-perpendicular samples, this ratio averages about twice what it does in the bedding-perpendicular samples. For the two sample orientations there is also a very consistent difference in the position of the lower angle neighbor of the mica (060) peak. In the cleavage-parallel samples this position is about 61.27°2θ CuK_{α}, whereas in the bedding-parallel samples it is about 60.82°2θ CuK_{α} (Fig. 32). These correspond to b-spacings of about 1.513 Å and 1.523 Å, respectively.

Another difference between the patterns produced from bedding-perpendicular samples and those produced from cleavage-perpendicular samples is the intensity of the peak around 59° 2θ. This is the (060) reflection for iron-rich chlorite. The average intensity of this peak compared to the quartz (211) peak is given in Figure 33. For the patterns run on bedding-perpendicular samples, this ratio averages about 0.32, whereas for the patterns run on cleavage-perpendicular samples it averages about 0.18.

Discussion of X-Ray Diffraction Data

XRD data obtained in this study is not necessarily directly comparable to that published in other works,

Figure 31. Bar graph of the ratio of the mica (060) peak to the interstratified (060) peak for chips cut perpendicular to bedding and perpendicular to cleavage.

Figure 32. Bar graph of the interstratified (060) peak position for pairs of chips cut parallel to bedding and parallel to cleavage.

Figure 33. Bar graph of the ratio Fe-rich chlorite (060)/ quartz (211) for pairs of chips cut parallel to bedding and parallel to cleavage.

because the nature of the samples analyzed was different here than in most other studies. Because this study compares differences in domains that are only microns wide, it was not feasible to separate samples of P domain material from samples of Q domain material. Instead whole rock chips were analyzed. The difficulty in comparing the data obtained from these samples to that obtained in studies using samples of the less than 2 micron grainsize fraction is that the whole rock samples are more heterogeneous in grainsize, mineralogy, and grain orientation. Nonetheless, because there is no data available for whole rock chip samples, the data obtained in this study are compared to information available from studies using less than 2 micron grainsize samples.

In the diffraction patterns run on the pairs of samples cut parallel to cleavage or to bedding there are two significant differences seen in the phyllosilicates. One is in the crystallinity or Kubler Index of the 10 Å peak and the other is in the ratio of the 10 Å peak intensity to the 7 Å peak intensity. For most pairs of chips cut from the same hand sample, the pattern produced from the cleavage-parallel sample has a somewhat smaller Kubler Index (higher illite crystallinity) than that measured in patterns run on bedding-parallel samples. The significance of illite crystallinity is not well established, but it is thought to be a measure of the

degree of crystal perfection. It may reflect such factors as density of defects or stacking faults as well as the presence or absence of minor amounts of interstratification with other phyllosilicate phases. Because this measurement generally decreases during prograde anchimetamorphism (e.g. Hunziker et al., 1986), these data suggest that the P domain phyllosilicates have, in comparison to the Q domain phyllosilicates, characteristics of grains that have reached a higher metamorphic grade.

The fact that peaks other than the 10 Å peak, also show a tendency toward smaller peak width at half height in the cleavage-parallel than in the bedding-parallel samples is difficult to interpret. It may indicate that these reflections are narrower for the P domain grains than for the Q domain grains because these grains contain fewer defects and incoherent grain boundaries. The explanation may, however, be simply that the Q domain grains tend to contain at least minor volumes of interstratified material, whereas the P domain grains are more likely to be pure phases. Even this, however, suggests that the P domain grains have been more affected by metamorphism than the Q domain grains have.

The significance of the mica (002)/(001) ratio is unclear. Several workers have suggested that there is a positive correlation between this measurement and increasing degree of diagenesis or metamorphism. Weaver et

al. (1984) plotted this ratio against grade and found that for the Conasauga shale it increases steadily up to the boundary between the anchizone and the epizone, and then reverses in the epizone. The ratio reaches a maximum value of about 0.5, and then drops to about 0.42 for their highest grade samples. Comparing the values obtained for samples in this study (Fig. 28) to their findings for the Conasauga shows that the fine-grained rocks from the western end of Ocoee Gorge lie close to the boundary between the anchizone and the epizone. The average value for the cleavage-parallel samples is about 0.48, whereas that for the bedding-parallel samples is about 0.53. Using the values found for the Conasauga, the P domain micas resemble epizone grade micas, whereas the Q domain micas resemble upper anchizone grade micas.

The data for the intensity ratio 2.80 Å/2.58 Å are particularly difficult to interpret because, as noted in other studies (e.g. Maxwell and Hower, 1967; Weaver et al., 1984), this ratio is strongly dependent on grain size. Because of this dependency, Maxwell and Hower used the less than 2 micron size fraction in calculating curves for determining the relative proportions of 1Md and 2M mica. Comparing the data from the patterns run on whole rock chips in this study to that given by Maxwell and Hower is of questionable value, but there is no more appropriate data base available for comparisons. Using their value of

0.25 as the point at which all 1Md mica has disappeared, there are only three samples that appear to have any 1Md mica. These three are all bedding-parallel samples. This suggests that more detrital mica may be preserved among the bedding-parallel Q domain grains, than among the cleavage-parallel P domains, but that most mica in both domains has completed the transition from the 1Md to the 2M polytype.

The transition in mica polytypes from the 1Md to 2M is reported to take place entirely in the anchizone, being completed near the epizone boundary, at a temperature of about 360°C (Weaver et al., 1984). According to this, the presence of 100% 2M mica in the P domains and a mixture of mostly 2M mica in the Q domains is consistent with the degree of metamorphism recorded by the illite crystallinity.

Comparison of the intensity of the 7 Å reflection and the 10 Å reflection indicates that this ratio is consistently higher for the bedding-parallel than for the cleavage-parallel chips (Fig. 27). This suggests that the proportion of chlorite to mica is greater for the bedding-parallel or Q domain grains than for the cleavage-parallel or P domain grains. Further evidence that the proportion of chlorite to mica is different in the two domain types is the difference in the intensities for the (060) mica and (060) chlorite peaks. Both these sets of measurements are in agreement with the probe data on individual grain

compositions and that on domain compositions. Microprobe analyses of individual phyllosilicate grains in Q domains were found to be far more likely to be chlorite than were analyses of P domain grains.

The XRD patterns run on samples cut perpendicular to cleavage or to bedding display two interesting differences in addition to the difference in the chlorite and mica peak intensities. These are in the position and the intensity of the peak or shoulder signifying the presence of interstratified material. The greater intensity and the lower 2θ position of the interstratified peak in the bedding-perpendicular patterns indicate both that there is more interstratified material present in Q domains and that the amount of chlorite in the interstratified Q domain grains is greater than in the interstratified P domain grains, a finding that is supported by the microprobe data.

In general, the X-Ray data obtained in this study indicate, when compared to data from other studies, that the Sandsuck Formation rocks from the western end of Ocoee Gorge are near the middle of the transition from detrital clays and micas to the metamorphic development of biotite. According to the phyllosilicate stability ranges given by Weaver et al. (1984) in Figure 7, P domain phyllosilicates plot near the anchizone-epizone boundary, whereas Q domain phyllosilicates plot near the diagenesis-anchizone boundary.

Microprobe Analyses of Phyllosilicates

Brief Review of Previous Studies

Three previous analytical studies of P and Q domain phyllosilicates are those of Knipe (1979), Stephens et al. (1979), and White and Johnston (1981). Knipe and White and Johnston found P domain micas to be richer in K and slightly more phengitic than Q domain micas. P domain chlorites were slightly lower in iron than Q domain chlorites. Knipe's data are summarized in Figure 8. Stephens et al. analyzed phyllosilicates from P and Q domains in relatively coarse-grained rocks (sandstone). Their findings were not consistent with Knipe's, but the differences appear to be due to the presence of detrital grains derived from high grade source areas.

Analytical Methods

All electron microprobe analyses, both those of individual grains and the traverses across compositional domains were made using an ARL-EMX three channel electron microprobe with Krisel automation operating at an accelerating voltage of 15KV. Bence-Albee correction factors (Bence and Albee, 1968; Albee and Ray, 1970) were used. Standards used were silicate standards of the University of Cincinnati Microprobe Laboratory, and are listed with compositions and beta factors in the Appendix. For analyses of individual grains, maximum count times of 20 seconds per element or 60 seconds per analysis were

used. Where grainsize was large enough, a slightly defocussed beam was used to minimize diffusive loss of Na and K.

In general grains along domain boundaries were avoided, as were poorly polished grains, because they gave low totals. The rejection of poorly polished grains may bias the data because they may represent a different population of grains than those that polished well. Grains cut perpendicular to (001) tend to polish better than those in other orientations. Because most of the thin sections analyzed were cut perpendicular to cleavage a disproportionately high number of grains not oriented parallel to cleavage have probably been excluded from the analyses. If grains in different orientations belong to different populations the compositional data may be biased.

Data

Analyses of phyllosilicate grains were obtained on Grains from both P and Q domains, and representative phyllosilicate analyses are given in Table 4 (P domain analyses) and Table 5 (Q domain analyses). The analyses used in these tables were of nine elements, Si, Al, Mg, Fe, K, Na, Ti, and Mn, whereas the data used to construct the plots are form analyses that did not include Na, Mn, or Ca. All phyllosilicate analyses are given in the appendix.

The phyllosilicate analyses obtained fall into three general categories: illite or white mica (muscovite or

TABLE 4. Representative electron microprobe analyses of P domain white mica, chlorite, and interstratified mica/chlorite

	1	2	3	4	5	6	7	8	9
SiO2	43.74	48.43	35.34	47.94	48.88	38.5	47.27	48.99	40.19
TiO2	0.24	0.41	0.03	0.29	0.25	0.29	0.19	0.33	0.2
Al2O3	27.74	30.18	24.31	28.98	30.31	27.74	31.87	29.86	25.32
FeO	11.12	3.47	18.21	4.89	2.11	11.53	2.89	2.62	13.07
MnO	0.09	0	0.21	0	0.1	0.2	0	0.09	0.15
MgO	4.06	10.96	8.5	2.67	2.2	6.49	1.66	2.08	6.04
CaO	0.3	0.37	0.38	0.79	0.25	0.33	0.27	0.29	0.3
Na2O	0.13	0.1	0.94	0.2	0.2	0.11	0.74	0.18	0.17
K2O	7.84	10.96	3.08	10.27	10.47	6.49	9.63	10.24	6.47
Total	95.26	96.21	91	96.02	94.77	91.68	94.52	94.66	91.92
	recalculated on the basis of 11 oxygens (total Fe as Fe2+ only)								
Si	3.05	3.24	2.68	3.23	3.28	2.81	3.19	3.29	2.94
Al	0.95	0.76	1.32	0.77	0.72	1.19	0.81	0.71	1.06
sum	4	4	4	4	4	4	4	4	4
Al	1.33	1.62	0.85	1.53	1.68	1.2	2.72	1.66	1.12
Ti	0.01	0.02	0	0.01	0.01	0.02	0.01	0.02	0.01
Fe	0.65	0.19	1.16	0.27	0.12	0.7	0.16	0.15	0.8
Mn	0	0	0.01	0	0	0.01	0	0	0.01
Mg	0.42	0.23	0.96	0.27	0.22	0.71	0.17	0.21	0.66
Ca	0.02	0.03	0.03	0.06	0.02	0.03	0.02	0.02	0.02
Na	0.02	0.01	0.14	0.03	0.03	0.02	0.1	0.02	0.02
K	0.7	0.93	0.3	0.88	0.9	0.6	0.83	0.88	0.6
sum	3.15	3.02	3.44	3.05	2.96	3.28	2.99	2.95	3.25
sample #	WC26A M	WC26A C/M	WC26A C/M	WC29 M	WC29 M	WC15 C/M	WC15 M	WC26B M	WC26B C/M

Where M = mica
C = chlorite
C/M = interstratified chlorite/mica

TABLE 5. Representative electron microprobe analyses of Q domain white mica, chlorite, and interstratified mica/chlorite

	1	2	3	4	5	6	7	8
SiO2	23.91	47.64	41.26	24.85	43.48	48.08	26.38	37.8
TiO2	0.08	0.11	0.12	0.04	0.13	0.31	0.01	0.06
Al2O3	24.64	36.21	31.53	22.88	17.36	29.61	24.23	29.4
FeO	29.6	0.84	8.25	29.49	16.65	2.47	24.85	11.95
MnO	0.13	0	0.07	0.13	0.01	0	0.31	0.13
MgO	11.41	0.59	3.57	12.78	5.86	1.99	11.51	6.79
CaO	0.32	0.25	0.27	0.34	0.28	0.29	0.34	0.26
Na2O	0.11	0.91	0.7	0.26	0.56	0.12	0.2	0.11
K2O	0.06	9.01	6.4	0.04	7.31	10.91	0.53	4.81
Total	90.27	95.57	92.18	90.81	91.64	93.79	88.36	91.3
recalculated on the basis of 11 oxygens (total Fe as Fe2+ only)								
Si	1.96	3.12	2.91	2.03	3.27	3.28	2.15	2.75
Al	2.04	0.88	1.09	1.97	0.73	0.72	0.85	1.25
sum	4	4	4	4	4	4	4	4
Al	0.34	1.91	1.53	0.23	1.19	1.66	1.48	1.27
Ti	0	0.01	0.01	0	0.01	0.01	0	0
Fe	2.03	0.04	0.49	2.01	1.05	0.14	1.7	0.73
Mn	0.01	0	0	0.01	0	0	0.02	0.01
Mg	1.4	0.06	0.58	1.55	0.66	0.2	1.4	0.73
Ca	0.03	0.02	0.02	0.03	0.02	0.02	0.03	0.02
Na	0.02	0.11	0.1	0.04	0.08	0.02	0.03	0.01
K	0	0.75	0.58	0	0.7	0.95	0.05	0.45
sum	3.83	2.9	3.09	3.87	3.33	2.99	3.71	3.21
sample #	WC40 C	WC40 M	WC40 C/M	WC15 C	OG11 C/M	WC26 M	WC26 C	WC26 C/M

Where M = mica
C = chlorite
C/M = interstratified chlorite/mica

phengite), chlorite (ripidolite), and interstratified chlorite/muscovite. Because it was not possible to distinguish between mica, chlorite, and interstratified grains while selecting grains for microprobe analyses, all phyllosilicate formulae were calculated on the basis of the number of oxygens in mica, not the number in chlorite. Therefore the chlorite and interstratified analyses included in Tables 4 and 5 have correct weight percents (upper half of table), but incorrect cation counts (lower half of table). For comparison, a few chlorite analyses from Deer et al. (1975) are shown in Table 6. Comparing the third column in Table 6 (a ripidolite) to the first, fourth, and seventh columns in Table 5 (Q domain chlorites) it can be seen that the weight percents for Si, Al, Fe, and Mg are similar, in spite of the apparently disparate formula calculations. This disparity arises from basing the formula calculations on the mica formula rather than on the chlorite formula. It should be noted that many of the figures in this section are plots of formula units and all analyses plotted were calculated as mica. In other words, formula representations of analyses of chlorite and interstratified chlorite are correctly represented in a qualitative, but not a quantitative sense. The triangular plots in Figures 34 through 35, however, are based on weight percent and should be quantitatively correct for both mica and chlorite.

TABLE 6. Selected chlorite analyses from Deer et al. (1975)

	1	2	3	4
SiO2	23.2	27.64	25.62	26.4
TiO2	0	0.22	0.88	0
Al2O3	24.42	22.48	21.19	18.23
Fe2O3	3.48	0.06	3.88	5.7
FeO	13.4	12.06	21.55	25.87
MnO	0	0.02	0.35	0.04
MgO	22.76	24.32	15.28	11.35
CaO	1.04	0	0.16	0.42
Na2O	0	0.17	0	0.17
K2O	0	0.06	0	0.17
Total	88.3	87.03	88.91	87.36
	recalculated on the basis of 14 oxygens			
Si	2.32	2.76	2.68	2.87
Al	1.68	1.24	1.32	1.13
sum	4	4	4	4
Al	1.2	1.41	1.29	1.21
Ti	0	0.02	0.07	0
Fe+3	0.26	0	0.31	0
Fe+2	1.13	1.08	1.89	2.82
Mn	0	0	0.03	0
Mg	3.4	3.62	2.38	1.84
Ca	0.11	0	0.02	0.05
Na	0	0	0	0.04
K	0	0	0	0.02
sum	6.1	6.13	5.99	5.98

1: Dark green corundophilite, emery deposit, Chester County, Massachusetts
2: Sheridanite, dravite-chlorite rock, Nelson, New Zealand
3: Ripidolite, chlorite-epidote-albite schist, south Devon
4: Green oolitic chamosite, siltstone, Wickwar, Gloucestershire

Microprobe analyses of phyllosilicate grains found in P domains (both sub-domains 1 and 3) indicate considerably more white mica is present than chlorite, and that most of the chlorite present is interstratified with mica (Figs. 34-36). Of 134 P domain phyllosilicates analyses plotted on these figures only one is pure chlorite. The other analyses are either pure mica or are intermediate between mica and chlorite and plot along a straight line on an AKF diagram (Fig. 34a). The vast majority of these grains have fewer than 7.3 cations per half cell, as compared to 7 for a dioctahedral mica with full occupancy of the interlayer sites. This indicates that chlorite makes up less than half the layers in a typical P domain mixed-layer phyllosilicate. This is clear in Figs. 34a and 34b, where it can be seen that P domain phyllosilicates cluster near the mica end member.

In P domains the composition of end member mica grains (average of analyses with 7.1 or fewer cations per half cell formula) averages $K_{0.9}(Mg_{0.2}Fe_{0.2}Al_{1.6})Al_{0.8}Si_{3.2}O_{10}(OH)_2$. This composition is intermediate between muscovite and phengite (their compositions are plotted in Figure 37). Table 7 gives average compositions for various ranges of total cations for both P and Q domain analyses. Ti, Na, and Mn, have been excluded from the formulae in Table 7 because they are present only in trace amounts.

Figure 34. AFK and AFM diagrams of 134 P domain analyses. In a. A = Al_2O_3/SiO_2, F = FeO/SiO_2, M = MgO/SiO_2. A + F + M = 100. In b. A = Al_2O_3/SiO_2, F = $(FeO+MgO)/SiO_2$, K = K_2O/SiO_2. A + F + K = 100. Total iron was calculated as FeO.

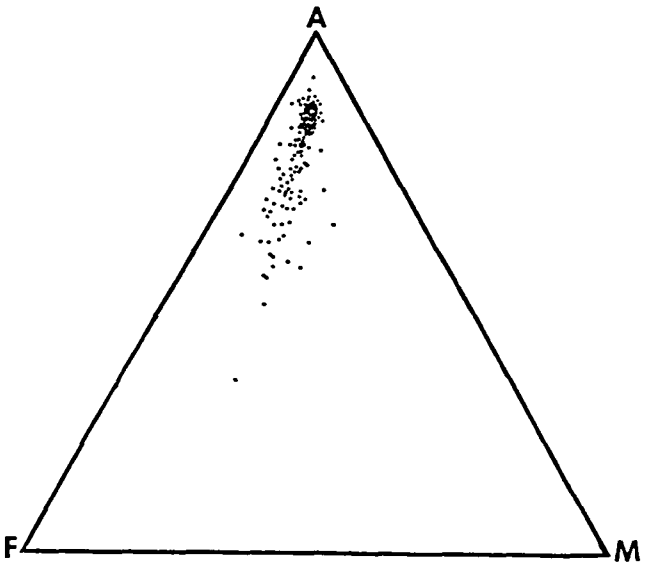

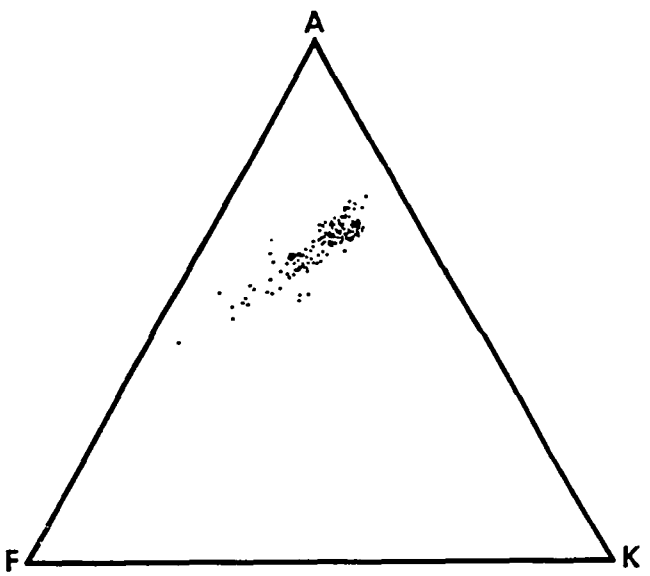

Figure 35. AFK and AFM diagrams of 63 Q domain analyses. In a. A = Al_2O_3/SiO_2, F = FeO/SiO_2, M = MgO/SiO_2. A + F + M = 100. In b. A = Al_2O_3/SiO_2, F = $(FeO+MgO)/SiO_2$, K = K_2O/SiO_2. A + F + K = 100. Total iron was calculated as FeO.

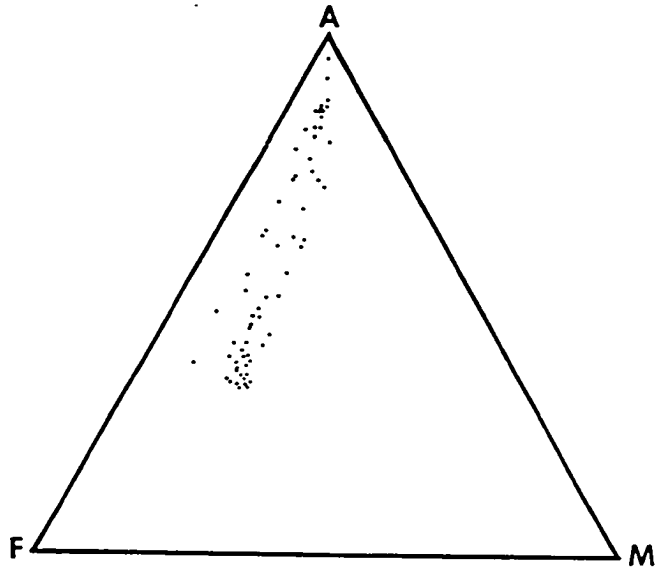

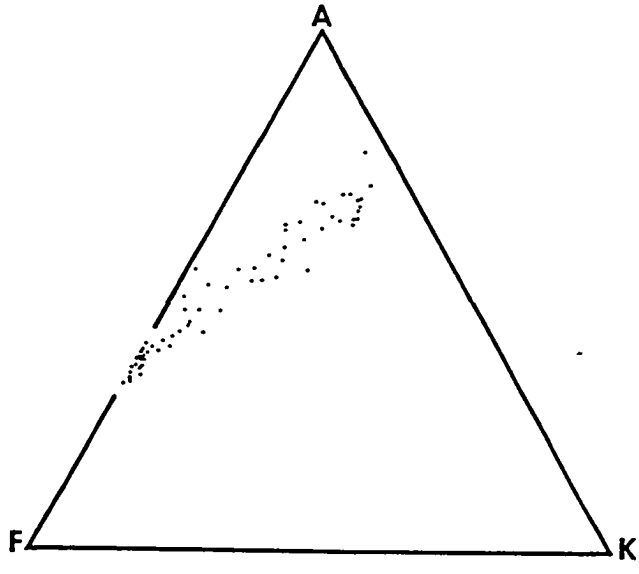

Figure 36. AFK and AFM diagrams of analyses of chlorite porphyroblasts.
In a. A = Al_2O_3/SiO_2, F = FeO/SiO_2,
M = MgO/SiO_2. A + F + M = 100.
In b. A = Al_2O_3/SiO_2, F = $(FeO+MgO)/SiO_2$,
K = K_2O/SiO_2. A + F + K = 100.
Total iron was calculated as FeO.

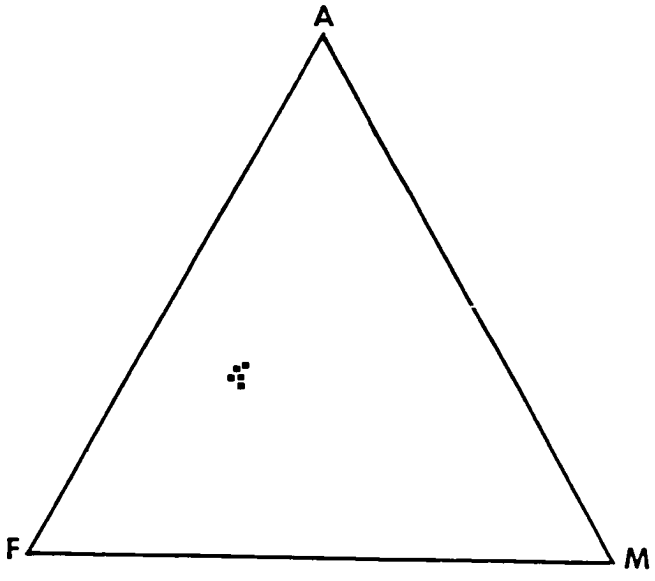

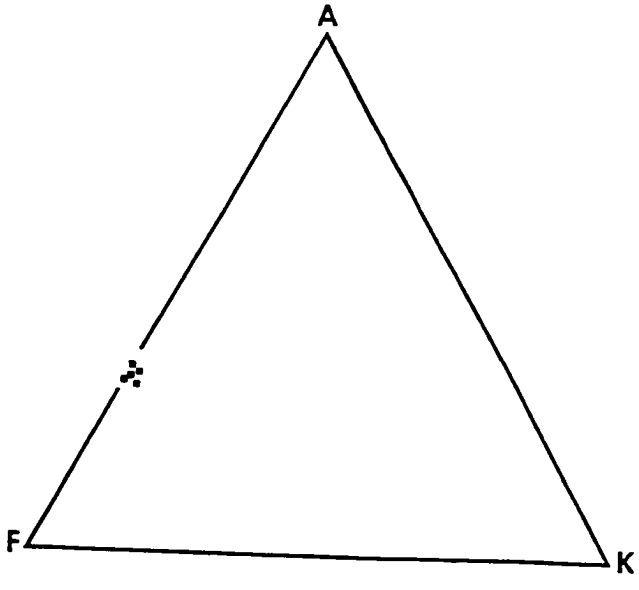

TABLE 7 AVERAGE PHYLLOSILICATE COMPOSITIONS

Average of all analyses:

a. P domain: $K_{0.9}(Mg_{0.3}Fe_{0.3}Al_{1.5})Al_{0.99}Si_{3.1}O_{10}(OH)_2$
b. Q domain: $K_{0.4}(Mg_{0.7}Fe_{1.0}Al_{1.0})Al_{1.3}Si_{2.7}O_{10}(OH)_2$

7.3 or fewer total cations per half cell:

c. P domain: $K_{0.9}(Mg_{0.3}Fe_{0.3}Al_{1.5})Al_{0.9}Si_{3.1}O_{10}(OH)_2$
d. Q domain: $K_{0.7}(Mg_{0.4}Fe_{0.4}Al_{1.5})Al_{0.9}Si_{3.1}O_{10}(OH)_2$

7.2 or fewer total cations per half cell:

e. P domain: $K_{0.9}(Mg_{0.3}Fe_{0.3}Al_{1.5})Al_{0.9}Si_{3.1}O_{10}(OH)_2$
f. Q domain: $K_{0.7}(Mg_{0.3}Fe_{0.4}Al_{1.5})Al_{0.8}Si_{3.2}O_{10}(OH)_2$

7.1 or fewer total cations per half cell:

g. P domain: $K_{0.9}(Mg_{0.2}Fe_{0.2}Al_{1.6})Al_{0.8}Si_{3.2}O_{10}(OH)_2$
h. Q domain: $K_{0.7}(Mg_{0.3}Fe_{0.3}Al_{1.5})Al_{0.8}Si_{3.2}O_{10}(OH)_2$

Figure 37. Compositions of muscovite (M), phengite (Ph), illite (I) (Bailey, 1984), ripidolite (R) Deer et al., 1975), P domain white mica (p), Q domain white mica (q), P domain average phyllosilicate (P), and Q domain average phyllosilicate (Q). A = Al_2O_3/SiO_2, F = $(FeO+MgO)/SiO_2$, K = K_2O/SiO_2. A + F + K = 100. Total iron was calculated as FeO.

Figure 37 shows the average P and Q domain white mica compositions (the averages for analyses with fewer than 7.1 cations) and the average P and Q domain phyllosilicate compositions (average of all analyses) in relation to pure muscovite, phengite, and illite (all three compositions are from Bailey, 1984) and to a ripidolite analysis given by Deer et al. (1975). Average Si content in the P and Q domain white mica grains is slightly lower than the typical phengitic muscovite found in greenschist facies pelitic rocks (Turner, 1981) and is also lower than the P domain phengitic micas reported in other slaty cleavage studies (Stephens, et al. 1979; Knipe, 1979; and Johnston, 1981).

In contrast to P domain phyllosilicates, Q domain phyllosilicates (Figs. 35a and 35b) range completely from pure white mica to pure chlorite. Many individual analyses fall within the muscovite or phengite fields, and many more fall into the range of interstratified chlorite/mica, or pure chlorite. In contrast to those seen in P domains, the interstratified grains found in Q domains range from 0 to 100 percent chlorite. Another difference between Q and P domain phyllosilicates is the chemical variation in analyses. This variation shows up not just as an increased range between phengite and chlorite, but also as an increase in scatter off either side of the line.

Chlorite found in the two types of domains cannot be compositionally distinguished from one another, nor can

they be distinguished from rare chlorite porphyroblasts. Figures 36a and 36b show that chlorite porphyroblasts plot within the compositional range of the Q domain chlorites. In both domains, fine-grained chlorite commonly falls within the compositional range of ripidolite (Fig. 38). The most notable difference between Q domain chlorites and P domain chlorites is simply that pure end-member chlorites are common in Q domains and practically non-existent in P domains.

Comparing analyses that plot near the mica end of the compositional range, there are several differences in the average compositions of P and Q domain mica grains. Figures 39 through 41 plot formula units of K, (Mg + Fe), and Si each against total cations. As in the AFK and AFM diagrams, the range in composition between white mica and chlorite is apparent. The mica grains cluster near the lefthand end of this range. Figure 39 shows that K content in P domain grains is both greater on average and is less variable than in Q domain grains. Figure 40 shows that (Mg + Fe) content tends to be somewhat higher as well as being more variable in the Q domain mica grains than in the P domain mica grains. In Figure 41, the difference between Si content of the mica grains in the two domains can be seen to be less marked than the differences in K or (Mg + Fe), but the average content in P domain grains is slightly greater than in Q domain grains.

Figure 38. Chlorites from Deer et al. (1975).

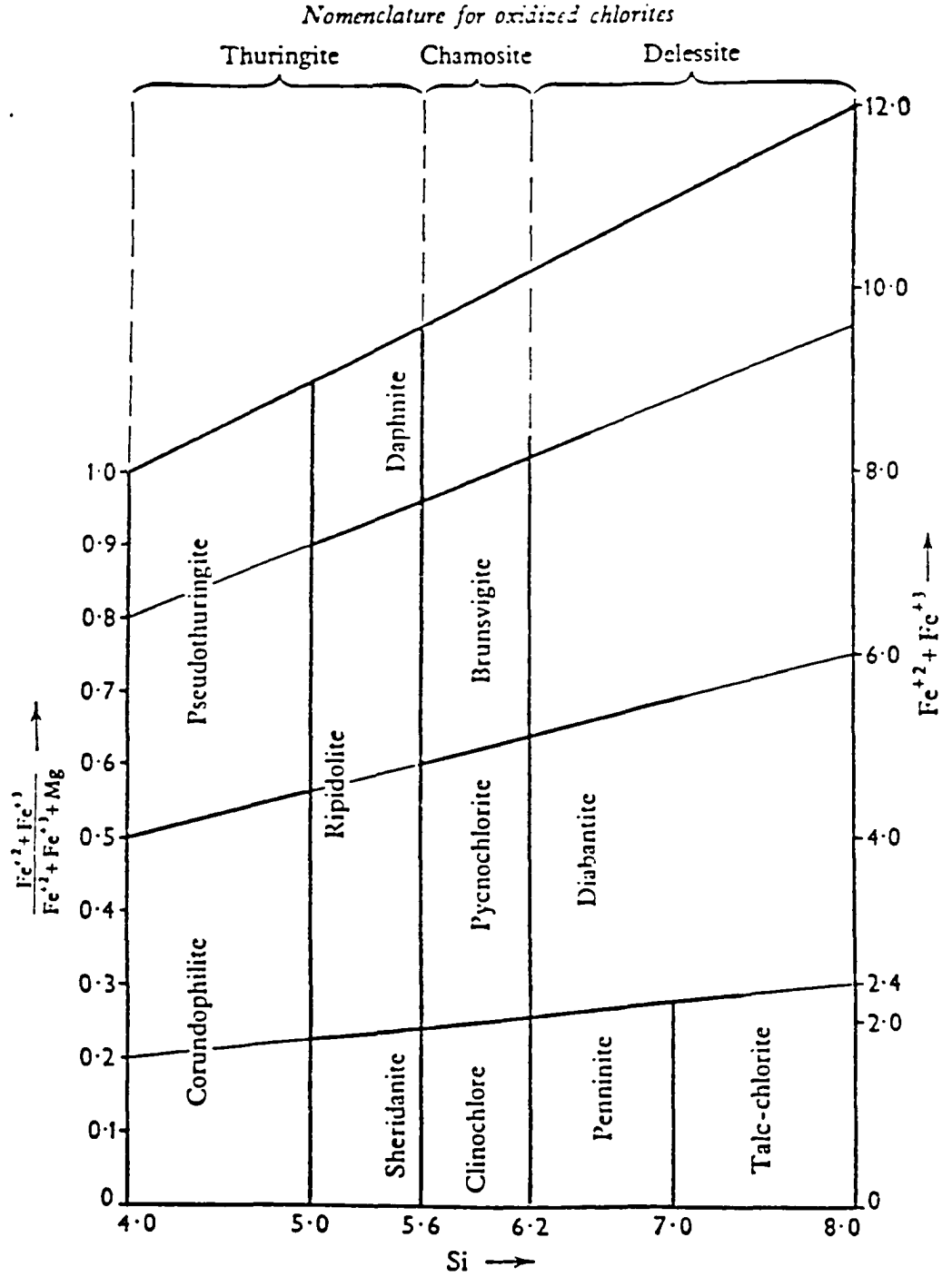

Nomenclature of chlorites and oxidized chlorites (after Hey, M. 1954, Min. Mag., *vol.* 30, *p.* 277).

Figure 39. Plot of K versus total cations for microprobe analyses of phyllosilicates. Straight lines are linear regressions for the P and Q domain analyses, with R^2 values 0.33 and 0.65, respectively.

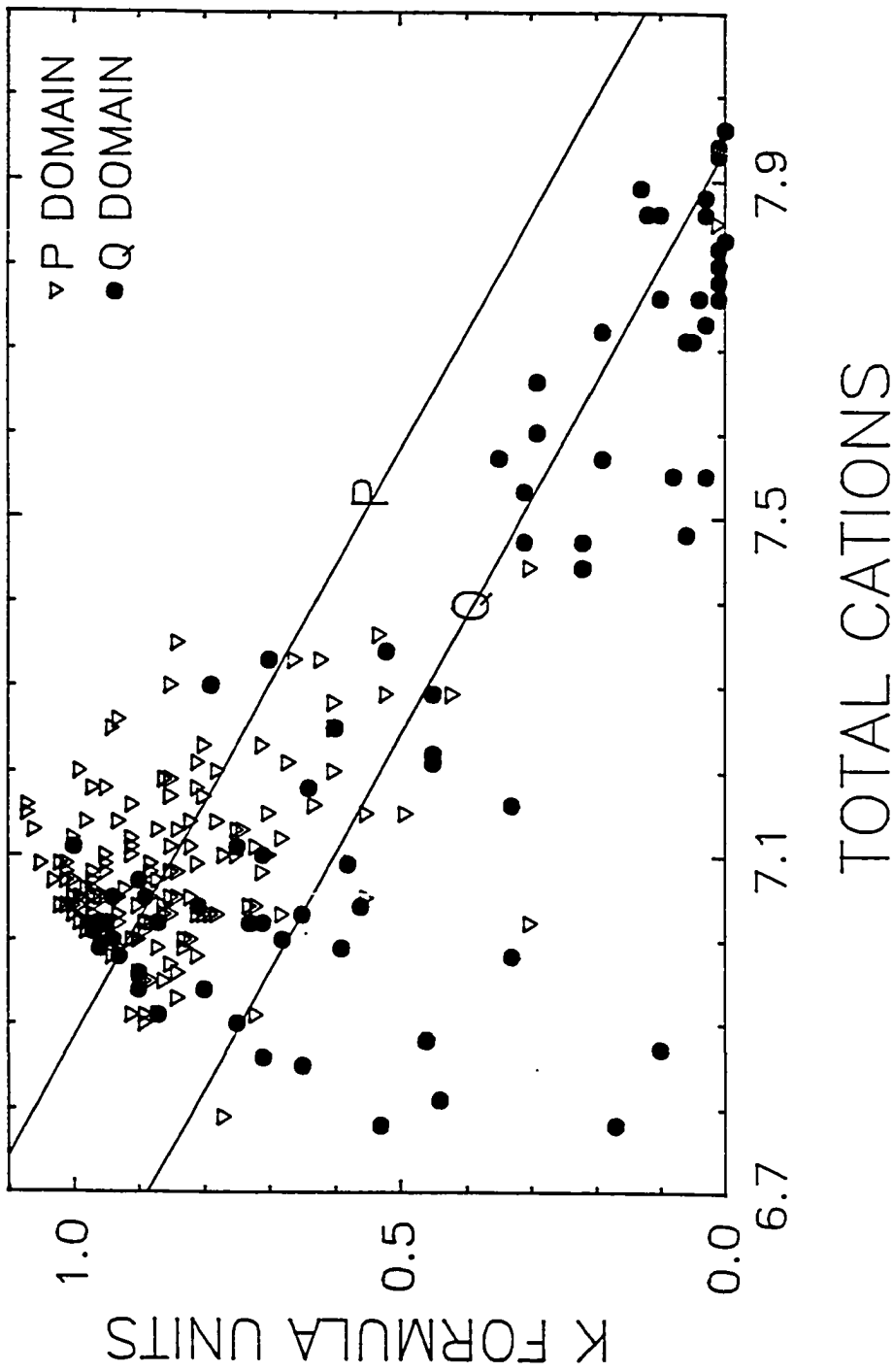

Figure 40. Plot of Mg + Fe versus total cations for microprobe analyses of phyllosilicates. Straight lines are linear regressions for the P and Q domain analyses, with R^2 values 0.70 and 0.90, respectively.

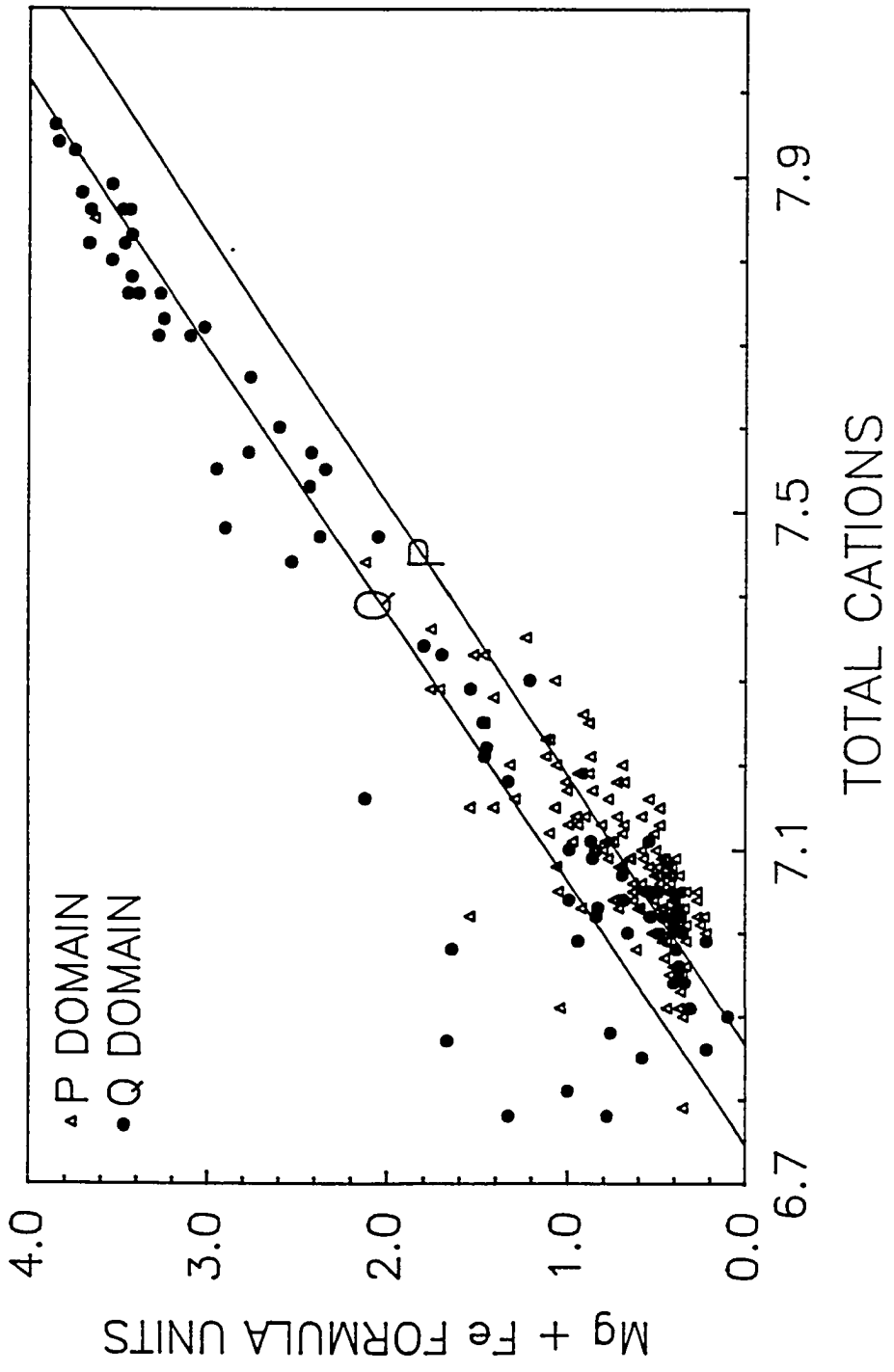

Figure 41. Plot of Si versus total cations for microprobe analyses of phyllosilicates. Straight lines are linear regressions for the P and Q domain analyses, with R^2 values 0.79 and 0.91, respectively.

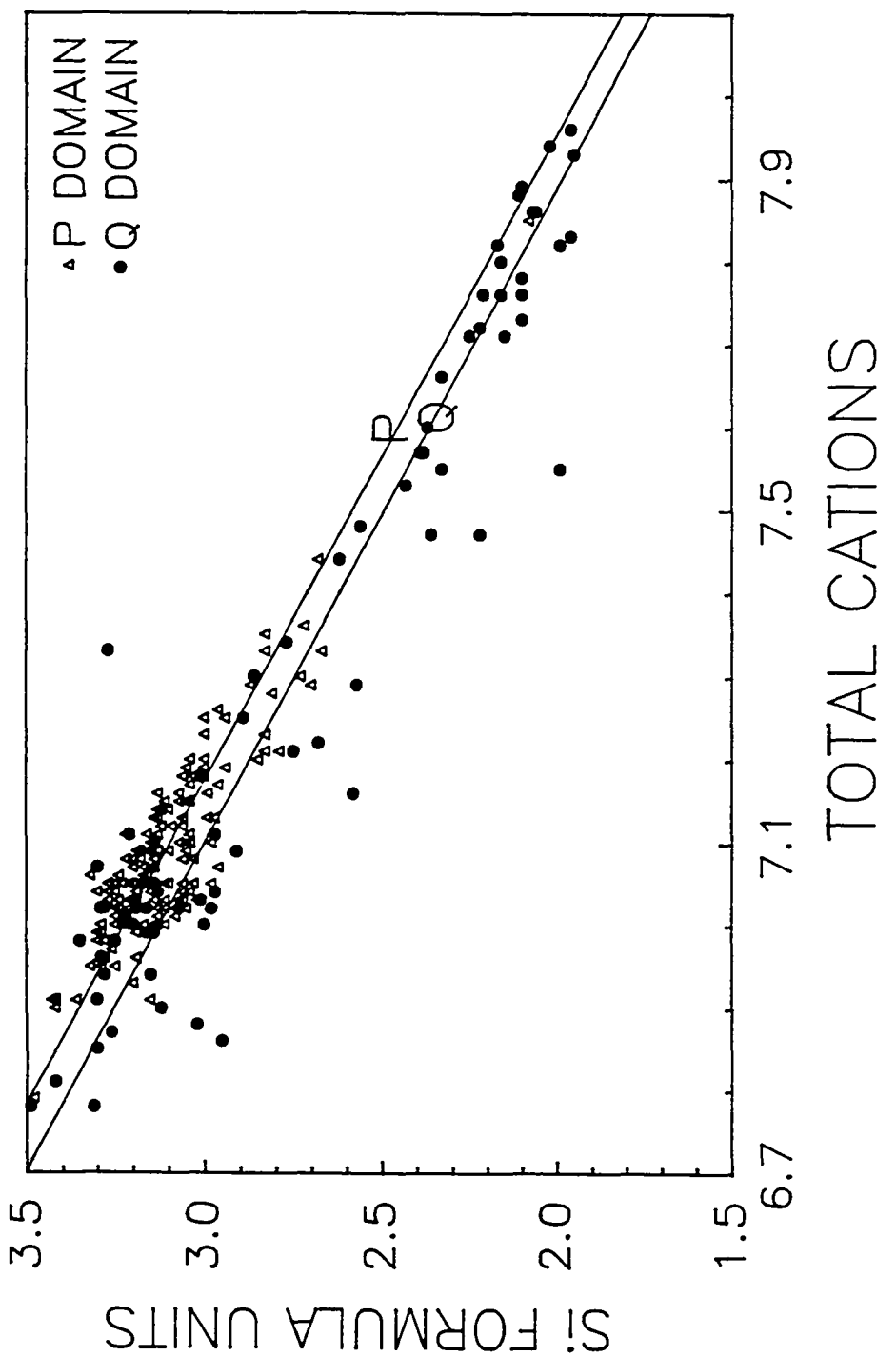

Figure 42. Plot of K versus Si for microprobe analyses of phyllosilicates. Straight lines are linear regressions for the P and Q domain analyses, with R^2 values 0.44 and 0.72, respectively.

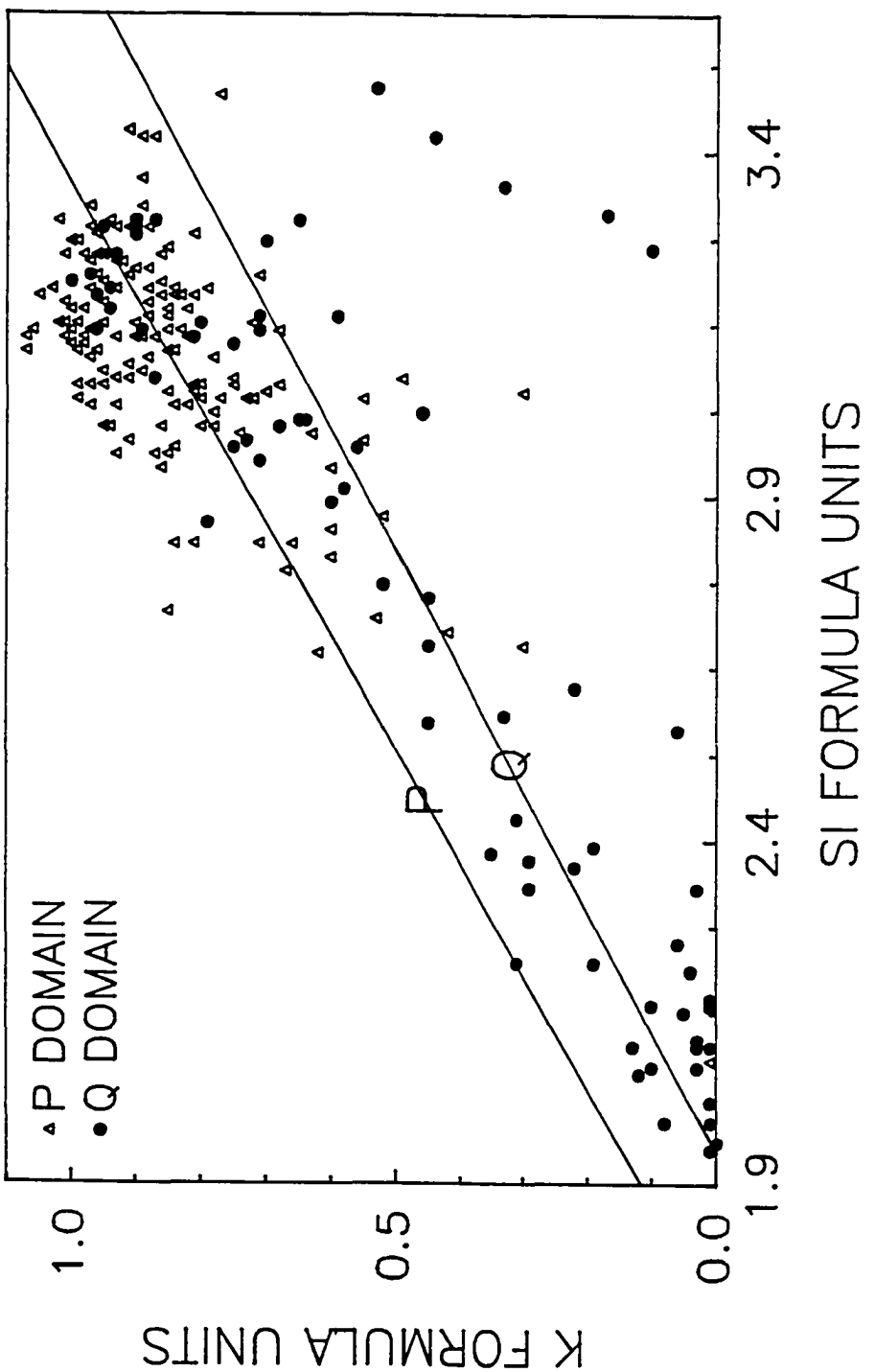

In a plot of K versus Si (Fig. 42) the K/Si ratio of P domain micas is both greater and less variable than that of Q domain micas. As in the plot of K versus total cations, there are some Q domain analyses that fall within the cluster formed by the P domain analyses. Total Al versus Si (Fig. 43) shows P domain grains to have a slightly greater average Al/Si ratio than Q domain grains have, indicating that a greater proportion of the Al in P domain grains is in octahedral sites. In a plot of Al versus total cations (Fig. 44) there is little difference in P and Q domain Al content at the mica end of the compositional range. Al is separated in Figures 45 and 46, where Al^{IV} and Al^{VI} are plotted against total cations. Figures 45 and 46 illustrate the difference in Al distribution between the P and Q domain grains suggested by Figure 43, showing that Q domain grains contain somewhat more Al^{IV} and P domain grains contain somewhat more Al^{VI}.

As shown in Figures 47 and 48, Fe content varies markedly with total cations (Fig. 47), and with total (Mg + Fe) (Fig. 48). There is no clear difference in the relationships Fe/(Fe + Mg) or Fe/total cations for the P and Q domain grains. There is, however, a small difference in the average Fe/Si and (Mg + Fe)/Si ratios of P and Q domain grains (Figs. 49 and 50), as indicated in the formulae given in Table 7. Both in these figures and in Table 7, Q domain grains are shown to have slightly higher

Figure 43. Plot of total Al versus Si for microprobe analyses of phyllosilicates. Straight lines are linear regressions for the P and Q domain analyses, with R^2 values 0.02 and 0.00, respectively.

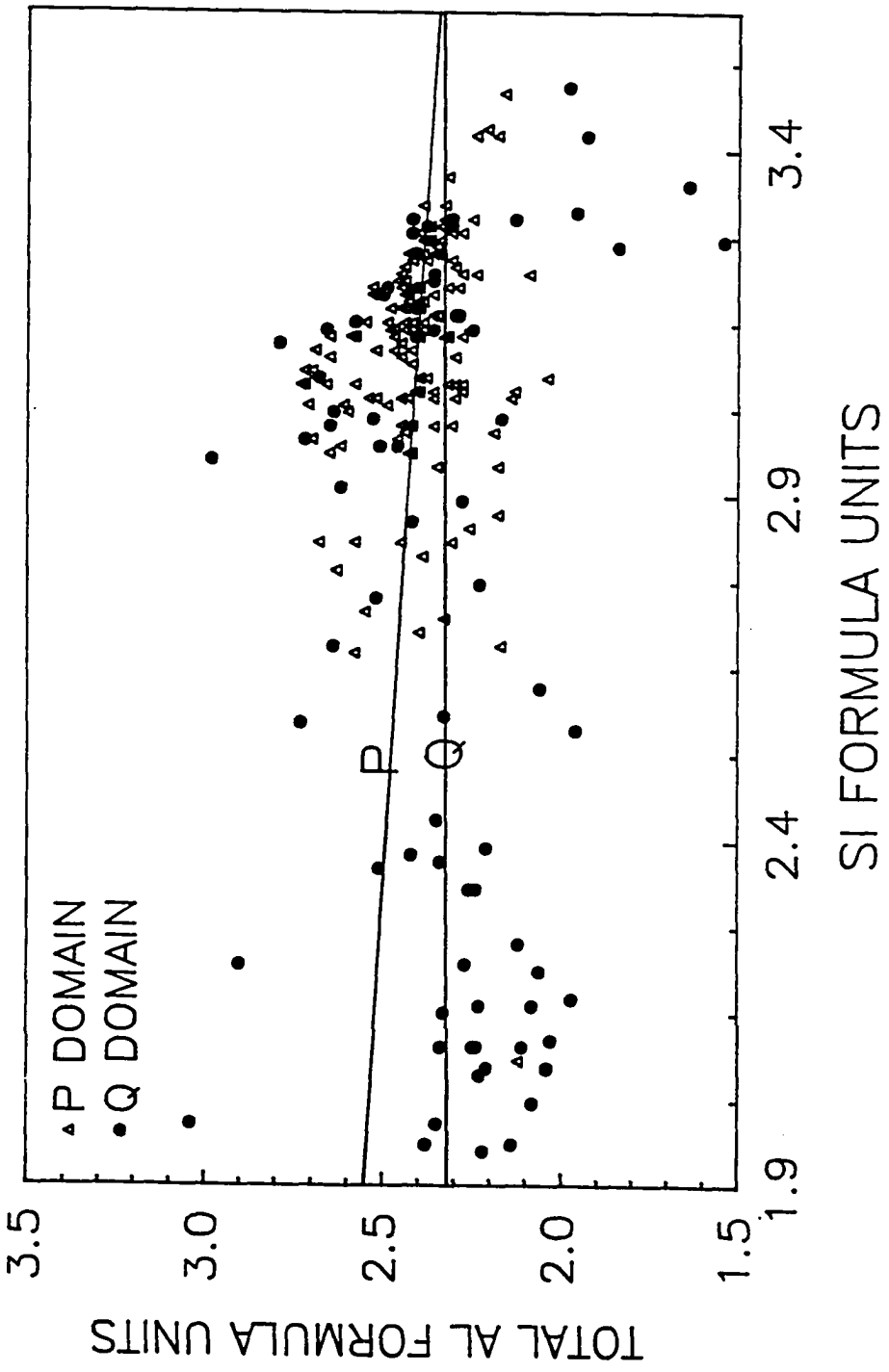

Figure 44. Plot of total Al versus total cations for microprobe analyses of phyllosilicates. Straight lines are linear regressions for the P and Q domain analyses, with R^2 values 0.02 and 0.07, respectively.

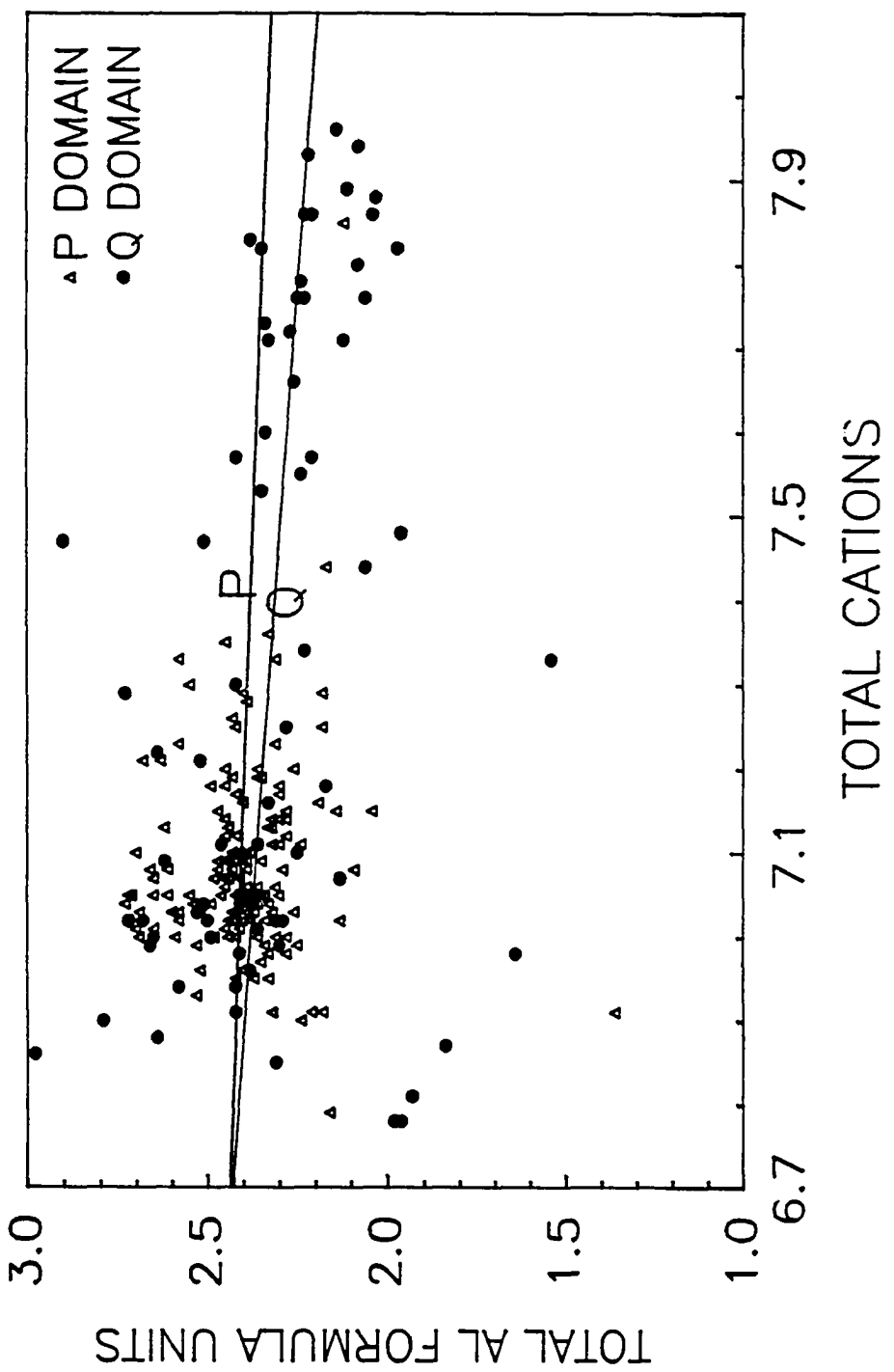

Figure 45. Plot of Al^{IV} versus total cations for microprobe analyses of phyllosilicates. Straight lines are linear regressions for the P and Q domain analyses, with R^2 values 0.79 and 0.91, respectively.

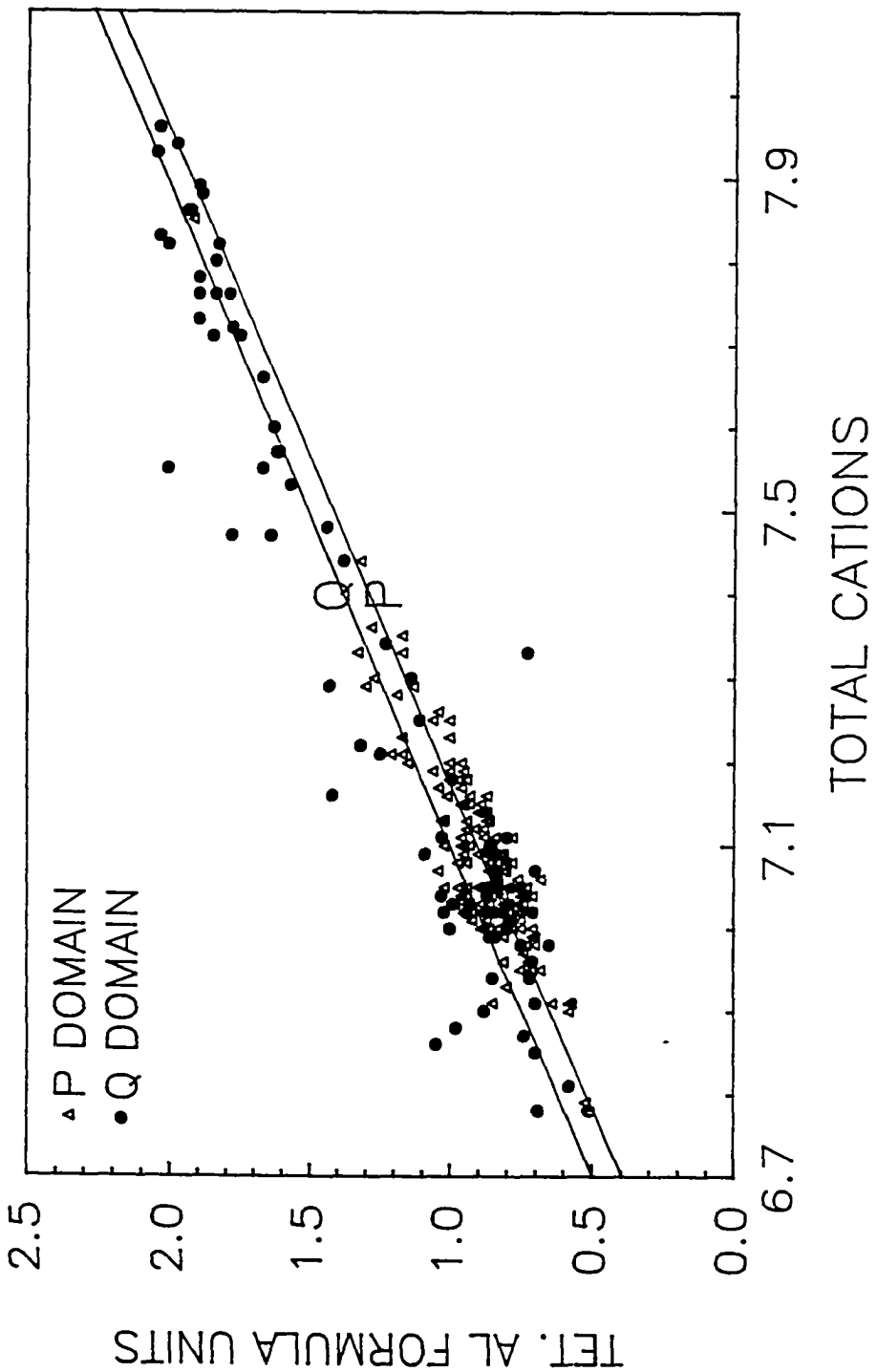

Figure 46. Plot of Al^{VI} versus total cations for microprobe analyses of phyllosilicates. Straight lines are linear regressions for the P and Q domain analyses, with R^2 values 0.70 and 0.89, respectively.

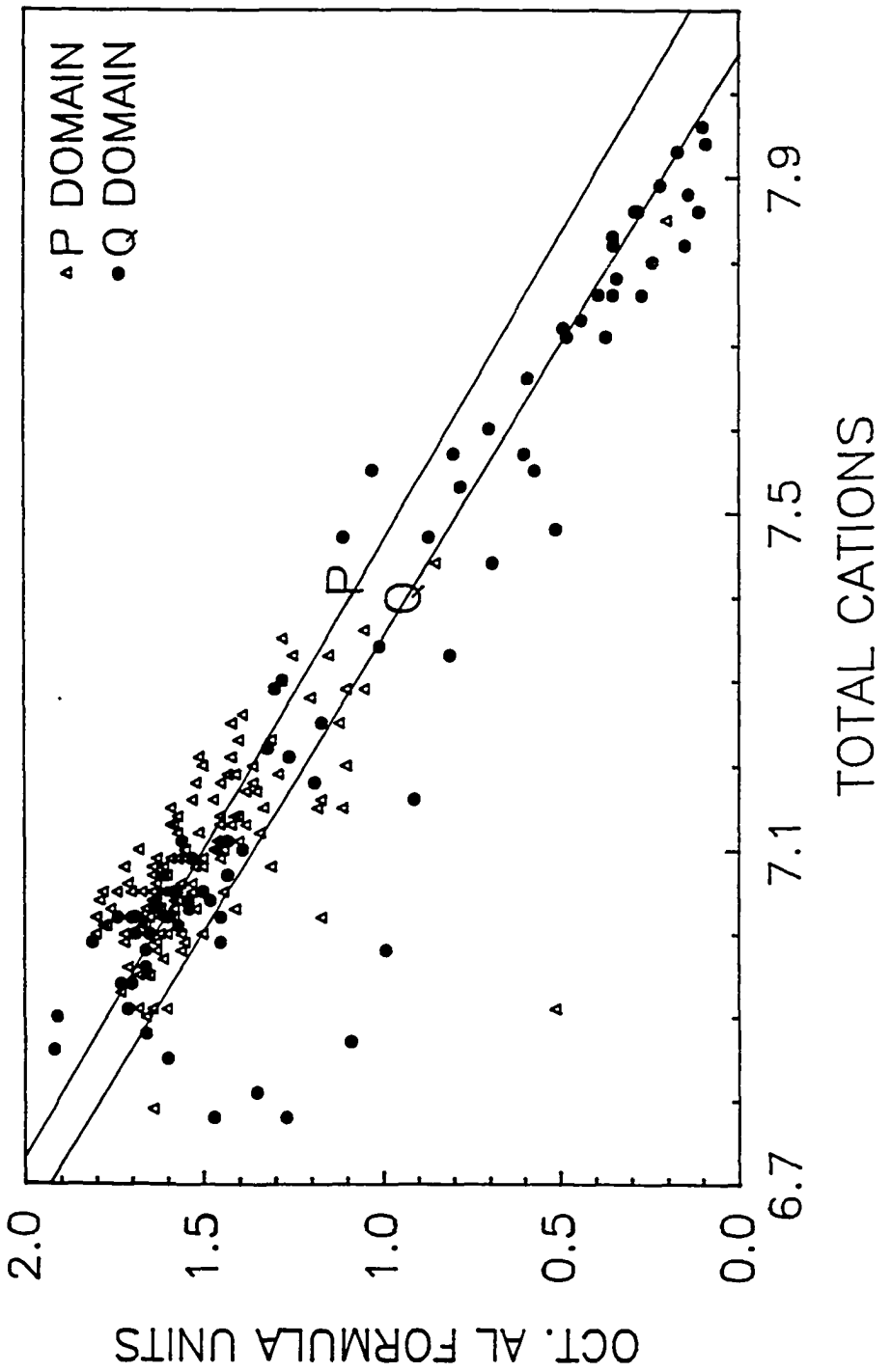

Figure 47. Plot of Fe versus total cations for microprobe analyses of phyllosilicates. Straight lines are linear regressions for the P and Q domain analyses, with R^2 values 0.78 and 0.89, respectively.

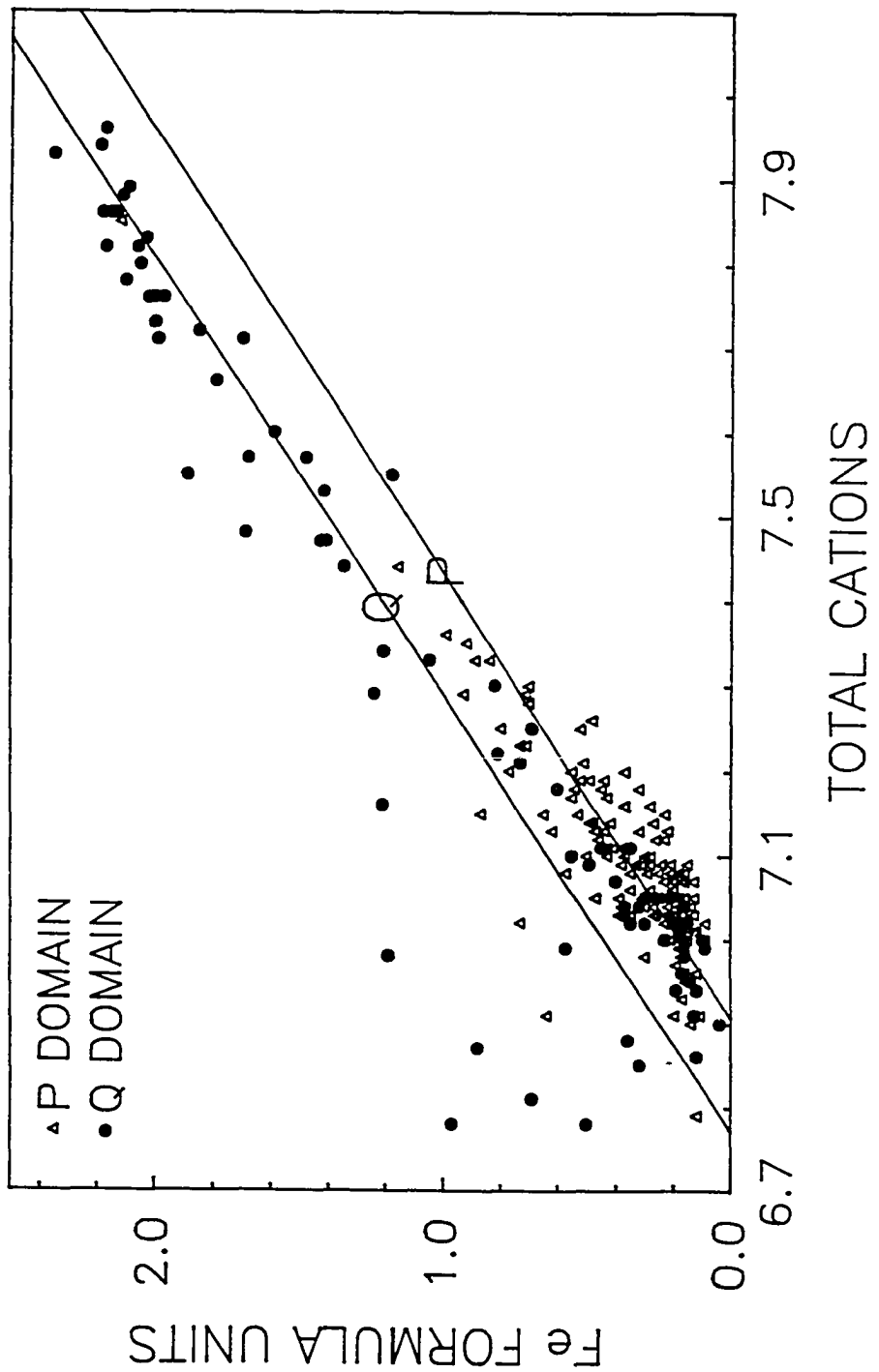

Figure 48. Plot of Fe versus Fe + Mg for microprobe analyses of phyllosilicates.

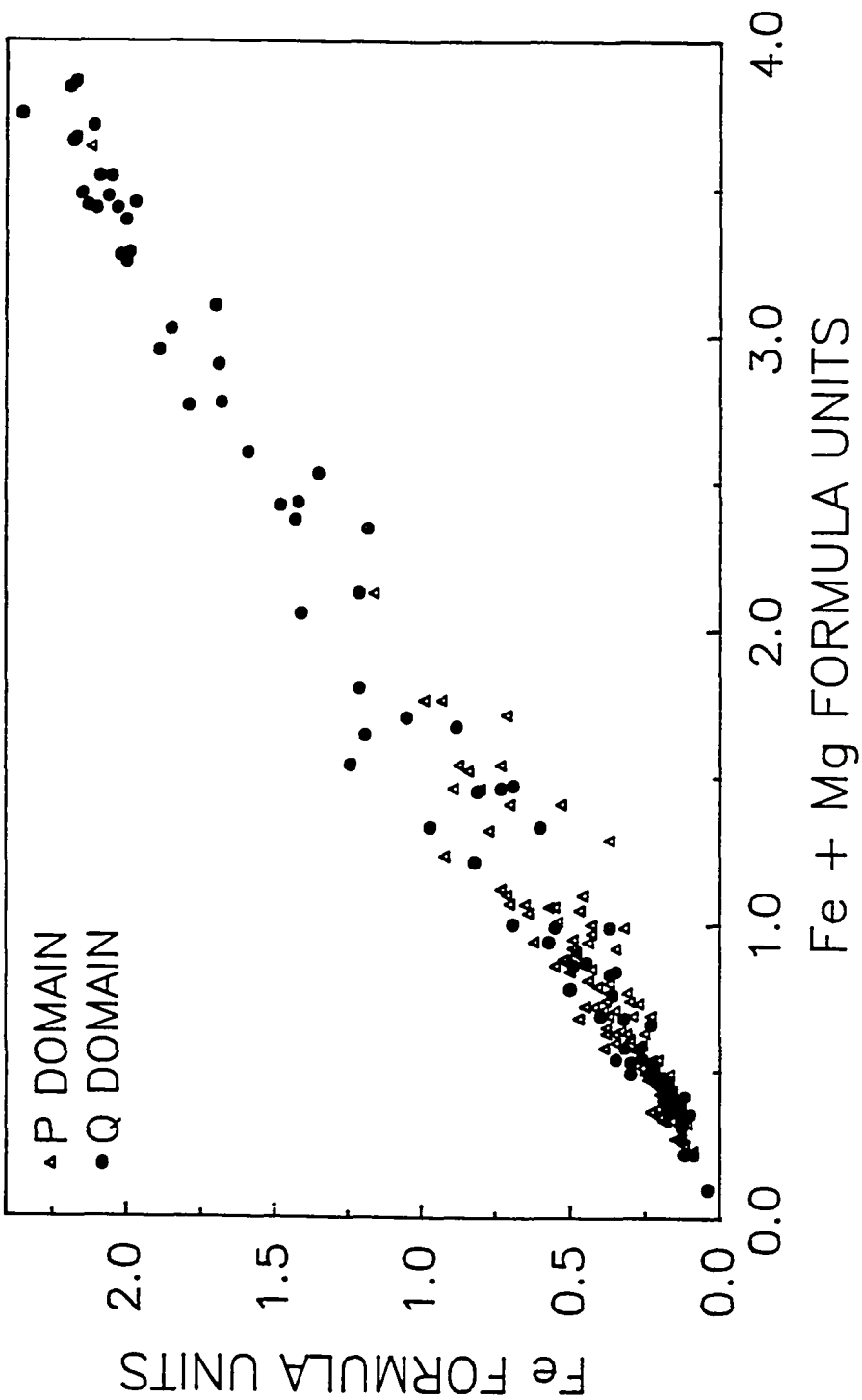

Figure 49. Plot of Mg + Fe versus Si for microprobe analyses of phyllosilicates. Straight lines are linear regressions for the P and Q domain analyses, with R^2 values 0.66 and 0.85, respectively.

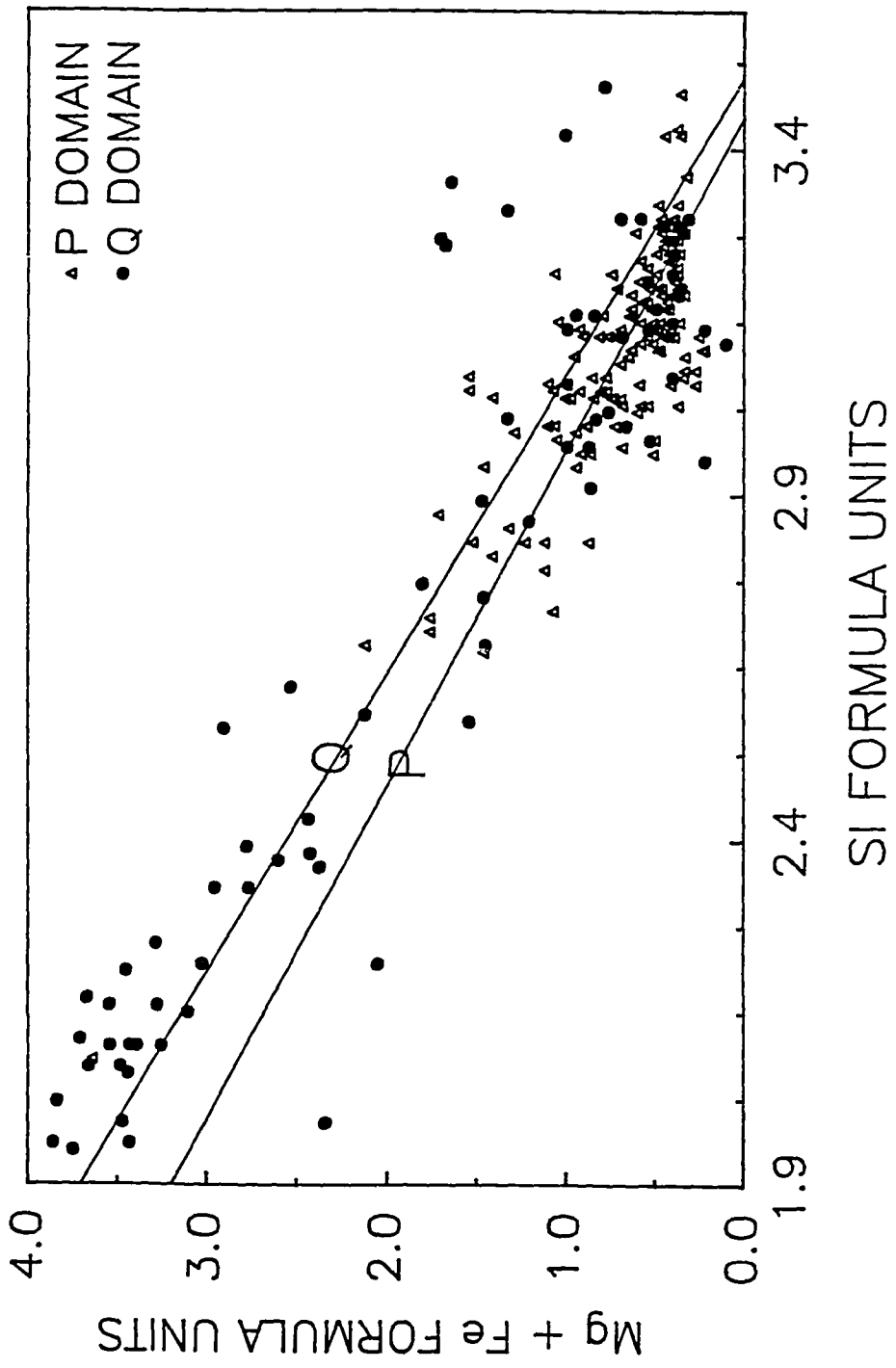

Figure 50. Plot of Fe versus Si for microprobe analyses of phyllosilicates. Straight lines are linear regressions for the P and Q domain analyses, with R^2 values 0.66 and 0.85, respectively.

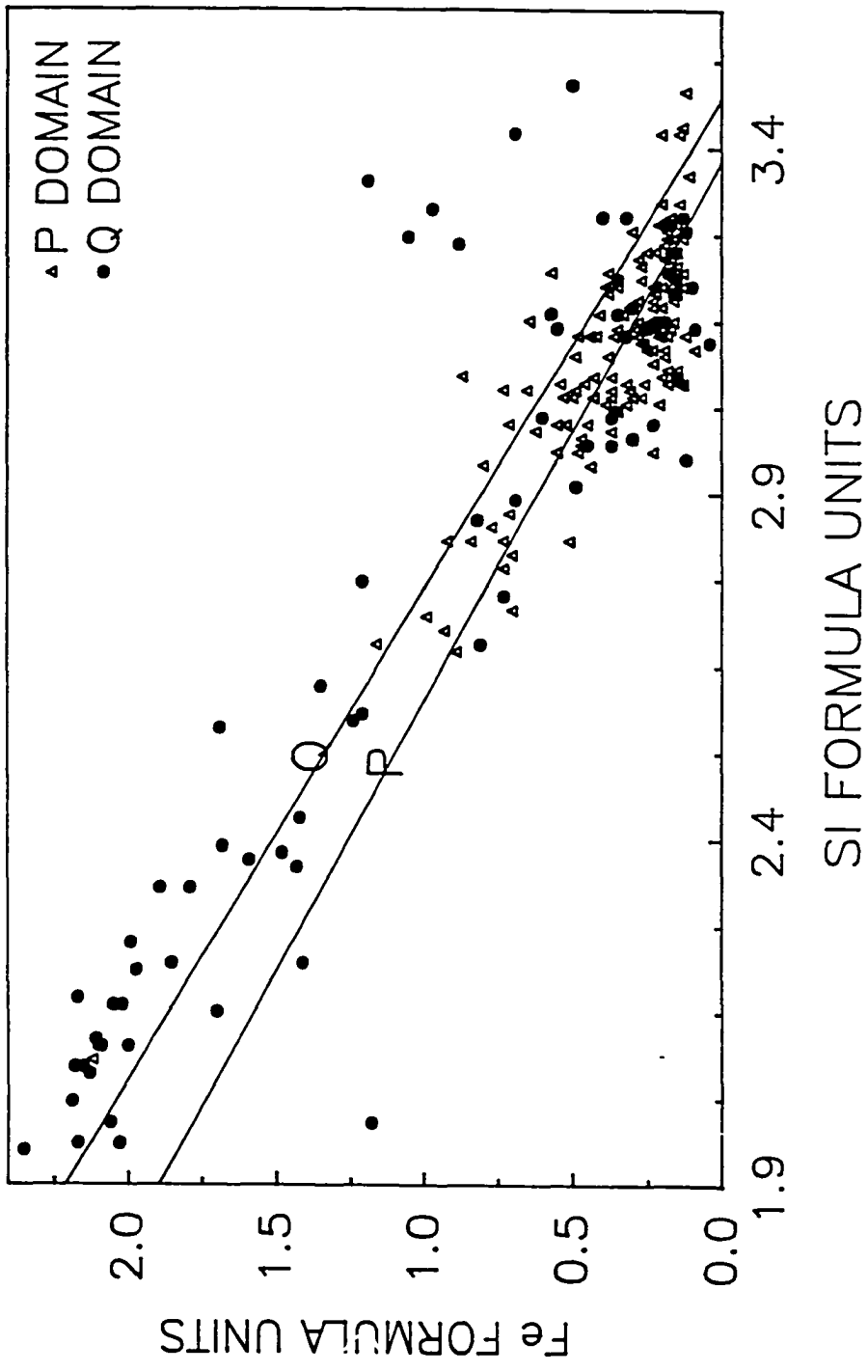

average Fe/Si and (Mg + Fe)/Si content than P domain grains have.

Discussion of Microprobe Analyses of Phyllosilicates

The microprobe analyses obtained for individual phyllosilicate grains show several differences between the average P and Q domain micas and chlorites. In general, when compared to findings from studies of the regional-scale metamorphic evolution of micas and chlorite (e.g. Weaver et al., 1984, Hunziker et al., 1986), P domain phyllosilicates are found, when compared to Q domain phyllosilicates, to have crystal chemical characteristics typical of a higher metamorphic grade. One of the most striking differences between the two groups of analyses is that P domain grains have a higher average K content, a finding consistent with the view that these grains are further along the evolutionary path from illite to muscovite than are their Q domain counterparts.

The data obtained during this study on the compositions of phyllosilicates in P and Q domains can be compared to data produced in two previous studies, those of Knipe (1979) and White and Johnston (1981). As in those studies, white mica was found to have a higher average K content in P domains than in Q domains. The trend toward more phengitic mica reported in those studies, however, was not seen here. Nor was the tendency for Q domain chlorite grains to have higher Fe contents than P domain grains

(Knipe) seen. One possibly significant difference between the rocks analyzed in both these other studies and those analyzed here is the Na content of the white micas. The considerably greater paragonite content reported in these studies than found in the Ocoee Gorge rocks may indicate a difference in metamorphic grade .

The difference in P domain and Q domain K content seen in the Ocoee Gorge rocks is not consistent with data reported in the study by Stephens et al. (1979) of coarser grained P and Q domains. The high K contents they found in Q domain grains may be due, however, to survival of K in detrital muscovites rather than to acquisition of K by these grains during or after the development of the domainal fabric.

The generally greater variability in Q domain than in P domain analyses for a fixed mica/chlorite ratio (e.g. Fig. 39) suggests that the set of Q domain grains retains evidence of a more complex history than do the P domains. This may be due to the preservation of detrital material in the Q domains. If the P domain grains have undergone a greater degree of metamorphic recrystallization than have the Q domain grains, it is not surprising that the Q domain grains would be more variable in composition. This seems particularly likely if, as is the case for the rocks studied by Stephens et al., the source area for the detrital grains experienced a higher grade of metamorphism

than that achieved during the development of the P domains.

Another significant difference between the P and Q domain phyllosilicates in this study is the overall range of mica/chlorite compositions, the Q domain analyses ranging from white mica to chlorite, and the P domain analyses ranging between white mica and an intermediate composition that is less than half chlorite. From these analyses it appears that many Q domain grains are mica/chlorite interstratifications, with no limit on the percentage of chlorite in a given grain. Interstratified P domain grains, on the other hand, appear to be limited to less than half chlorite.

The intermediate analyses that plot between chlorite and mica cannot, on the basis of probe data alone, identified with certainty as being analyses of interstratifications rather than analyses of mixtures of discrete grains of fine-grained mica and chlorite. Because of the large size of the electron beam and its associated excitation area, relative to the size of some phyllosilicate grains, it is difficult to distinguish analyses of interstratified grains from analyses of mixtures of discrete grains of fine-grained material. There are, however, several factors that indicate that many of the intermediate analyses obtained may in fact be analyses of interstratified material. One is that interstratified mica and chlorite have been reported in

studies of slates that employed techniques with greater resolution than that of the microprobe (e.g. Lee et al., 1984, 1986).

Another factor suggesting the presence of interstratified grains is that the analyses themselves have rather a peculiar compositional distribution for analyses produced by mixtures of discrete grains. The P domain analyses nearly all cluster at compositions that are less than half chlorite. Examination of Figures 39-41 shows that only very rare P domain grains exceed 7.3 total cations. If these analyses were from discrete mixtures it seems likely that there would be greater variability than this in the P domain data. Even if the P domains were made up of considerably more white mica than chlorite. there should be individual analyses where the beam fell on more chlorite than mica grains. The fairly narrow composition range in which the P domain grains cluster seems likely to be the result of a maximum limit on the percentage of chlorite present in interstratified grains.

Assuming that these intermediate analyses are in fact analyses of interstratified grains, the data suggest again that the P domain grains are typical of a higher metamorphic grade than are the Q domain grains. Weaver et al. (1984) found decreasing abundance of chlorite with increasing grade throughout the anchizone and epizone and evidence that Fe-rich chlorite was dissolving and being

replaced by phengite. Perhaps layers of chlorite might gradually either be removed from a chlorite/mica interstratified grain or might be replaced by phengite layers.

The differences seen in Figures 40 and 41 in both (Mg + Fe) and Si plotted versus total cations are somewhat difficult to explain in terms of ideal phengitic or muscovitic compositions. Ideal muscovite is lower in Si and in (Mg + Fe) than is ideal phengite. Hence, the data in Figure 40 seem to indicate that the Q domain grains are more phengitic and the P domain grains are more muscovitic, whereas Figure 40 seems to indicate the opposite. Along the solid solution between muscovite and phengite, the increase in Si, Mg, and Fe content is offset by decreasing Al in both the tetrahedral and octahedral sites. Total Al is about the same in P and Q domain grains. Q domain grains, however, are higher in Al^{IV}, whereas P domain grains are higher in Al^{VI}. This also suggests that the differences in the sets of grains are not due to differences in the percentages of phengitic and muscovitic components. A possible explanation for these differences is that Q domain grains plotting near the mica end of the total cation range may contain small amounts of interstratified chlorite. If the lower average K content of Q domain micas is due to vacancies in the interlayer cation sites, the total number of cations for an average

mica should be somewhat lower in Q domains than in P domains. Therefore Q domain grains that are mostly mica, but that contain minor amounts of interstratified chlorite, might plot at the same point along the X-axis (total cations) as P domain grains that are pure mica.

Microprobe Traverses

Brief Review of Previous Work

Two previous studies have been done on the bulk compositions of P and Q domains, but neither was a quantitative microprobe study. Holcombe (1973) obtained qualitative microprobe scan data on P and Q domains in the Ocoee Gorge rocks. These data indicate that K, Al, and Ti are concentrated in P domains, whereas Si, Ca, Mn, Mg, and Fe are concentrated in the Q domains. Stephens et al. analyzed P and Q domain material from a sandstone, using X-Ray Fluorescence (XRF) spectrometry. They found K, Ti, and Al to be concentrated in P domains.

Analytical Methods

Microprobe data on the bulk compositions of the P and Q domains were obtained using a defocussed beam to analyze a series of relatively large spots along a straight traverse. Several traverses were made, with a typical traverse line being a few millimeters long and oriented roughly perpendicular to the domain boundaries. In general, the beam width was greater than the distance between the centers of the spots analyzed, so that neighboring analyses overlap. The beam width varied somewhat from one traverse to another, but was typically about 50 microns measured parallel to the line of traverse. This beam width was great enough to ensure that any given analysis was an analysis of several grains, thus diluting

the effect of any single grain while providing data similar to that of a modal analysis. The beam shape was also varied for some traverses. For two traverses run perpendicular to domains, the beam spot shape was changed, making it elongate parallel to the domain boundaries. This served to increase the area analyzed without increasing the number of analyses that straddle domain boundaries.

The maximum count time per element was 15 seconds and the maximum count time per analysis was 15, 30, or 45 seconds, depending on whether 3, 6, or 9 elements were analyzed. Most traverses were run along a line perpendicular to domain boundaries, although two were parallel to domains, one along a P domain and one along a Q domain. Neither of these traverses showed any recognizable trends in composition and they will not be discussed further.

During each traverse, analyses were made for either three elements, K, Ti, and Mg; for six elements, Si, Al, Fe, Mg, Ti, and K; or for nine elements, the six previous elements plus Ca, Na, and Mn. These nine elements effectively outlined the distribution of all the common mineral phases. The distribution of all nine elements showed some relationship to the domain type. In particular, K, Al, and Si, were strongly related to the domainal fabric; the other elements showed a weaker relationship to this fabric.

Data

The results of all traverses are not identical, but the patterns of each are roughly the same. Much of the variation that is seen among traverses is due to the presence or absence of carbonates. In all traverses K is clearly concentrated in the P domains and must outline the concentration of K bearing mica, since no other K-bearing phases are present in the Walden Creek phyllites. Si and Al vary less than K, but they also clearly reflect the type of zone being analyzed; Q domains are relatively rich in Si, whereas P domains are relatively rich in Al. Both Si and Al are present in phases which may be concentrated in P domains and or in Q domains. Quartz and albite are concentrated in Q domains, mica is concentrated in P domains, and chlorite is common in both types of domain.

Ti tends to be somewhat concentrated in the P domains, and in places follows the K distribution very well. In other traverses, however, Ti distribution is irregular, and in traverses that cross boundaries between siltstone and phyllite layers, Ti is found to be concentrated along the layer boundaries. This bedding-parallel zone of high Ti coincides with the thin layer of opaques found along the base of many siltstone layers.

Fe and Mg both tend to be concentrated in the P domains, but their patterns of concentration do not coincide with the domain boundaries as well as do those of

K, Si, and Al. The concentration patterns of Fe and Mg are complicated because they depend on the distribution of both mica and chlorite. There is also some Mg and Fe in scattered carbonate blebs, and some Fe in pyrite. The irregularities in Mg and Fe concentration, however, do not generally correlate well with calcium concentration. In some traverses, the Fe distribution is "noisier" than that of Mg, possibly because of the presence of pervasive fine-grained pyrite or less common hematite staining.

Na distribution closely follows that of Si. Only albite, which is concentrated in the Q domains, contains Na in more than trace amounts. Ca is somewhat more concentrated in Q than in P domains, but has an irregular distribution, with large spikes signifying the presence of isolated carbonate patches. The feldspar commonly found in these rocks is pure albite, and none of the other silicates are calcium bearing. Mn is present in such small amounts that it is difficult to characterize its distribution, but it also appears to slightly prefer the Q domains, and tends to follow the Ca distribution rather closely. The only phases in which Mn has been found are the carbonates, which typically have 1-2 weight percent, and chlorite which has up to 0.5 weight percent.

Figure 51 displays a series of plots, one each for K, Al, Si, Fe, Mg, and Ti, from a six element traverse across three P domains and two Q domains. Each curve is a plot of

Figure 51. Microprobe traverse of sample OG3. Beam spot was circular and about 100 microns in diameter. X axis is traverse direction and is 3 mm long. Traverse crossed 3 P domains, each well-defined by highs in K_2O.

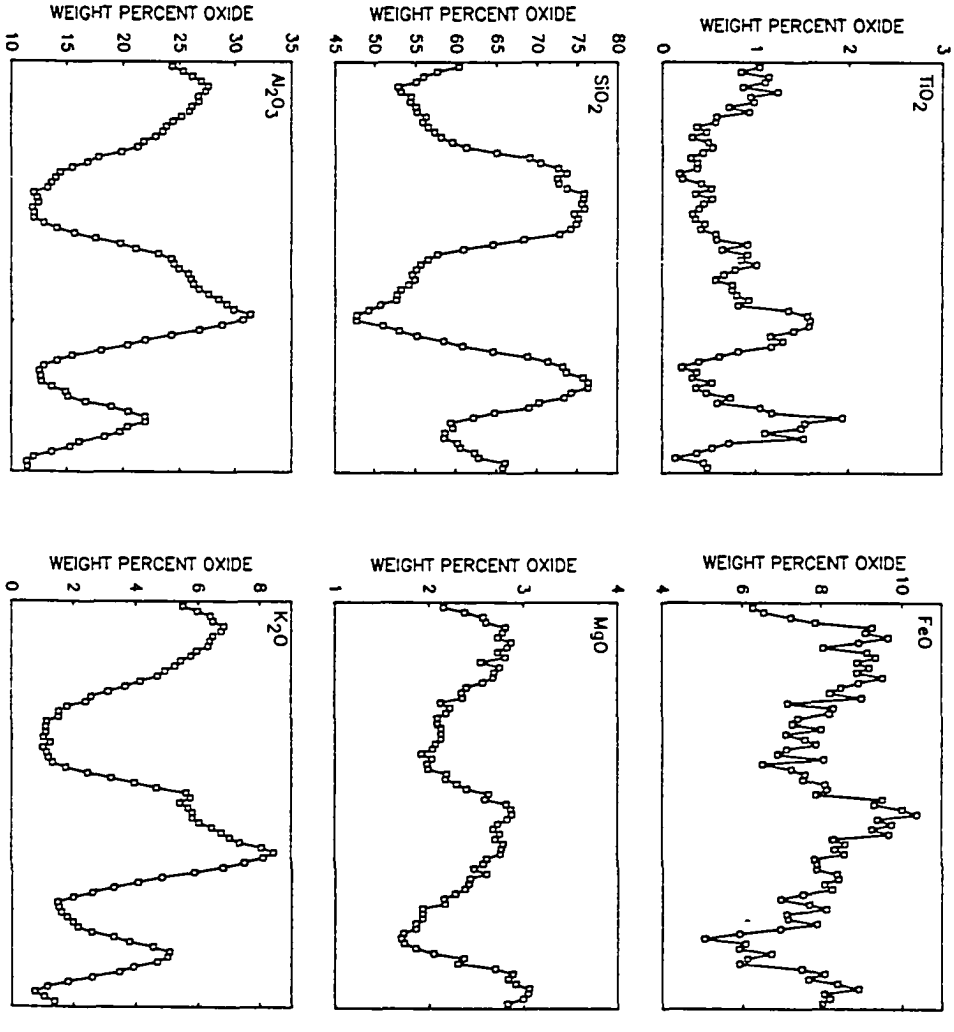

weight percent oxide versus position along the traverse. This particular traverse was made with a circular beam spot about 100 microns in diameter. The entire traverse is about 3 mm long and was confined to a siltstone layer.

K, Al, and Si exhibit the distributions seen in all traverses, e.g. Al is high in P domains and low in Q domains. Along each of these curves the boundaries between domains are clearly defined by steep slopes. Comparing the high and low values along the traverse K varies by a factor of about five, as compared to Al by a factor less than three, and Si by a factor less than two. In this particular traverse, the other three elements tend to have higher values in the P domains, although for Mg and Fe the variation between high and low values is considerably less than a factor of two. Ti shows greater variation than some of the other elements, but is present in such small amounts that a single Ti-rich grain would appear as a great increase in its concentration. In this traverse Ti follows K fairly closely.

Figures 52 and 53 are scatter plots showing Fe and Mg, respectively, versus K for the traverse shown in Figure 51. In both scatter plots there is a slight positive correlation between Fe or Mg and K, up to about six weight percent K. At higher K values, Fe decreases slightly, and Mg is nearly constant.

A 5 mm long, 9 element traverse that crosses between

Figure 52. Scatter plot of FeO versus K_2O for the microprobe traverse of sample OG3 shown in Figure 51.

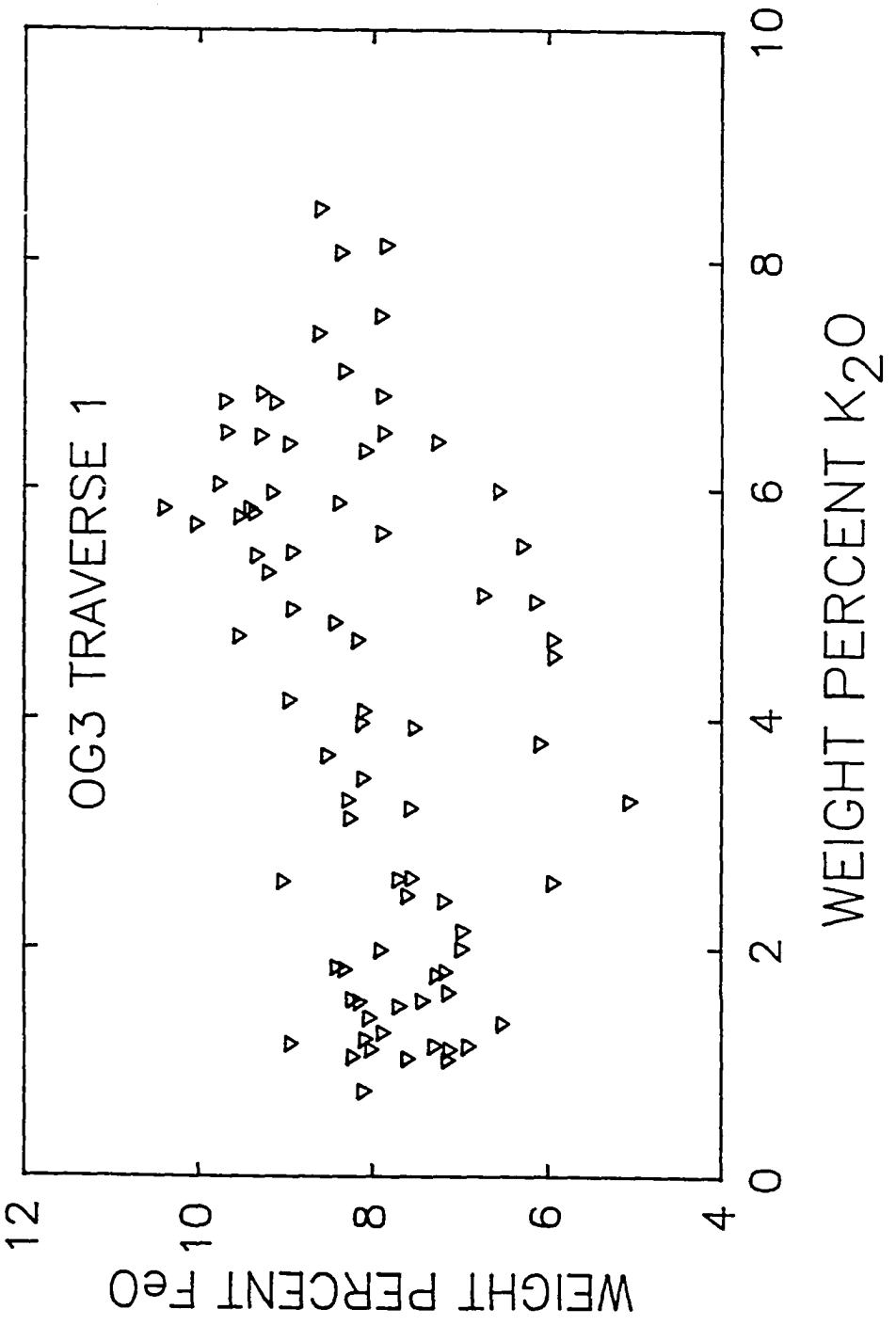

Figure 53. Scatter plot of MgO versus K_2O for the microprobe traverse of sample OG3 shown in Figure 51.

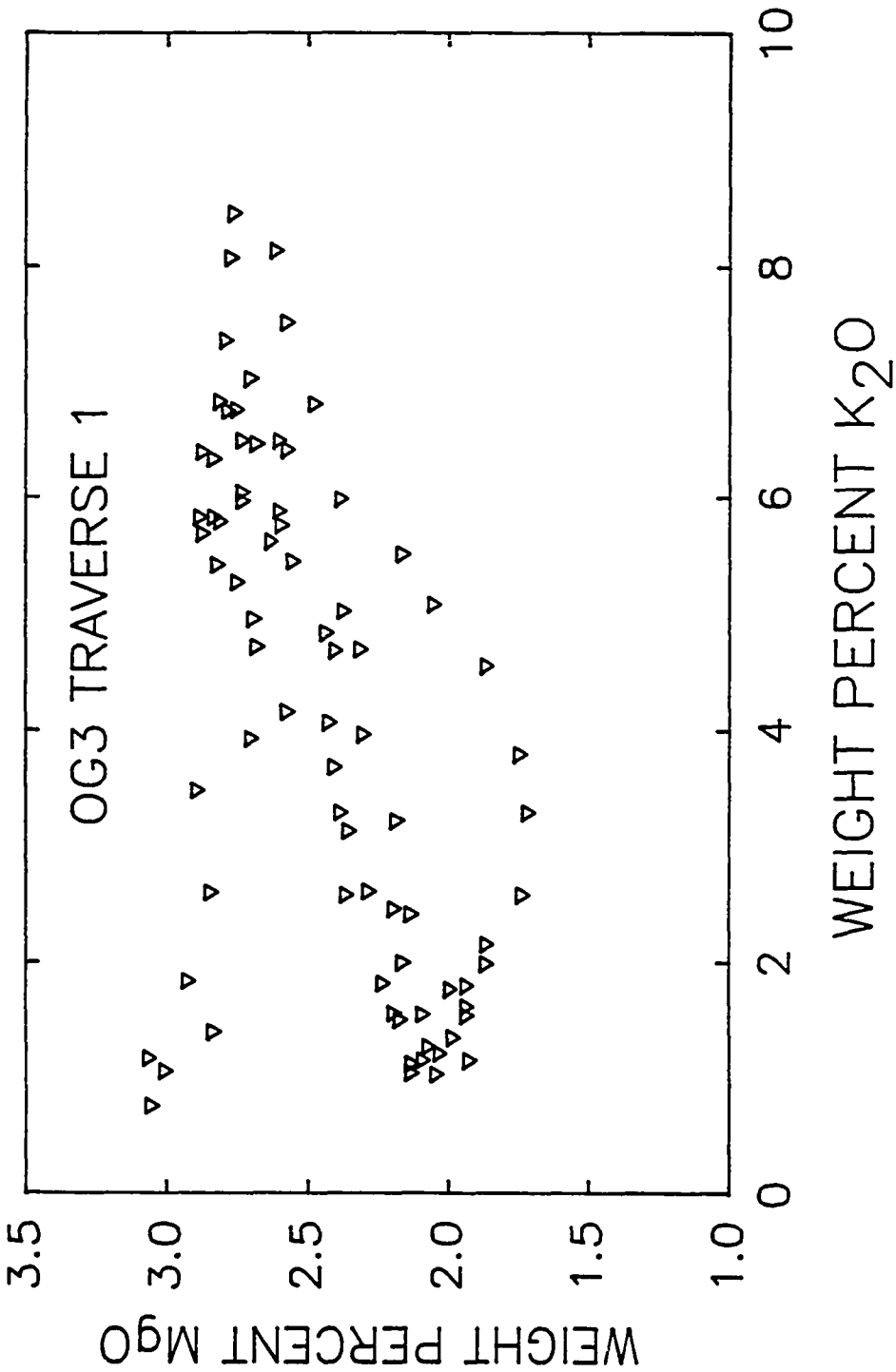

Figure 54. Microprobe traverse of sample WC26A. Beam spot was elliptical with a major axis of about 80 microns and a minor axis of about 20 microns. X axis is traverse direction and is 5 mm long. Traverse ran from siltstone (lefthand 0.5 mm), through phyllite (center 4 mm), back into siltstone (righthand 0.5 mm). Within the phyllite, it crossed 3 P domains, each well -defined by highs in K_2O.

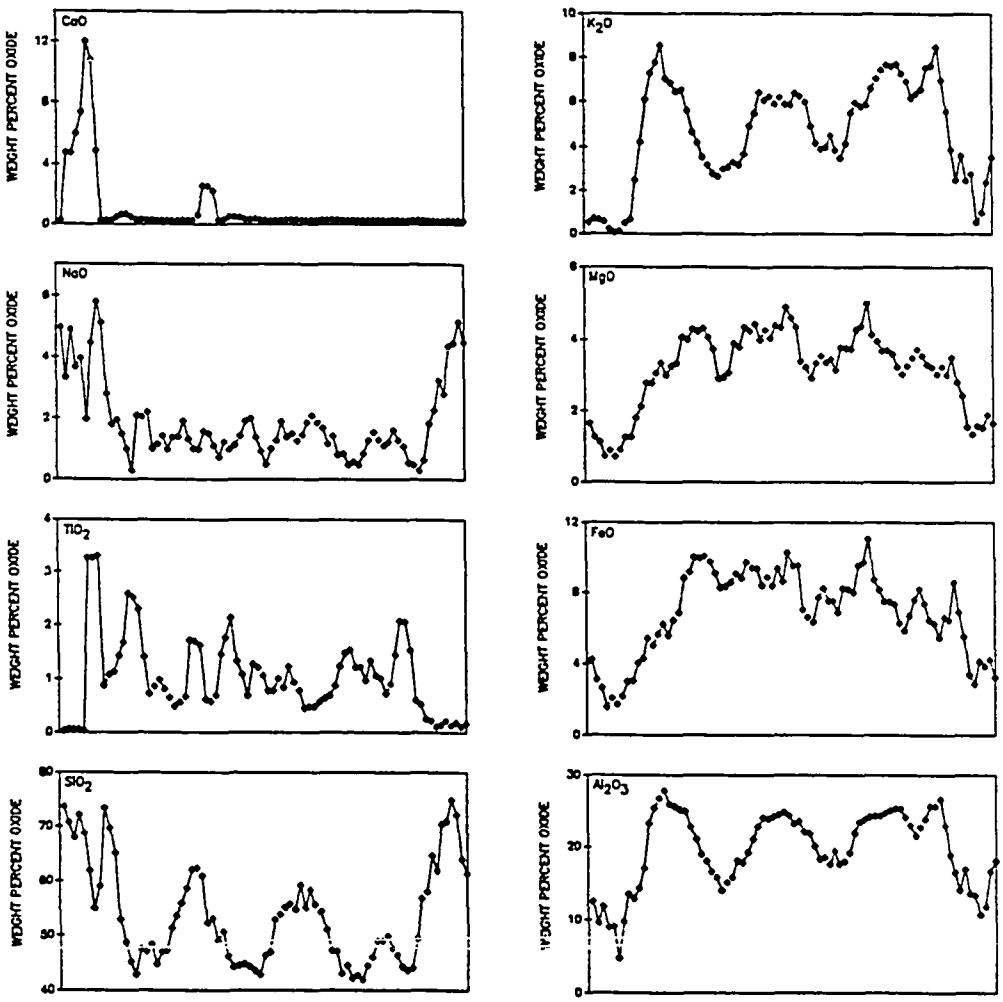

siltstone and phyllite layers is shown in Figure 54. The left and right ends of this traverse are in Q domains within a siltstone layer, whereas the central 4/5's is in a phyllite layer. The considerably greater variability seen in the analyses in the siltstone is due to larger grainsize. An increase in grainsize increases the proportional contribution of individual grains in a given analysis. For this traverse, the beam spot was elliptical, with the major axis about 80 microns long and the minor axis about 20 microns long. The spot was aligned with its major axis roughly parallel to domain boundaries.

As in the traverse shown in Figure 51, K, Si and Al all show very clear concentration patterns that mark the locations of the three P domains and two Q domains. Mg and Fe concentration, however, show a stronger correlation with bedding layer type than with domain type. They are both concentrated in the phyllite layer relative to the siltstone layer. Within the phyllite layer, Mg concentration appears to have a very slight preference for P domains. There is no discernible relationship between Fe concentration and domain type.

As in all the traverses, Na tends to be slightly more concentrated in the Q domains than in the P domains, but in this traverse it also shows a much stronger concentration in the siltstone than in the phyllite. Ti is slightly more concentrated in the P domains than in the Q

domains, but has its greatest concentration along the boundary between the siltstone and the phyllite. Ca is found only in two places along the traverse, making it difficult to generalize about its distribution. Both places are, however, in Q domains, one in siltstone and one in phyllite.

Mn distribution for the same traverse has concentrations in both Q and P domains and is shown in Figure 55, along with the same Fe, Ca, and Mg plots shown in Figure 54. These four elements are the cations found in the carbonates. The most common type of carbonate in these samples is ferroan dolomite, although calcite and rarer Mg-Fe carbonate are also present. Comparing the Mn and Ca plots in Figure 55, it can be seen that the greatest concentration of Mn coincides with the greatest concentration of Ca. The smaller Mn concentrations, however, follow the Mg and Fe distribution rather than the Ca distribution.

Scatter plots of Fe versus K (Fig. 56) and Mg versus K (Fig. 57) show both Fe and Mg to increase as K increases, up to a maximum at about five weight percent K. Above that K value, both Fe and K decrease, dropping to values of less than half their maximum values for analyses richest in K.

A traverse run across a relatively carbonate-rich sample is shown in Figure 58. There are two well-defined P domains on either end of the traverse, each neighboring two

Figure 55. Same microprobe traverse shown in Figure 54.

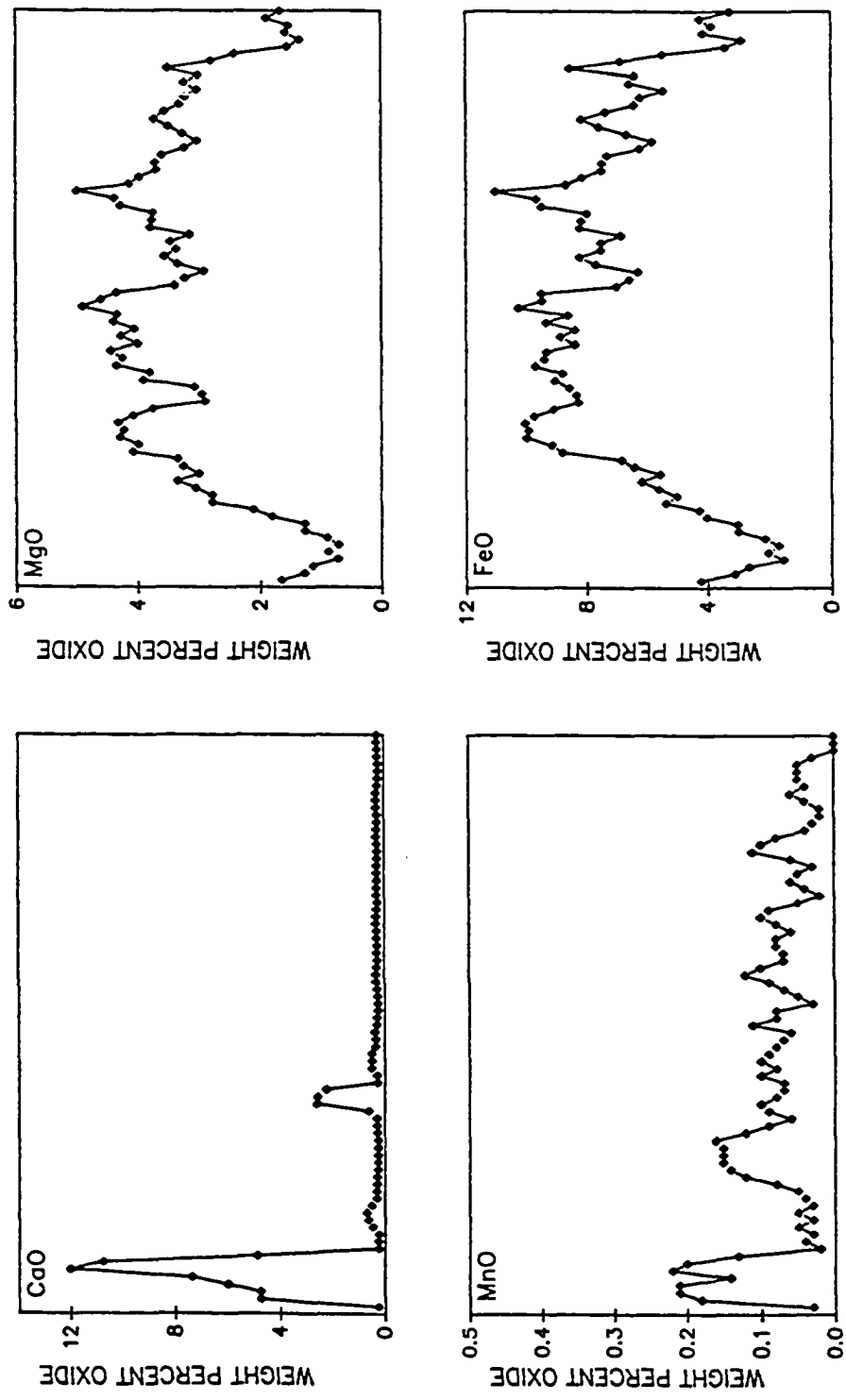

Figure 56. Scatter plot of FeO versus K_2O for the microprobe traverse of sample WC26A shown in Figures 54 and 55.

Figure 57. Scatter plot of MgO versus K_2O for the microprobe traverse of sample WC26A shown in Figures 54 and 55.

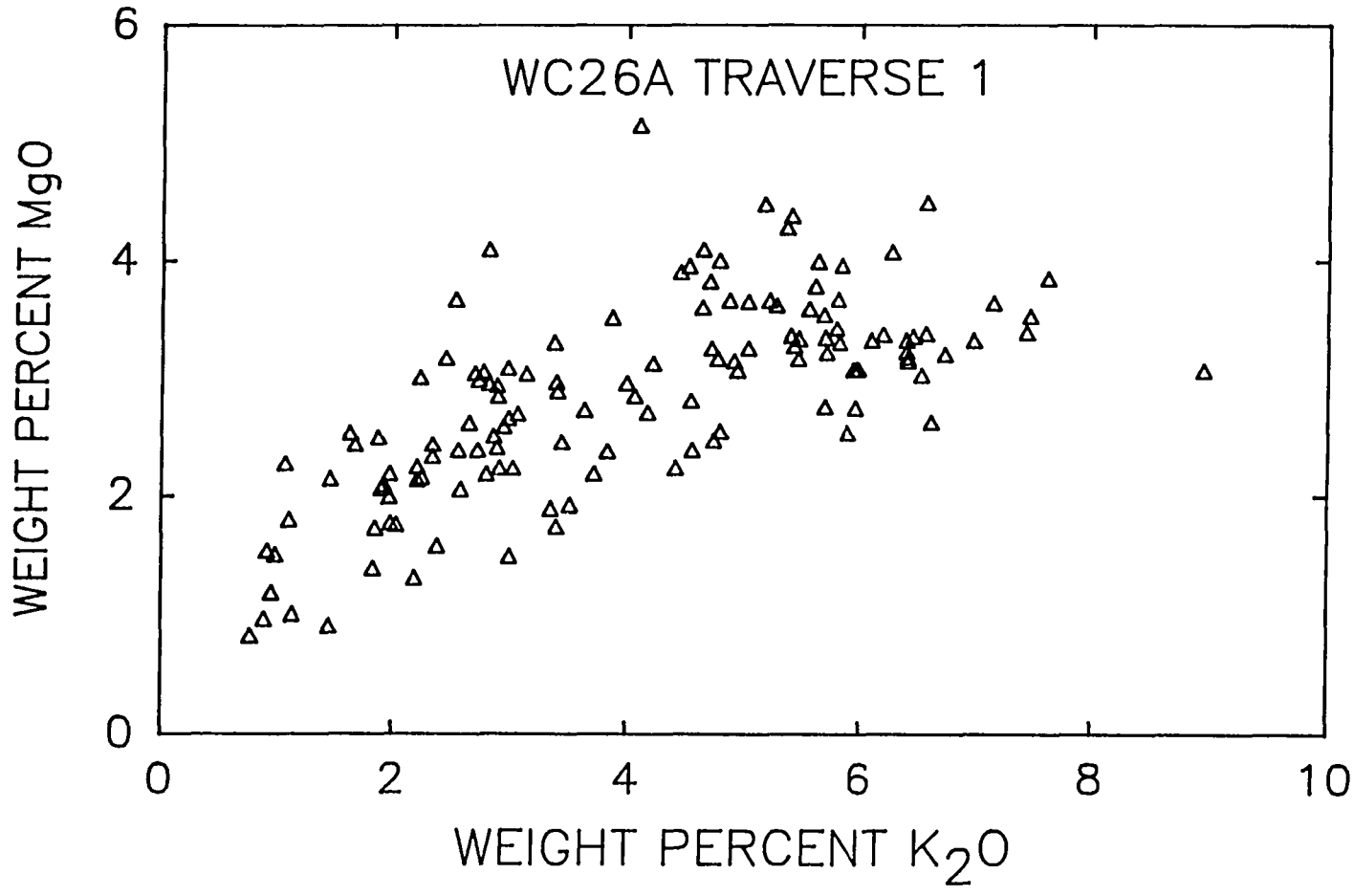

Figure 58. Microprobe traverse of sample OG17. Beam spot was elliptical with a major axis of about 100 microns and a minor axis of about 25 microns. X axis is traverse direction and is 4 mm long. The traverse crossed P domains, a patch of carbonate grains, and then 2 more P domains. The P domains are defined by highs in K_2O, the patch of carbonate by high CaO_2.

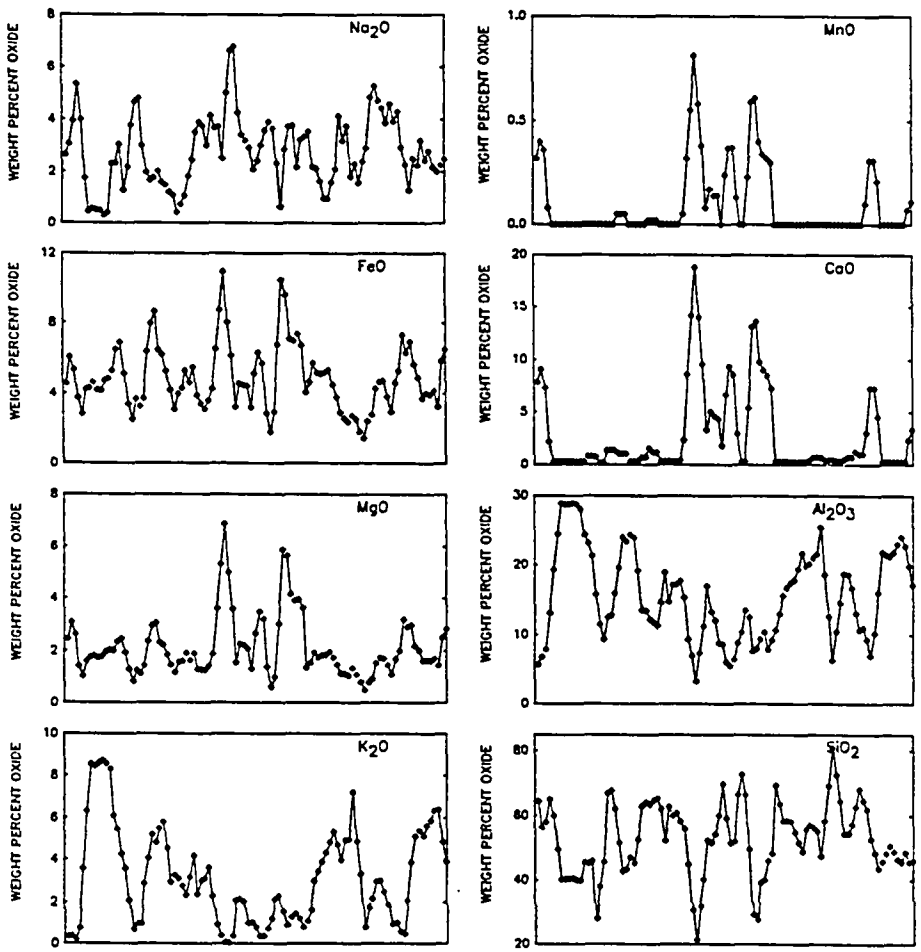

more poorly defined ones. The presence of carbonate, particularly near the middle of the traverse, obscures the domainal nature of the elemental distributions.
Near the center is a broad Q domain that envelops a carbonate patch. The positions of these domains are reflected in the distributions of K, Al and Si. The carbonate blebs are well-outlined by the Ca, Mn, Mg, and Fe distributions. In this traverse there is no apparent correlation between location of P and Q domains and concentrations of Fe or Mg. Na distribution in this traverse does not show a strong domainal pattern, but when compared to the K and Si distributions, it appears to follow the Si or Q domain distribution more closely .

Scatter plots of Fe versus K (Fig. 59) and Mg versus K (Fig. 60) are considerably different for this carbonate-rich traverse than for the carbonate-poor traverses shown in Figures 51 and 54. Both Fe and Mg are most concentrated at the lowest K values. They decrease steadily as K increases up to about six weight percent K. Above that K value Fe and Mg are roughly constant.

Discussion of Traverse Data

The compositional data generated during the microprobe traverses made perpendicular to the domainal fabric reveal several interesting features. An obvious observation is that the K distribution seen in every traverse clearly indicates that white mica, the only K-bearing phase

Figure 59. Scatter plot of FeO versus K_2O for the microprobe traverse of sample OG17 shown in Figure 58.

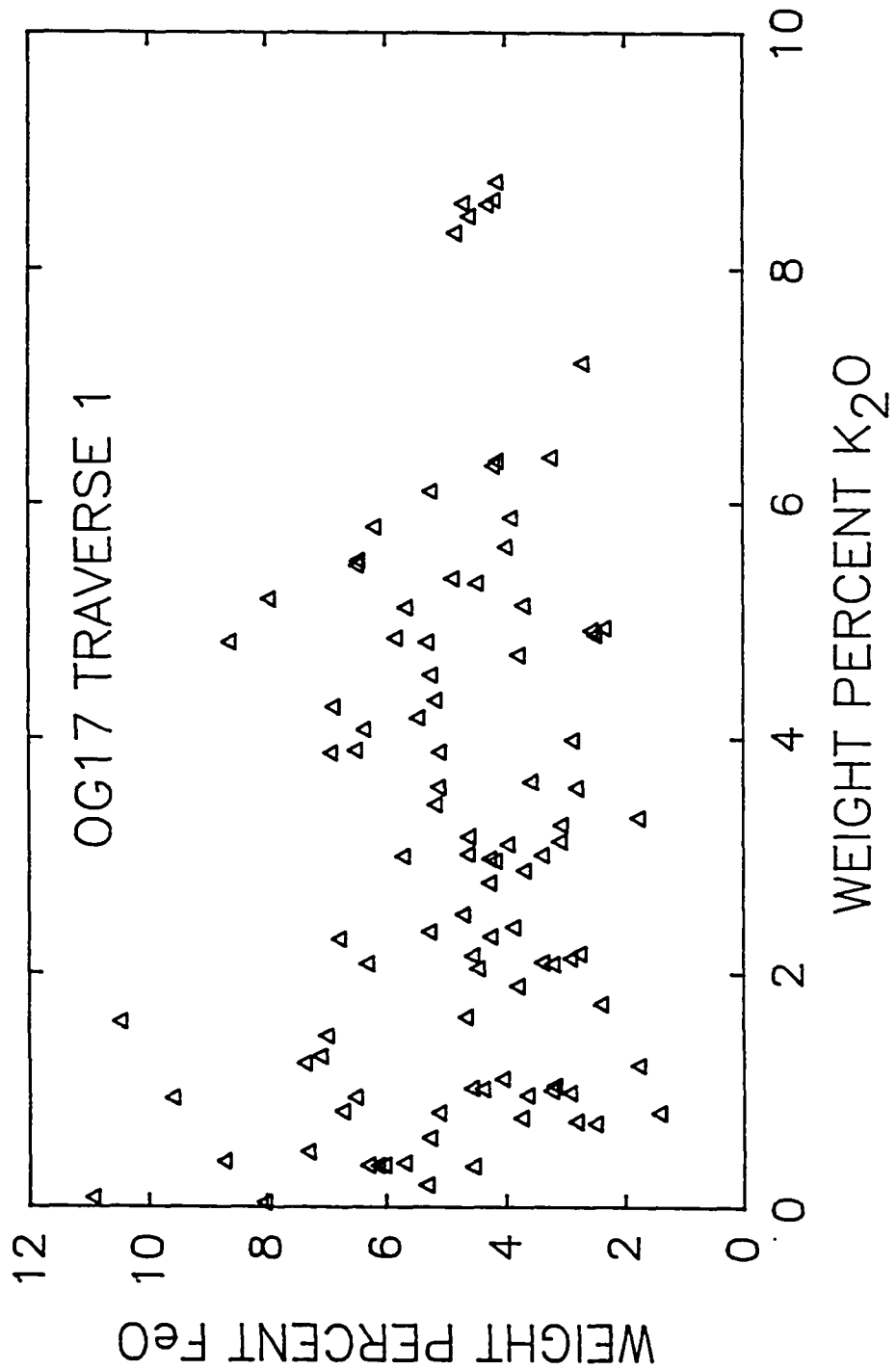

Figure 60. Scatter plot of MgO versus K_2O for the microprobe traverse of sample OG17 shown in Figure 58.

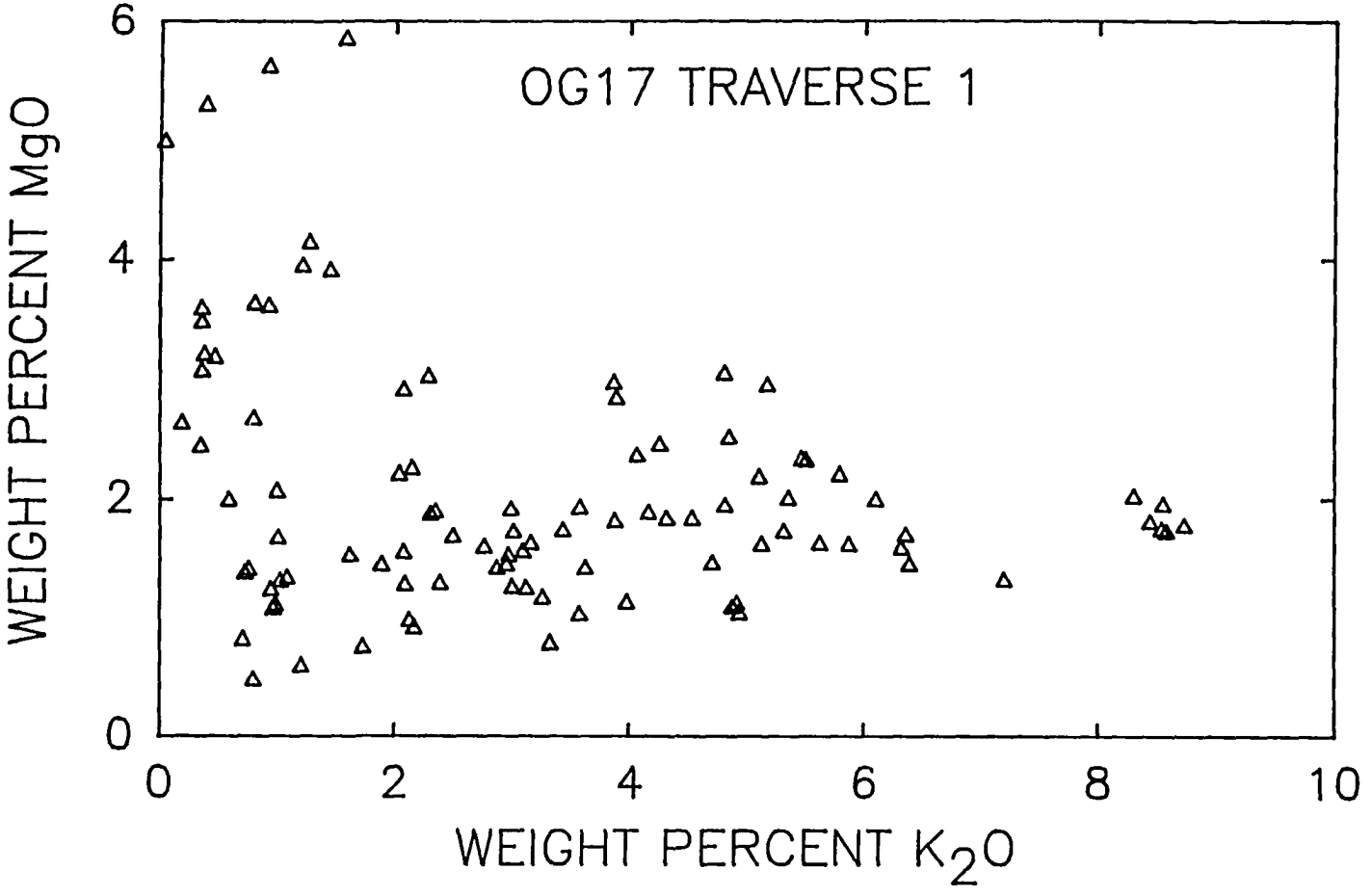

present, is concentrated in the P domains. The distribution of chlorite, the other common phyllosilicate, is less obvious, but the traverse data suggests that it is more concentrated in Q domains than in P domains. Because there are no elements that are unique to chlorite there is, however, no straightforward way to read chlorite distribution from the traverse plots.

In the absence of carbonates, two elements that are generally more concentrated in chlorite than in any other phase are Fe and Mg. There should therefore be some relationship between concentrations of these elements and concentrations of chlorite. The difficulty, however, is in determining how great their concentrations must be before they signify chlorite concentration. The Mg and Fe plots shown in Figure 51 show a slight tendency for these elements to be concentrated in P domains. In the traverse plotted in Figure 54, however, the domainal nature of these concentrations is less obvious, and in the traverse plotted in Figure 55 they correlate not with K and P domain distribution, but with Ca and Mn concentrations.

Both Fe and Mg are present in white mica, as well as in chlorite and carbonates, if in smaller amounts. Strong concentrations of K should therefore be accompanied by moderate concentrations of Fe and Mg even where no chlorite is present. In other words, if mica were concentrated in P domains, chlorite were uniformly distributed between P and

Q domains, and there were no carbonate, there should be concentrations of Mg and Fe in the P domains. Even if the volume of chlorite was slightly lower in P domains than in Q domains, there might still be a slight concentration of Fe and Mg in P domains, if there were a great enough concentration of white mica in P domains.

The fact that in only one (Fig. 51) of the three traverses shown is there a clear concentration of Mg and Fe in P domains indicates that only in this traverse is there any possibility that chlorite concentration accompanys mica concentration. Even in this traverse the increase in Fe and Mg in the P domains may be due primarily to mica concentration rather than to chlorite concentration. The five-fold difference in K concentration found in P and Q domains here (Fig. 51) should be accompanied by a five-fold difference in the amount of Mg and Fe in white mica in the two domains, assuming the composition of white mica is roughly the same in the two domains. The fact that Fe and Mg are concentrated by a factor of less than two suggests that there may actually be somewhat less chlorite in the P domains than in the Q domains in this traverse.

Because the mineralogy of these samples is fairly simple it is possible to use data from the traverses to estimate the relative proportions of chlorite and mica in the domains. To make this estimate it is first necessary to calculate how much of the Al in a given analysis is tied

up in albite, the only non-phyllosilicate Al-bearing phase common in these samples. This has been done by using the amount of Na, which is generally present only in albite, to calculate the amount of albite for a given analysis. The Al accounted for in the albite has been subtracted from the total Al, and the remainder partitioned between mica and chlorite. K is only found in mica, so the average end-member P domain mica composition (average of P domain analyses with less than 7.1 cations per half cell formula) was used with the K data to calculate the amount of mica present in each analysis along the traverse. Finally the Al unaccounted for in albite or mica has been used to calculate how much chlorite is in each spot analyzed. The chlorite composition used in this calculation is that of end-member Q domain chlorite.

Figure 61 shows the estimated proportions of chlorite and mica along the traverse shown in Fig. 54. Again, both ends of the traverse are in a siltstone layer and the remainder of the traverse crosses three P domains and two Q domains. The estimate indicates that within the phyllite Q domains, about 55-60 % of the phyllosilicates are mica, whereas in the phyllite P domains, 80-90 % are mica. Within the siltstone at either end of the plot, the relationship between the two phyllosilicates seems difficult to generalize; at the left end chlorite is more prevalent than mica, whereas at the right end the reverse

Figure 61. Plot of mica and chlorite distributions for the microprobe traverse shown in Figures 54 and 55.

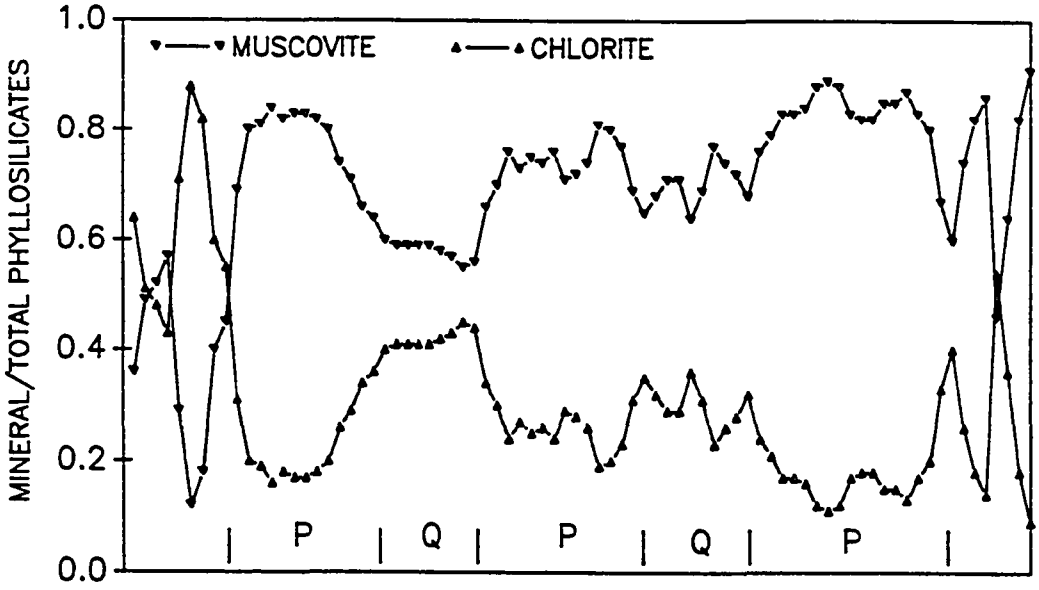

WC26A TRAVERSE 3

is true.

The scatter plots of traverse data for Mg and Fe plotted versus K indicate that unless there is significant carbonate present, there is at least a slight positive correlation between mica distribution and Fe and Mg distribution. The fact that this correlation flattens out at high K contents suggests that high K values may correspond to low percentages of interstratified chlorite, and hence low Mg contents, whereas moderate K contents are found for spots containing considerable interstratified material. Taken as a whole the microprobe traverse data strongly suggests that there is little tendency for discrete chlorite grains to be concentrated in P domains, and that in fact they are probably somewhat more concentrated in Q domains.

The fact that in carbonate-rich samples Fe and Mg concentration patterns are very well matched to Ca and Mn patterns suggests that where there is much carbonate there is relatively little chlorite. Textural evidence from thin sections suggests that some, but not all, carbonate blebs developed after the foliation (and, presumably, after the domainal fabric had developed). Perhaps these late stage carbonates are the sink for Fe and Mg left over as chlorite is replaced by mica, as Hower, et al. (1976) suggested takes place during burial diagenesis of Gulf Coast sediments.

The microprobe traverse data generated during this study are generally consistent with the rather limited data available on P and Q domain compositions. Holcombe's (1973) analyses were only qualitative, but also indicate that white mica is concentrated in the P domains. Without quantitative information it is difficult to know whether his Mg and Fe concentrations in the Q domains are due to chlorite concentration, carbonate concentration, or both. There is nothing in his data, however, that is inconsistent with the chlorite being more concentrated in Q domains than in P domains.

BRIEF SUMMARY OF CONCLUSIONS

In general, both the XRD and the microprobe data indicate, when compared to other studies, that P domain phyllosilicate grains, relative to Q domain phyllosilicate grains, have crystal chemical characteristics typical of a higher metamorphic grade. Specifically, P domain phyllosilicates have a higher K content, a finding consistent with virtually every study done on the regional changes undergone by illite during prograde diagenesis and low-grade metamorphism, lower Kubler index values (greater crystallinity), less interstratification, and less variability in composition. All these specific differences have been reported in regional studies on the prograde evolution of white mica (e.g. Hunziker, et al., 1986). Differences in the overall mineralogical characteristics of the domains also include a higher mica/chlorite ratio in P domains than in Q domains. According to the findings of Weaver, et al. (1984), this increase in mica/chlorite is also typical of the prograde evolution of phyllosilicates during early metamorphism.

CHAPTER VII

MECHANISMS OF FABRIC DEVELOPMENT

Many of the outcrop and petrographic observations made here and in other cleavage studies provide some insight into the mechanical and chemical processes that operated during the development of slaty cleavage fabric. These observations by themselves, however, are of limited value; in fine-grained rocks, such as the Walden Creek Group's Sandsuck Formation, the scale on which they are made is large relative to many important structural and mineralogical details of the fabric. The scale of the fabric is one of the reasons that the origin of slaty cleavage remains controversial after more than a century of active research on the topic, and it was one of the motivations for using the microprobe and XRD to obtain analytical data on the mineralogy and composition of the microstructural domains. The microprobe and XRD data yield vital information that when evaluated in conjunction with the petrographic observations make it possible to assess the relative merit of the various mechanisms that have been proposed as contributing to the development of slaty cleavage.

The two basic elements of the cleavage fabric that must be accounted for are the preferred orientation of mica grains and the domainal fabric that crosscuts bedding. It

is clear both from observations and from analytical data that there are some significant differences in the characteristics of P and Q domains. These differences not only include differences in domain morphology, bulk composition, and development of preferred orientation, but also differences in the crystal chemical characteristics of particular mineral phases. The object in identifying these differences is to try to understand the mechanisms by which the two types of domains, and hence slaty cleavage, develop.

Preferred orientation has been proposed to develop by means of many different processes, including rotation of platy minerals, rotation of platy minerals during dewatering of sediments, rotation of platy minerals accompanied by pressure solution of other phases, particularly quartz, solid state recrystallization and reorientation of pre-existing grains, and growth of new grains in the preferred orientation. The processes that have been proposed for the development of domainal fabric include mechanical transposition of sedimentary layering during isoclinal folding, passive concentration of insoluble mineral grains during pressure solution of soluble minerals, and mass transfer, either by diffusion or flow, of components of mica and/or quartz.

The development of slaty cleavage is discussed in the following paragraphs, taking into consideration

observations of the microstructures within the Ocoee Gorge rocks, some selected observations reported in other studies, analytical data gathered during this study, and some selected analytical data reported in other studies. Because some of the mechanisms that have been proposed could lead to the development of both preferred orientation and domainal fabric, no effort has been made to discuss the development of these characteristics separately.

Transposition of Layering

The only strictly mechanical process that has been proposed to account for the development of both domainal fabric and preferred orientation is the mechanical transposition of pre-existing layering during folding (e.g. Turner and Weiss, 1963). This process would entail the gross attenuation of pre-existing layering during isoclinal folding. There are several objections that can be raised to such a process having contributed to the development of domainal fabric and foliation, here or elsewhere. In the Walden Creek Group rocks exposed in Ocoee Gorge, bedding and other sedimentary structures are well preserved, easily identified, and clearly crosscut by the domainal fabric. What is more, the only folding episode experienced by these rocks produced open, not isoclinal, folds. In higher grade regions that have been subjected to multiple folding episodes, such as the French Slate in the Medicine Bow Mountains of Wyoming, it is common to find a younger

domainal fabric overprinting an older one that is still easily traced for tens of centimeters (Fig. 62). The continuity of the older domainal fabric makes it clear that the younger layering has not been produced by the isoclinal folding of the earlier layering. Clearly the development of domainal fabric requires redistribution of mineral phases by some means other than extreme stretching and rotation of sedimentary layering.

Mechanical Rotation

One other strictly mechanical process has been proposed as contributing to the development of preferred orientation. This is the mechanical rotation of phyllosilicate grains into the foliation-parallel orientation. Several petrographic observations, however, indicate that mechanical rotation alone cannot account for the development of preferred orientation of mica grains parallel to cleavage. The uniformity of orientation, particularly in the type 1 sub-domains, and the lack of optical scale evidence of internal strain within these mica grains indicates that they did not reorient strictly by mechanical rotation. Some of the P domain mica grains are so thin and elongate that they should be very fragile, an observation that makes it difficult to believe they rotated tens of degrees without becoming deformed.

The fact that within Q domains, foliation-parallel mica grains are smaller and more elongate than bedding-

Figure 62. Domainal fabric (axial planar to recumbent fold) cross-cutting earlier domainal fabric in French Slate, Medicine Bow Mountains, Wyoming. Pencil is 14 cm long.

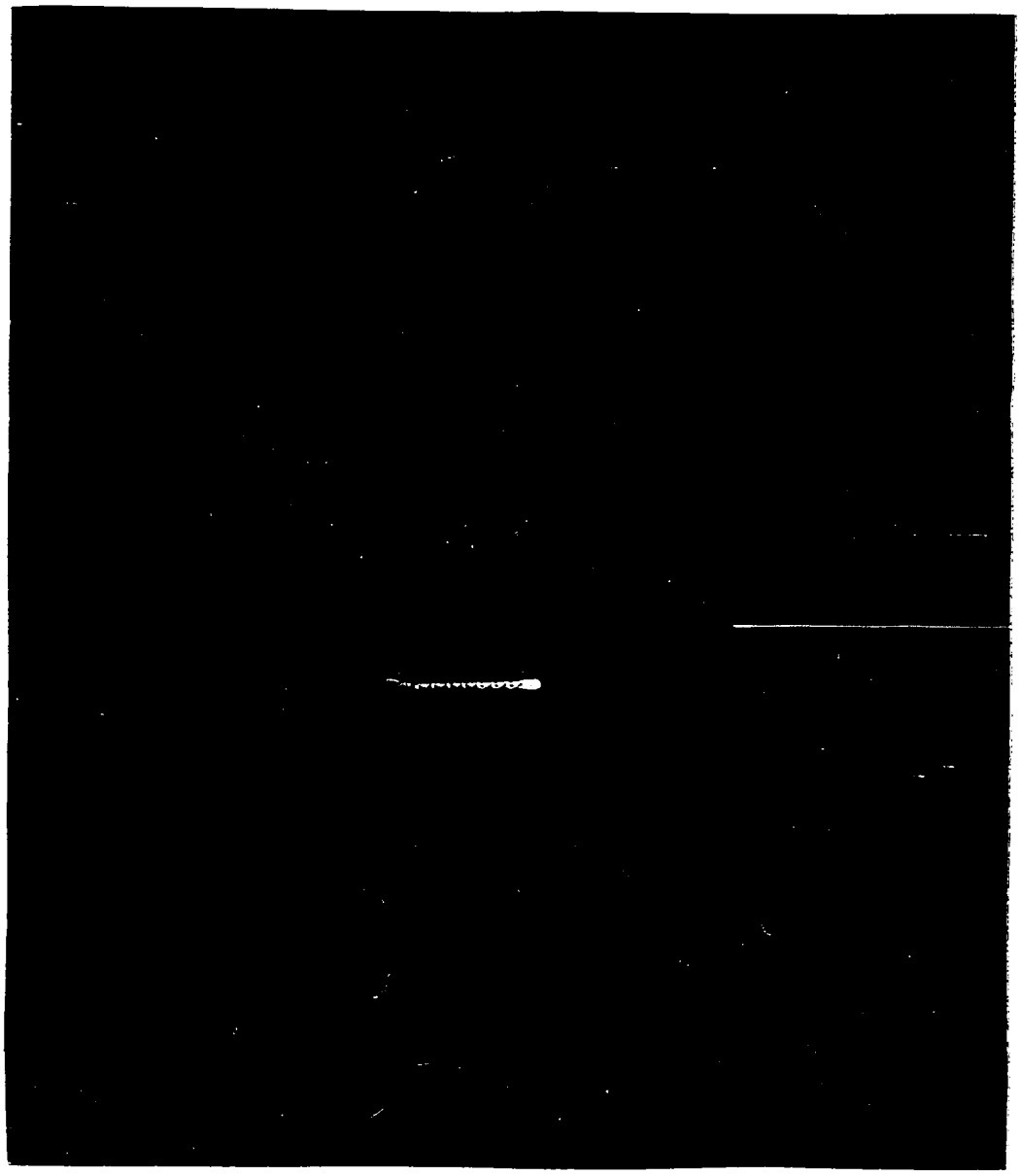

parallel mica grains suggests that the foliation-parallel grains are new grains, not selectively rotated pre-existing grains. If rotation were acting alone, it is difficult to understand why the somewhat larger and more heterogeneous bedding-parallel grains would be completely spared, while the tiny, isolated, needle-shaped grains are rotated into a preferred orientation parallel to the foliation.

As in the case of the petrographic observations, there are analytical data that are difficult to reconcile with a strict mechanical rotation origin for the fabric. These data indicate that there are significant differences in the phyllosilicate populations of the P and Q domains. The XRD finding that a higher proportion of the chlorite than of the mica is oriented parallel to bedding certainly rules out mechanical reorientation as the primary agent by which the preferred orientation was achieved; both chlorite and mica occur as flat, platy mineral grains, that should respond similarly to stresses causing mechanical rotation.

Both the probe data on differences in the typical phyllosilicate compositions and the XRD data on differences in the white mica populations of the two types of domains, e.g. the Kubler index, indicate that the P domain phyllosilicates are characteristic of a higher metamorphic grade than are their Q domain counterparts. This data, coupled with the P domain grain shapes and uniformity of orientation, strongly suggest that most of the P domain

grains are new grains that grew during the fabric development, not old grains that have been rotated into a new preferred orientation. It is possible, however, that rotation of some grains has made a minor contribution to the development of the fabric.

Mechanical Rotation during Sedimentary Dewatering

Many of the objections raised to mechanical rotation also apply to mechanical rotation during sedimentary dewatering. In particular the mineralogical differences in the P and Q domain phyllosilicates, and the difference between average chlorite and average mica grain orientations, seem to rule out dewatering as a mechanism that could, by itself, account for the development of this fabric. One argument made in favor of this mechanism is that high water contents might cushion and lubricate the grains, permitting a high degree of reorientation with little or no grain-scale deformation (e.g. Clark 1970a, 1970b). As in the case of mechanical rotation without dewatering, however, the differences in the proportions of chlorite and mica that have been reoriented, and the compositional differences in the P and Q domain white micas are difficult to explain as a result of sedimentary dewatering.

Mechanical Rotation and Passive Concentration of Mica

The combination of mechanical rotation and passive concentration of mica has been suggested as a means of

generating both preferred orientation and domainal fabric (e.g. Holcombe, 1973). The idea is that soluble phases (usually quartz) found between mica grains undergo pressure solution and are removed, allowing mica grains to rotate into a parallel arrangement and become concentrated. The driving force behind the dissolution of the soluble phases is assumed to be stress concentration developing along grain boundaries. It is rather difficult, however, to reconcile this combination of mechanisms with the mineralogical differences in the phyllosilicate populations found in the two domains. These differences might, however, be accounted for by a chemical process taking place in the P domains after the domainal fabric has developed by rotation and passive concentration. Perhaps after the P domains developed they became avenues for fluid flow, and the fluids permitted localized metamorphic reactions within the P domains.

This explanation requires, at least for the Ocoee Gorge rocks, that internal strain suffered by the mica grains during rotation has not been preserved. It seems unlikely, however, that much annealing of deformed mica grains took place under the relatively low-grade metamorphic conditions these rocks experienced. It is difficult to understand why the unstrained foliation-parallel mica grains found in type 1 sub-domains, would have been completely annealed, whereas deformed mica grains

found in type 4 sub-domains, were not annealed at all. Heat and time, the factors that are generally suggested to control annealing (e.g. Spry, 1969), should have had the same effect in both types of sub-domains.

A further objection to this combination of mechanisms is the lack of evidence of significant pressure solution of quartz grains along their foliation-parallel boundaries. Where ragged boundaries or inequant grain shapes suggest that pressure solution may have occurred it appears to be geometrically unrelated to the foliation. In many samples the quartz grains show no evidence of pressure solution, making it seem unlikely that the fragile mica grains were cushioned during rotation by a quartz matrix that took up strain and decreased the stress transmitted to the mica grains by undergoing pressure solution.

In addition to the bedding-parallel and foliation-parallel preferred orientations, there is a third, less common orientation of mica grains in type 4 sub-domains: strings of grains oriented between 30 and 60 degrees away from the foliation-parallel orientation. These strings of grains swing back and forth between two orientations that are each roughly parallel to the grain boundaries of large quartz grains. The development of these mica strings could be caused by passive concentration accompanying pressure solution only if the material undergoing pressure solution has been completely removed, leaving behind large, equant

quartz grains with smooth grain boundaries. It seems more likely that the mica grains have grown between the quartz grains and have simply followed the orientations of the quartz grain boundaries, less energy being required to grow between the quartz grains than to grow through them.

A petrographic observation that has been cited by other workers (e.g. Williams, 1972; Holcombe, 1973; Swager, 1985) as evidence of passive concentration of mica is the concentration of an insoluble residue of opaque mineral grains along P domains. In this study, however, no evidence has been found for the concentration of insoluble opaques along the P domains, and in any case it is not clear that their presence would necessarily indicate that mica was also a passively concentrated insoluble material. In the Walden Creek Group thin sections, optical-scale opaque grains, including those detectable only with an oil-immersion objective, show no greater concentration in P domains than in Q domains.

It is possible, however, that sub-microscopic opaque grains are concentrated along P domains. Some data for evaluating this suggestion come from another study; Holcombe (1973) performed qualitative probe scans, two that he interpreted as showing some concentration of Ti along P domains and two that clearly do not show such a concentration. The quality of the scan photographs, however, is too poor to interpret with certainty. Further,

without quantitative information there is no way of distinguishing Ti in white mica from Ti in rutile or ilmenite. The microprobe traverse data obtained during the present study, indicate some concentration of Ti along P domains, but the average value of this concentration is in a range that could be accounted for by Ti in white mica.

The dark color of many P domains is cited by both Holcombe (1973) and Williams (1972) as evidence that P domains represent an insoluble residue accumulated during the pressure solution of other phases. White and Johnston (1981), however, using electron microscopy to examine the microstructure of slate, found that the dark color they observed in some P domains is due not to the presence of an insoluble residue of opaque minerals, but rather to iron oxide staining along P domains. They also reported that P domains become as pale as their surroundings if thin sections were ground sufficiently thin. In comparing P and Q domains they actually found opaque grains occupied a smaller per cent of the total volume in P domains than in Q domains. In this study of Walden Creek Group rocks iron oxide staining was also observed along some P domains. Considering the warm, humid climate in which these rocks have been exposed, weathering would seem to be a more likely explanation for hematite staining than would passive concentration of an insoluble residue. The fact that the hematite staining is preferentially located along P domains

rather than along Q domains suggests that P domains are zones of high permeability.

In the Walden Creek Group rocks concentrations of opaque grains are common only as thin sedimentary layers, usually along the base of siltstone layers. Not only are these detrital opaques not particularly concentrated along P domains, but the layers they form are actually completely disrupted by cross-cutting P domains (Fig. 23). In other words, these sedimentary accumulations of opaques are more concentrated in Q domains than in P domains.

Solid State Recrystallization of Phyllosilicates

Solid state recrystallization of phyllosilicates is a mechanism that could account for several of the features noted in the petrographic observations, as well as for many aspects of the analytical data. Two general types of grains might be particularly susceptible to recrystallization. One type is deformed grains possessing high strain energy. These might recrystallize as strain free grains. The other type is grains that are in thermodynamically less stable orientations. Because of the anisotropic nature of mica and the anisotropic nature of tectonic stress fields, such as that applied to these rocks during deformation, these grains might tend to recrystallize in more stable orientations.

Recrystallization could account for both the strain free nature of P domain mica grains and for their preferred

orientation. It could also account for the higher illite crystallinity of the P domain grains, and possibly for some of the differences in P and Q domain phyllosilicate compositions, including the higher K content of P domain micas and the P domain limit on how much chlorite may be present in interstratified mica/chlorite. If mica were more susceptible than chlorite to recrystallization that could account for the difference in proportions of chlorite and mica found in the foliation-parallel versus the bedding-parallel orientations.

The domainal fabric, however, is difficult to explain as being a result of recrystallization. The compositional differences in P and Q domains require that some type of mass transport has taken place. Further, the tapering shape of P domains in siltstone layers suggests that P domains have propagated upward from phyllite layers, also requiring mass transport of the components of mica.

Growth of New Grains

A mechanism that might account for the development of both preferred orientation and domainal fabric is the growth of new mica grains. Dissolution of some detrital mineral grains, particularly biotite, chlorite, clays, and K feldspar probably supplies the components from which new phyllosilicate grains can be grown. These components may then be redeposited in new white mica or, possibly, chlorite growing in the preferred orientation.

Several petrographic observations suggest that at least some growth of new mica grains took place during the development of this fabric. One of these observations is that the opaque layers found at the base of some siltstone layers appear to have been pushed aside and out into the siltstone layer by the propagation of the P domains into the siltstone layers from the underlying phyllite layers. This suggests that mica grains within P domains, and in fact the siltstone P domains themselves, developed as mica components were supplied from the underlying phyllite layer; it is difficult to envisage a mechanical process that could force thin, elongate mica grains up through the opaque layer and on into or across the siltstone layer without deforming the mica grains. It seems far more likely that these P domains propagated into the siltstone layers by means of growth of new mica grains from the components of mica available in pore fluid from the breakdown of pre-existing phases.

The morphology of the type 3 sub-domains also suggests that the P domains have propagated into siltstone layers from neighboring phyllite layers. The fading away or tapering of P domains crossing Q domains suggests that they grew outward from phyllite layers and failed to completely cross neighboring siltstone layers. Type 3 sub-domains can be tens of mica grains thick close to their source phyllite layers, but then taper to nothing within a few mm. Where

spacing between P domains is fairly small, a significant volume of the portion of the siltstone layer closest to the phyllite layer is occupied by P domains which are nearly pure mica. If this mica were concentrated passively by the removal of intervening quartz grains, it would represent a substantial volume loss within this portion of the siltstone layer, since there is, by volume, relatively little mica found within the parts of siltstone layers not occupied by P domains, and these parts should be akin to the parent material in which the passive concentration took place. This volume reduction would not be matched in the middle of the layer where P domains are few and thin. If there were such a change in volume reduction across the siltstone layer there should be significant deformation within the layer, but there is no evidence preserved of such deformation.

Based on grainscale observations, there are certain conclusions that can be drawn about the redistribution of mineralogical components within this system. The scarceness of corroded grain boundaries on quartz grains in Q domains suggests that there has not been any significant dissolution or removal of quartz from these domains. Similarly, in P domains there is no compelling textural evidence that much quartz has been lost to pressure solution. There are in both types of domains some quartz grain boundaries that appear to be ragged or corroded and

some that appear to have overgrowths. These grain boundaries, however, have no discernible preferred orientation, i. e. the corroded boundaries are as likely to be normal to the foliation as perpendicular to it.

Among the mica grains, the only grain boundary corrosion is seen on some of the large, apparently detrital mica grains found in the Q domains and the rare large grains found in P domains. In addition, some large grains show signs of dissolution within the grain, particularly if they are bent. There is no optical scale evidence of dissolution within or along any of the smaller mica grains.

The bedding-parallel orientation of mica grains within Q domains probably predates deformation. If these grains have been reoriented during deformation, they have rotated with the bed to which they belong, not independently of it. These grains are probably either detrital grains that have been bedding-parallel since deposition or compaction, or they are grains that have replaced pre-existing bedding-parallel phyllosilicate, maintaining the same crystallographic orientation during the replacement process. The microprobe data on the compositions of these grains suggest that at least some of them are detrital. The variability in compositions, the low average K content, and the complete range of mica/chlorite interstratifications, contrast these grains with their P domain counterparts, and support the view that these grains

have not been significantly altered during metamorphism or deformation and may still be in their original sedimentary orientation.

The growth of foliation-parallel mica grains, both those within P domains and the rarer ones within Q domains, does not appear to predate metamorphism and deformation, and is intimately related to the development of the domainal fabric itself. This oriented growth might be due to either or both of two causes. One is that the grains grew in an anisotropic tectonic stress field that favored growth in this particular orientation. Considering that phyllosilicates are highly anisotropic in their structure and physical properties it seems reasonable to expect that them to grow in such a preferred orientation. That assumes, however, that there are no other constraints on their growth direction.

The other possible cause of oriented grain growth is that the grains grew from components carried in a fluid phase that moved upward in a direction parallel to the direction of grain growth. As the fluid migrated the mica may have simply grown along the pathways available for fluid flow, i.e. along the grain boundaries of the larger quartz and feldspar grains. The fact that many P domains branch out and fade shortly after entering the bottom of a siltstone layer suggests that the mica-component bearing fluid was following a well defined path of reoriented mica

within the phyllite layer,but not within the siltstone layer. The morphology of the P domains suggests that once the fluid reached the more permeable siltstone, it was able to follow a several branching flow paths and flow along many different quartz and feldspar grain boundaries. Perhaps in the development of more continuous P domains, a mica-rich zone slowly grew upward into the siltstone, and eventually channelled the flow as a continuous P domain developed.

Many workers have studied the changes that take place in phyllosilicates during late diagenesis and early metamorphism and the associated development of preferred orientation (e.g. Lewis, 1980; Pique, 1982; Weaver et al., 1984; Lee et al., 1984, 1986). Their findings generally indicate that phyllosilicates undergo significant chemical and structural changes during late diagenesis and low-grade metamorphism. This indicates that at least some components of these minerals are mobile during the early development of slaty cleavage. Further, at least one study (Knipe, 1979) has found that phyllosilicate composition is related both to microstructural domain type and to grain orientation. This strongly suggests that grains in different orientations did not develop at the same time.

Lewis (1980) examined phyllosilicates (primarily chlorite and white mica) in the Martinsburg Formation at Lehigh Water Gap, Pennsylvania, where one exposure grades

over a distance of tens of meters from an unfoliated mudstone to a slate with a well developed cleavage. He noted several changes that suggested that recrystallization or crystallization, not rotation, was the dominant deformation mechanism operating here. Among these changes are compositional differences between the chlorite and white mica in the bedding plane orientation and those in the cleavage orientation, a greater illite crystallinity in the cleavage-parallel grains than in bedding-parallel material, and the disappearance of 1M mica from the cleavage parallel material. Lewis found, as did Holeywell and Tullis (1975) in their study of the same outcrop, that chlorite and white mica do not attain the cleavage plane-parallel orientation at the same place along the outcrop.

Another of Lewis' observations suggests that recrystallization or new grain growth were the dominant mechanisms for the development of preferred orientation. He found there to be few large phyllosilicate grains in orientations part way between bedding and cleavage, contrary to what might be expected for progressive rotation. He also found that aspect ratios of phyllosilicate grains in the cleavage plane orientation are much greater than those for phyllosilicate grains in the bedding plane orientation. Further evidence indicating that at least some recrystallization or new growth has taken place is the crosscutting relationship observed

between cleavage-parallel phyllosilicates and bedding plane-parallel phyllosilicates; the latter commonly truncate the former.

In many respects the observations of Lewis and the other workers who have studied the Lehigh Water Gap rocks are similar to or lend support to observations made in this study. An important difference, however, between Lewis' study of the Lehigh Water Gap rocks and this study of the rocks exposed in western Ocoee Gorge is that he traced changes that occurred in the fabric and phyllosilicates along the length of the outcrop, whereas this study has focussed on differences found between P and Q domains. It is interesting that the differences seen in the mudstone to slate transition at Lehigh Water Gap appear to be so similar to the differences seen in the P and Q domains of the Sandsuck phyllites. Because P and Q domains were not identified in Lewis' study its difficult to say whether recrystallization alone could account for the development of the fabric there.

White and Knipe (1978), in a high voltage electron microscopy (HVEM) study of three slates exhibiting varying degrees of foliation development, observed that new P domains are initiated where individual phyllosilicate grains are highly deformed, and that metamorphic reactions take place there, where strain energy is highest. They suggested that kinks and microfolds in phyllosilicates

introduce a periodicity into the fabric which may control the spacing of the developing P domains. If, however, spacing were determined by the wavelength of bending in detrital mica grains in phyllite layers, it does not seem likely that it would be the same for sets of P domains that developed in different phyllite layers as is observed in the siltstone layers of Walden Creek rocks. Perhaps spacing is controlled by the rates at which mineral components become available and can migrate within the system. In other words the rate at which unstable minerals dissolve and the rate at which their components can be made available to growing P domain grains may influence the spacing that develops. Alternatively, if P domains develop along pathways for expulsion of fluid during compaction, diagenesis, and metamorphism, fluid pressure may control the spacing of P domains.

Gregg (1985) hypothesized, on the basis of his observations on cleavage in psammites, that single mica grains crystallize in the cleavage orientation, then form the nuclei of films, which link up and gradually become continuous mica-rich zones. He saw no evidence that the mica films are insoluble residue left behind after dissolution and removal of soluble materials or of deformation of mica grains indicating that the grains may have been mechanically rotated. Further, he observed that the process of films linking up with one another involves

fracturing of clastic grains as mica films "grow" through them. He also suggested that in higher-grade rocks evidence of fracturing is commonly obscured by later pressure solution, but it is visible in the rocks he examined because little pressure solution has taken place. Once continuous mica films have formed they act as fluid conduits and neighboring clastic grains are dissolved, resulting in passive thickening of the mica films. Gregg studied a different rock type than that present in western Ocoee Gorge, but the suggestion that the initial mica grain need not be mechanically rotated or be part of a system of micro-crenulations to become reoriented in the foliation-parallel direction is an interesting one. Certainly before deformation of these rocks began there would have been a few grains in unusual orientations that might have served as P domain nuclei.

Taking into account the above discussion, it is possible to speculate about a sequence of events in the development of slaty cleavage. There seem to be three general requirements for cleavage development. The first of these is the establishment of appropriate conditions for diagenesis or low-grade metamorphism to take place. Presumably these conditions have to do with temperature, pressure, presence of fluids, and tectonic stress. In addition there are some limitations on the lithologies in which cleavage will develop, although cleavage or some type

of metamorphic foliation has been reported in a remarkable variety of rock types. The second requirement is that P domains nucleate, probably around single grains that either are in the orientation of the developing foliation or are deformed and have high strain energy, making them particularly susceptible to dissolution or recrystallization. The third requirement is the thickening and lengthwise propagation of P domains from these reoriented platy mineral grains. In this study it is how these second and third requirements are met that is of particular interest.

The second requirement, the nucleation of cleavage (P domains), requires the presence of a least a few mica grains in what will become the foliation-parallel orientation, but it is not clear that reorientation of any grains is necessary. There may already be sufficient grains in the preferred orientation, in other words there may already be scattered grains in the primary rock fabric that are not parallel to bedding, but are roughly parallel to the direction in which the foliation-parallel preferred orientation develops.

There are at least two ways that reorientation might be achieved if it is necessary. One possibility for reorientation suggested by Gregg (1985) in his study of cleavage in psammitic rocks, and possibly applicable in pelitic rocks is the crystallization of individual mica

grains in the new preferred orientation. What the preferred orientation will be is determined by the orientation of the applied stresses as explained by Kamb (1959, 1961) in his analysis of growth of anisotropic crystals in an anisotropic stress field. The chief difficulty with this type of reorientation is that the direction of growth of the new grain may be controlled by the orientations of the grain boundaries of pre-existing. bedding-plane parallel mica grains that surround the growing grain rather than by the orientation of the applied stress. The direction of growth may, however, be controlled by the average direction in which fluid is migrating. This might account for the amount of variation that is seen in mica grain orientations among grains that have an average orientation parallel to foliation.

The second way that the initial reorientation of a few mica grains might be achieved is by the bending or microfolding of a few grains. A single, large grain might become bent during the initial stages of deformation. If the bent grain has a sharp hinge, this part of the grain will be likely to dissolve because of high strain energy, a style of deformation reported in detrital biotite grains by Bell (1981). New grains, oriented parallel to the hinge or parallel to the developing preferred orientation, will then crystallize in the region where high strain has caused dissolution. Evidence that this process takes place has

been reported by White and Knipe (1978). They observed small white mica grains oriented along and parallel to dissolved hinges of large, bent grains.

An alternative to the bending of a few large grains is the microfolding or crenulation of entire phyllite layers. In this case the reorientation of mica occurs along all the hinges of the crenulations and the spacing between the P-domains is controlled by the wavelength of the crenulations. An objection to this, at least for the Walden Creek Group rocks, is that the Q domain phyllosilicate grains are parallel to bedding, not to the limbs of set of microfolds.

Once a few P domains have nucleated, that is once a few clusters of reoriented mica grains have formed, the next step in cleavage development is the propagation of these incipient P domains outward from these reoriented clusters. Regardless of how the initial reorientation has occurred, once a small cluster of grains has formed parallel to the developing preferred orientation, there is probably a tendency for more grains to crystallize in the same orientation, as well as for the first reoriented grains to grow larger. There are at least two reasons for this. One reason is that these clusters of long, flat grains arranged parallel to one another contain long, flat pore spaces that link up easily to create a zone of relatively high permeability. As the rock undergoes prograde metamorphism,

it will expel fluid, and it is likely that a disproportionately high volume of this fluid passes through these newly developing zones of high permeability. This relatively high volume of fluid flow nourishes the growth of grains in these zones by supplying them with a steady stream of dissolved mineral components.

The other reason new grains may tend to grow in a direction that extends these zones is that individual grains may perturb the local stress field, establishing mean stress gradients, and hence chemical potential gradients around their perimeters. If these grains are effectively stiffer than the surrounding material, and the greatest compressive stress is perpendicular to the flat sides of the grains, there will be gradients around the edges of the grains in the chemical potentials of the components of the grains. These gradients will tend to drive diffusion of dissolved material away from the flat sides and toward the edges of the grains. This means that the mica grains will have anisotropic growth rates not only because of their anisotropic structure, but they may also have anisotropic growth rates because of an anisotropic supply of nutrients; growth will occur most readily along the edges of the grains in the direction that will tend to extend the P domains lengthwise. The difficulty with this model is that it assumes that mica grains are stiffer than their surroundings, an unlikely condition if the

surrounding material is quartz.

Another factor contributing to the development of this fabric is the breakdown of thermodynamically unstable minerals. This breakdown may occur more readily along P domains than along Q domains, because the higher permeability along P domains permits the flow of a relatively high volume of fluid. This breakdown of material provides the components needed for new growth of mica grains along developing P domains. Unstable mineral grains located in the path of these propagating domains may be broken down and removed, leaving behind more stable grains and a trail of new mica grains that have grown along the pathway of the fluid.

The textural evidence and the analytical data taken as a whole suggest that the typical P domain mica grains are new grains that have grown during the diagenesis and low-grade metamorphism these rocks have experienced. The bedding-plane parallel grains typical of the Q domains, on the other hand, appear to be detrital or possibly diagenetically altered grains that were in place before the rocks were deformed, and hence before the slaty cleavage developed. The rarer foliation-parallel Q domain grains probably developed at the same time as the foliation-parallel P domain grains. New grain growth is the only mechanism that is consistent with all the evidence.

This assessment does not rule out the possibility that

some other mechanisms have contributed to the development of the fabric. In particular, it is possible that recrystallization accounts for some of the differences in the P and Q domain phyllosilicates. A minor degree of mechanical rotation cannot be ruled out; if rotation took place, the affected grains might have been particularly susceptible to recrystallization because of their higher strain energy. Therefore, the expected grainscale deformation might not have been preserved. Rotation followed by recrystallization cannot, however, account for the development of the domainal fabric, and it seems unlikely that it could account for the greater tendency for chlorite to be parallel to bedding.

New grain growth and propagation of P domains from phyllite layers into siltstone layers can account for both the petrographic observations made and the analytical data gathered during this study. This growth requires the presence of intergranular fluid, probably a flowing intergranular fluid.

CHAPTER VIII

SUMMARY AND CONCLUSIONS

The slaty cleavage exposed in the fine-grained metasediments of eastern Ocoee Gorge is defined by zones enriched in cleavage-parallel white mica (P domains), alternating with zones enriched in quartz and feldspar (Q domains). Significant growth of new mica as well as possible solid state recrystallization of clays and mica occurred in conjunction with the development of the domainal fabric. The fact that this new growth generated mica grains that are oriented parallel to the mesoscopic foliation is not surprising. Metamorphism in these rocks was accompanied by a tectonic stress field that generated outcrop scale folds. This same stress field would have made highly anisotropic mica grains grow much more easily in one orientation than in others, and may also have controlled the direction in which fluid flowed through the rock, and providing components to growing mica grains.

Little, if any, rotation and passive concentration of mica grains took place during the development of this fabric. Further, there is evidence that suggests the nucleation and growth of P domains may involve the expulsion of fluids, either sedimentary or metamorphic. Part of this evidence is textural and part includes the differences in the phyllosilicate populations in the two

domain types.

The textural observations and mineralogical data that support these conclusions are as follows:

1. The distribution of opaque grains supports the conclusion that passive concentration of mica could not have been the principal mechanism by which the fabric developed. A thin layer of detrital opaque minerals (probably ilmenite) deposited along the base of many of the silt beds is disrupted by the P domains as they cross from phyllite to silt layers. In addition, there is no concentration of opaque grains along or within the P domains. Neither of these observations is consistent with P domain mica concentrations forming by passive concentration as grains of quartz and feldspar are dissolved and removed from between mica grains. If passive concentration had taken place, the opaque layers should be concentrated along the P domains rather than being disrupted by them.

2. Passive concentration of mica was not important in the development of this fabric. There is no pressure solution along quartz grain boundaries oriented parallel to the foliation. There is some evidence of pressure solution of along quartz grain boundaries, but the orientations of these ragged grain boundaries are unrelated to the orientation of the foliation. Similarly, quartz overgrowths are as likely to be perpendicular to foliation

as parallel to it, suggesting that the development of both ragged grain boundaries and overgrowths may be unrelated to the development of the foliation. Possibly, quartz pressure solution did not take place during the deformation that generated the slaty cleavage.

It may be more appropriate to consider passive concentration of quartz and albite than of mica. Growth of new mica requires a supply of K and the most obvious sources are K feldspar or detrital mica. K feldspar is present in the coarser grained psammites of the Great Smoky Group and in the rare quartzite, but not in the phyllite or siltstone, of the Walden Creek Group. Whatever K feldspar was deposited with the finer-grained Walden Creek Group sediments disappeared during the early stages of metamorphism. The K this liberated could then have migrated to the developing P domains, probably in a flowing fluid. The destruction of K feldspar and the migration and concentration of at least one of its components would have acted to passively concentrate the quartz left behind in the Q domains.

3. The shapes of many P domains suggest that they have formed by growth of new grains from a fluid rather than by passive concentration of pre-existing grains. Within phyllite layers P domains tend to be roughly constant in thickness, but within siltstone layers many of them taper upward. Commonly P domains that are thick and well

developed at the base of a siltstone layer taper and anastomose further up into the siltstone. The shapes of these domains suggest that they propagated upward into the siltstone layers from underlying phyllite layers.

P domains may die out for several reasons, as they continue into siltstone layers. First, the further from the underlying phyllite layer a P domain gets, the further it is from its source of new material, i.e. mica components appear to be supplied by a fluid originating in the phyllite layer. Second, if P domains grew from components carried in a moving fluid, the path the fluid followed may have been well defined within the phyllite and at the boundary between the phyllite and the siltstone, but not in the more permeable siltstone. Within the phyllite, once a zone of reoriented mica began to develop, flow would have been concentrated along that zone rather than in regions to either side of the zone, where it would have had to follow a tortuous course around bedding-parallel mica grains. Once flow along a zone of reoriented grains was established and "channelled", mica components moving along the zone were supplied to growing grains, allowing the zone of foliation-parallel mica to thicken. As the fluid continued up into the siltstone, however, there may have been so many pathways for it among the quartz and feldspar grains, that the fluid followed the anastomosing course now preserved by the trains of mica grains.

4. The new white mica that has developed in the P domains is not identical to the white mica found in intervening Q domains. It appears in fact to be mica that is characteristic of "higher grade" metamorphism than that in the Q domains. The unit cell K content is greater in the P domain micas than in the Q domain micas, a finding consistent with the prograde changes seen in the transition from illite to either muscovite or phengite. In addition, the illite crystallinity index for P domain grains is smaller than for Q domain grains, also indicating that the P domain grains are more crystalline. Another indication that the Q domain white mica grains have not undergone the same prograde changes as the P domain white mica grains is that the Q domain grains are more variable in composition than are the P domain grains. Such variability is more common in detrital than in low grade metamorphic mineral populations.

5. The compositions of the interstratified mica/chlorite observed in each domain suggests that P domain phyllosilicate grains are characteristic of a higher metamorphic grade than are those found in Q domains. Interstratifications of mica and chlorite are found in both domain types, but the interstratifications in the P domains have an upper limit to their chlorite content of about 1/3, whereas there is no apparent limit for the Q domain interstratifications. This difference in the amount of

chlorite that is found in interstratified grains suggests that as the P domain grains evolve there is a tendency for chlorite strata to be cleaned out or converted to mica.

6. The distribution of discrete chlorite and white mica between the two domain types is different. The ratio of bedding-parallel chlorite to cleavage-parallel chlorite is greater than the ratio of bedding parallel mica to cleavage parallel mica, i.e. a greater proportion of mica is oriented parallel to foliation, and more mica than chlorite is in P domains. Because chlorite develops during anchimetamorphism and then gradually disappears during epimetamorphism, this also suggests that the P domain phyllosilicates resemble a higher grade assemblage than do the Q domain phyllosilicates.

The fact that these two types of domains occur together alternating on a scale of tenths of millimeters, indicates that if they contain mineral populations that are typical of different metamorphic grades, then at least one of them must not have equilibrated at the prevailing metamorphic conditions. The fact that the Q domain phyllosilicates are more variable in composition and compositionally more characteristic of lower grade than the P domain grains suggests that the Q domain grains did not approach metamorphic equilibrium as closely as the P domain grains did. The factors that control the development of metamorphic mineral assemblages are, in addition to bulk

composition, pressure, temperature, and the presence of fluids. Temperature and pressure are not likely to have varied over the scale at which these domains have developed. Therefore, the availability of fluid is probably the factor that controlled the mineralogical differences that developed between the P and Q domains.

Kinetic controls on the dissolution or transformation of the lower grade Q domain grains may have preserved their lower grade character as temperature and pressure of the rock increased. P domain grains may not have actually undergone greater changes than the Q domain grains, but rather a much larger proportion of them may be entirely new growth. These new P domain mica grains grew under higher grade conditions than those at which the grains in the Q domain grains grew.

If my interpretation that P domain grains have undergone greater changes than the Q domain grains is correct, there are two possible reasons for this difference. The first is greater fluid flow along developing P domains. Fluids may have supplied components to growing grains, and because fluids flowed more readily along incipient P domains than along regions between domains, it is along P domains that most of the new grain growth occurred and it is along P domains that preexisting illite is most likely to have received the additional K required to become muscovite or phengite. The factor that

limited the development of P domains nay have been the supply of K; if most of the K was derived from the breakdown of K-feldspar, the disappearance of this phase may have stopped the development of P domains.

The second reason for the "higher grade" of P domains may be that P domains nucleate around bent detrital mica grains. Detrital grains have been reported in other cleavage studies (e.g. White and Knipe, 1978) to become bent during layer-parallel compression, then dissolve along their hinges because of higher strain energy at those locations. These hinge regions would then grow new, unstrained mica parallel to the axial plane of the bent grain, and, presumably, also parallel to the developing foliation. The new grains, growing at the prevailing pressure and temperature, might in fact belong to a higher grade assemblage than that of neighboring detrital grains.

Summary

Development of P domains may be initiated by rotation of grains caused by the upward expulsion of sedimentary or metamorphic fluids. Then, as diagenesis and metamorphism proceed the P domains continue to develop by growth of new mica grains and compositional re-equilibration of older grains as more fluid is expelled, preferentially travelling along incipient P domains into overlying silt layers. The components from which these new micas grew may have been at least partly supplied by the dissolution of K feldspar.

Thus, the complete disappearance of K feldspar may be the factor that limits the growth of new mica.

The fact that proportionately more chlorite than mica is oriented parallel to bedding suggests that much of the chlorite grew early in diagenesis, and predates the development of the P domains and foliation. As low-grade metamorphism proceeded, chlorite, particularly chlorite interstratified with mica, began to disappear. Fe- and Mg-rich carbonates, many of which overprint the foliation and some of which are overprinted by the foliation, provided a sink for the Fe and Mg that was lost from chlorite as chlorite was either dissolved or transformed into mica.

REFERENCES

Albee, A. L. and Ray L., 1970. Correction factors for electron probe microanalysis of silicates, oxides, carbonates, phosphates, and sulfates. Anal. Chem. 42: 1408-1414.

Bailey, S. W., 1984. Classification and Structure of the Micas. Reviews in Mineralogy 13: 1-12.

Bakewell, R., 1815. An introduction to Geology. Harding, London, 2nd ed., 429 p.

Bayly, B. M., 1974. Cleavage not parallel to strain ellipsoid's xy-plane: discussion. Tectonophysics 23: 205-207.

Bayly, B. M., Borradaile, G. J., and Powell, C. McA., 1977. Atlas of Rock Cleavage. Univ. of Tasmania, provisional edition.

Becker, G. F., 1893. Finite homogeneous strain, flow and rupture of rocks. GSA Bull. 4: 13-90.

Becker, G. F., 1896. Schistosity and slaty cleavage. J. Geol. 4: 429-448.

Bence, A. E. and Albee, A. L., 1968. Empirical correction factors for the electron microprobe analyses of silicates and oxides. J. Geol. 76: 382-403.

Bilby, B. A., Eshelby, J. D., and Kundu, A. K., 1975. The change in shape of a viscous ellipsoidal region embedded in a slowly deforming matrix having a different viscosity. Tectonophysics 28: 255-279.

Bilby, B. A., Eshelby, J. D., Kolbuszewski, M. L., and Kundu, A. K., 1976. The change of shape of a viscous ellipsoidal region embedded in a slowly deforming matrix having a different viscosity - some comments on a discussion by N. L. Gray. Tectonophysics 35: 408-410.

Borradaile, G. J. and Johnson, H. D., 1973. Finite-strain estimates from the Dalradian Dolomitic Formation, Islay, Argyll, Scotland. Tectonophysics 18: 249-259.

Borradaile, G. J., 1979. Strain study of the Caledonides in the Islay region, SW Scotland: implications for

strain histories and deformation mechanisms in greenschists. J. Geol. Soc. Lond. **136**: 77-88.

Borradaile, G. J., 1981. Particulate flow of rock and the formation of cleavage. Tectonophysics 72: 321-350.

Braddock, W. A., 1970. The origin of slaty cleavage: evidence from Precambrian rocks in Colorado. GSA Bull. **81**: 589-600.

Butler, J. R., 1972. Age of Paleozoic regional metamorphism in the Carolinas, Georgia, and Tennessee Southern Appalachians. Am. Jour. Sci. **272**: 319-333.

Carpenter, R. H., 1970. Metamorphic history of the Blue Ridge Province of Tennessee and North Carolina. GSA Bull. **81**: 749-762.

Clark, B. R., 1970a, Origin of slaty cleavage in the Coeur d'Alene district, Idaho. GSA Bull. **81**: 3061-3072.

Clark, B. R., 1970b, Mechanical formation of preferred orientation in clays. Am. Jour. Sci. **269**: 250-266.

Cosgrove, J. W., 1976. The formation of crenulation cleavage. J. Geol. Soc. Lond. **132**: 155-178.

Curtis, C. D., Ireland, B. J., Whiteman, J. A., Mulvaney, R., and Whittle, C. K., 1984. Authigenic chlorites: problems with chemical analysis and structural formula calculation. Clay Minerals **19**: 471-481.

Curtis, C. D., Hughes, C. R., Whiteman, J. A., and Whittle, C. K., 1985. Compositional variation within some sedimentary chlorites and some comments on their origin. Min. Mag. **49**: 375-386.

Darwin, C., 1846. Geological Observations. D. Appleton and Co., New York.

deBoer, R. B., 1977. On the thermodynamics of pressure solution - Interaction between chemical and mechanical forces. Geochim. Cosmochim. Acta **41**: 249-256.

Deer, W. A., Howie, R. A., and Zussman, J., 1975. An Introduction to the Rock-forming Minerals. Longman, London. 528 p.

Dewey, J. J., 1965. Nature and origin of the kink-band. Tectonophysics **1**: 459-494.

Dieterich, J. H., 1969. Origin of cleavage in folded rocks. Am. Jour. Sci. **267**: 155-165.

Dixon, J. M., 1976. Apparent double rotation of porphyroblasts during a single progressive deformation. Tectonophysics **34**: 101-116.

Durney, D. W., 1972. Solution-transfer, an important geological deformation mechanism. Nature **235**: 315-317.

Durney, D. W. and Ramsey, J. G., 1973. Incremental strains measured by syntectonic crystal growths, in DeJong, K. A., and Scholten, R., eds., Gravity and Tectonics. J. Wiley & Sons, New York, p. 67-96.

Elliot, D., 1973. Diffusion flow laws in metamorphic rocks. GSA Bull. **89**: 2645-2662.

Emmons, S. F. and Laney, F. B., 1926. Geology and Ore Deposits of the Ducktown Mining District, Tennessee. USGS Prof. Paper **139**.

Epstein, J. B. and Epstein, A. G., 1969. Geology of the Valley and Ridge Province between Delaware Water Gap and Lehigh Gap, Pennsylvania in Subitzky, S., ed., Geology of selected areas in New Jersey and eastern Pennsylvania and guidebook of excursions. 1969 Ann. Meeting GSA in Atlantic City, N. J. Rutgers Univ. Press, New Brunswick, p. 132-205.

Etheridge, M. A., Wall, V. J., and Vernon, R. H., 1983. The role of the fluid phase during regional metamorphism and deformation. Jour. Metamorphic Geol. **1**: 205-226.

Fairbairn, H. W., 1935. Notes on the mechanics of rock foliation. J. Geol. 43: 591-608.

Fairbairn, H. W., 1949. Structural Petrology of Deformed Rocks. Addison-Wesley, Cambridge, 344 p.

Ferguson, C. C., 1979. Rotation of elongate particles in slow non-Newtonian flows. Tectonophysics **60**: 247-262.

Fisher, O., 1884. On cleavage and distortion. Geol. Mag., New Ser., III **1**: 396-406.

Ghosh, S. K. and Ramberg, H., 1978. Reversal of the spiral direction of inclusion trails in paratectonic porphyroblasts. Tectonophysics **51**: 83-98.

Gonzales-Bonorino, F., 1960. The mechanical factor in the formation of schistosity. Int. Geol. Congr., 21st, Copenhagen, 1960, Rep. Ses. Norden 18: 303-316.

Granath, J. W., 1978. Strain history and metamorphism of the Burra Burra Anticline at Ducktown, Tennessee. Southeastern Geology 19: 231-240.

Gray, D. R., 1977. Some parameters which affect the morphology of crenulation cleavages. J. Geol. 85: 763-780.

Gray, D. R., 1978. Cleavages in deformed psammitic rocks from southeastern Australia: their nature and origin. GSA Bull. 89: 577-590.

Gregg, W. J., 1985. Microscopic deforamation mechanisms associated with mica film formation in cleaved psammitic rocks. Jour. Struct. Geol. 7: 45-56.

Groshong, R. H., 1975. "Slip" cleavage caused by pressure solution in a buckle fold. Geology 3: 411-413.

Groshong, R. H., 1976. Strain and pressure solution in the Martinsburg Slate, Delaware Water Gap, New Jersey. Amer. Jour. Sci. 276: 1131-1146.

Guidotti, C. V., 1984. Micas in Metamorphic Rocks. Reviews in Mineralogy 13: 357-469.

Hadley, J. B., 1970. The Ocoee Series and its possible correlatives, in Studies of Appalachian Geology: Central and Southern. Edited by Fisher, G. W., Pettijohn, F. J., Reed, J. C., Jr., and Weaver, K. N., Interscience Publishers, New York, 460 p.

Harker, A., 1885. The cause of slaty cleavage, compression vs shearing. Geol. Mag. 2: 15-17.

Harker, A., 1886. Slaty cleavage and related rock structures.

Haughton, S., 1856. On slaty cleavage and the distortion of fossils. Philos. Mag. 12: 409-412.

Hayes, J. B., 1970. Polytypism of chlorite in sedimentary rocks. Clays and Clay Min. 18: 285-306.

Heald, M. T., 1956. Cementation of Simpson and St. Peter Sandstones in parts of Oklahoma, Arkansas, and Missouri. J. Geol. 64: 16-30.

Hernon, R. H., 1968. Geology of the Ducktown, Isabella, and Persimmon Creek quadrangles, Tennessee and North Carolina. USGS Open File Report.

Holcombe, R. J., 1973. Mesoscopic and microscopic analysis of deformation and metamorphism near Ducktown, Tennessee. Ph.D. dissertation, Stanford Univ., 225 p.

Holeywell, R. C. and Tullis, T. E., 1975. Mineral reorientation and slaty cleavage in the Martinsburg Formation, Lehigh Gap, Pennsylvania. GSA Bull. **86**: 1296-1304.

Hower, J., Eslinger, E., Hower, M. E., and Perry, E. A., 1976. Mechanism of burial metamorphism in argillaceous sediments: 1. Mineralogical and chemical evidence. GSA Bull. **87**: 725-737.

Hunziker, J. C., Frey M., Clauer, N., Dallmeyer, R. D., Friedrichsen, H., Flehmig, W., Hochstrassen, K., Roggwiler, P., Schwander, H., 1986. The evolution of illite to muscovite: mineralogical and isotopic data from the Glarus Alps, Switzerland. Contr. Min. Pet. **92**: 157-180.

Hurst, J. V. and Schlee, J. S., 1962. Field excursions, Ocoee metasediments north central Georgia - Southeast Tennessee. Annual Meeting Southeastern GSA.

Jeffrey, G. B., 1922. The motion of ellipsoidal particles immersed in a viscous fluid. Royal Soc. London Proc., Ser. A. **102**: 161-179.

Kamb, W. B., 1959. Theory of preferred crystal orientation developed by crystallization under stress. J. Geol. **67**: 153-170.

Kamb, W. B., 1961. The thermodynamic theory of nonhydrostatically stressed solids. Jour. Geophys. Res. **66**: 259-271.

King, P. B., Hadley, J. B., Newman, R. B., Hamilton, W., 1958. Stratigraphy of Ocoee Series, Great Smoky Mountains, Tennessee and North Carolina. GSA Bull. **69**: 947-966.

Kinkel, A. R., Thomas, H. H., Marvin, R. F., and Walthall, F. G., 1965. Age and metamorphism of some massive sulfide deposits in Virginia, North Carolina, and Tennessee. Geochim. Cosmochim. Act. **29**: 717-724.

Knipe, R. J. and White, S. H., 1977. Microstructural

variation of an axial plane cleavage around a fold. A H.V.E.M. study. Tectonophysics 39: 355-381.

Knipe, R. J., 1979. Chemical changes during slaty cleavage development. Bull. Mineral. 102: 206-209.

Knipe, R. J., 1981a. The interaction of deformation and metamorphism in slates. Tectonophysics 78: 249-272.

Labotka, T. C., 1971. Slaty Cleavage at Madden Branch, Tennessee. Bachelor's Thesis, University of Illinois, Champaign-Urbana, Illinois.

Lee, J. H., Peacor, D. R., Lewis, D. D., and Wintsch, R. P., 1984. Chlorite-illite/muscovite interlayered and interstratified crystals: a TEM/STEM study. Contr. Min. Pet. 88: 372-385.

Lee, J. H., Peacor, D. R., Lewis, D. D., and Wintsch, R. P., 1986. Evidence for Syntectonic Crystallization for the Mudstone to Slate Transition at Lehigh Gap, Pennsylvania. Jour. Struct. Geol. 8: 767-780.

Leith, C. K., 1905. Rock Cleavage. USGS Bull. 239, 216 p.

Lewis, D. D., 1980. An Investigation of the Preferred Orientation of Phyllosilicates in the Martinsburg Slate, Lehigh Gap Area, Pennsylvania. Master's thesis, Indiana University.

Lipshie, S. R., Oertel, G., and Christie, J. M., 1976. Measurement of preferred orientation of phyllosilicates in schists. Tectonophysics 39: 91-99.

Magee, M., 1970. Geology and ore deposits of the Ducktown District, Tennessee, in Ridge, J. D., ed., Ore Deposits of the United States 1933-1967, Graton-Sales Vol.; AIME, New York, p.207-241.

March, A., 1932. Mathematische Theorie der Regelung nach der Korngestalt bei affiner Deformation. Z. Kristallogr., Kristallgeom., Kristallphys., Kristallchem. 81: 285-298.

Maxwell, J. C., 1962. Origin of slaty and fracture cleavage in the Delaware Water Gap area, New Jersey and Pennsylvania, in Petrologic Studies (Buddington Volume). GSA, New York, p. 281-311.

Maxwell, D. T. and Hower, J, 1967. High-grade diagenesis and low-grade metamorphism of illite in the Precambrian Belt series. Am. Min. 52: 843-857.

Means, W. D., 1977. Experimental contributions to the study of foliations in rocks: a review of research since 1960. Tectonophysics **39**: 329-354.

Moench, R. H., 1966. Relation of S2 schistosity to metamorphosed clastic dikes, Rangeley-Phillips area, Maine. GSA Bull. **77**: 1449-1462.

Morris, A. P., 1981. Competing deformation mechanisms and slaty cleavage in deformed, quartzose meta-sediments. J. Geol. Soc. Lond. **138**: 455-462.

Nesbitt, B. E., 1979. Regional metamorphism of the Ducktown, Tennessee massive sulfides and ajoining portions of the Blue Ridge Province. Ph.D. dissertaition, Univ. of Michigan.

Nesbitt, B. E. and Essene, E. J., 1982. Metamorphic thermometry and barometry of a portion of the southern Blue Ridge province. Amer. Jour. Sci. **282**: 701-729.

Nicholson, R., 1966. Metamorphic differentiation in crenulated schists. Nature **209**: 68-69.

Nickelson, R. P., 1979. Attributes of rock cleavage in some mudstones and limestones of the Valley and Ridge Province, Pennsylvania. Proceedings of the Pennsylvania Academy of Science **46**: 107-112.

Oertel, G., 1970. Deformation of a slaty lapillar tuff in the Lake District, England. GSA Bull. **81**: 1173-1188.

Oertel, G. and Phakey, P. P., 1972. The texture of a slate from Nantlle Cernarvoa, North Wales. Texture, 1: 1-8.

Owens, W. H., 1973. Strain modification of angular density distributions. Tectonophysics **16**: 249-261.

Phillips, J., 1884. On certain movements in the parts of stratified rocks. Rep. Br. Assoc. Adv. Sci. **1843**: 60-61.

Pique, A., 1982. Relations between stages of diagenetic and metamorphic evolution and the development of a primary cleavage in the northwestern Moroccan Meseta. Jour. Struct. Geol. **4**: 491-500.

Powell, C. McA., 1969. Intrusive sandstone dykes in the Siamo Slate near Negaunee, Michigan. GSA Bull. **80**: 2585-2594.

Powell, C. McA., 1972. Tectonic dewatering and strain in the Michigamme Slate, Michigan. GSA Bull. 83: 2149-2158.

Powell, C. McA., 1979. A morphological classification of rock cleavage. Tectonophysics 58: 21-34.

Rast, N., 1965. Nucleation and growth of metamorphic minerals, in Pitcher, W. S. and Flinn, G. W., eds., Controls on Metamorphism. J. Wiley & Sons, New York, p. 73-102.

Rast, N. and Kohles, K. M., 1986. The origin of the Ocoee Supergroup. Amer. Jour. Sci. 286: 593-616.

Robin, P.-Y. F., 1978. Pressure solution at grain-to-grain contacts. Geochim. Cosmochim. Acta 42: 1383-1389.

Robin, P.-Y. F., 1979. Theory of metamorphic segregation and related processes. Geochim. Cosmochim. Acta 43: 1587-1600.

Safford, J. M., 1856. A Geological Reconnoissance of the State of Tennessee. First Biennial Report, State Geologist. 164 p.

Safford, J. M., 1869. Geology of Tennessee, Tennessee Office of Geologist and Mineralogist, Nashville, 551 p.

Sassi, F. P. and Scolari, S. B., 1974. The b_o value of the potassic white micas as a barometric indicator in low-grade metamorphism of pelitic schists. Contr. Min. Pet. 45: 143-152.

Sedgewick, A., 1835. Remarks on the structure of large mineral masses, and especially on the chemical changes produced in the aggregation of stratified rocks during different periods after their deposition. Trans. Geol. Soc. Lond. 2nd ser., 3: 461-486.

Sharpe, D., 1847. On slaty cleavage. Q. J. Geol. Soc. Lond. 3: 74-104.

Sharpe, D., 1849. On slaty cleavage. Q. J. Geol. Soc. Lond. 5: 111-115.

Sibley, D. F. and Blatt, H., 1976. Intergranular pressure solution and cementation of the Tuscarora orthoquartzite. J. Sed. Petrology 46: 881-896.

Siddans, A. W. B., 1972. Slaty cleavage - a review of research since 1815. Earth Sci. Reviews **8**: 205-232.

Sorby, H. C., 1853. On the origin of slaty cleavage. New Philos. J. Edinb. **55**: 137-148.

Sorby, H. C., 1856. On slaty cleavage, as exhibited in the Devonian limestones of Devonshire. Philos. Mag. **11**: 20-37.

Sorby, H. C., 1857. On some facts connected with slaty cleavage. Rep. Br. Assoc. Adv. Sci. **1857** (part 2), p. 92-93.

Spry, A. H., 1969. Metamorphic Textures. Pergamon, Oxford, 350p.

Stephens, M. B., Glasson, M. J., and Keays, R. R., 1979. Structural and Chemical Layering Development in Metasediments from Clunes, Australia. Amer. Jour. Sci. **279**: 129-160.

Stose, G. W. and Stose, A. J., 1944. The Chilhowee group and Ocoee Series of the southern Appalachians. Amer. Jour. Sci. **242**: 367-390.

Stose, G. W. and Stose, A. J., 1949. The Ocoee Series of the southern Appalachians. GSA Bull. **60**: 267-320.

Swager, N., 1985. Solution transfer, mechanical rotation and kink-band boundary migration during crenulation-cleavage development. Jour. Struct. Geol. **7**: 421-429.

Talbot, J. L. and Hobbs, B. E., 1968. The relationship of metamorphic differentiation to other structural features at three localities. Jour. Geology **76**: 581-587.

Tullis, T. E., 1971. Experimental development of preferred orientation of mica during recrystallization. Ph.D. Thesis, Univ. of California, Los Angeles, California. 262 p.

Tullis, T. E., 1976. Experiments on the origin of slaty cleavage and schistosity. GSA Bull. **87**: 745-753.

Turner, F. J. and Weiss, L. E., 1963. Structural Analysis of Metamorphic Tectonites. McGraw-Hill, New York.

Turner, F. J., 1981. Metamorphic Petrology. McGraw-Hill, New York.

Van Hise, C. R., 1896. Principles of North American Pre-Cambrian geology. Rep. USGS, **16**: 517-843.

Vernon, R. H., 1975. Metamorphic Processes. Halsted Press, New York, 247 p.

Voll, G. 1960. New work on petrofabrics. Liverp. Manch. Geol. J. **2**: 503-567.

Weaver, C. E., 1979. Geothermal Alteration of Clay Minerals and Shales: Diagenesis. Technical Report ONWI-21 for Battelle-Office fo Nuclear Waste Isolation. 176 p.

Weaver, C.E. and Pollard, L. D., 1973. The Chemistry of Clay Minerals. Elsevier, Amsterdam. 239 p.

Weaver, C. E. and Associates, 1984. Shale-Slate Metamorphism in the Southern Appalachians. Elsevier, Amsterdam, 239 p.

Weyl, P. K., 1959. Pressure solution and the force of crystallization - a phenomenological theory. J. Geophys. Res. **64**: 2001-2025.

White, S. H. and Knipe, R. J., 1978. Microstructure and cleavage development in selected slates. Contr. Min. Pet. **66**: 165-174.

White, S. H. and Johnston, D. C., 1981. A microstructural and microchenical study of cleavage lamellae in a slate. Jour. Struct. Geol. **3**: 279-290.

White, S. H., Huggett, J. M., and Shaw, H. F., 1985. Electron-optical studies of phyllosilicate intergrowths in sedimentary and metamorphic rocks. Min. Mag. **49**: 413-423.

Williams, P. F., 1972. Development of metamorphic layering and cleavage in low grade metamorphic rocks at Bermagui, Australia. Amer. Jour. Sci. **272**: 1-47.

Williams, P. F., 1976. Relationships between axial-plane foliations and strain. Tectonophysics **30**: 181-196.

Williams, P. F., 1977. Foliation: a review and discussion. Tectonophysics **39**: 305-328.

Wood, D. S., 1974. Current views of the development of slaty cleavage. Ann. Rev. Earth Plan. Sci. **2**: 369-401.

APPENDICES

APPENDIX 1

X-RAY DIFFRACTION PATTERNS

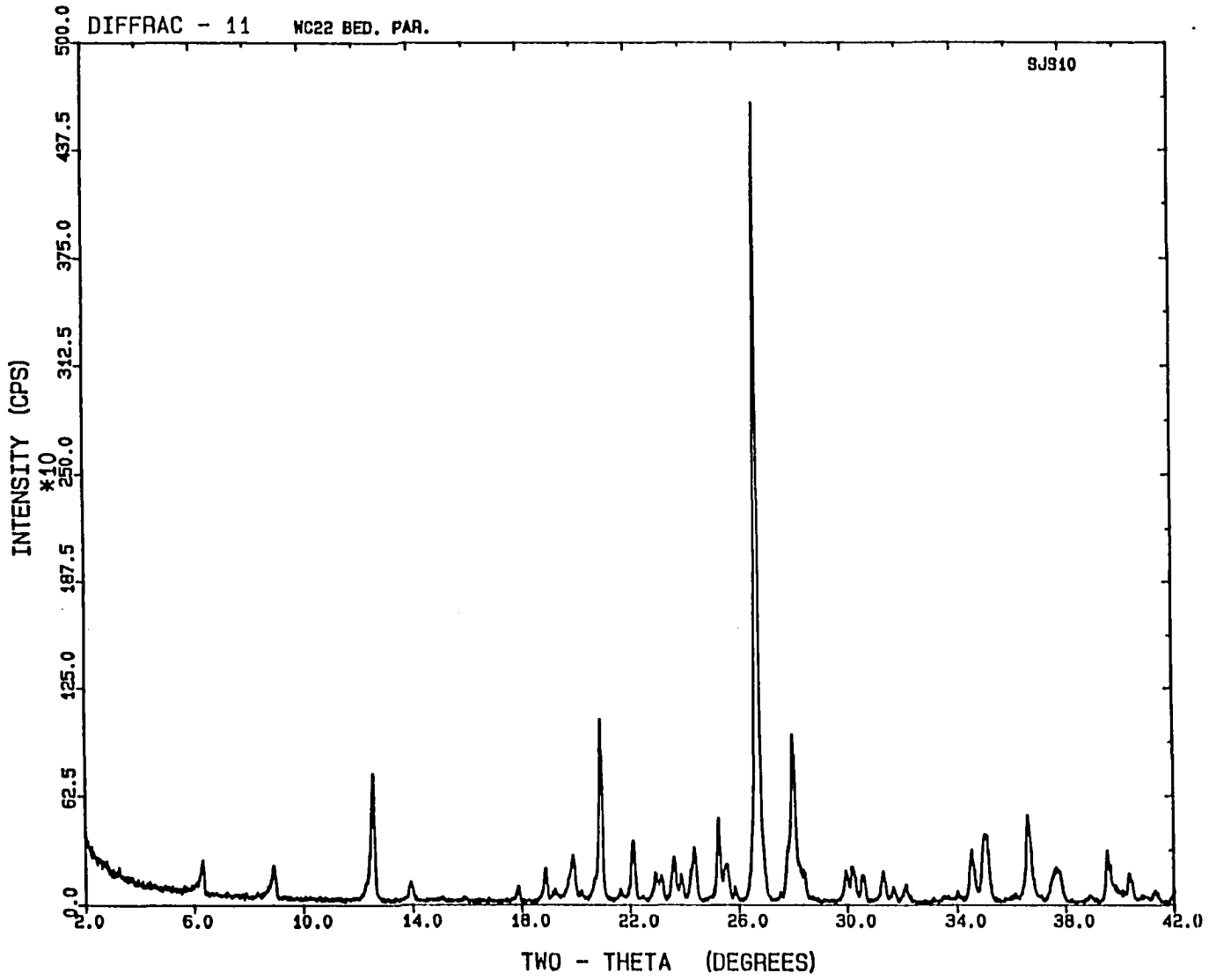

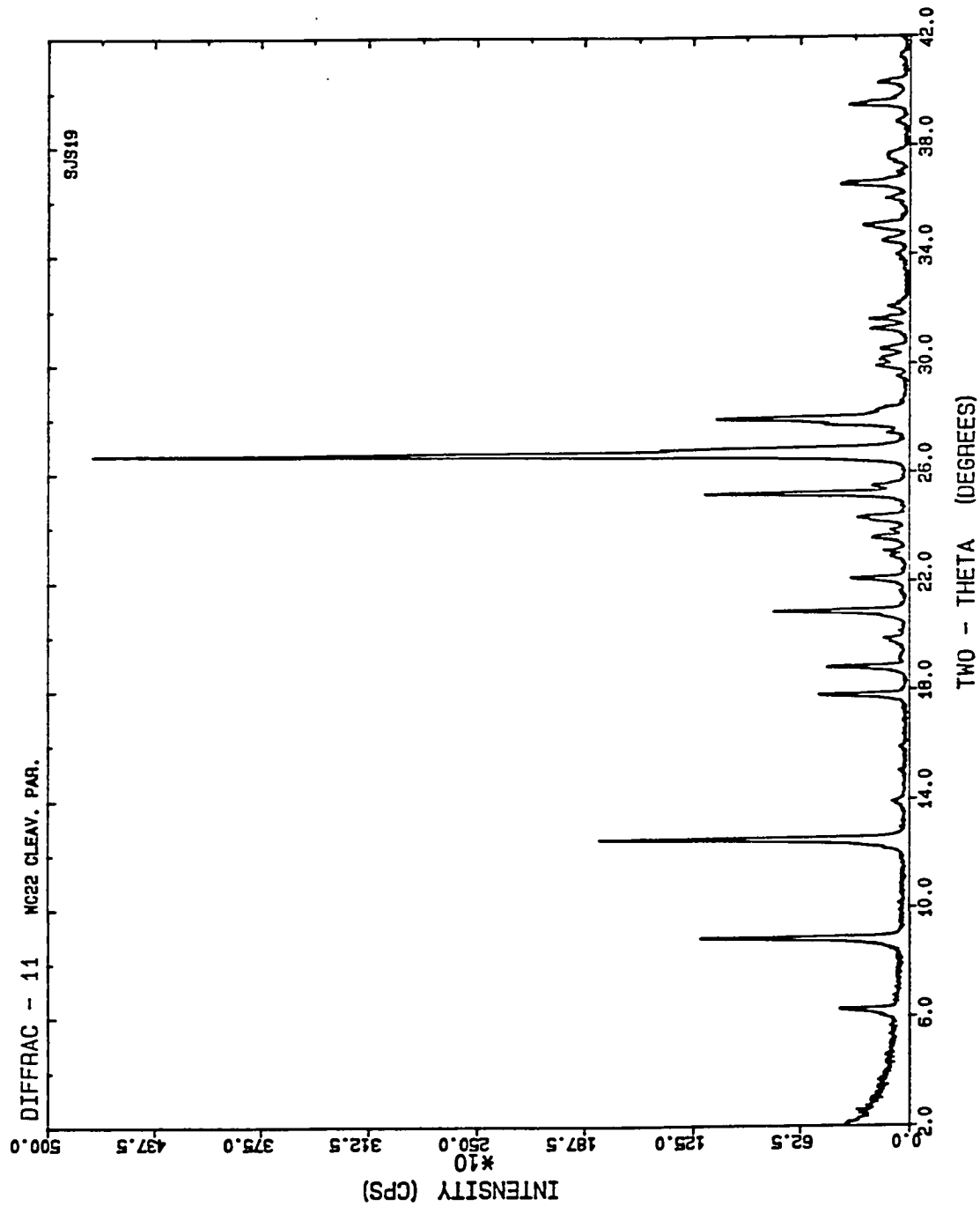

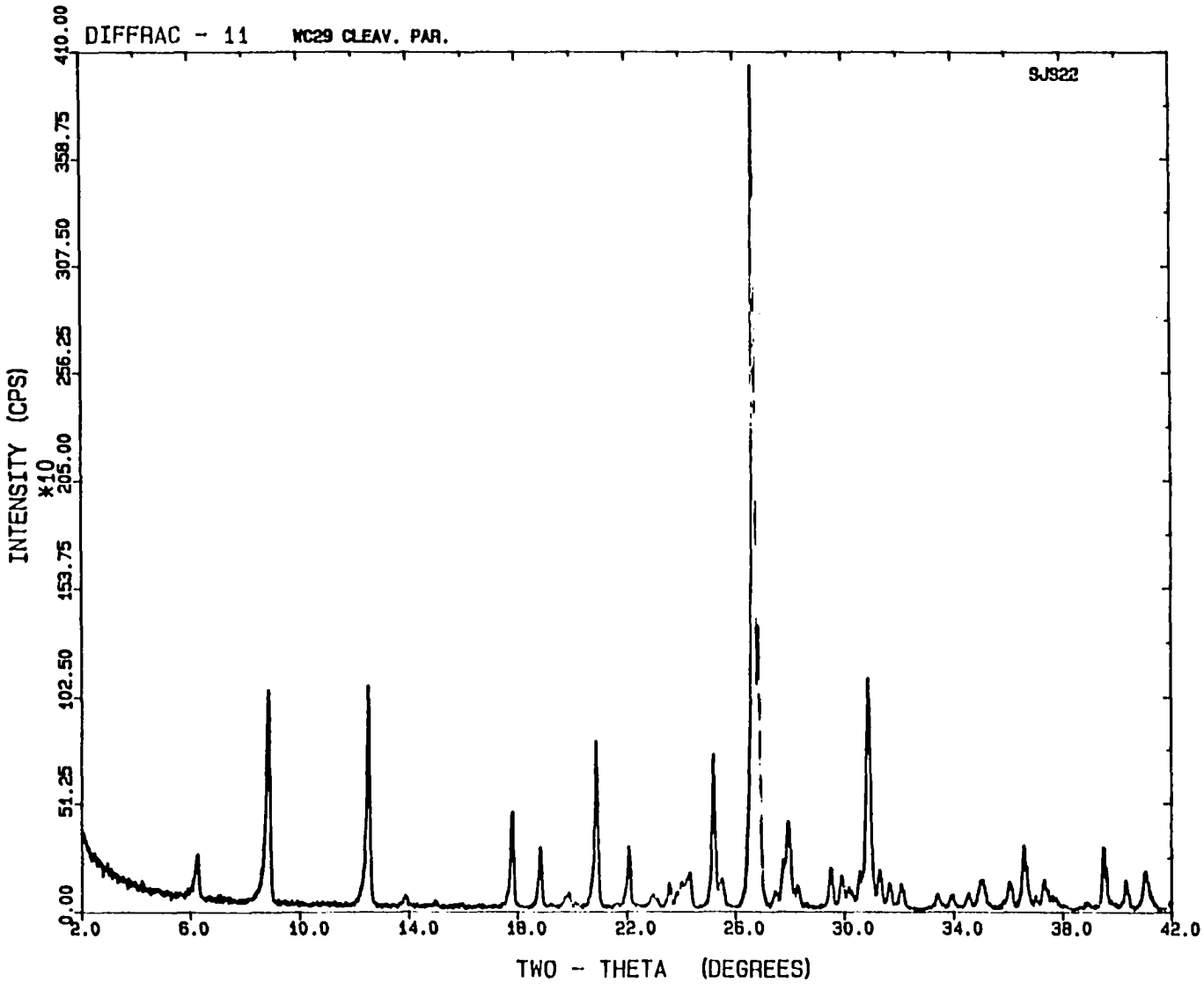

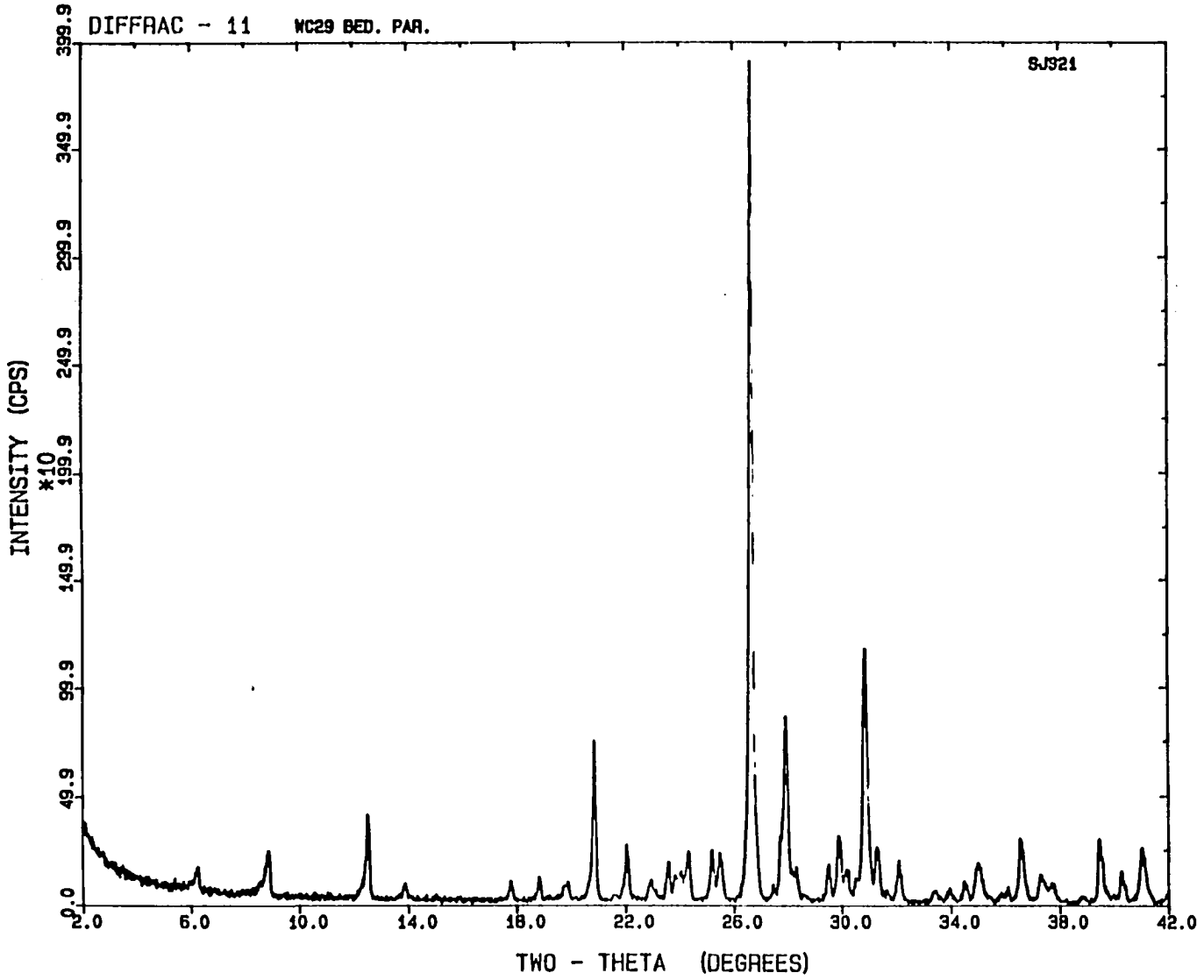

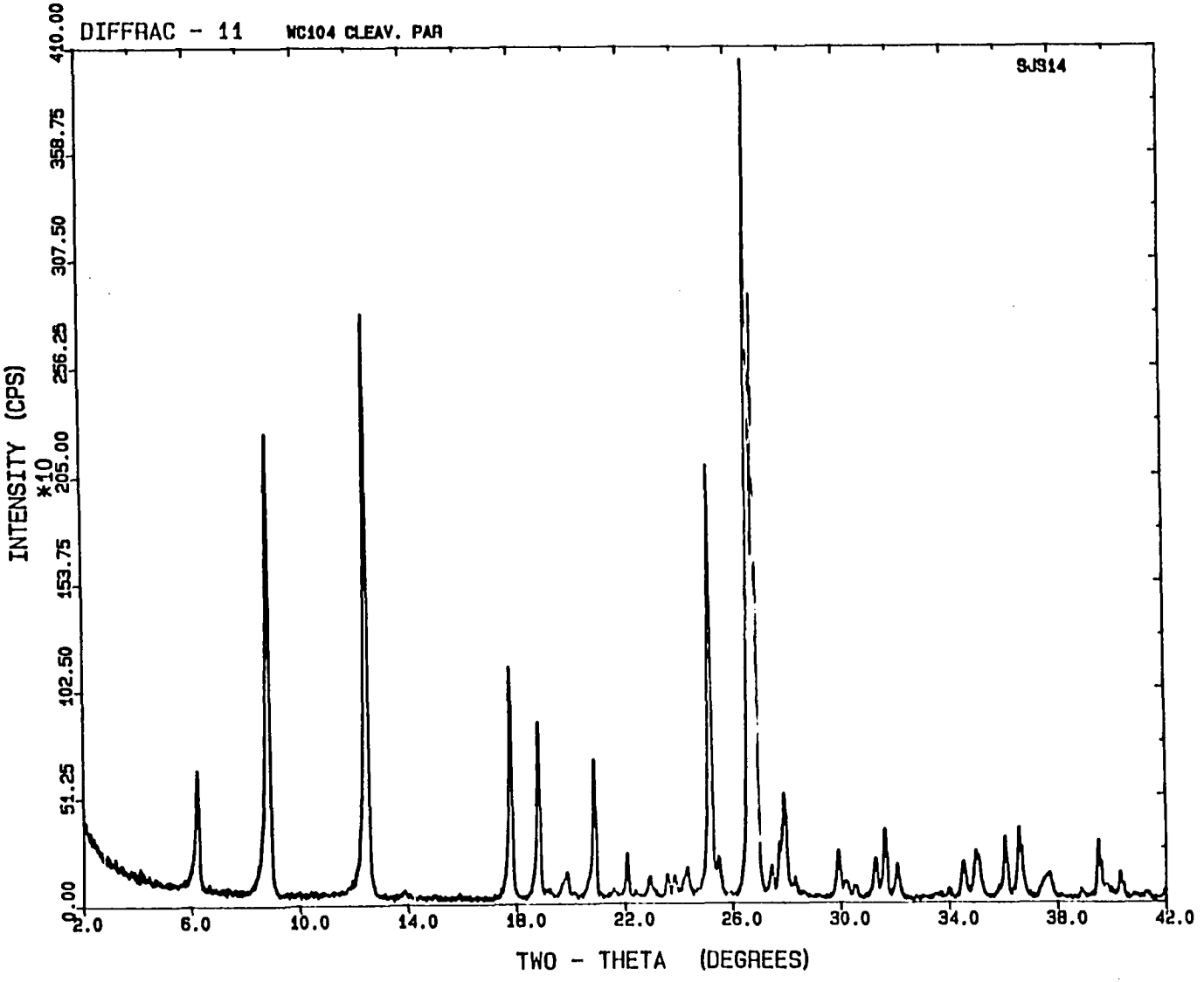

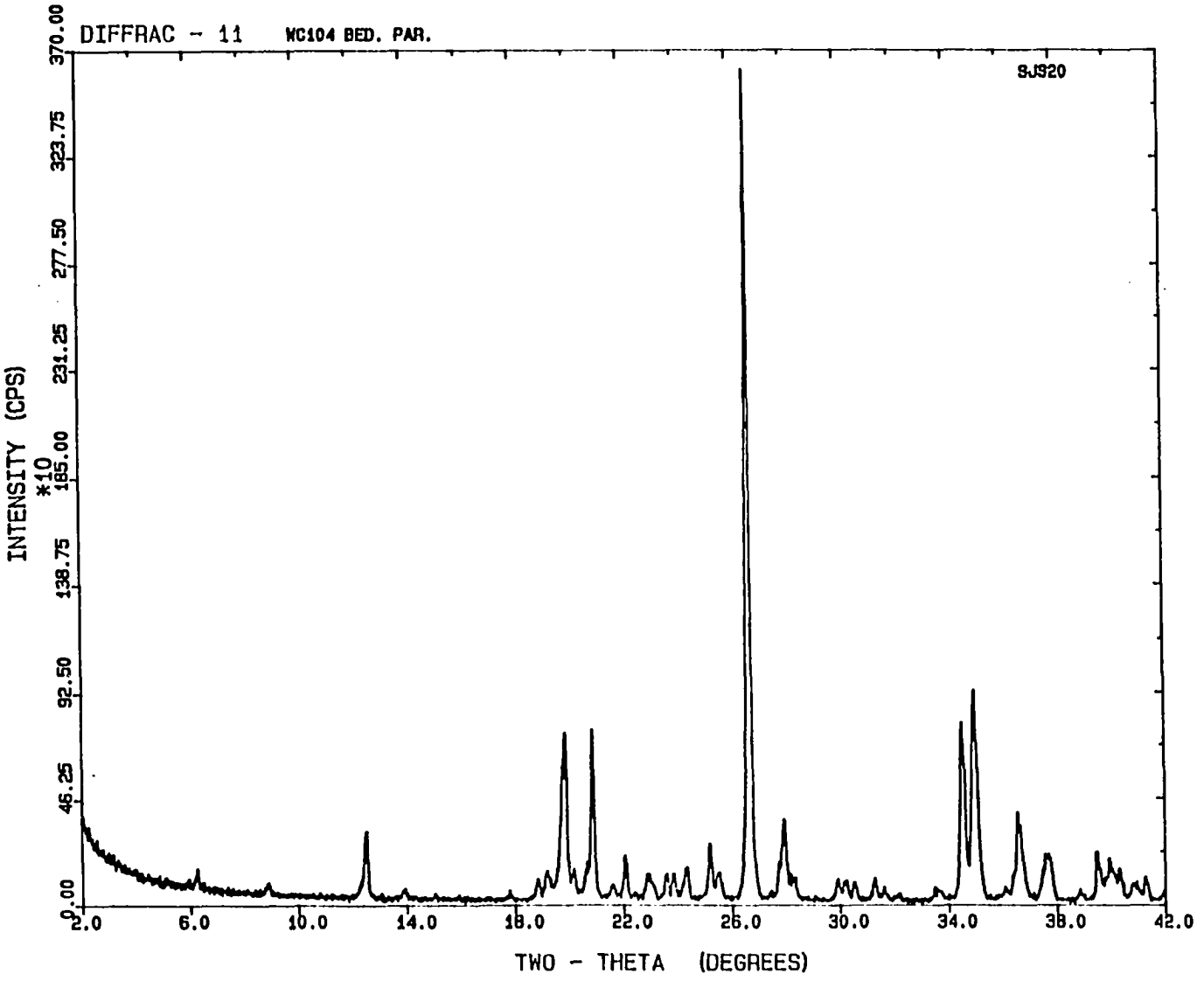

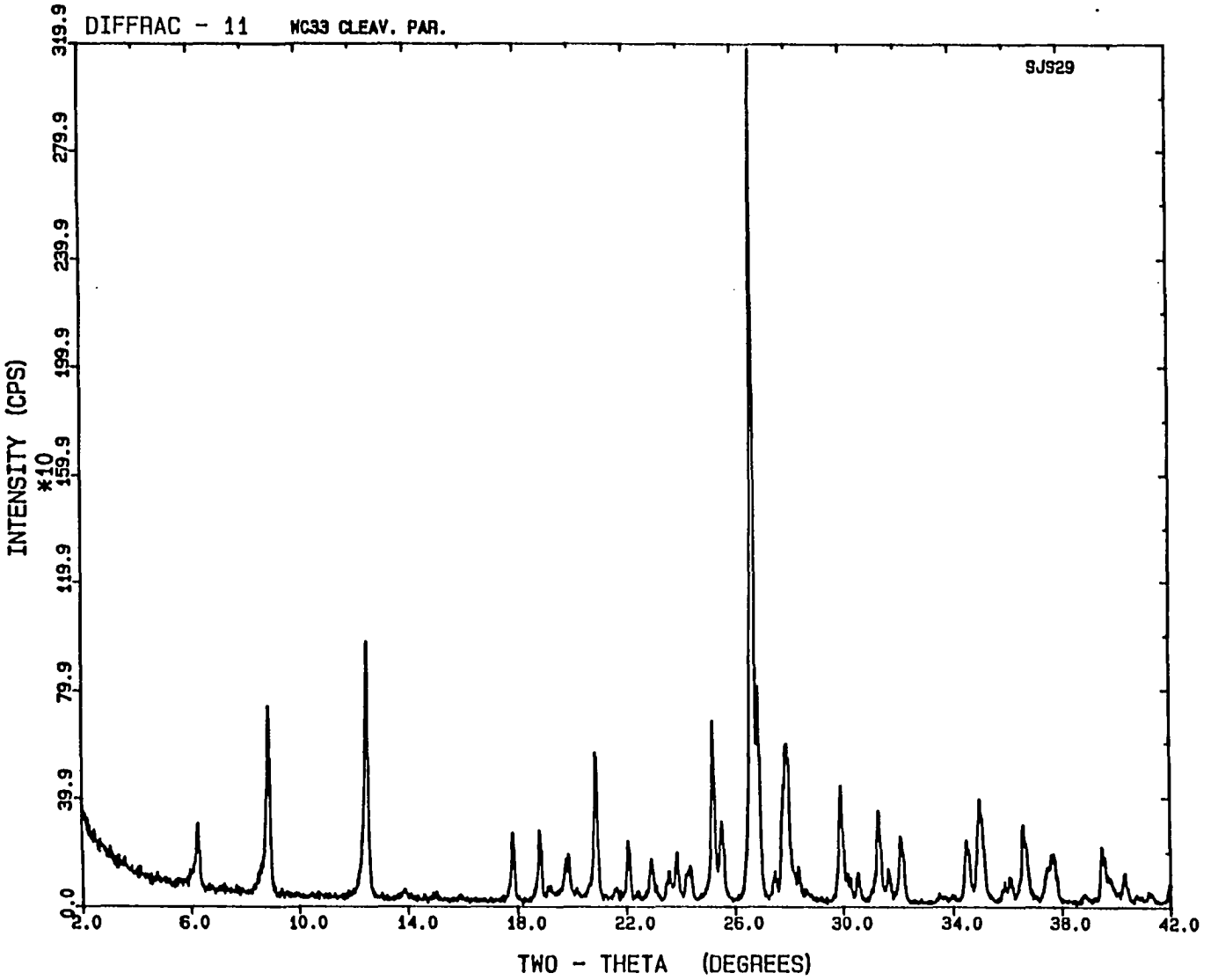

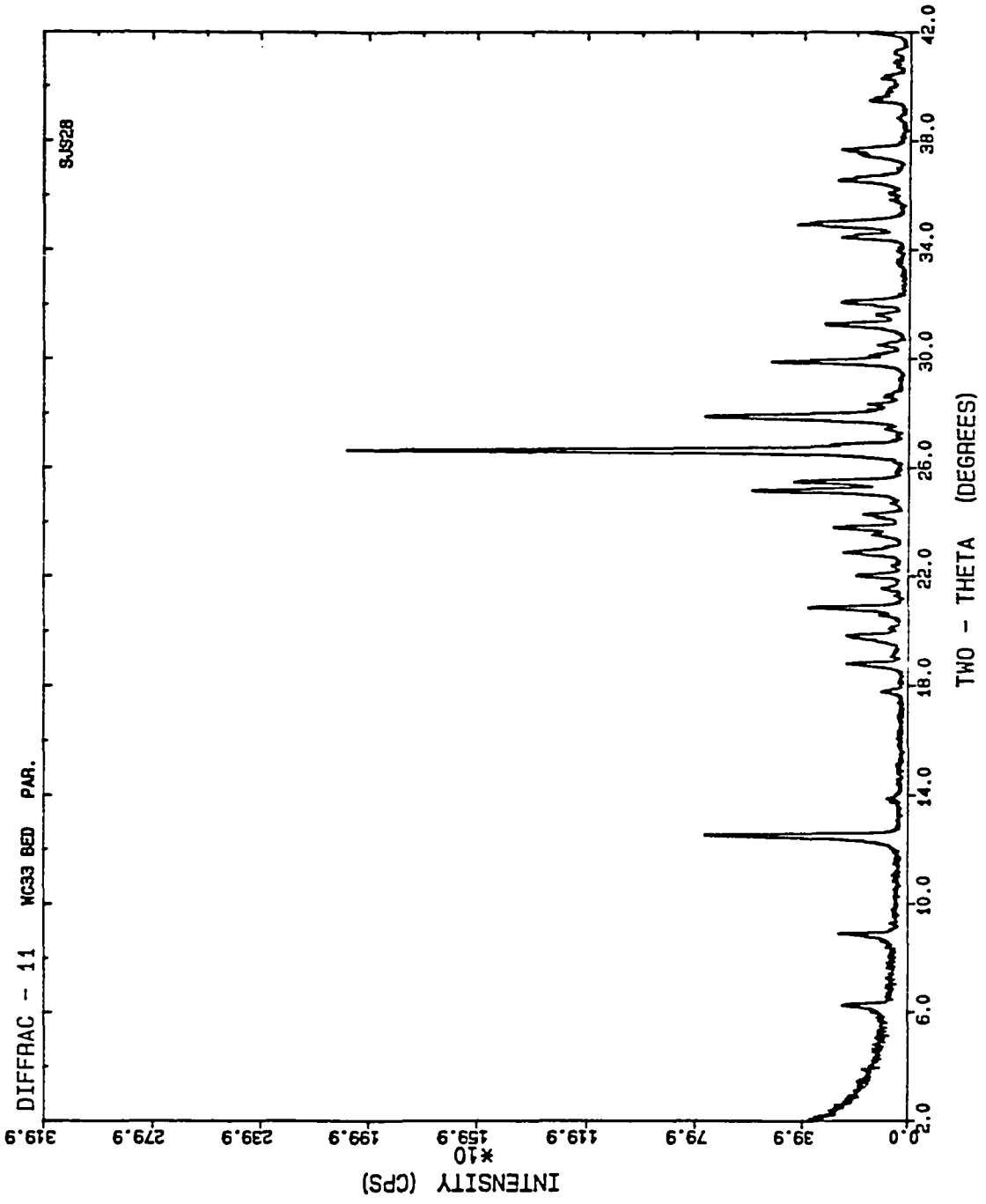

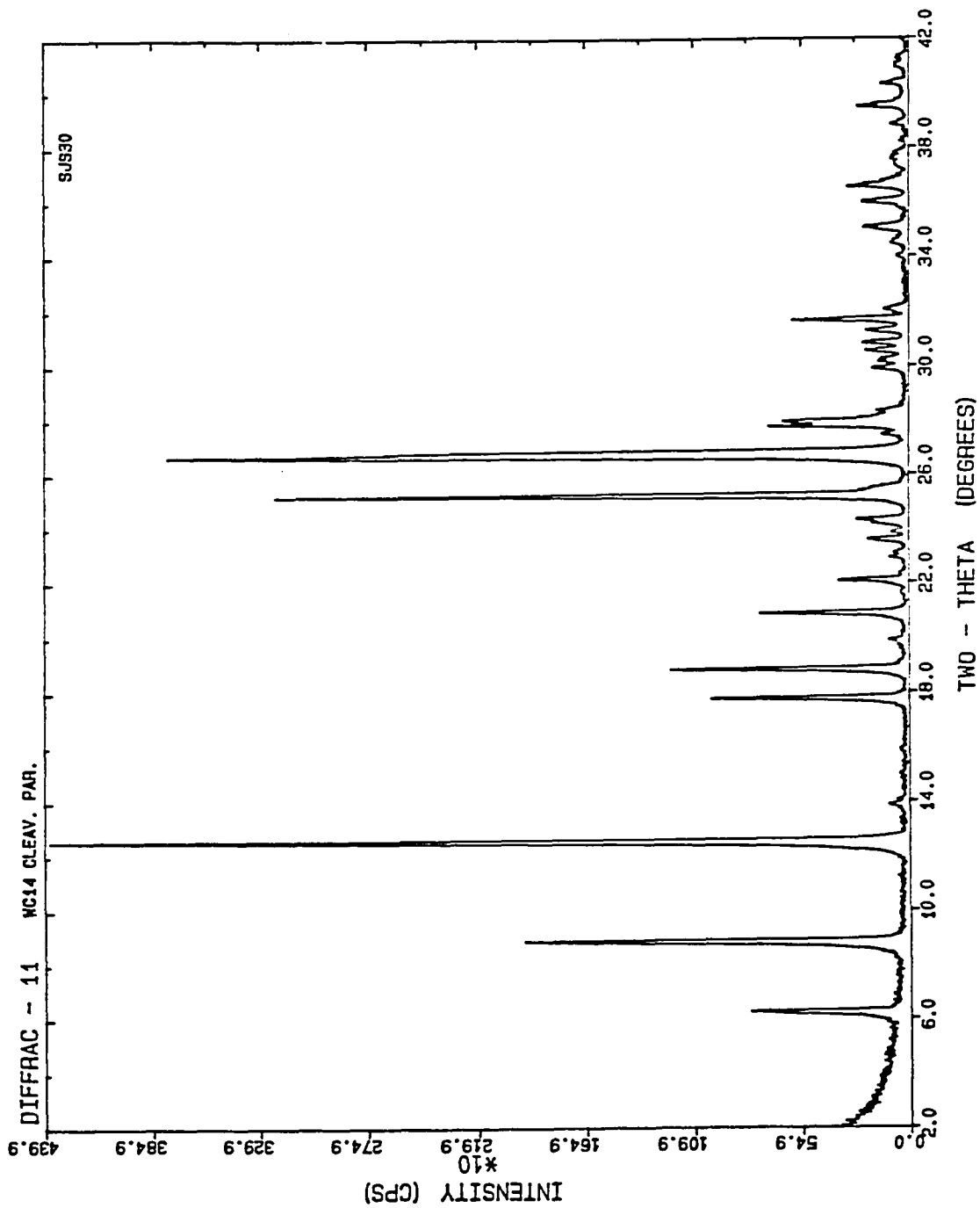

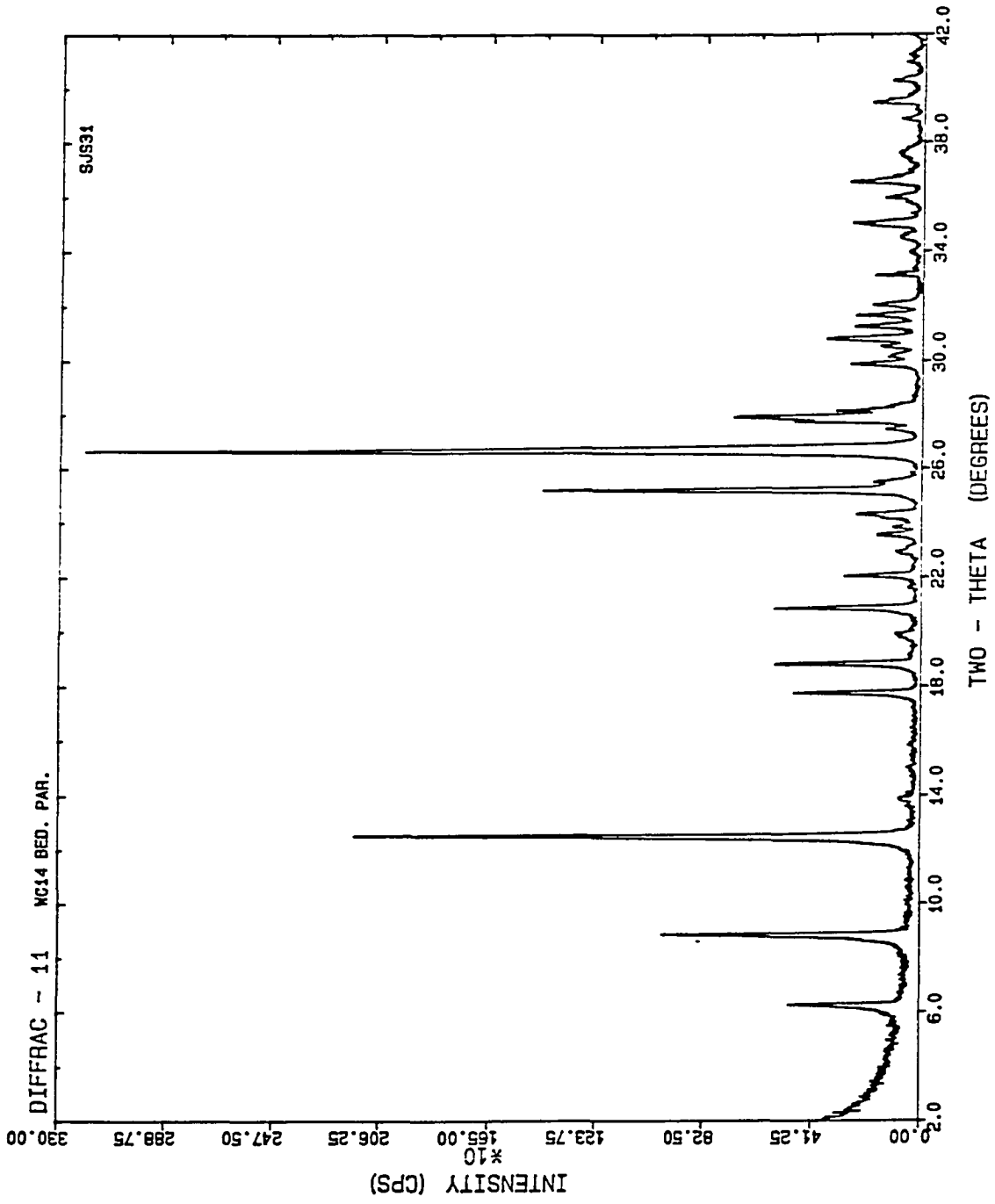

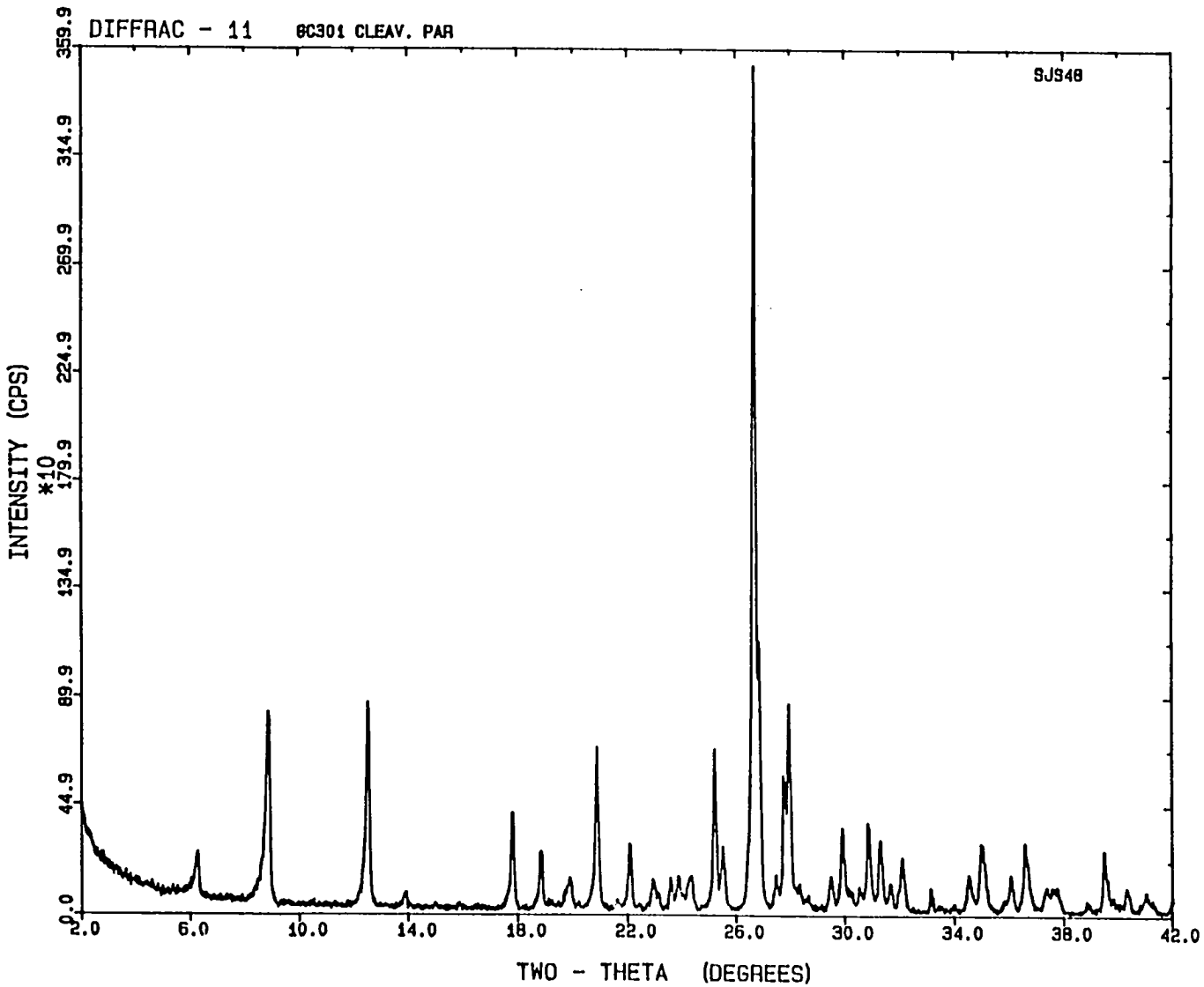

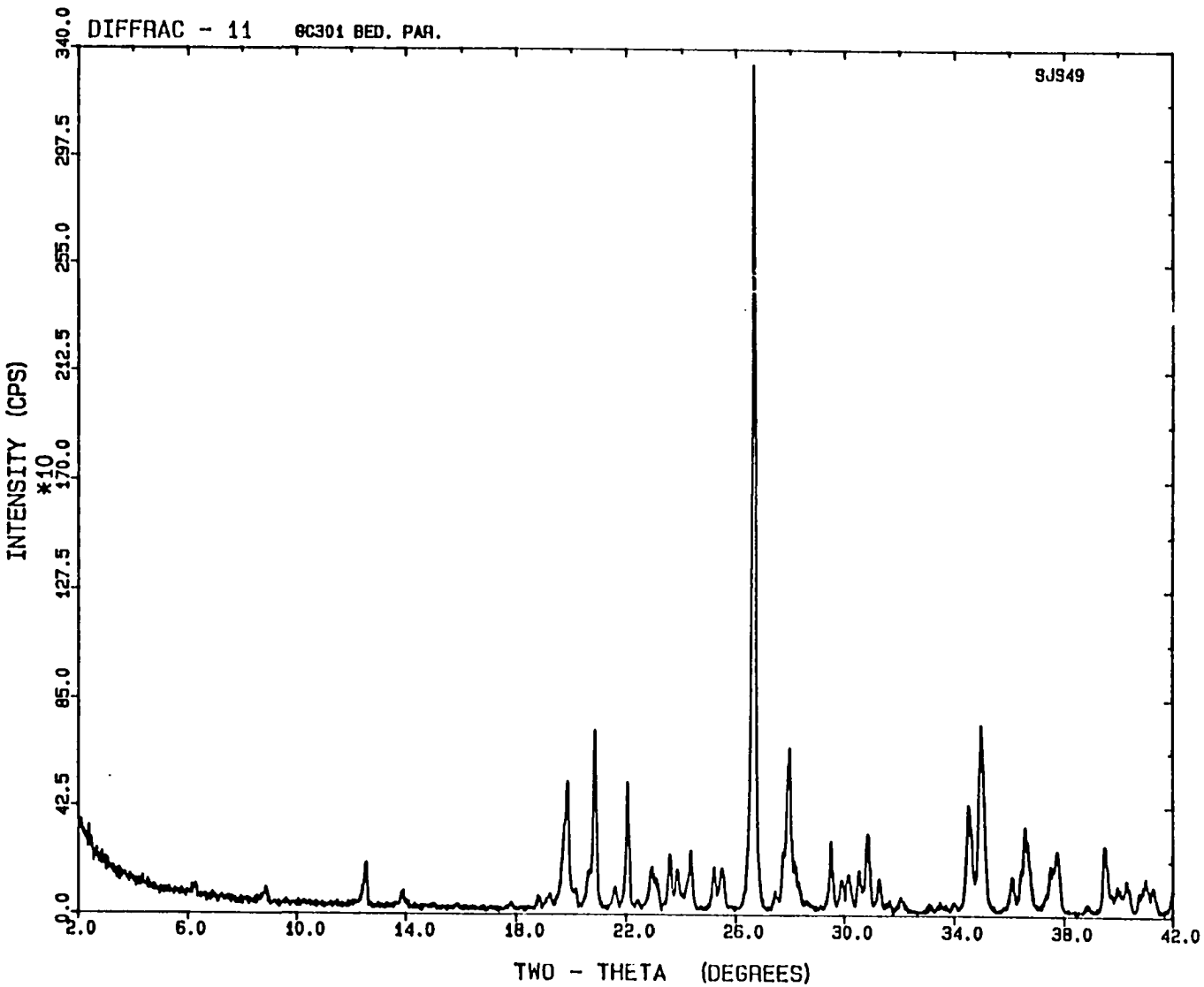

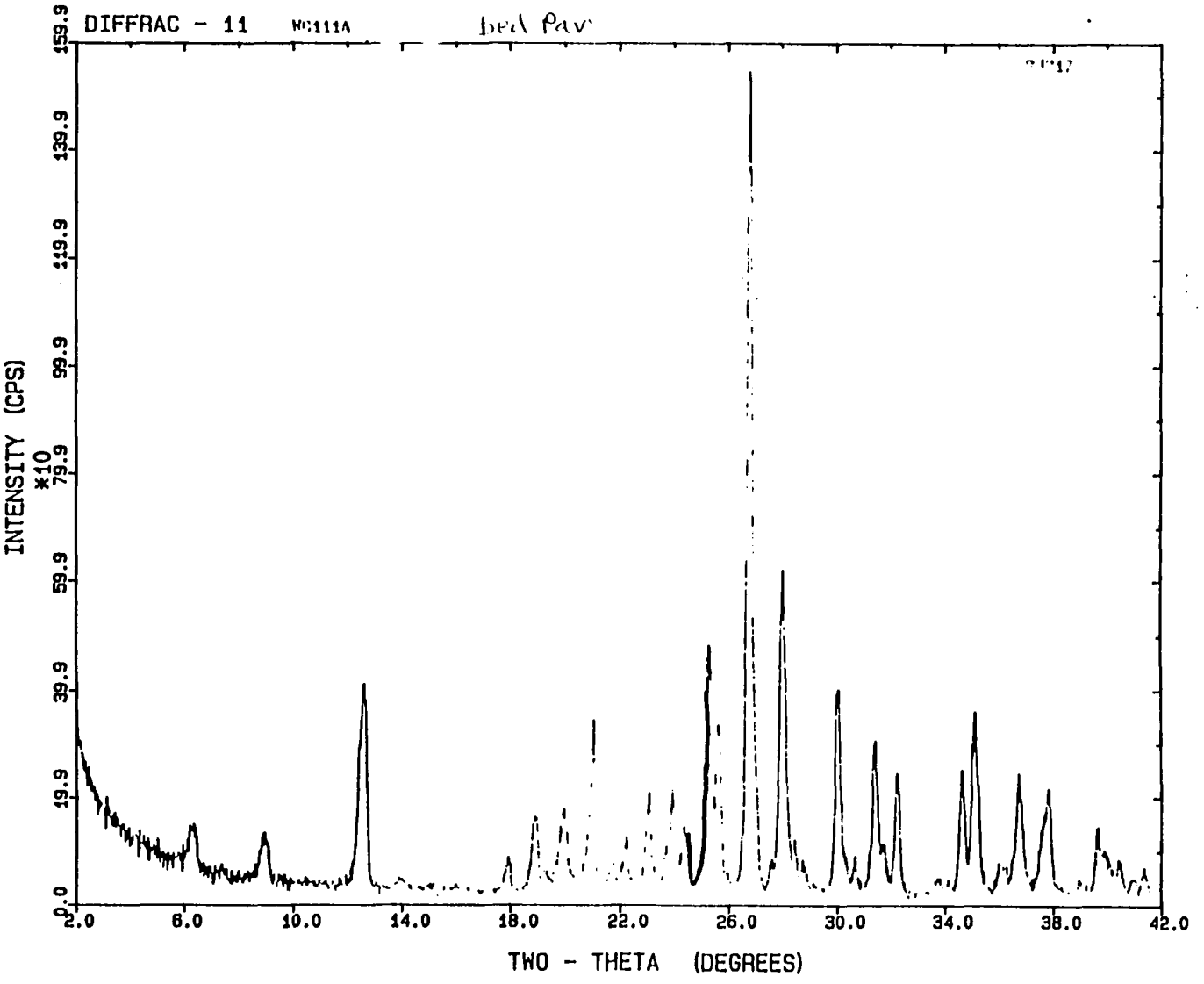

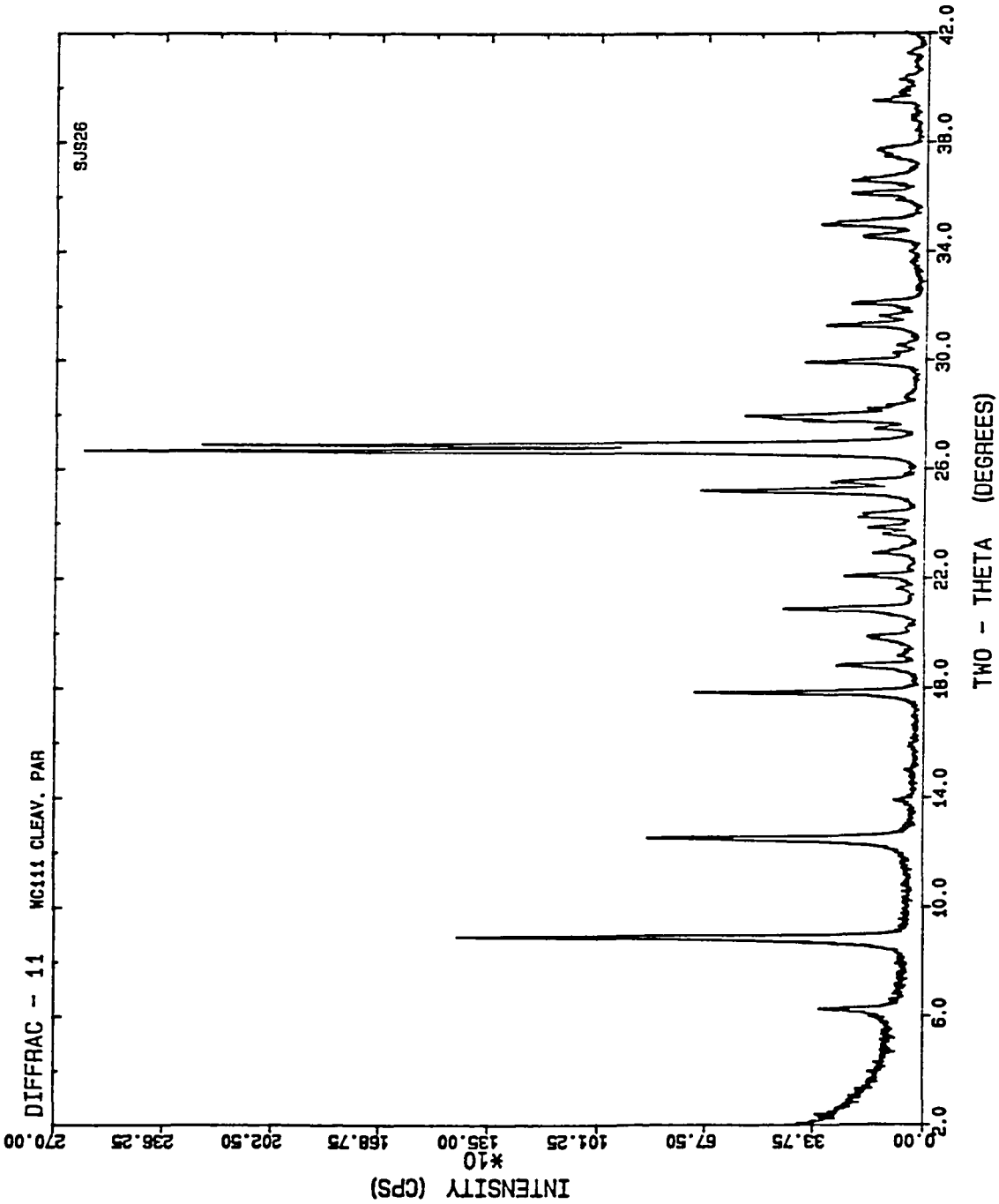

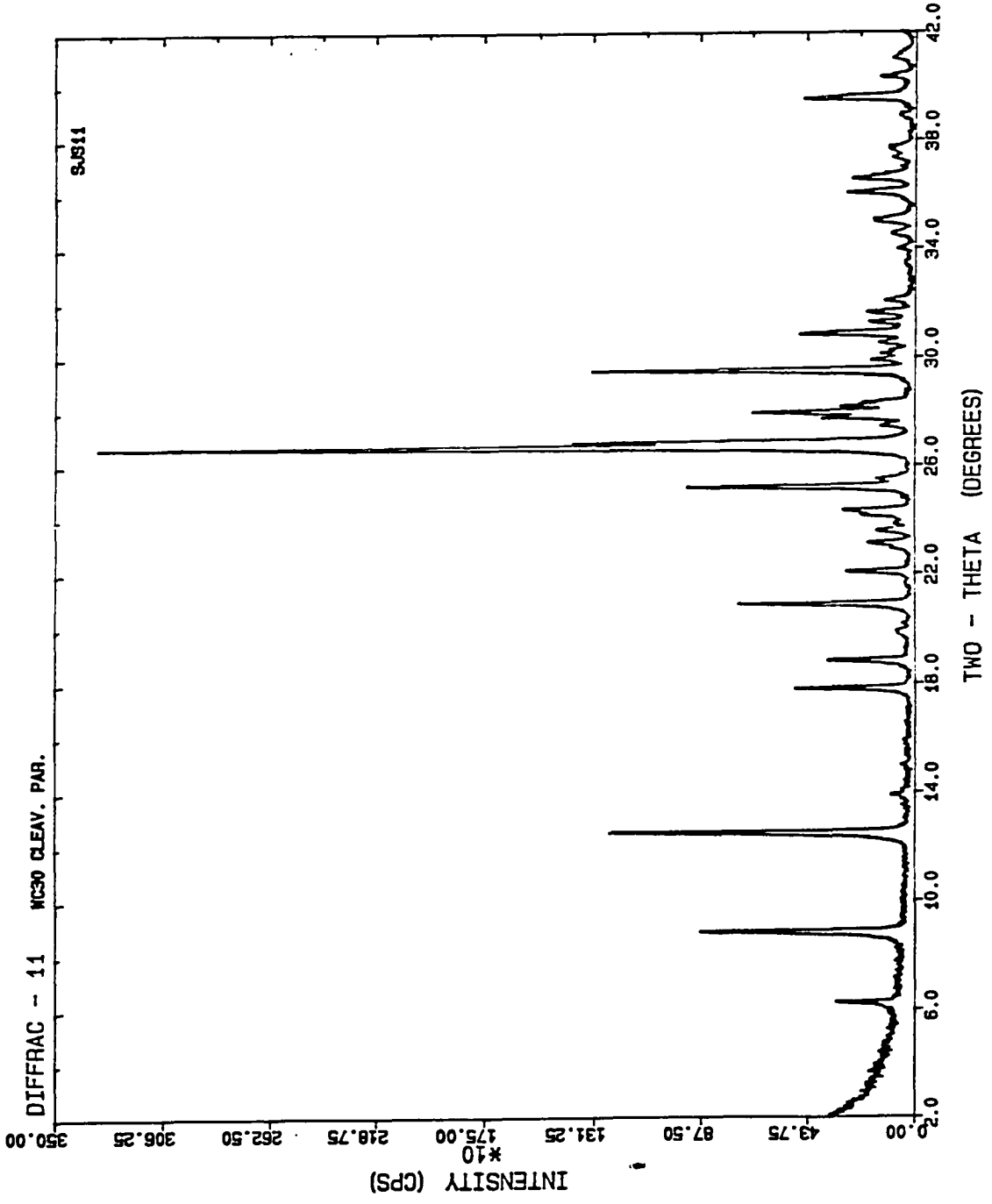

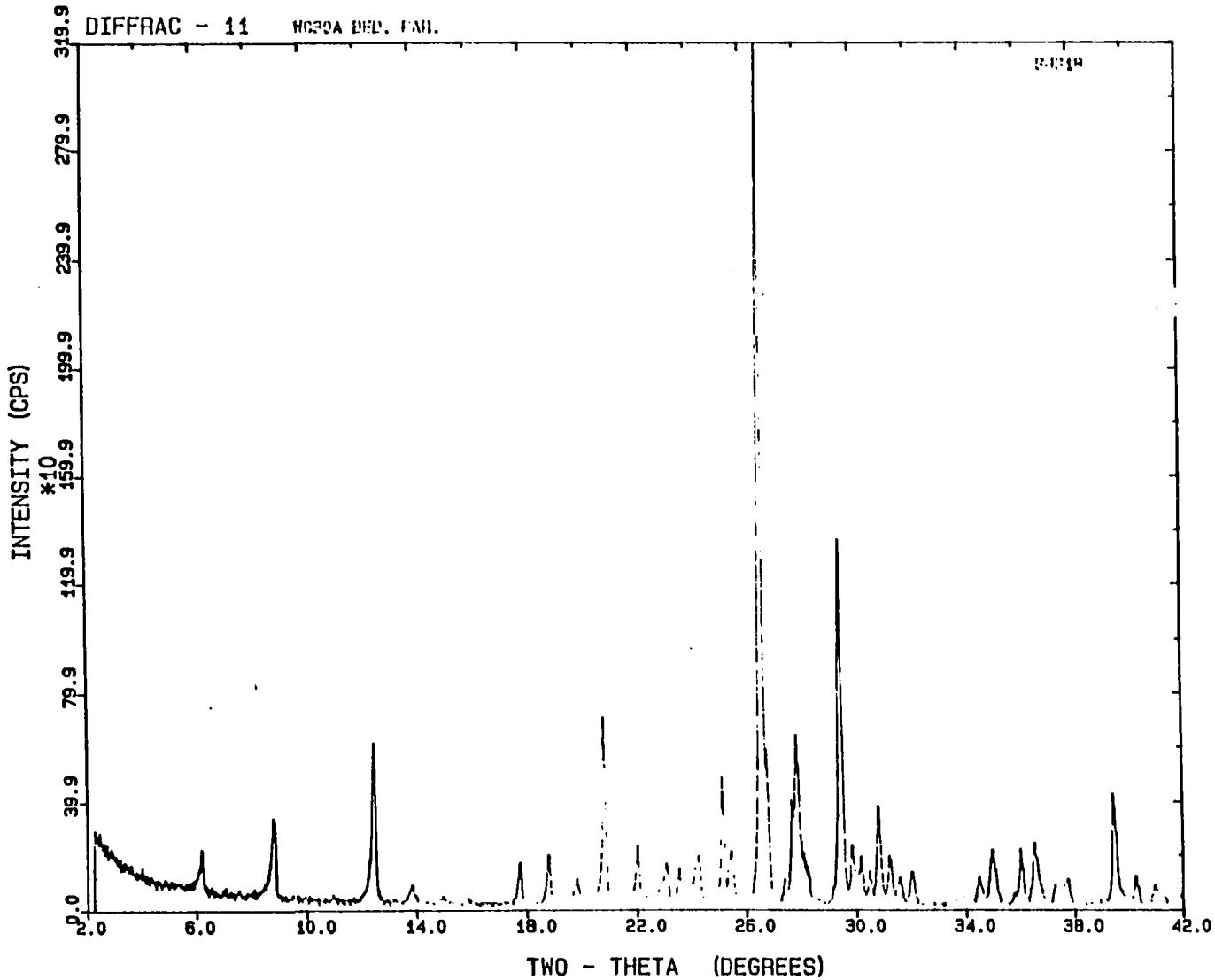

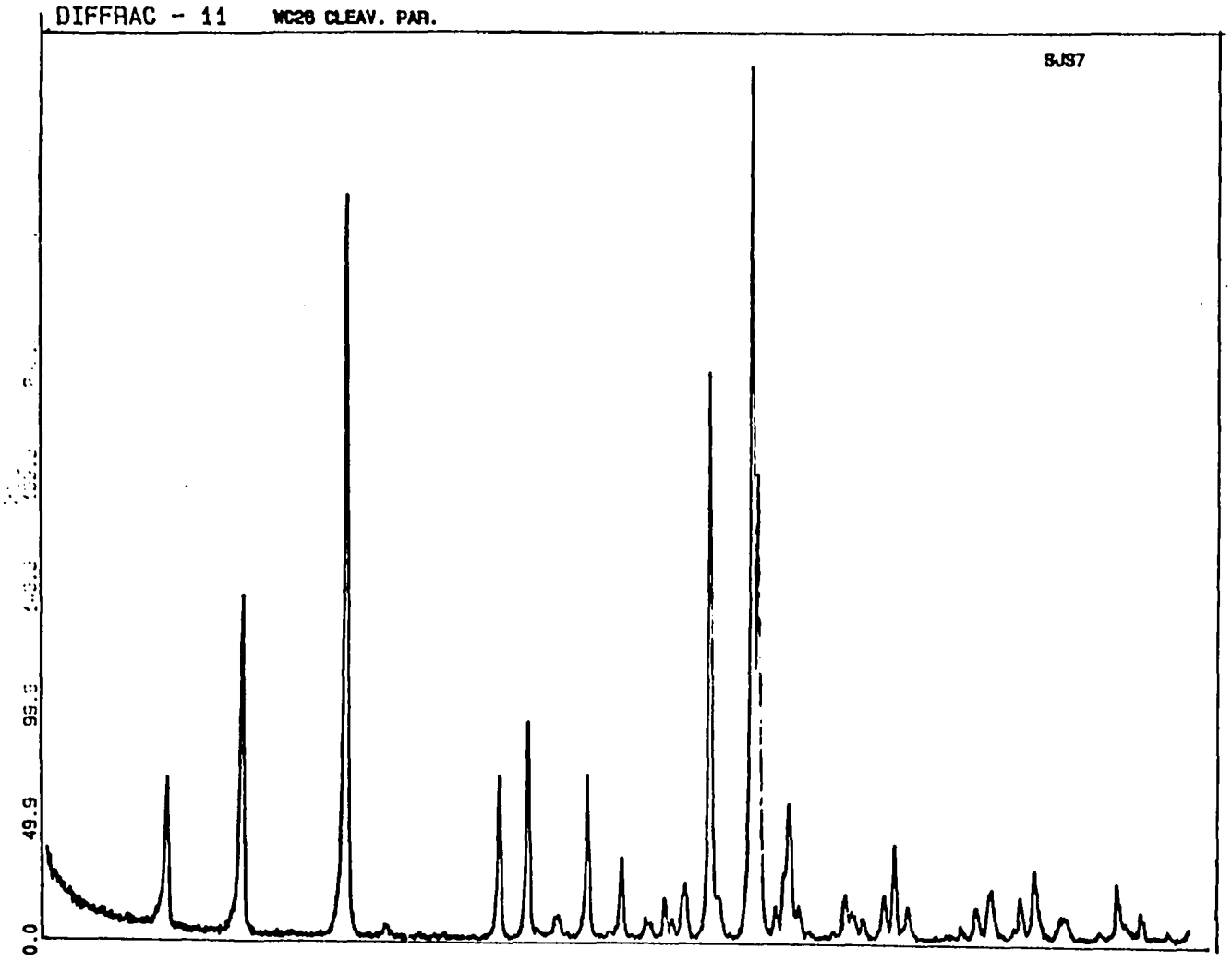

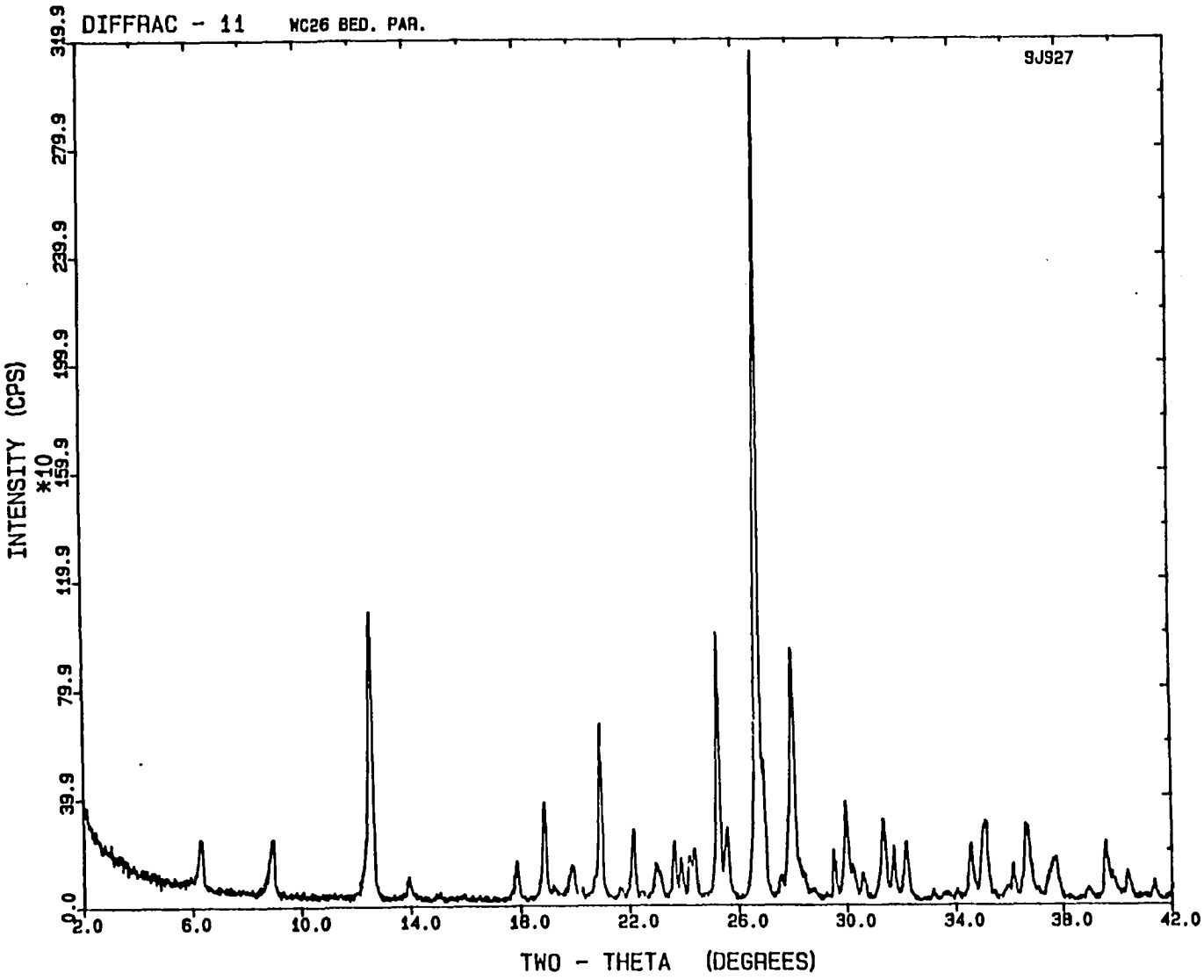

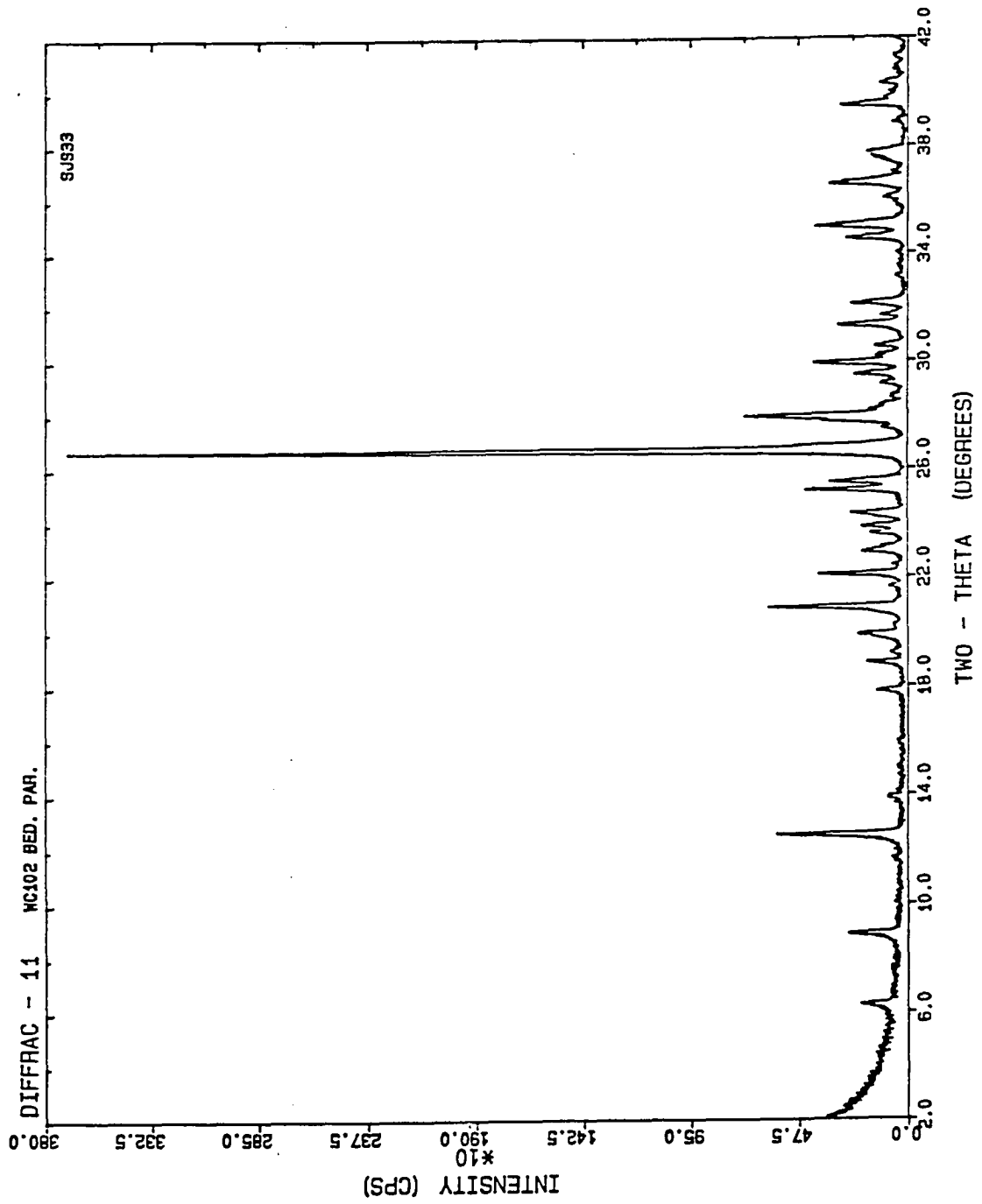

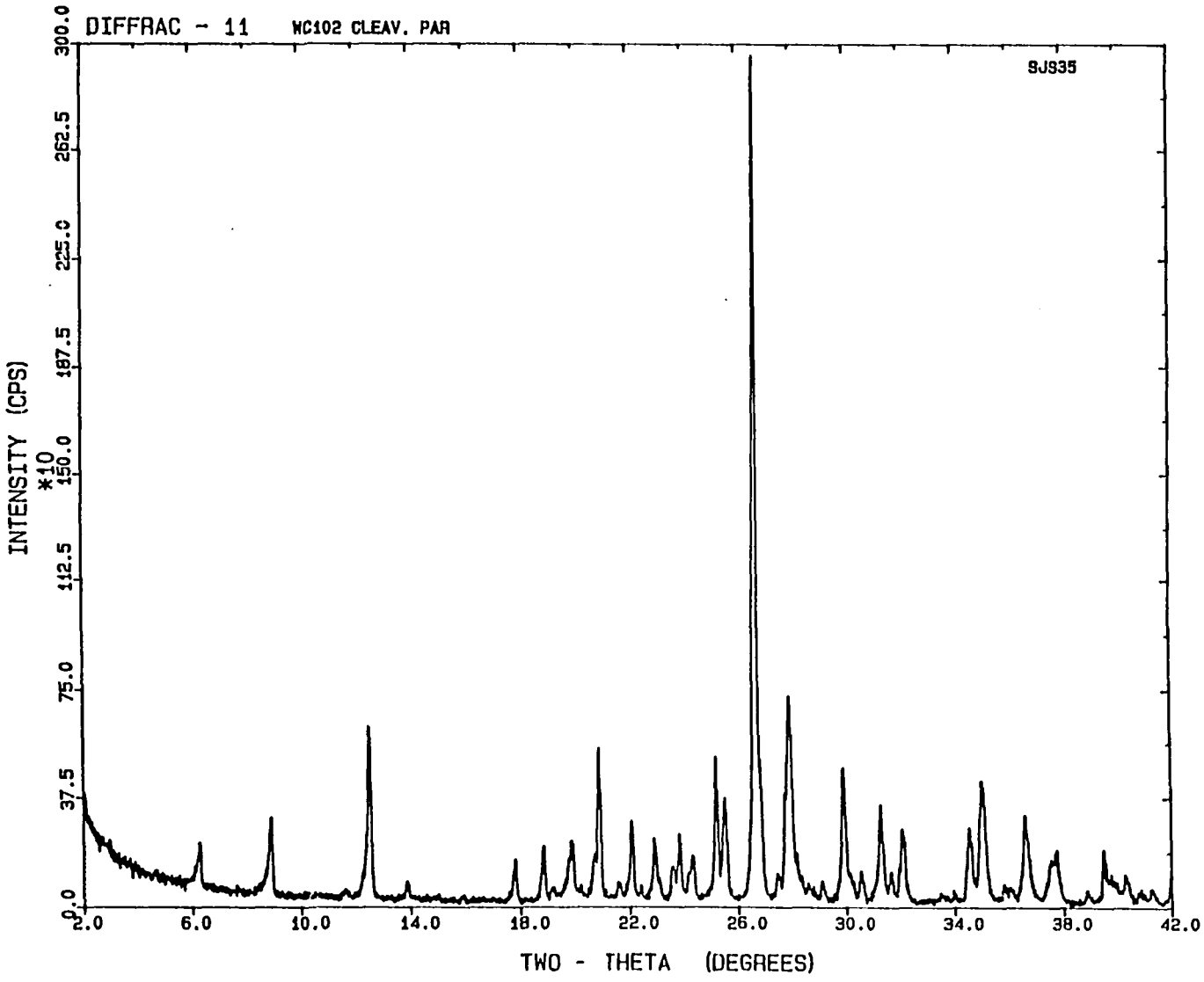

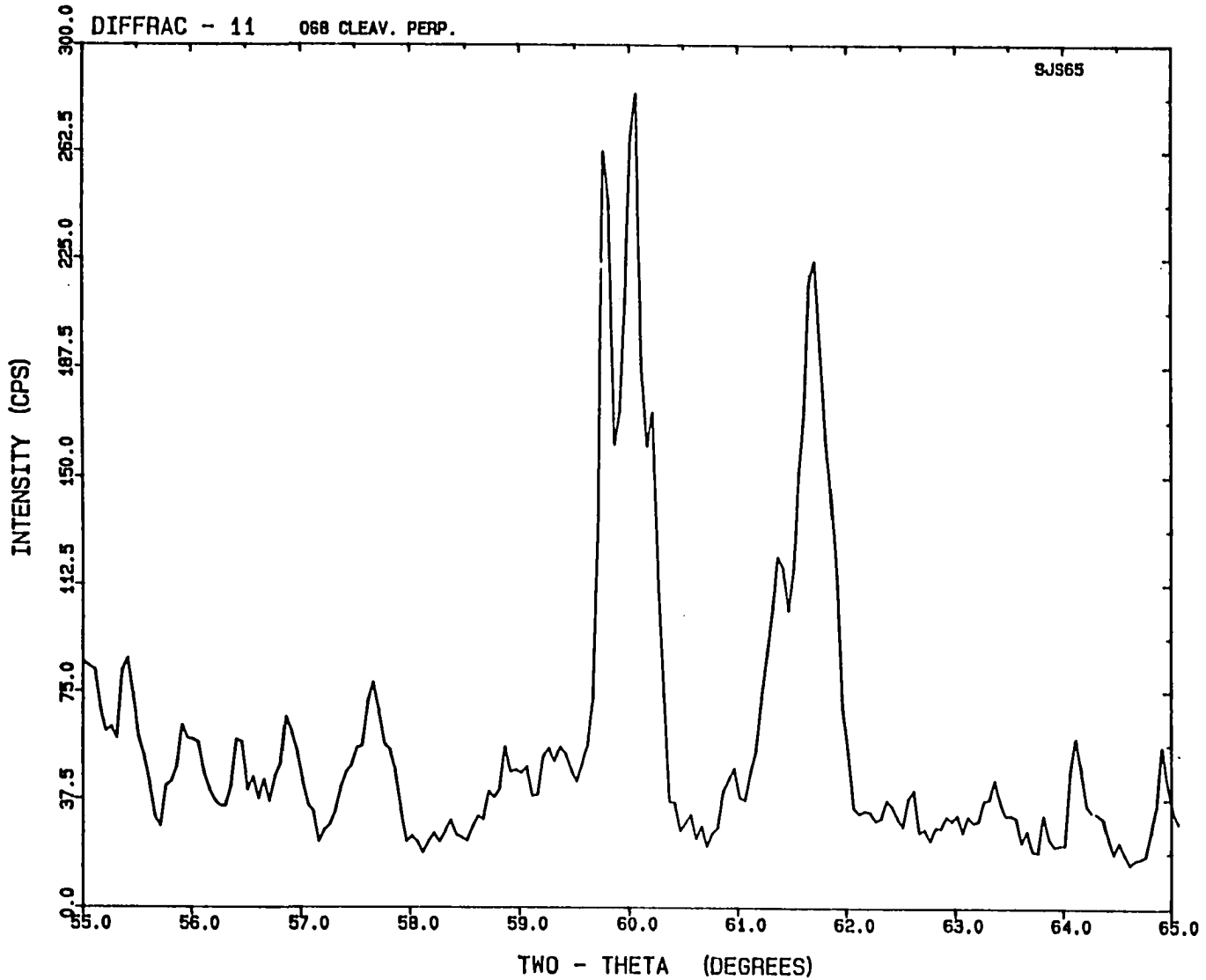

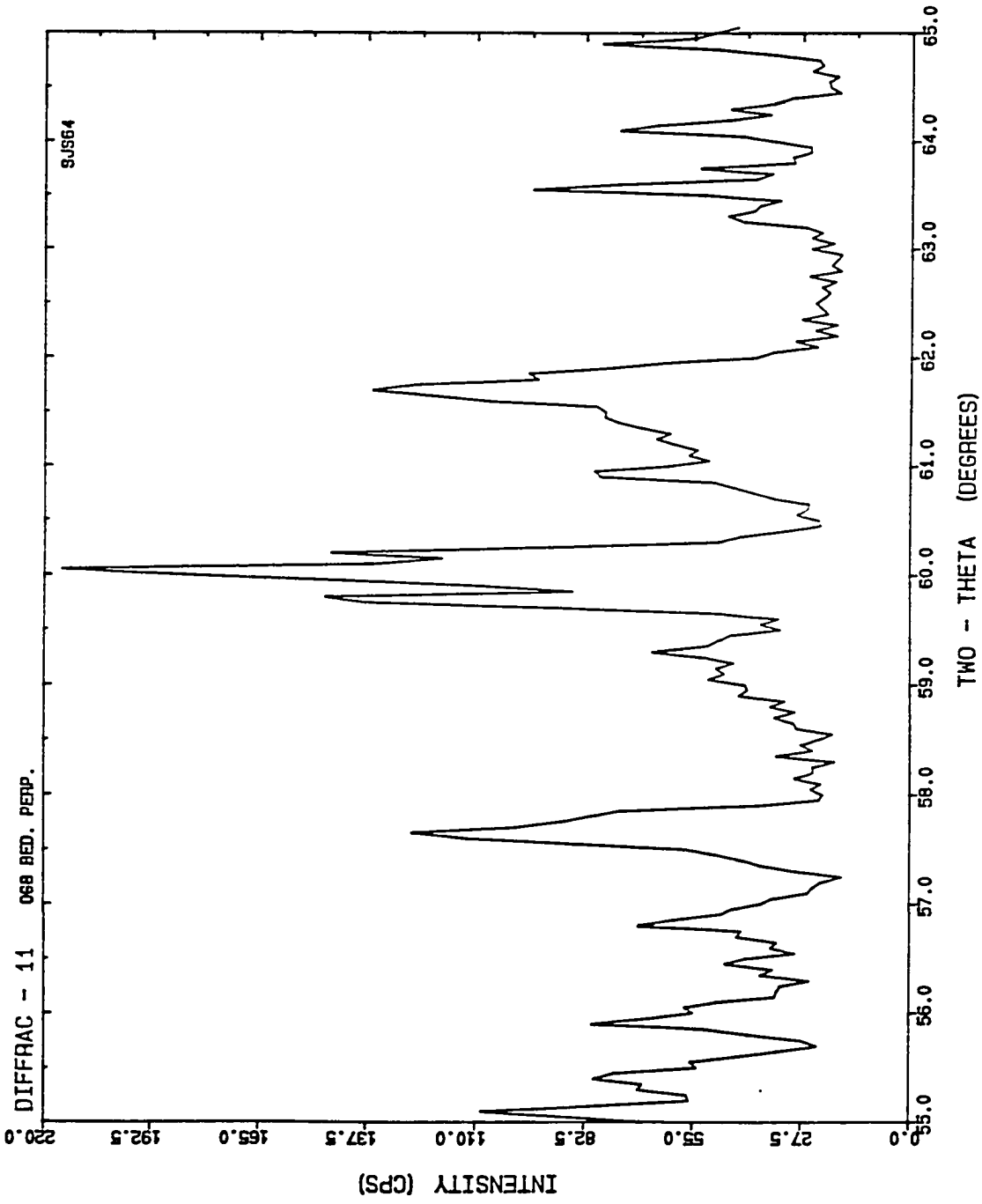

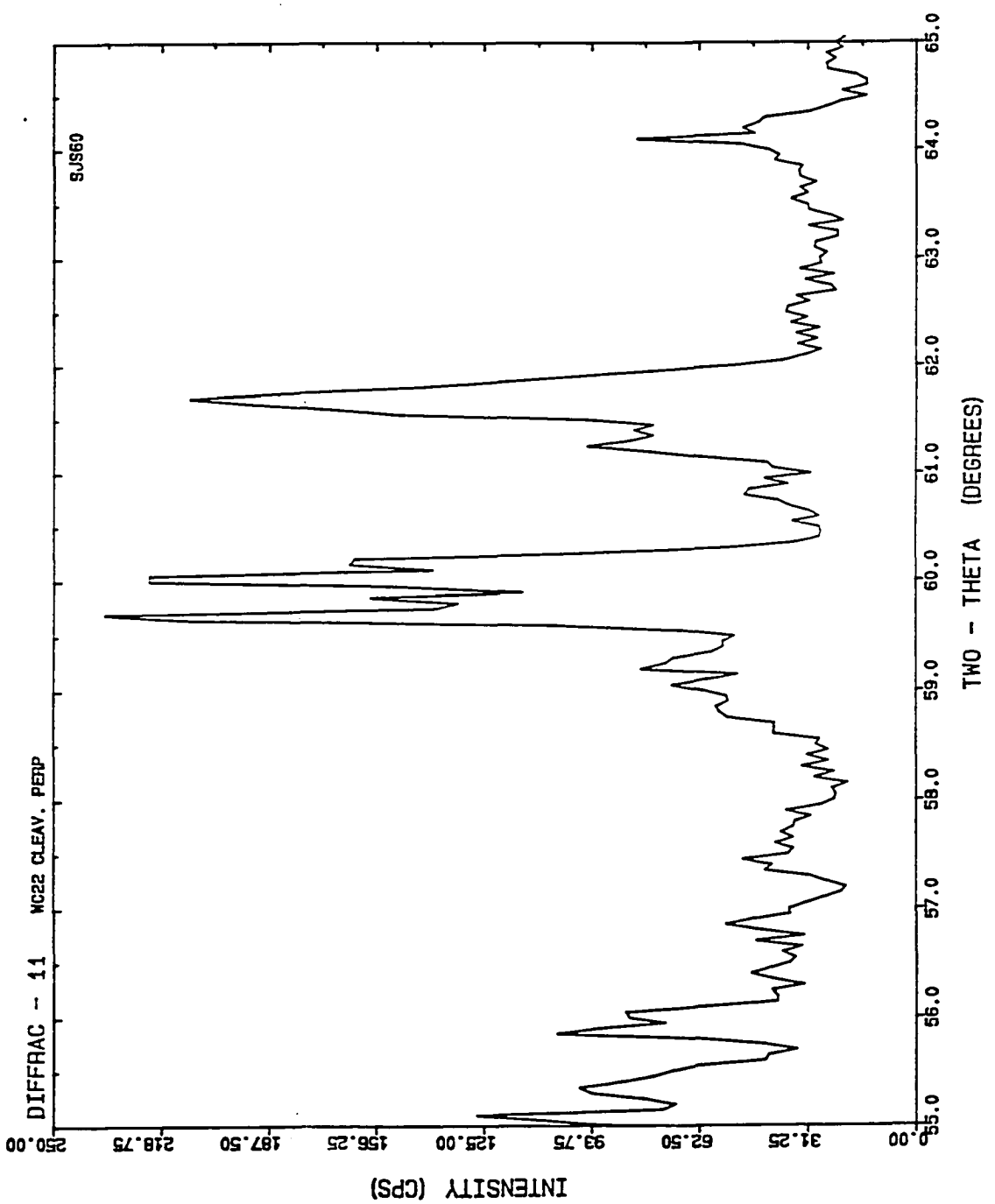

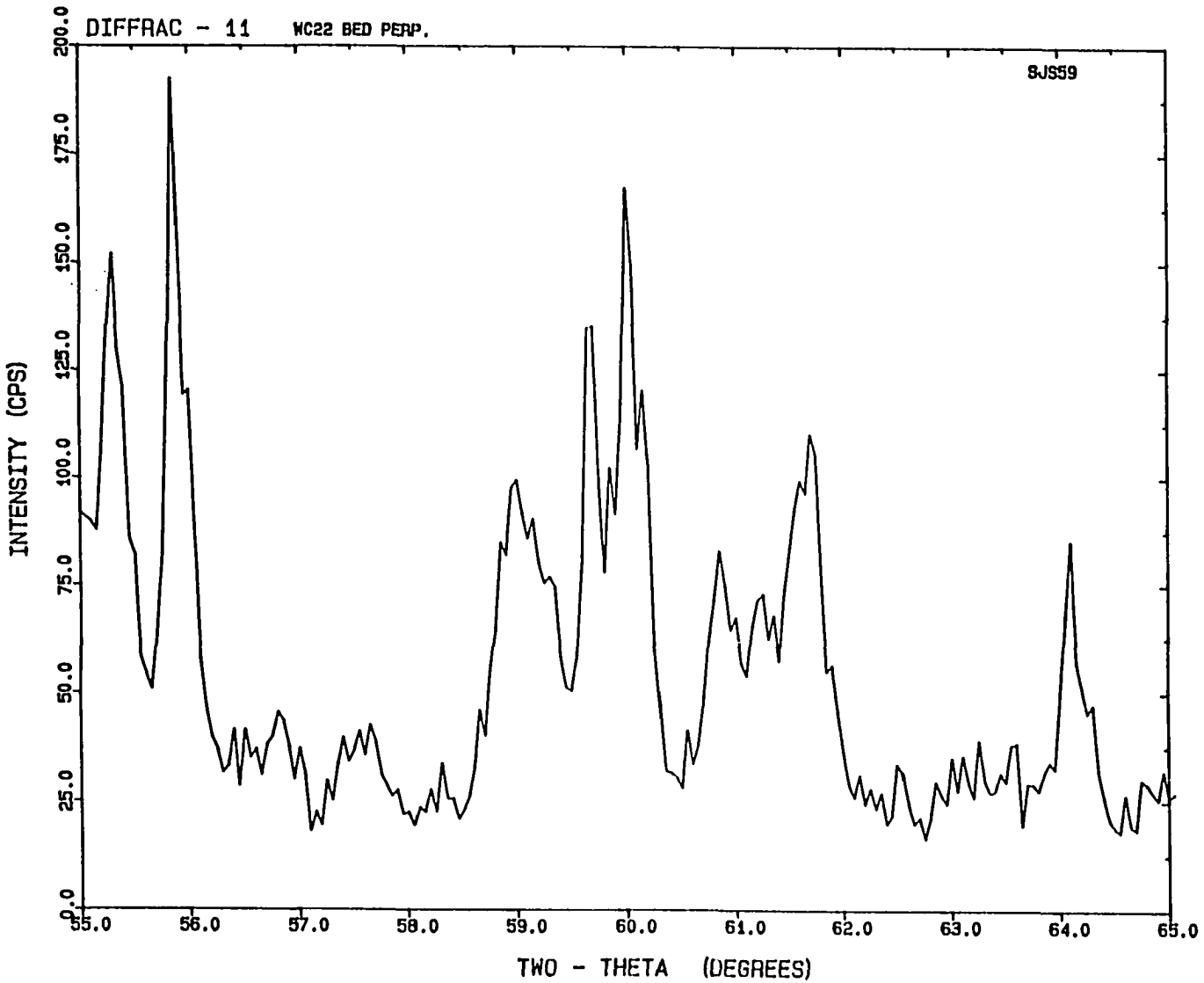

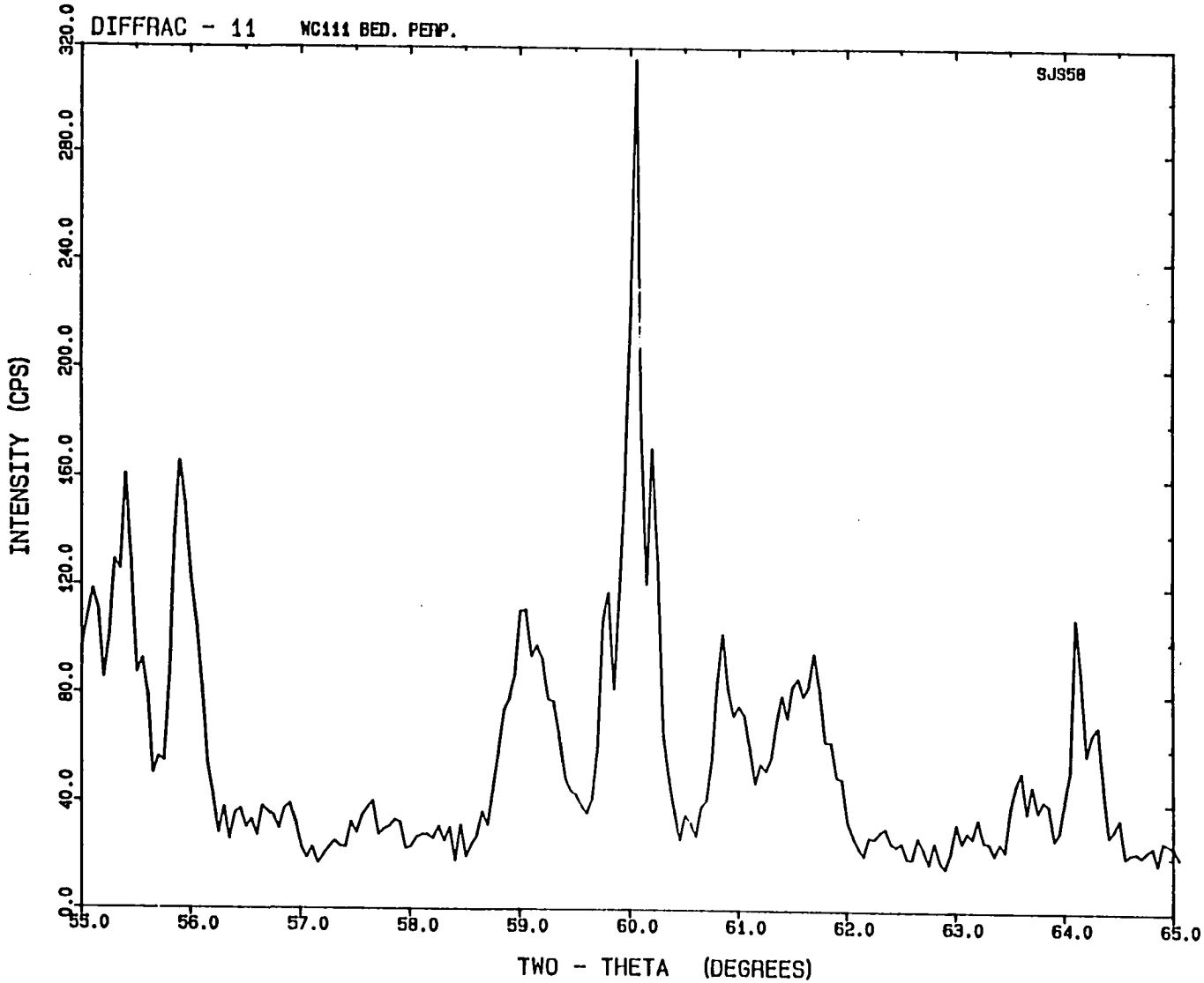

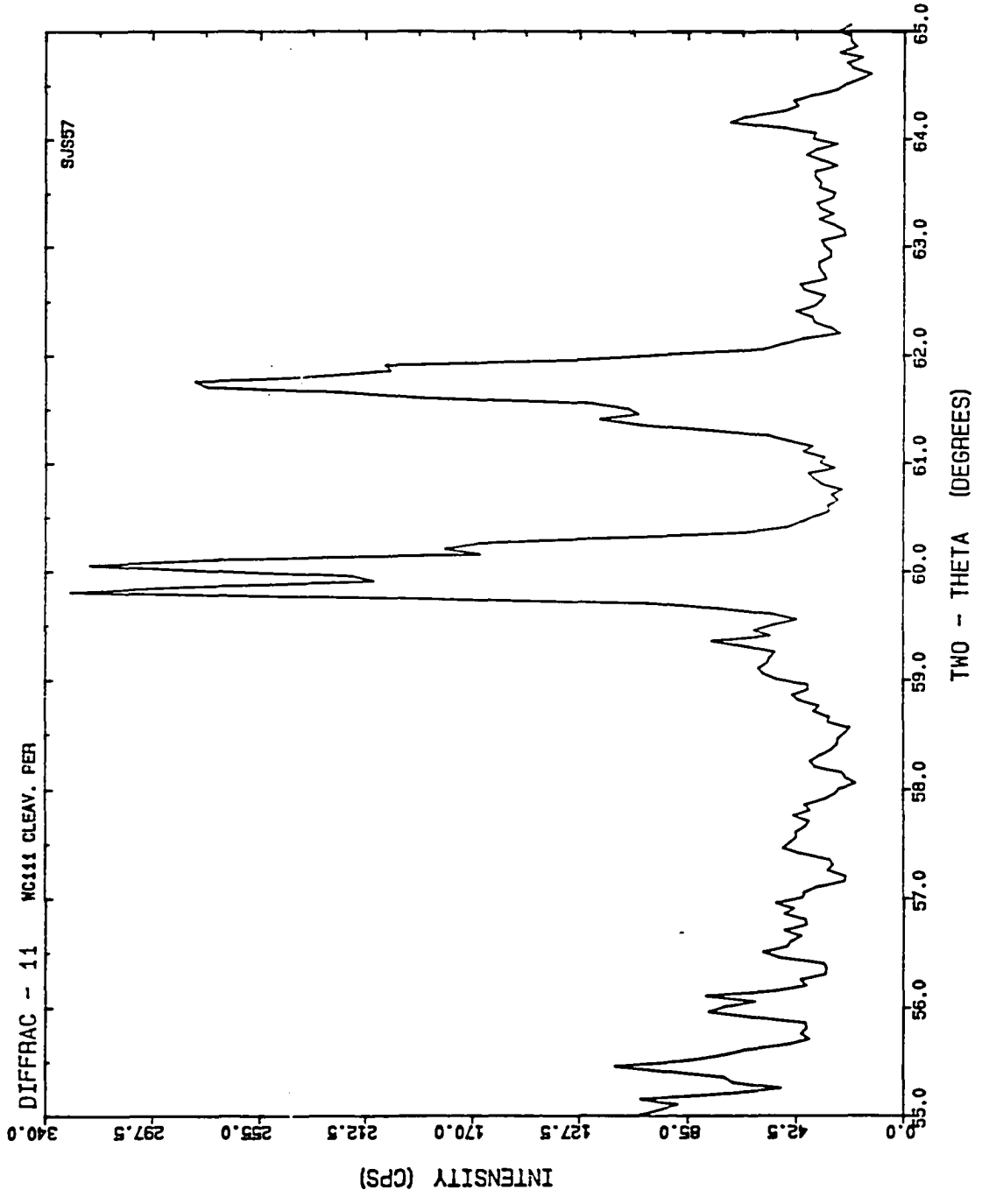

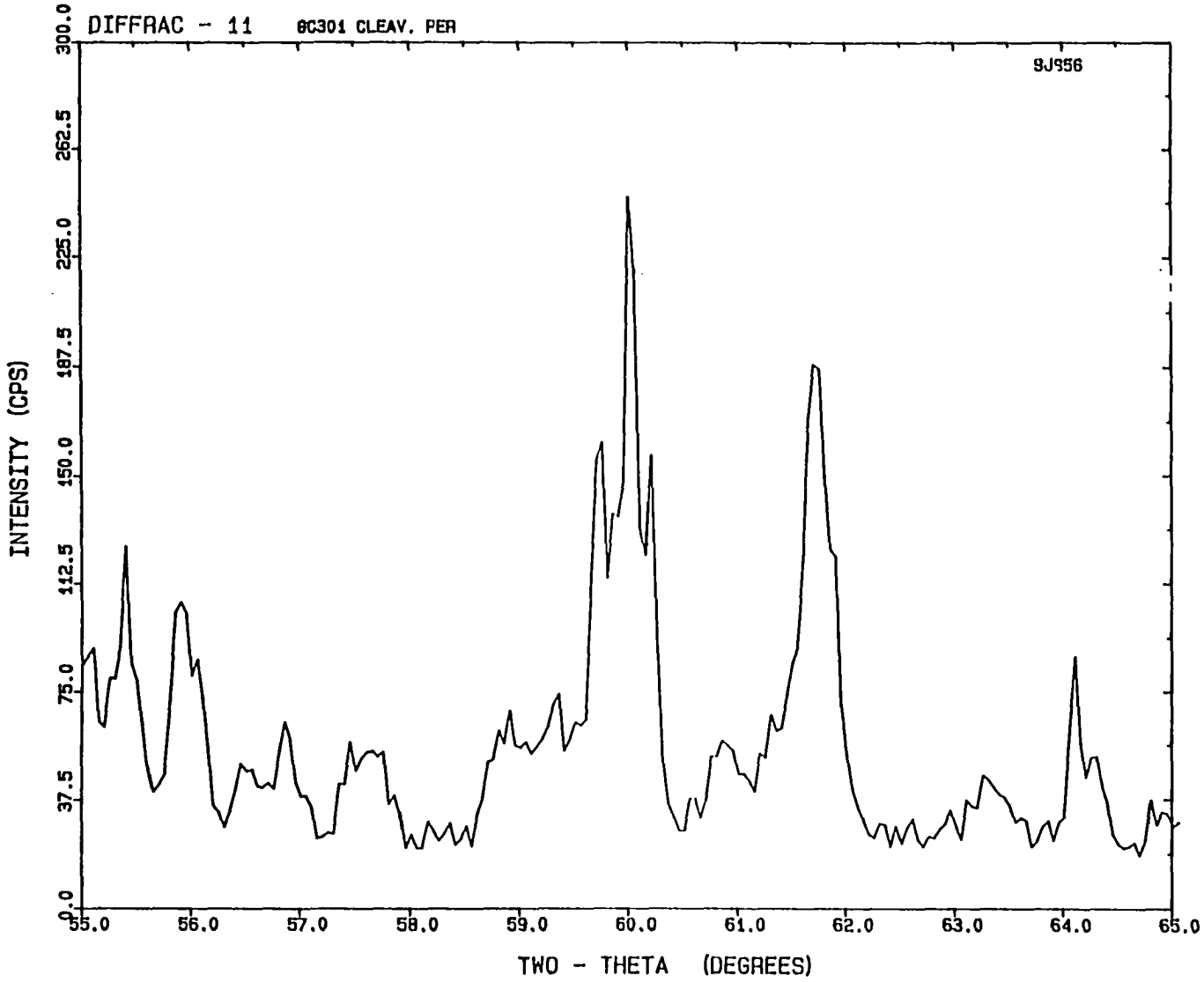

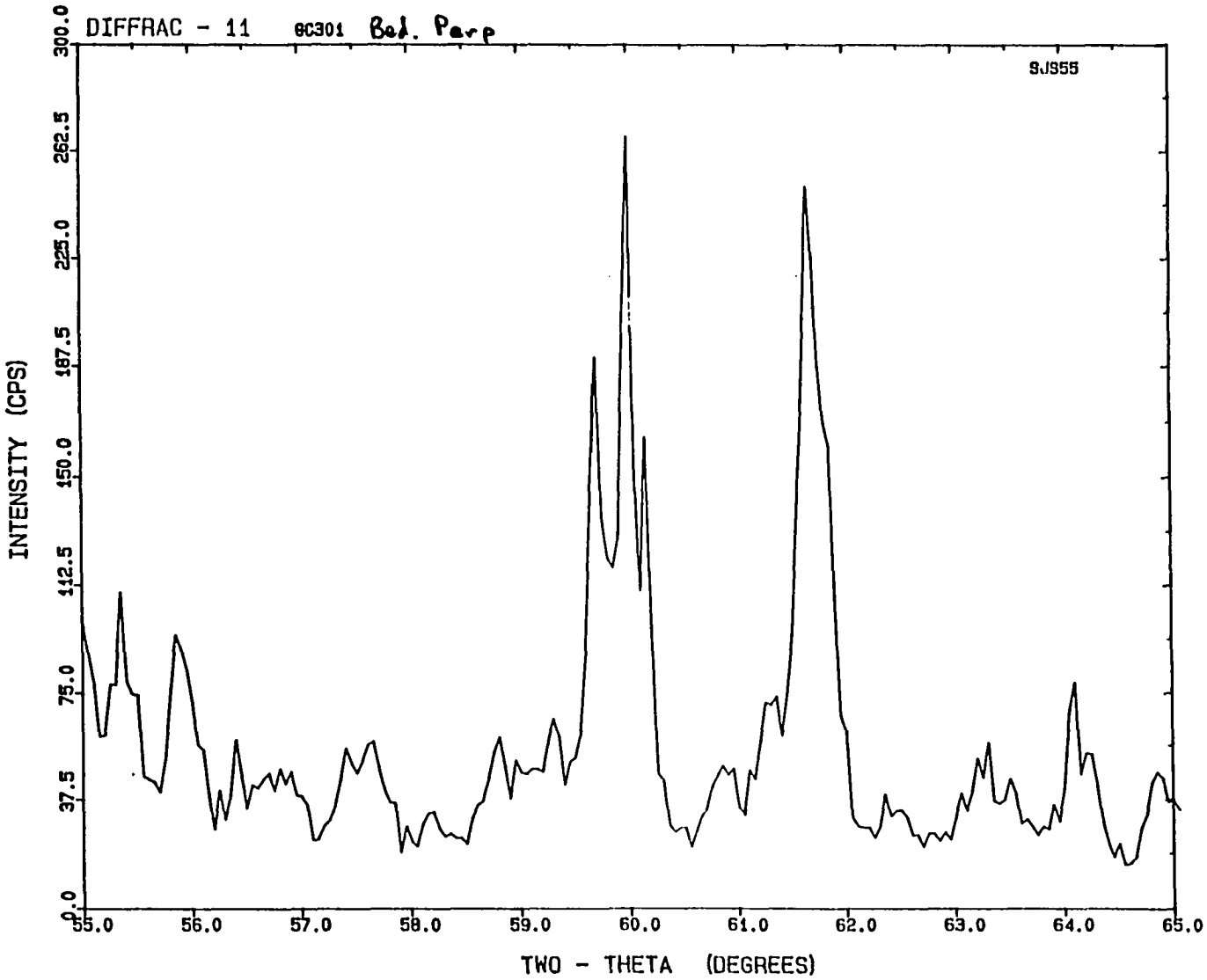

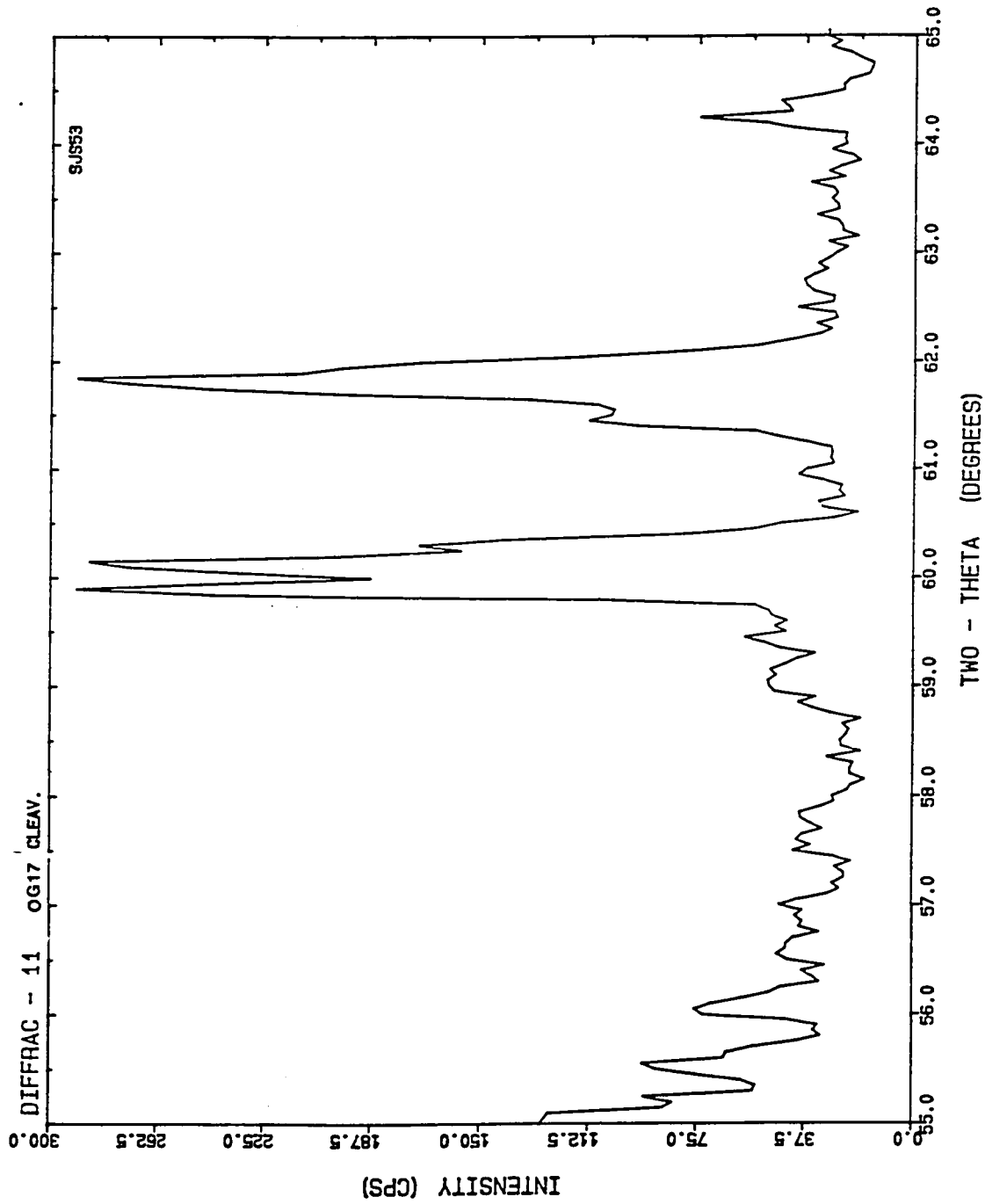

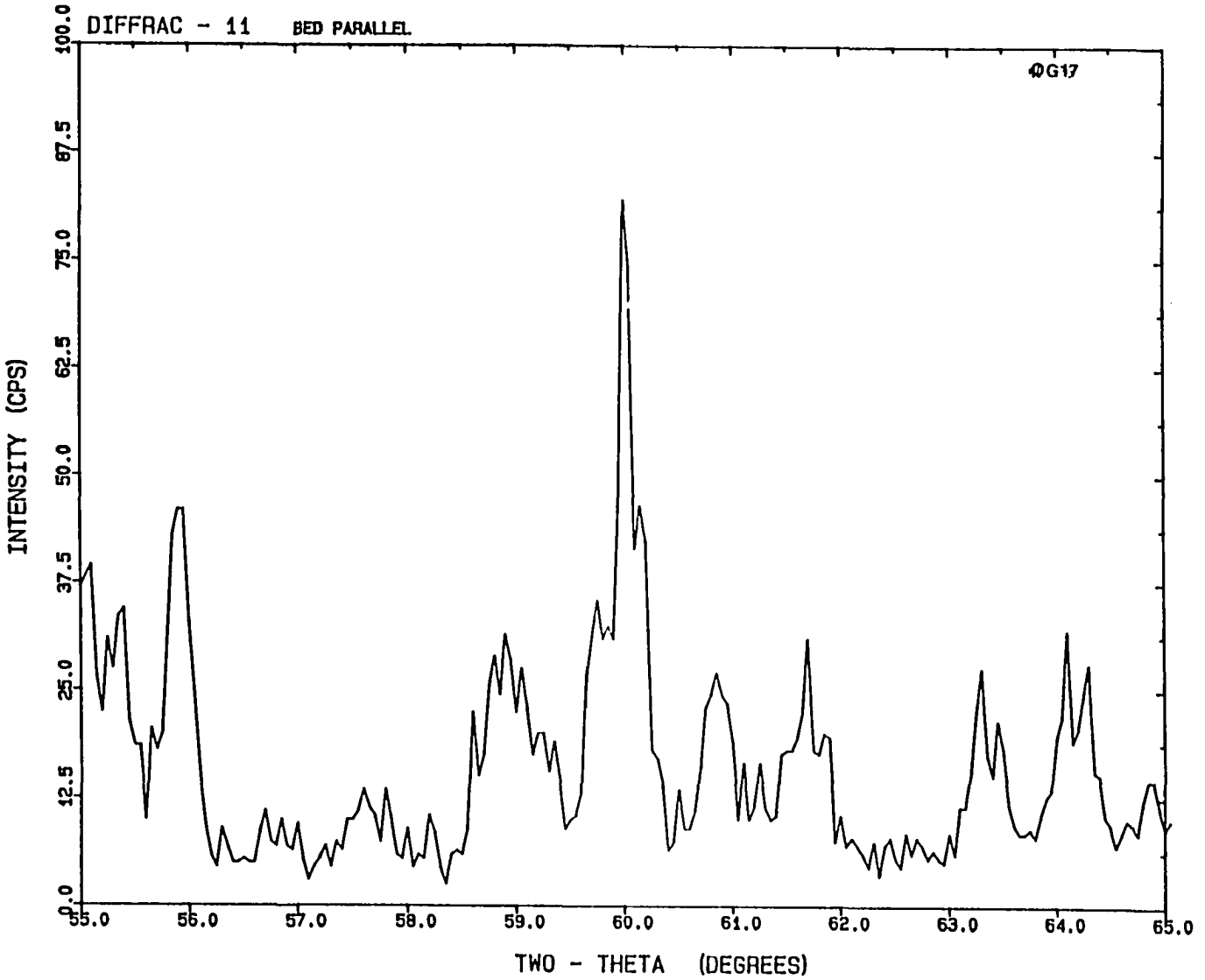

APPENDIX 2

MICROPROBE STANDARDS

APPENDIX 2

University of Cincinnati Microprobe Standards Used.

	Element	% oxide	% metal	β factor
Penn. State Microcline:	Si	65.1	30.43	1.056
	Al	17.3	9.16	1.022
	K	16.1	13.37	1.164
Penn. State Albite:	Si	68.2	31.9	1.097
	Al	19.7	10.4	1.071
	Na	11.8	8.72	1.230
Penn. State Garnet:	Si	36.50	17.1	1.133
	Al	20.60	10.9	1.150
	Fe	22.70	17.7	1.092
	Mn	19.30	15.0	1.128
	Ca	0.34	0.24	1.040
Penn. State Diopside:	Si	54.37	25.43	1.060
	Mg	18.25	11.00	1.126
	Ca	25.38	18.15	1.119
	Ti	2.00	1.20	1.155

For all silicate analyses and microprobe traverses reported in this study microcline was used as the K standard; albite as the Si, Al, and Na standards; garnet as the Fe and Mn standards; and diopside as the Mg, Ca, and Ti standards.

APPENDIX 3

MICROPROBE DATA

Six Element Probe Analyses of P Domain Phyllosilicates

sample:		Ti	K	Mg	Fe	Si	Al	Total
WC26A	Wt.%	_	9.66	2.90	4.14	47.59	21.52	95.90
	Form.	_	0.82	0.29	0.23	3.17	2.48	7.00
WC26A	Wt.%	_	10.22	2.63	3.00	49.53	31.31	96.69
	Form.	_	0.86	0.26	0.16	3.25	2.42	6.95
WC26A	Wt.%	_	11.65	2.44	3.03	49.38	31.27	97.81
	Form.	_	0.97	0.24	0.17	3.24	2.42	7.03
WC26A	Wt.%	_	11.08	2.39	4.34	47.70	29.16	94.67
	Form.	_	0.96	0.24	0.25	3.25	2.34	7.05
WC26A	Wt.%	_	9.82	3.07	4.67	46.43	29.17	93.18
	Form.	_	0.86	0.32	0.27	3.21	2.37	7.03
WC26A	Wt.%	_	10.02	3.22	5.67	47.76	30.63	97.30
	Form.	_	0.85	0.32	0.31	3.17	2.40	7.05
WC26A	Wt.%	_	11.53	2.19	3.05	47.73	28.64	93.18
	Form.	_	1.02	0.23	0.17	3.30	2.33	7.04
WC26A	Wt.%	_	11.10	2.38	2.99	48.61	30.53	95.69
	Form.	_	0.95	0.24	0.17	3.25	2.41	7.01
WC26A	Wt.%	_	11.09	2.60	3.34	50.33	30.30	97.70
	Form.	_	0.93	0.25	0.18	3.29	2.34	6.99
WC26A	Wt.%	_	10.04	3.77	7.71	46.25	29.17	96.95
	Form.	_	0.87	0.38	0.44	3.13	2.33	7.13
WC26A	Wt.%	_	10.69	3.48	9.07	43.35	29.62	96.21
	Form.	_	0.94	0.36	0.52	3.00	2.42	7.25
WC26A	Wt.%	_	11.61	2.19	2.84	47.66	30.96	95.25
	Form.	_	1.00	0.22	0.16	3.21	2.46	7.05
WC26A	Wt.%	_	11.34	3.10	4.84	46.17	30.72	96.27
	Form.	_	0.98	0.31	0.27	3.12	2.45	7.14
WC26A	Wt.%	_	11.04	2.23	3.37	47.84	28.88	93.46
	Form.	_	0.97	0.23	0.19	3.29	2.34	7.02
WC26A	Wt.%	_	11.43	2.28	3.25	48.11	29.64	94.71
	Form.	_	0.99	0.23	0.18	3.27	2.37	7.04
WC26A	Wt.%	_	9.12	4.64	8.68	46.13	29.10	97.83
	Form.	_	0.78	0.46	0.49	3.10	2.30	7.14

WC26A	Wt.%	_	10.53	2.31	2.36	50.58	27.70	93.50
	Form.	_	0.91	0.23	0.13	3.43	2.21	6.91
WC26A	Wt.%	_	9.04	3.13	6.74	46.45	28.55	94.01
	Form.	_	0.79	0.32	0.39	3.20	2.32	7.03
WC26A	Wt.%	_	11.88	2.38	2.40	49.26	30.66	96.61
	Form.	_	1.00	0.23	0.13	3.27	2.39	7.03
WC26A	Wt.%	_	8.13	4.79	9.96	47.03	25.82	95.75
	Form.	_	0.71	0.49	0.57	3.22	2.09	7.08
WC26A	Wt.%	_	9.34	4.10	8.30	45.34	27.98	95.16
	Form.	_	0.82	0.42	0.48	3.13	2.28	7.14
WC26A	Wt.%	_	11.21	2.76	3.56	47.01	30.03	94.60
	Form.	_	0.97	0.28	0.20	3.20	2.41	7.07
WC26A	Wt.%	_	10.18	2.18	3.56	45.80	32.09	93.85
	Form.	_	0.89	0.22	0.20	3.13	2.58	7.02
WC26A	Wt.%	_	10.57	2.93	4.85	47.23	28.62	94.21
	Form.	_	0.92	0.30	0.28	3.24	2.31	7.06
WC26A	Wt.%	_	10.38	2.43	3.70	52.32	28.38	97.26
	Form.	_	0.87	0.24	0.20	3.42	2.18	6.91
WC26A	Wt.%	_	11.47	2.55	2.82	47.84	29.48	94.17
	Form.	_	1.00	0.26	0.16	3.27	2.37	7.05
WC26A	Wt.%	_	11.48	2.31	2.73	47.15	29.46	93.14
	Form.	_	1.01	0.24	0.16	3.25	2.39	7.04
WC26A	Wt.%	_	10.23	3.42	6.55	46.06	27.19	93.45
	Form.	_	0.91	0.36	0.38	3.22	2.24	7.11
WC26A	Wt.%	_	11.00	2.74	3.43	46.70	29.44	93.55
	Form.	_	0.97	0.28	0.20	3.32	2.39	7.06
WC26A	Wt.%	_	11.40	2.59	3.10	47.33	28.68	93.13
	Form.	_	1.00	0.27	0.18	3.27	2.34	7.05
WC26A	Wt.%	_	10.90	3.06	4.11	47.92	30.51	96.55
	Form.	_	0.93	0.30	0.23	3.20	2.40	7.05
WC26A	Wt.%	_	9.93	3.80	7.25	46.95	29.00	96.97
	Form.	_	0.85	0.38	0.41	3.16	2.30	7.11
WC26A	Wt.%	_	9.30	4.61	9.50	45.05	28.70	97.29
	Form.	_	0.81	0.47	0.54	3.06	2.30	7.18

WC26A	Wt.%	_	11.20	2.68	4.02	48.50	29.86	96.32
	Form.	_	0.95	0.27	0.22	3.25	2.35	7.05
WC26A	Wt.%	_	8.71	4.81	9.33	42.40	28.30	93.68
	Form.	_	0.78	0.51	0.55	3.00	2.36	7.20
WC26A	Wt.%	_	11.44	1.34	3.97	46.35	31.90	95.05
	Form.	_	0.99	0.13	0.23	3.15	2.55	7.05
WC26A	Wt.%	_	9.59	4.19	8.39	43.84	28.82	94.92
	Form.	_	0.85	0.43	0.49	3.05	2.36	7.19
WC26A	Wt.%	_	10.66	2.77	3.70	48.95	29.21	95.92
	Form.	_	0.91	0.28	0.21	3.29	2.31	7.00
WC26A	Wt.%	_	10.83	2.89	4.80	46.11	29.36	94.04
	Form.	_	0.95	0.30	0.28	3.18	2.39	7.09
WC26A	Wt.%	_	11.63	2.38	2.80	48.30	29.81	94.96
	Form.	_	1.00	0.24	0.16	3.27	2.38	7.04
WC26A	Wt.%	_	11.28	2.06	2.65	47.88	30.38	94.27
	Form.	_	0.98	0.21	0.15	3.25	2.43	7.02
WC26A	Wt.%	_	9.88	3.39	6.07	45.99	27.93	93.33
	Form.	_	0.88	0.35	0.35	3.20	2.29	7.08
WC26A	Wt.%	_	10.61	2.87	4.04	47.45	31.89	96.95
	Form.	_	0.90	0.28	0.22	3.15	2.49	7.04
WC26A	Wt.%	_	10.46	2.12	2.50	51.25	28.57	94.93
	Form.	_	0.89	0.21	0.14	3.42	2.24	6.90
WC26A	Wt.%	_	9.35	3.11	5.22	48.16	28.50	94.40
	Form.	_	0.81	0.32	0.30	3.28	2.28	6.98
WC26A	Wt.%	_	7.26	6.33	14.07	39.55	27.42	94.73
	Form.	_	0.66	0.67	0.84	2.83	2.31	7.33
WC26A	Wt.%	0.68	10.68	2.90	7.40	45.61	28.75	96.02
	Form.	0.03	0.93	0.30	0.42	3.13	2.32	7.14
WC26A	Wt.%	1.22	7.39	9.35	6.54	44.68	27.71	96.89
	Form.	0.06	0.63	0.92	0.37	2.99	2.19	7.16
WC26A	Wt.%	0.34	10.64	4.06	6.57	45.76	30.35	97.72
	Form.	0.02	0.91	0.41	0.37	3.07	2.40	7.16
WC26A	Wt.%	0.44	11.06	2.19	3.01	49.31	29.49	95.50
	Form.	0.02	0.94	0.22	0.17	3.30	2.33	6.98
WC26A	Wt.%	0.43	12.39	2.46	2.72	48.02	31.19	97.21

	Form.	0.02	1.05	0.24	0.15	3.19	2.44	7.09
WC26A	Wt.%	0.36	12.29	2.55	3.93	46.57	30.76	96.46
	Form.	0.02	1.06	0.26	0.22	3.14	2.44	7.13
WC26A	Wt.%	0.48	10.61	4.18	8.32	42.87	29.86	96.32
	Form.	0.02	0.93	0.43	0.48	2.96	2.43	7.26
WC26A	Wt.%	0.36	12.51	2.48	4.16	46.51	31.36	97.37
	Form.	0.02	1.07	0.25	0.23	3.11	2.47	7.15
WC26A	Wt.%	0.53	12.24	2.51	4.96	45.65	29.62	95.51
	Form.	0.03	1.07	0.26	0.28	3.13	2.40	7.16
WC22	Wt.%	1.01	11.70	2.56	2.78	46.65	30.68	95.37
	Form.	0.05	1.01	0.26	0.16	3.15	2.44	7.07
WC22	Wt.%	0.42	10.91	3.48	5.54	43.67	30.40	94.43
	Form.	0.02	0.97	0.36	0.32	3.03	2.49	7.18
WC22	Wt.%	0.33	12.25	2.43	2.39	48.28	31.41	97.15
	Form.	0.02	1.03	0.24	0.13	3.20	2.45	7.07
WC22	Wt.%	0.37	10.98	3.03	4.90	46.50	29.96	95.75
	Form.	0.02	0.95	0.31	0.28	3.15	2.39	7.10
WC22	Wt.%	1.50	9.71	3.05	9.51	43.07	29.91	96.75
	Form.	0.08	0.85	0.31	0.55	2.96	2.42	7.17
WC22	Wt.%	0.17	7.81	6.37	8.00	44.96	28.36	95.67
	Form.	0.01	0.68	0.65	0.46	3.06	2.28	7.12
WC22	Wt.%	1.25	10.87	2.65	7.84	43.96	30.43	97.01
	Form.	0.06	0.95	0.27	0.45	3.00	2.45	7.18
WC22	Wt.%	0.44	11.50	3.13	6.58	45.03	30.79	97.46
	Form.	0.02	0.99	0.32	0.37	3.04	2.45	7.20
WC29	Wt.%	0.75	11.61	2.47	4.64	45.97	30.69	96.12
	Form.	0.04	1.00	0.25	0.26	3.12	2.45	7.12
WC29	Wt.%	0.52	11.87	2.52	3.55	48.00	31.41	97.86
	Form.	0.03	1.00	0.25	0.20	3.17	2.44	7.07
WC29	Wt.%	2.09	9.88	4.96	7.76	43.22	29.32	97.23
	Form.	0.11	0.86	0.50	0.44	2.94	2.35	7.19
WC29	Wt.%	0.21	8.79	6.79	5.75	46.14	29.61	97.30
	Form.	0.01	0.75	0.67	0.32	3.06	2.32	7.13
WC29	Wt.%	0.19	9.13	2.87	15.39	39.37	28.96	95.90
	Form.	0.01	0.84	0.31	0.92	2.83	2.45	7.35

WC29	Wt.%	0.35	10.63	4.67	4.05	46.21	30.65	96.56
	Form.	0.02	0.91	0.47	0.23	3.09	2.42	7.12
WC29	Wt.%	0.55	11.80	2.78	2.83	47.43	30.86	96.25
	Form.	0.03	1.01	0.28	0.16	3.18	2.43	7.08
WC29	Wt.%	0.75	11.58	2.26	4.15	45.75	29.76	94.25
	Form.	0.04	1.02	0.23	0.24	3.15	2.42	7.09
WC29	Wt.%	0.08	11.94	2.48	3.79	47.16	31.55	97.67
	Form.	0.04	1.01	0.25	0.21	3.13	2.47	7.09
WC29	Wt.%	0.64	11.04	2.60	4.02	48.42	31.16	97.88
	Form.	0.03	0.93	0.26	0.22	3.19	2.42	7.03
WC29	Wt.%	0.54	9.27	5.71	7.54	44.96	28.84	96.86
	Form.	0.03	0.80	0.58	0.43	3.04	2.30	7.17
WC29	Wt.%	0.23	6.49	8.80	9.58	45.57	27.29	97.96
	Form.	0.01	0.55	0.87	0.53	3.04	2.14	7.15
WC29	Wt.%	0.18	5.89	9.58	12.13	40.89	26.39	95.07
	Form.	0.01	0.52	1.00	0.71	2.87	2.18	7.29
WC29	Wt.%	0.25	8.89	3.73	11.95	42.27	27.63	94.73
	Form.	0.01	0.80	0.39	0.71	3.00	2.31	7.23
WC29	Wt.%	0.25	9.93	2.48	2.90	48.18	32.32	96.05
	Form.	0.01	0.84	0.24	0.16	3.19	2.52	6.96
WC29	Wt.%	0.19	9.65	2.14	8.17	43.23	32.42	95.79
	Form.	0.01	0.84	0.22	0.47	2.97	2.62	7.13
WC29	Wt.%	0.20	6.77	5.30	14.98	37.38	30.73	95.36
	Form.	0.01	0.62	0.56	0.89	2.67	2.58	7.33
WC29	Wt.%	0.18	3.41	7.88	12.47	43.86	25.94	93.73
	Form.	0.01	0.30	0.82	0.73	3.05	2.13	7.02
WC29	Wt.%	0.43	11.53	1.27	1.74	47.61	34.98	97.55
	Form.	0.02	0.96	0.12	0.09	3.11	2.69	7.00
WC29	Wt.%	0.14	7.40	3.67	12.41	39.30	31.46	94.38
	Form.	0.01	0.67	0.39	0.73	2.79	2.63	7.21
WC29	Wt.%	1.40	10.11	2.87	3.99	43.67	33.12	95.16
	Form.	0.07	0.87	0.29	0.23	2.96	2.65	7.07
WC29	Wt.%	0.59	8.95	2.42	6.18	44.16	32.19	94.48
	Form.	0.03	0.78	0.25	0.35	3.02	2.60	7.03

WC29	Wt.%	0.25	10.39	1.57	3.19	45.89	34.13	95.42
	Form.	0.01	0.89	0.16	0.18	3.08	2.70	7.01
WC29	Wt.%	0.25	9.34	3.21	4.73	45.51	32.55	95.59
	Form.	0.01	0.80	0.32	0.26	3.06	2.58	7.03
WC29	Wt.%	0.28	10.79	1.64	3.67	45.06	34.17	95.60
	Form.	0.01	0.93	0.16	0.21	3.03	2.71	7.05
WC29	Wt.%	0.29	9.28	1.92	6.70	43.72	31.99	93.90
	Form.	0.01	0.82	0.20	0.39	3.03	2.61	7.05
WC29	Wt.%	1.20	9.30	4.46	5.47	44.41	29.70	94.55
	Form.	0.06	0.81	0.46	0.31	3.05	2.40	7.09
WC29	Wt.%	0.51	8.42	3.13	10.86	43.42	30.05	96.39
	Form.	0.03	0.74	0.32	0.62	2.99	2.44	7.13
WC29	Wt.%	0.48	8.36	5.39	7.59	45.15	29.79	96.77
	Form.	0.02	0.72	0.54	0.43	3.04	2.36	7.11
WC29	Wt.%	0.96	9.98	3.82	4.61	47.20	31.14	97.72
	Form.	0.05	0.84	0.37	0.25	3.11	2.42	7.05
WC29	Wt.%	0.41	8.95	3.40	8.90	45.08	30.52	97.26
	Form.	0.02	0.77	0.34	0.50	3.04	2.43	7.10
WC29	Wt.%	0.23	10.52	1.96	5.38	44.11	33.86	96.07
	Form.	0.01	0.91	0.20	0.30	2.98	2.70	7.10
WC29	Wt.%	0.13	6.31	5.76	8.16	43.64	30.54	94.54
	Form.	0.01	0.55	0.59	0.47	2.98	2.46	7.05
WC29	Wt.%	0.39	9.06	3.42	8.73	40.13	32.18	93.91
	Form.	0.02	0.81	0.36	0.51	2.83	2.68	7.21
WC29	Wt.%	0.06	7.84	3.66	12.14	39.46	30.54	93.69
	Form.	0.00	0.71	0.39	0.73	2.83	2.58	7.23
WC29	Wt.%	0.06	9.87	1.92	3.12	48.09	32.19	95.25
	Form.	0.00	0.84	0.19	0.17	3.20	2.53	6.93
WC29	Wt.%	0.57	11.55	2.26	3.60	47.64	31.24	96.86
	Form.	0.13	0.98	0.22	0.20	3.17	2.45	7.06
WC29	Wt.%	0.96	11.38	2.34	2.92	45.66	30.58	93.84
	Form.	0.05	1.00	0.24	0.17	3.14	2.48	7.07
WC29	Wt.%	0.05	0.13	12.67	31.38	25.79	22.26	92.27
	Form.	0.00	0.01	1.52	2.12	2.08	2.12	7.85
WC29	Wt.%	0.56	10.00	3.03	3.98	46.11	29.61	93.29

	Form.	0.03	0.88	0.31	0.23	3.18	2.40	7.02
WC29	Wt.%	0.23	5.70	7.02	16.14	36.94	26.83	92.87
	Form.	0.01	0.53	0.77	0.99	2.72	2.33	7.36
WC29	Wt.%	0.13	4.58	7.69	15.29	37.29	28.08	93.06
	Form.	0.01	0.42	0.83	0.93	2.70	2.40	7.29
OG3	Wt.%	0.15	11.33	1.28	1.85	46.03	34.75	95.39
	Form.	0.01	0.97	0.13	0.10	3.08	2.74	7.02
OG3	Wt.%	0.15	8.29	4.13	9.52	41.09	31.32	94.50
	Form.	0.01	0.74	0.43	0.56	2.88	2.58	7.19
OG3	Wt.%	0.20	9.41	1.59	5.43	45.34	32.59	94.55
	Form.	0.01	0.82	0.16	0.31	3.09	2.61	6.99
OG3	Wt.%	0.12	7.32	4.62	13.52	37.84	30.36	93.77
	Form.	0.01	0.67	0.50	0.81	2.73	2.58	7.30
OG3	Wt.%	0.20	9.09	3.10	6.19	43.78	32.84	95.20
	Form.	0.01	0.79	0.31	0.35	2.98	2.63	7.08
OG3	Wt.%	0.19	8.26	5.49	3.14	46.00	32.77	95.86
	Form.	0.01	0.70	0.54	0.17	3.04	2.55	7.01
OG3	Wt.%	0.30	10.71	1.41	3.36	44.77	34.03	94.59
	Form.	0.01	0.93	0.14	0.19	3.04	2.72	7.03
OG3	Wt.%	0.07	5.92	4.85	16.37	37.51	29.65	94.37
	Form.	0.00	0.54	0.52	0.99	2.71	2.52	7.29
OG3	Wt.%	0.18	10.25	1.71	3.55	46.24	34.57	96.50
	Form.	0.01	0.87	0.17	0.20	3.07	2.70	7.00
OG3	Wt.%	0.30	10.80	1.30	2.03	47.80	35.09	97.32
	Form.	0.01	0.90	0.13	0.11	3.12	2.70	6.96
OG3	Wt.%	0.18	9.34	1.54	3.57	50.49	34.20	99.31
	Form.	0.01	0.76	0.15	0.19	3.21	2.56	6.94
OG3	Wt.%	0.05	8.31	2.38	4.18	48.55	31.03	94.50
	Form.	0.00	0.71	0.24	0.23	3.25	2.45	6.87
OG3	Wt.%	0.21	7.05	4.34	11.93	42.67	30.70	96.90
	Form.	0.01	0.61	0.44	0.68	2.92	2.47	7.13
OG3	Wt.%	0.82	4.72	1.13	3.58	60.25	23.50	94.00
	Form.	0.04	0.39	0.11	0.19	3.87	1.78	6.38
OG3	Wt.%	0.27	5.07	5.81	16.71	39.07	27.79	94.72
	Form.	0.02	0.46	0.62	1.00	2.80	2.34	7.24

OG3	Wt.%	0.50	6.45	5.10	13.90	38.79	30.70	95.45
	Form.	0.02	0.58	0.54	0.82	2.74	2.55	7.25
OG3	Wt.%	0.30	8.95	2.60	8.49	43.06	33.20	96.60
	Form.	0.01	0.77	0.26	0.48	2.92	2.66	7.11
OG3	Wt.%	1.11	9.15	2.77	7.90	43.23	33.21	97.38
	Form.	0.06	0.78	0.28	0.44	2.91	2.63	7.10
OG3	Wt.%	1.25	8.91	2.42	5.72	45.38	31.11	94.78
	Form.	0.06	0.77	0.25	0.33	3.08	2.49	6.98
OG3	Wt.%	0.89	7.44	2.23	3.09	51.46	29.92	95.03
	Form.	0.04	0.62	0.22	0.17	3.37	2.31	6.73
OG3	Wt.%	0.02	7.48	3.51	10.88	43.71	30.69	96.30
	Form.	0.00	0.65	0.36	0.62	2.99	2.47	7.09
OG3	Wt.%	0.34	7.08	3.64	10.05	45.24	29.30	95.66
	Form.	0.02	0.62	0.37	0.57	3.09	2.36	7.02
OG3	Wt.%	0.94	8.01	2.56	7.38	45.95	30.89	95.73
	Form.	0.05	0.69	0.26	0.42	3.10	2.46	6.97
OG3	Wt.%	0.54	4.56	3.23	7.64	51.06	27.13	94.16
	Form.	0.03	0.71	0.25	0.34	3.00	2.13	6.69
OG17	Wt.%	0.00	7.38	3.64	11.89	43.14	31.29	97.34
	Form.	0.00	0.64	0.37	0.68	2.94	2.51	7.13
OG17	Wt.%	0.76	5.73	4.34	11.75	44.16	28.43	95.16
	Form.	0.04	0.50	0.44	0.68	3.04	2.31	7.01
OG17	Wt.%	0.16	9.29	1.26	1.62	48.96	35.86	97.15
	Form.	0.01	0.76	0.12	0.09	3.15	2.72	6.85
OG17	Wt.%	0.31	7.18	3.28	8.09	40.29	36.42	95.55
	Form.	0.01	0.62	0.33	0.46	2.74	2.92	7.09
OG17	Wt.%	0.09	8.40	2.99	7.97	38.97	35.87	94.29
	Form.	0.00	0.75	0.30	0.46	2.71	2.94	7.18
OG17	Wt.%	0.34	10.88	1.32	1.91	48.14	34.99	97.59
	Form.	0.02	0.90	0.13	0.10	3.13	2.68	6.96
OG17	Wt.%	0.43	10.89	1.66	2.48	46.54	33.77	95.77
	Form.	0.02	0.93	0.16	0.14	3.11	2.66	7.01
OG17	Wt.%	0.31	11.20	1.45	3.45	45.87	34.62	96.90
	Form.	0.02	0.95	0.14	0.19	3.05	2.71	7.05

OG17	Wt.%	0.00	3.49	7.46	12.74	44.49	35.21	93.98
	Form.	0.00	0.31	0.77	0.74	3.08	2.69	2.11
OG17	Wt.%	0.39	11.03	1.47	1.76	46.27	33.98	94.90
	Form.	0.02	0.94	0.15	0.10	3.10	2.69	6.99
OG17	Wt.%	0.22	11.01	2.28	1.88	45.59	35.05	96.03
	Form.	0.01	0.93	0.22	0.10	3.03	2.75	7.04
OG17	Wt.%	0.17	11.10	1.26	1.64	47.57	34.34	96.17
	Form.	0.01	0.94	0.12	0.09	3.14	2.67	6.98
OG17	Wt.%	0.28	11.59	1.47	1.46	46.89	34.98	96.67
	Form.	0.01	0.97	0.14	0.08	3.09	2.72	7.02
OG17	Wt.%	0.41	10.71	1.75	1.75	45.10	34.97	94.70
	Form.	0.02	0.92	0.17	0.10	3.03	2.77	7.01
OG17	Wt.%	0.54	9.78	1.93	9.71	41.73	33.58	97.28
	Form.	0.03	0.85	0.20	0.55	2.85	2.71	7.19
WC26B	Wt.%	0.00	11.13	1.27	2.66	46.25	34.64	95.96
	Form.	0.00	0.95	0.13	0.15	3.08	2.72	7.02
WC26B	Wt.%	0.04	11.22	2.34	3.32	46.21	34.07	97.20
	Form.	0.00	0.95	0.23	0.18	3.06	2.66	7.08
WC26B	Wt.%	0.10	8.68	4.47	5.44	46.00	32.35	97.04
	Form.	0.00	0.73	0.44	0.30	3.04	2.52	7.04
WC26B	Wt.%	0.02	8.32	4.56	4.82	44.70	31.64	94.07
	Form.	0.00	0.72	0.46	0.27	3.04	2.54	7.04
WC26B	Wt.%	0.12	11.53	1.58	3.45	47.01	34.07	97.66
	Form.	0.01	0.97	0.15	0.19	3.10	2.65	7.05
WC26B	Wt.%	0.12	11.80	1.43	1.64	47.54	34.83	97.37
	Form.	0.01	0.99	0.14	0.09	3.11	2.69	7.02
WC26B	Wt.%	0.12	11.49	1.41	2.48	46.14	34.97	96.62
	Form.	0.01	0.97	0.14	0.14	3.06	2.73	7.04
WC26B	Wt.%	0.38	11.60	1.38	2.34	45.64	34.46	95.81
	Form.	0.02	0.99	0.14	0.13	3.06	2.72	7.05
WC26B	Wt.%	0.22	11.71	1.36	2.25	47.91	34.41	97.86
	Form.	0.01	0.98	0.13	0.12	3.13	2.65	7.01
WC26B	Wt.%		10.84	1.39	3.51	45.39	33.77	94.91
	Form.		0.93	0.14	0.20	3.07	2.69	7.03

WC26B	Wt.%		10.58	2.10	3.23	46.96	33.06	95.93
	Form.		0.90	0.21	0.18	3.13	2.59	7.00
WC26B	Wt.%	0.50	11.04	2.67	2.85	48.84	30.12	96.01
	Form.	0.02	0.94	0.26	0.16	3.25	2.36	7.00
WC26B	Wt.%	0.63	9.51	2.45	2.21	54.79	28.89	98.46
	Form.	0.03	0.77	0.23	0.12	3.48	2.16	6.79
WC26B	Wt.%	0.50	11.20	2.42	2.69	48.02	31.06	95.89
	Form.	0.02	0.95	0.24	0.15	3.21	2.44	7.02
WC26B	Wt.%	0.22	10.01	4.07	5.19	47.12	30.44	97.06
	Form.	0.01	0.85	0.40	0.29	3.14	2.39	7.08
WC26B	Wt.%	0.40	11.28	2.38	4.45	46.68	31.24	96.42
	Form.	0.02	0.97	0.24	0.25	3.14	2.47	7.08
WC26B	Wt.%	0.38	9.95	3.55	9.10	44.06	30.36	97.39
	Form.	0.02	0.86	0.36	0.52	3.00	2.43	7.19
WC26B	Wt.%	0.20	9.91	2.51	6.67	47.01	29.45	95.75
	Form.	0.01	0.86	0.25	0.38	3.19	2.36	7.04
WC15	Wt.%	0.32	10.07	2.60	6.62	45.12	30.19	94.92
	Form.	0.02	0.88	0.27	0.38	3.10	2.45	7.09
WC15	Wt.%	1.99	9.46	3.48	11.97	38.92	30.75	96.58
	Form.	0.11	0.85	0.37	0.70	2.73	2.55	7.30
WC15	Wt.%	0.32	11.07	2.35	2.31	47.67	30.73	94.46
	Form.	0.02	0.96	0.24	0.13	3.22	2.45	7.01
WC15	Wt.%	0.54	8.08	5.77	6.34	47.35	28.95	97.02
	Form.	0.03	0.68	0.57	0.35	3.14	2.26	7.03
WC15	Wt.%	1.84	10.84	3.28	3.10	48.75	29.34	97.14
	Form.	0.09	0.91	0.32	0.17	3.22	2.28	7.00
WC15	Wt.%	0.31	10.54	2.13	1.96	50.56	29.68	95.19
	Form.	0.02	0.89	0.21	0.11	3.36	2.32	6.91
WC15	Wt.%	0.30	11.17	2.83	3.22	48.82	29.21	95.55
	Form.	0.01	0.96	0.28	0.18	3.28	2.31	7.02
WC15	Wt.%	0.48	10.08	2.81	6.16	46.32	29.40	95.26
	Form.	0.02	0.88	0.28	0.35	3.16	2.36	7.06
WC15	Wt.%	0.37	11.05	2.41	4.01	48.50	31.13	97.47
	Form.	0.02	0.93	0.24	0.22	3.20	2.42	7.03

Electron Microprobe Analyses of Q Domain Phyllosilicates

sample:		Ti	K	Mg	Fe	Si	Al	Total
WC26A	Wt.%	_	10.01	2.59	4.46	51.25	26.6	94.91
	Form.	_	0.858	0.258	0.25	3.445	2.107	6.92
WC26A	Wt.%	_	9.12	2.36	3.82	56.27	26.02	97.59
	Form.	_	0.747	0.224	0.205	3.615	1.97	6.761
WC26A	Wt.%	0.07	0.09	11.91	30.93	25.87	19.89	88.76
	Form.	0.002	0.01	1.493	2.174	2.174	1.971	7.824
WC26A	Wt.%	0.43	3.58	8.34	19.8	35.26	27.01	94.43
	Form.	0.023	0.333	0.91	1.211	2.579	2.33	7.385
WC26A	Wt.%	0.5	3.58	8.34	19.8	35.26	27.01	92.11
	Form.	0.026	0.333	0.91	1.211	2.579	2.33	7.156
WC26A	Wt.%	1.28	8.76	4.14	8.05	44.11	31.03	97.38
	Form.	0.068	0.75	0.415	0.452	2.967	2.46	7.107
WC26A	Wt.%	0.14	2.99	8.82	24.7	30.81	25.81	93.29
	Form.	0.006	0.292	1.01	1.587	2.367	2.335	7.599
WC26A	Wt.%	0.11	0.96	10.05	29.02	25.94	22.66	88.75
	Form.	0.009	0.1	1.248	2.023	2.163	2.226	7.764
WC26A	Wt.%	0.39	1.85	9.18	25.37	30.11	23.64	90.54
	Form.	0.023	0.186	1.084	1.682	2.387	2.208	7.57
WC26A	Wt.%	0.29	10.3	2.85	4.5	46.09	30.7	94.74
	Form.	0.014	0.893	0.288	0.255	3.138	2.362	7.049
WC26A	Wt.%	0.36	8.49	5.1	6.34	48.24	29.69	98.23
	Form.	0.017	0.709	0.498	0.346	3.161	2.292	7.022
WC26A	Wt.%	0.25	11.33	2.11	2.84	48.11	31.99	96.62
	Form.	0.011	0.957	0.208	0.155	3.188	2.5	7.019
WC15	Wt.%	0.1	0.91	10.54	30.3	24.43	22.19	88.46
	Form.	0.005	0.097	1.33	2.145	2.067	2.214	7.857
WC15	Wt.%	0.23	1.13	10.43	30.05	24.35	22.39	88.57
	Form.	0.015	0.119	1.315	2.125	2.057	2.231	7.861
WC15	Wt.%	0.16	0.13	12.13	29.71	26.19	21.38	89.69
	Form.	0.009	0.012	1.491	2.048	2.159	2.077	7.795
WC15	Wt.%	0.27	1.93	9.96	28.14	28.27	24.43	93
	Form.	0.014	0.194	1.168	1.852	2.224	2.265	7.717
OG3	Wt.%	0.12	6.45	6.02	6.55	43.45	31.13	93.7
	Form.	0.006	0.563	0.612	0.374	2.973	2.511	7.039

OG3	Wt.%	0.1	3.56	8.18	22.96	30.84	26.54	92.18
	Form.	0.004	0.349	0.94	1.482	2.381	2.416	7.572
OG3	Wt.%	0.2	3.72	4.33	20.16	47.5	19.75	95.67
	Form.	0.01	0.333	0.455	1.188	3.349	1.641	6.977
OG3	Wt.%	0.12	3.3	9.02	22.74	32.43	26.62	94.22
	Form.	0.006	0.314	1.007	1.424	2.429	2.35	7.531
OG3	Wt.%	0.07	0.027	7.98	27.06	27.07	21.61	89.88
	Form.	0.002	0.026	1.062	1.885	2.332	2.239	7.545
OG3	Wt.%	0.26	7.58	4.53	6.64	44.79	31.95	95.75
	Form.	0.012	0.649	0.454	0.373	3.012	2.531	7.031
OG3	Wt.%	0.21	7.98	4.39	4.17	45.05	33.8	95.61
	Form.	0.009	0.677	0.433	0.23	2.996	2.649	6.995
OG3	Wt.%	0.17	6.18	2.76	8.86	51.6	24.85	94.41
	Form.	0.008	0.531	0.277	0.5	3.486	1.979	6.781
OG3	Wt.%	0.24	9.41	2.05	3.5	47.46	33.02	95.69
	Form.	0.011	0.795	0.203	0.193	3.151	2.583	6.936
OG3	Wt.%	0.26	2.28	8.21	22.28	30.91	27.84	91.89
	Form.	0.013	0.222	0.936	1.429	2.362	2.508	7.469
OG3	Wt.%	0.09	3.11	5.55	21.89	28.79	31.86	91.29
	Form.	0.004	0.305	0.638	1.409	2.219	2.896	7.471
OG11	Wt.%	0.25	0.07	11.37	29.07	25.53	23.27	89.57
	Form.	0.014	0.007	1.391	1.997	2.098	2.252	7.759
OG11	Wt.%	0.07	0.33	10.11	28.69	25.19	23.86	88.24
	Form.	0.002	0.034	1.255	1.999	2.099	2.344	7.733
OG11	Wt.%	0.24	10.36	2.57	2.64	46.59	34.5	96.9
	Form.	0.011	0.869	0.25	0.145	3.065	2.675	7.016
OG11	Wt.%	0.09	1.16	7.63	15.34	47.29	22.61	94.12
	Form.	0.004	0.101	0.782	0.883	3.259	1.835	6.865
OG11	Wt.%	0.11	0.1	11.41	34.26	23.76	22.88	92.52
	Form.	0.004	0.009	1.396	2.353	1.95	2.216	7.929
OG11	Wt.%	0.19	11.45	1.36	1.55	47.71	34.29	96.55
	Form.	0.007	0.96	0.133	0.085	3.143	2.662	6.991
WC26B	Wt.%	0.02	0.52	5.29	33.43	26.62	22.34	88.22
	Form.	0	0.055	0.671	2.383	2.271	2.245	7.624
WC26B	Wt.%	0.35	5.19	3.18	12.24	50.89	24.4	96.25
	Form.	0.018	0.443	0.317	0.686	3.417	1.931	6.812
WC26B	Wt.%	0.32	0.11	10.48	30.62	25.51	20.52	87.55
	Form.	0.02	0.01	1.331	2.181	2.173	2.061	7.774

WC26B	Wt.%	0.03	0.04	14.06	32.24	24.35	22.5	93.21
	Form.	0	0.002	1.689	2.172	1.963	2.136	7.962
WC40	Wt.%	0.24	11.02	2.36	2.87	49.29	31.06	96.83
	Form.	0.011	0.926	0.23	0.156	3.248	2.412	6.984
WC40	Wt.%	0.55	7.37	7.17	10.58	44.29	27.13	97.09
	Form.	0.028	0.639	0.727	0.601	3.013	2.174	7.181
WC40	Wt.%	0.25	11.22	2.73	3.53	49.65	29.63	97.01
	Form.	0.011	0.946	0.268	0.194	3.286	2.311	7.016
WC40	Wt.%	1.42	11.2	2.23	3.11	47.44	29.51	94.91
	Form.	0.071	0.966	0.225	0.175	3.215	2.356	7.008
WC40	Wt.%	0.3	5.4	5.16	19.09	36.48	24.93	91.36
	Form.	0.015	0.522	0.584	1.213	2.773	2.233	7.341
WC40	Wt.%	0.1	2.22	10.27	20.75	33.82	22.59	89.76
	Form.	0.004	0.218	1.186	1.345	2.622	2.064	7.44
WC40	Wt.%	0.08		1.92	6.16	47.6	29.71	97.18
	Form.	0.004	1.003	0.191	0.346	3.205	2.357	7.106
WC40	Wt.%	0.68	11.06	1.96	5.34	47.61	30.65	97.3
	Form.	0.033	0.939	0.193	0.297	3.174	2.409	7.047
WC40	Wt.%	0	0.07	13.32	31.54	24.3	21.25	90.49
	Form.	0	0.007	1.649	2.188	2.017	2.078	7.938
WC40	Wt.%	0.24	10.87	2.28	2.19	50.77	31.77	98.11
	Form.	0.011	0.895	0.218	0.117	3.281	2.42	6.942
WC40	Wt.%	0.34	10.86	2.07	3.17	50.42	30.92	97.77
	Form.	0.015	0.903	0.201	0.172	3.288	2.377	6.956
WC40	Wt.%	0.37	9.59	3.64	5.8	47.41	30.97	97.78
	Form.	0.017	0.806	0.358	0.319	3.128	2.41	7.039
WC40	Wt.%	0.05	0.29	12.48	29.53	24.65	20.11	87.12
	Form.	0.002	0.03	1.593	2.113	2.11	2.027	7.875
WC40	Wt.%	0.24	2.86	8.13	26.83	29.15	24	91.21
	Form.	0.014	0.291	0.969	1.793	2.331	2.263	7.66
WC40	Wt.%	0.36	6.74	7.5	11.73	41.31	27.68	95.33
	Form.	0.018	0.598	0.781	0.685	2.886	2.279	7.247
WC40	Wt.%	0.1	0.38	12.45	29.77	27.91	22.05	92.66
	Form.	0.004	0.037	1.471	1.974	2.214	2.06	7.761
WC40	Wt.%	0.16	0.6	10.41	26.11	33.02	21.41	91.72
	Form.	0.009	0.059	1.203	1.692	2.558	1.956	7.476
WC40	Wt.%	0.36	8.8	3.76	13.81	40.44	29.04	96.21

	Form.	0.019	0.792	0.396	0.815	2.859	2.419	7.3
WC40	Wt.%	0.05	1.25	11.7	30.02	25.26	21.49	89.75
	Form.	0.002	0.132	1.453	2.091	2.104	2.111	7.893
WC40	Wt.%	0.1	0.55	10.44	28.78	27.17	21.76	88.8
	Form.	0.004	0.056	1.287	1.991	2.249	2.123	7.71
.WC40	Wt.%	0.95	0.28	11.74	30.84	24.46	20.47	88.75
	Form.	0.06	0.03	1.479	2.182	2.068	2.041	7.859
WC40	Wt.%	1.87	10.34	2.38	3.92	45.71	30.23	94.46
	Form.	0.094	0.899	0.24	0.222	3.122	2.432	7.009

NINE ELEMENT PHYLLOSILICATE ANALYSES
P domain:

	Fe	Ca	Al	Mn	K	Mg	Ti	Si	Na	Total
WC26A:										
wt %	11.12	0.30	27.74	0.09	7.84	4.06	0.24	43.74	0.13	95.26
form.	0.65	0.02	2.28	0.00	0.70	0.42	0.01	3.05	0.02	7.15
wt %	3.99	0.24	30.13	0.09	9.57	2.85	1.28	46.00	0.12	94.26
form.	0.23	0.02	2.42	0.00	0.83	0.29	0.06	3.14	0.02	7.00
wt %	10.53	0.39	15.75	0.07	7.71	3.65	11.05	43.09	0.04	92.28
form.	0.64	0.03	1.36	0.00	0.72	0.40	0.61	3.15	0.00	6.91
wt %	3.47	0.37	30.18	0.00	10.96	2.29	0.41	48.43	0.10	96.21
form.	0.19	0.03	2.38	0.00	0.93	0.23	0.02	3.24	0.01	7.02
wt %	3.43	0.21	30.25	0.02	10.17	2.67	0.47	49.49	0.16	96.86
form.	0.19	0.01	2.35	0.00	0.85	0.26	0.02	3.26	0.02	6.97
wt %	2.59	0.30	29.81	0.01	10.50	2.30	0.12	50.18	0.21	96.01
form.	0.14	0.02	2.33	0.00	0.89	0.23	0.01	3.32	0.03	6.95
wt %	12.57	0.36	26.11	0.17	6.42	5.05	2.21	38.77	0.14	91.81
form.	0.77	0.03	2.26	0.01	0.60	0.55	0.12	2.85	0.02	7.20
wt %	6.43	0.32	29.79	0.16	8.00	4.21	0.53	44.43	0.70	94.56
form.	0.37	0.02	2.41	0.01	0.70	0.43	0.03	3.05	0.09	7.10
wt %	7.39	0.37	28.65	0.08	8.38	4.01	0.29	43.54	0.08	92.80
form.	0.43	0.03	2.38	0.00	0.75	0.42	0.01	3.07	0.01	7.10
wt %	18.21	0.38	24.31	0.21	3.08	8.50	0.03	35.34	0.94	91.00
form.	1.16	0.03	2.17	0.01	0.30	0.96	0.00	2.68	0.14	7.44
wt %	3.45	0.29	31.59	0.13	9.82	2.71	0.48	45.93	0.30	94.71
form.	0.19	0.02	2.52	0.01	0.85	0.27	0.02	3.11	0.04	7.03
wt %	6.31	0.25	28.91	0.11	9.46	3.99	0.43	45.96	0.29	95.71
form.	0.36	0.02	2.32	0.01	0.82	0.40	0.02	3.13	0.04	7.11
wt %	5.82	0.30	28.97	0.06	10.00	3.00	0.38	45.93	0.29	94.73
form.	0.33	0.02	2.35	0.00	0.88	0.31	0.02	3.16	0.04	7.09
wt %	4.05	0.27	31.03	0.09	10.49	2.38	0.32	47.96	0.18	96.77
form.	0.22	0.02	2.43	0.00	0.81	0.23	0.02	3.19	0.02	7.03
wt %	3.11	0.30	28.31	0.04	10.05	2.84	0.59	48.97	0.48	94.69
form.	0.17	0.02	2.25	0.00	0.87	0.29	0.03	3.30	0.06	6.99
wt %	2.70	0.30	30.94	0.09	10.58	2.25	0.30	48.18	0.16	95.49
form.	0.15	0.02	2.44	0.00	0.90	0.22	0.01	3.23	0.02	7.00

wt %	3.59	0.29	32.18	0.07	9.61	3.25	0.25	44.04	0.18	93.47
form.	0.21	0.02	2.61	0.00	0.84	0.33	0.01	3.03	0.02	7.08
WC29:										
wt %	4.89	0.79	28.98	0.00	10.27	2.67	0.29	47.94	0.20	96.02
form.	0.27	0.06	2.30	0.00	0.88	0.27	0.01	3.23	0.03	7.05
wt %	2.11	0.25	30.31	0.10	10.47	2.20	0.25	48.88	0.20	94.77
form.	0.12	0.02	2.40	0.00	0.90	0.22	0.01	3.28	0.03	6.96
WC15:										
wt %	2.89	0.27	31.87	0.00	9.63	1.66	0.19	47.27	0.74	94.52
form.	0.16	0.02	2.53	0.00	0.83	0.17	0.01	3.19	0.10	6.99
wt %	11.53	0.33	27.74	0.20	6.49	6.49	0.29	38.50	0.11	91.68
form.	0.70	0.03	2.39	0.01	0.60	0.71	0.02	2.81	0.02	7.28
WC26B:										
wt %	2.62	0.29	29.86	0.09	10.24	2.08	0.33	48.99	0.18	94.66
form.	0.15	0.02	2.37	0.00	0.88	0.21	0.02	3.29	0.02	6.95
wt %	13.07	0.30	25.32	0.15	6.47	6.04	0.20	40.19	0.17	91.92
form.	0.80	0.02	2.18	0.01	0.60	0.66	0.01	2.94	0.02	7.25

NINE ELEMENT PHYLLOSILICATE ANALYSES
Q domain:

	Fe	Ca	Al	Mn	K	Mg	Ti	Si	Na	Total
wt %	29.60	0.32	24.64	0.13	0.06	11.41	0.08	23.91	0.11	90.27
form.	2.03	0.03	2.38	0.01	0.00	1.40	0.00	1.96	0.02	7.83
wt %	0.84	0.25	36.21	0.00	9.01	0.59	0.11	47.64	0.91	95.57
form.	0.04	0.02	2.79	0.00	0.75	0.06	0.01	3.12	0.11	6.90
wt %	18.49	0.29	33.72	0.14	0.87	10.16	0.13	26.01	0.41	90.21
form.	1.18	0.02	3.04	0.01	0.08	1.16	0.01	1.99	0.06	7.55
wt %	8.25	0.27	31.53	0.07	6.40	3.57	0.12	41.26	0.70	92.18
form.	0.49	0.02	2.62	0.00	0.58	0.38	0.01	2.91	0.10	7.09
WC15:										
wt %	29.49	0.34	22.88	0.13	0.04	12.78	0.04	24.85	0.26	90.81
form.	2.01	0.03	2.20	0.01	0.00	1.55	0.00	2.03	0.04	7.87
OG11:										
wt %	16.65	0.28	17.36	0.01	7.31	5.86	0.13	43.48	0.56	91.64
form.	1.05	0.02	1.54	0.00	0.70	0.66	0.01	3.27	0.08	7.33
WC26A:										
wt %	2.47	0.29	29.61	0.00	10.91	1.99	0.31	48.08	0.12	93.79

form.	0.14	0.02	2.38	0.00	0.95	0.20	0.01	3.28	0.02	6.99
wt %	24.85	0.34	24.23	0.31	0.53	11.51	0.01	26.38	0.20	88.36
form.	1.70	0.03	2.33	0.02	0.05	1.40	0.00	2.15	0.03	7.71
wt %	26.97	0.35	21.24	0.32	0.17	11.95	1.79	24.23	0.78	87.79
form.	1.90	0.03	2.11	0.02	0.02	1.50	0.11	2.04	0.13	7.85
wt %	6.80	0.29	25.73	0.03	10.02	2.80	0.32	46.97	0.15	93.11
form.	0.40	0.02	2.13	0.00	0.90	0.29	0.02	3.30	0.02	7.07
wt %	11.95	0.26	29.40	0.13	4.81	6.79	0.06	37.80	0.11	91.30
form.	0.73	0.02	2.52	0.01	0.45	0.73	0.00	2.75	0.01	7.21
WC11:										
wt %	5.21	0.23	33.18	0.05	8.17	2.21	0.31	42.78	0.24	92.39
form.	0.30	0.02	2.72	0.00	0.73	0.23	0.02	2.98	0.03	7.02

Representative Probe Analyses of Calcite
from Sandsuck Formation Phyllites and Siltstones

Weight percent:					Formula units:				
Ca	Mg	Fe	Mn	Total	Ca	Mg	Fe	Mn	Total
50.72	0.77	1.15	0.67	53.30	1.91	0.04	0.03	0.02	2.00
52.45	1.12	0.98	0.37	54.93	1.91	0.06	0.03	0.01	2.00
52.71	0.73	1.24	0.47	55.16	1.91	0.04	0.04	0.01	2.00
52.47	0.73	1.46	0.47	55.14	1.91	0.04	0.04	0.01	2.00
52.88	0.66	1.31	0.57	55.42	1.91	0.03	0.04	0.02	2.00
53.90	0.76	1.18	0.25	56.09	1.92	0.04	0.03	0.01	2.00
53.21	0.89	1.49	0.49	56.07	1.90	0.04	0.04	0.01	2.00
54.03	0.73	1.27	0.63	56.65	1.91	0.04	0.04	0.02	2.00
50.95	0.81	1.19	0.44	53.39	1.91	0.04	0.03	0.01	2.00
55.00	0.68	0.64	0.38	56.71	1.94	0.03	0.02	0.01	2.00
55.61	0.71	1.24	0.57	58.34	1.92	0.03	0.03	0.02	2.00
55.33	0.70	1.18	0.56	57.76	1.92	0.03	0.03	0.02	2.00
54.29	0.89	1.56	0.84	57.57	1.89	0.04	0.04	0.02	2.00
55.51	0.62	1.11	0.63	57.87	1.92	0.03	0.03	0.02	2.00
53.84	0.69	1.46	0.68	56.66	1.91	0.03	0.04	0.02	2.00
54.87	0.73	1.27	0.50	57.36	0.03	1.92	0.03	0.01	2.00
54.11	0.73	1.42	0.60	56.86	1.91	0.04	0.04	0.02	2.00
51.55	0.64	1.87	0.61	54.67	1.90	0.03	0.05	0.02	2.00
52.52	0.60	1.34	0.45	54.91	1.92	0.03	0.04	0.01	2.00
52.10	0.45	1.05	0.67	54.27	1.93	0.02	0.03	0.02	2.00
52.84	0.59	1.41	0.59	55.42	1.91	0.03	0.04	0.02	2.00
53.50	0.68	1.58	0.68	56.44	1.90	0.03	0.04	0.02	2.00
54.88	0.73	1.36	0.55	57.53	1.91	0.03	0.04	0.02	2.00
54.16	0.63	1.30	0.38	56.47	1.92	0.03	0.04	0.01	2.00
52.41	0.77	1.71	0.76	55.65	1.89	0.04	0.05	0.02	2.00
52.70	0.89	2.10	0.60	56.29	1.88	0.04	0.06	0.02	2.00
53.52	0.84	1.39	0.63	56.39	1.90	0.04	0.04	0.02	2.00

Representative Probe Analyses of Feldspars from Sandsuck Formation phyllites and siltstones.

Fe	Ca	Al	Mn	K	Mg	Ti	Si	Na	Total
0.27	0.21	18.71	0.14	0.05	0.38	0	68.02	12.85	100.6
0.13	0.27	20.27	0	0.14	0.04	0.09	68.82	11.36	101.1
0.09	0.3	19.45	0	0.07	0.03	0.2	66.7	11.19	98.02
0.09	0.32	20.17	0	0.1	0.02	0	67.65	10.46	98.82
0.48	0.3	19.79	0	0.13	0.3	0	66.27	10.41	97.68
	0.01	18.97		0			66.78	11.46	97.21
		19.34		0			67	11.49	97.64
0	0.21	20.06	0.12	0.06	0.02	0	68.38	11.28	100.1
0.09	0.2	19.95	0	0	0	0	67.99	10.58	98.52
0	0.2	20.72	0	0	0	0	66.77	11	100.6
0	0.17	20.81	0	0	0	0	66.92	11.18	99.08
0	0.2	20.28	0	0	0	0.05	66.7	11.13	98.36
0.02	0.14	18.82	0.09	0.07	0	0	69.19	12.36	100.6
0	0.21	18.82	0.09	0.02	0	0	70.2	12.23	101.5
0	0.14	19.05	0.06	0.01	0	0.01	69.82	11.91	101.0
0	0.17	17.94	0.05	0	0.02	0	67.5	13.32	99
0.12	0.13	19.57	0.04	0.02	0.02	0	68.92	12.32	101.1
0.45	0.17	20.48	0	0.04	0.04	0	69.27	11.24	101.6
0.16	0.24	21.23	0	0	0	0	68.48	10.09	100.4
0.11	0.19	19.64	0	0	0.01	0	67.89	11.8	99.64
0.06	0.21	19.78	0	0	0.04	0	68.18	11.91	100.1
0.14	0.23	19.98	0.01	0.02	0	0	68.42	11.56	100.3
0.09	0.18	19.23	0.02	0	0	0	67.98	11.45	98.95

Nine Element Traverse of OG17

Analyses calculated as weight percent oxide

step	Fe	Ca	Al	Mn	K	Mg	Ti	Si	Na	Total
1	4.56	7.84	5.67	0.32	0.35	2.45	0.02	64.39	2.64	88.24
2	6.04	9.05	6.83	0.40	0.36	3.08	0.00	56.29	3.06	85.12
3	5.33	7.33	7.87	0.36	0.19	2.64	0.05	58.02	3.94	85.73
4	3.74	2.19	13.05	0.08	0.76	1.41	0.13	64.89	5.34	91.61
5	2.81	0.27	19.31	0.00	3.58	1.03	1.28	59.91	3.99	92.19
6	4.21	0.30	24.49	0.00	6.32	1.59	2.42	49.35	1.74	90.42
7	4.31	0.31	28.91	0.00	8.54	1.75	3.31	40.21	0.45	87.77
8	4.61	0.31	28.71	0.00	8.44	1.81	2.37	40.33	0.56	87.15
9	4.19	0.31	28.78	0.00	8.58	1.73	1.64	40.43	0.51	86.17
10	4.15	0.30	28.91	0.00	8.73	1.78	0.94	40.59	0.49	85.89
11	4.71	0.29	28.73	0.00	8.55	1.96	1.38	39.93	0.29	85.84
12	4.84	0.28	28.07	0.00	8.30	2.03	1.37	39.91	0.41	85.22
13	5.26	0.27	24.40	0.00	6.10	2.00	1.12	45.46	2.29	86.91
14	6.49	0.78	23.16	0.00	5.46	2.34	0.58	45.05	2.33	86.19
15	6.88	0.78	21.31	0.00	4.26	2.46	0.19	45.81	3.03	84.71
16	5.12	0.70	15.72	0.00	3.58	1.93	0.18	28.10	1.28	84.72
17	3.38	0.19	11.48	0.00	2.09	1.28	0.06	38.06	2.17	86.81
18	2.50	0.18	9.36	0.00	0.71	0.82	0.22	45.56	3.77	91.24
19	3.65	1.32	12.46	0.00	0.95	1.24	0.22	66.73	4.65	91.22
20	3.24	1.35	12.77	0.00	0.99	1.11	0.31	67.55	4.79	92.12
21	3.69	1.37	15.86	0.00	2.88	1.42	0.49	62.04	2.99	90.74
22	6.37	1.05	19.58	0.05	4.07	2.37	0.81	51.35	1.97	87.63
23	7.95	1.03	23.99	0.05	5.17	2.96	0.95	42.72	1.66	86.47
24	8.62	1.04	23.41	0.05	4.80	3.06	0.75	43.33	1.77	86.83
25	6.47	0.30	24.33	0.00	5.50	2.33	0.75	46.86	2.01	88.54
26	6.19	0.29	23.89	0.00	5.79	2.21	0.90	45.29	1.60	86.17
27	5.26	0.28	19.18	0.00	4.53	1.84	0.70	52.40	1.47	85.66
28	4.18	0.67	13.51	0.00	2.96	1.45	0.79	62.74	1.22	87.53
29	3.07	0.69	13.36	0.00	3.27	1.17	2.16	64.01	1.07	88.79
30	3.96	1.53	12.20	0.02	3.10	1.56	2.18	63.26	0.42	88.23
31	4.28	1.15	11.80	0.02	2.77	1.60	1.77	64.54	0.72	88.64
32	5.28	1.14	11.32	0.02	2.35	1.90	0.42	65.20	1.06	88.68
33	4.62	0.30	14.57	0.00	3.17	1.63	0.81	62.00	1.82	88.91
34	5.47	0.32	18.88	0.00	4.17	1.89	0.89	52.17	2.45	86.24
35	3.87	0.33	14.66	0.00	2.39	1.29	0.49	62.68	3.51	89.22
36	3.39	0.32	17.07	0.00	3.01	1.26	0.56	59.94	3.89	89.43
37	3.09	0.32	17.11	0.00	3.13	1.25	0.80	60.81	3.74	90.26
38	3.57	0.41	17.64	0.00	3.63	1.42	1.00	58.30	3.01	88.98
39	4.26	2.32	15.28	0.05	2.31	1.88	0.51	55.74	4.13	86.49
40	6.52	8.60	9.35	0.32	0.93	3.61	0.20	44.80	3.68	78.00
41	8.72	14.13	6.92	0.55	0.39	5.31	0.00	30.84	3.73	70.59
42	10.94	18.77	3.28	0.81	0.08	6.86	0.00	21.33	2.51	64.59
43	8.03	13.98	7.34	0.58	0.04	5.00	0.00	32.04	5.01	72.03
44	6.14	9.56	11.21	0.38	0.36	3.59	0.00	40.21	6.61	78.07
45	3.21	3.28	16.92	0.08	2.08	1.55	0.73	52.07	6.77	86.71
46	4.56	5.01	13.24	0.17	2.15	2.26	0.96	51.45	4.25	84.08
47	4.47	4.57	12.03	0.14	2.04	2.21	0.98	54.03	3.41	83.90
48	4.40	4.29	8.84	0.14	1.00	2.07	0.31	60.02	3.20	84.28
49	3.18	1.80	8.61	0.00	1.03	1.31	0.08	69.58	2.92	88.55
50	5.13	6.66	6.07	0.24	0.80	2.68	0.09	59.26	2.09	83.03

51	6.31	9.32	5.55	0.37	0.36	3.48	0.47	51.43	2.41	79.72
52	5.71	8.56	6.43	0.37	0.38	3.21	0.49	51.91	3.01	80.06
53	2.82	2.91	8.81	0.13	0.73	1.38	0.53	66.48	3.57	87.36
54	1.77	0.28	10.38	0.00	1.21	0.60	0.48	72.55	3.90	91.17
55	2.91	0.33	13.45	0.00	2.13	0.98	0.50	66.41	3.65	90.37
56	6.78	5.38	12.54	0.23	2.29	3.03	0.45	49.44	2.32	82.44
57	10.47	13.09	7.66	0.59	1.58	5.86	0.06	29.50	0.63	69.43
58	9.60	13.57	8.03	0.61	0.92	5.63	0.15	27.91	2.85	69.28
59	7.10	9.78	9.40	0.40	1.28	4.15	0.15	39.15	3.72	75.13
60	6.99	8.99	10.35	0.34	1.46	3.91	0.35	40.13	3.76	76.23
61	7.36	8.49	7.94	0.32	1.22	3.95	0.30	45.96	2.17	77.65
62	6.73	7.26	9.22	0.30	0.81	3.63	0.30	48.08	3.21	79.48
63	4.06	0.32	10.68	0.00	1.09	1.34	0.16	69.15	3.34	90.13
64	4.67	0.32	12.97	0.00	1.63	1.53	0.16	63.58	3.53	88.38
65	5.72	0.31	15.57	0.00	3.00	1.92	0.13	58.31	2.19	87.14
66	5.18	0.31	16.65	0.00	3.44	1.74	0.23	58.43	2.11	88.08
67	5.11	0.29	17.36	0.00	3.88	1.82	0.27	58.21	1.62	88.55
68	5.18	0.28	17.80	0.00	4.32	1.84	0.31	54.70	0.96	85.40
69	5.32	0.27	19.42	0.00	4.81	1.95	0.20	51.48	0.95	84.41
70	4.49	0.29	21.69	0.00	5.31	1.73	0.59	48.80	1.57	84.47
71	3.78	0.31	19.90	0.00	4.70	1.46	0.87	55.63	2.09	88.76
72	2.88	0.33	20.14	0.00	3.98	1.13	0.83	56.98	4.12	90.39
73	2.56	0.68	20.95	0.00	4.91	1.12	0.58	56.12	3.18	90.10
74	2.35	0.69	21.55	0.00	4.93	1.04	0.31	54.91	3.74	89.52
75	2.71	0.68	25.41	0.00	7.20	1.32	0.56	47.36	1.80	87.05
76	2.50	0.41	18.58	0.00	4.87	1.09	0.36	58.30	2.29	88.40
77	1.77	0.45	12.61	0.00	3.33	0.79	0.30	69.11	1.56	89.91
78	1.42	0.47	6.32	0.00	0.80	0.48	0.04	80.93	2.38	92.82
79	2.40	0.37	10.43	0.00	1.74	0.76	0.78	72.45	2.90	91.82
80	2.76	0.33	14.52	0.00	2.17	0.92	1.13	64.42	4.84	91.09
81	4.28	0.47	18.70	0.00	2.98	1.53	1.17	54.19	5.27	88.59
82	4.64	0.73	18.56	0.00	3.02	1.73	0.78	54.26	4.71	88.42
83	4.72	0.71	16.64	0.00	2.50	1.69	0.57	57.21	4.43	88.48
84	3.80	1.23	13.09	0.00	1.89	1.45	0.54	62.63	3.86	88.49
85	2.93	0.98	10.72	0.00	0.97	1.08	0.20	67.99	4.58	89.46
86	4.58	1.01	11.00	0.00	1.01	1.68	0.07	64.63	3.92	87.90
87	5.28	3.04	9.32	0.10	0.59	2.00	0.17	61.87	4.29	86.68
88	7.30	7.28	6.98	0.31	0.47	3.19	0.22	52.58	2.93	81.26
89	6.31	7.26	10.22	0.31	2.08	2.92	1.84	48.34	2.26	81.53
90	6.92	4.53	16.03	0.21	3.87	2.98	1.86	43.65	1.28	81.31
91	5.67	0.29	21.91	0.00	5.10	2.19	1.95	45.72	2.49	85.32
92	4.89	0.29	21.48	0.00	5.35	2.01	0.65	48.07	2.24	84.98
93	3.70	0.29	21.26	0.00	5.12	1.62	0.58	50.31	3.19	86.08
94	4.00	0.29	21.82	0.00	5.62	1.63	0.65	48.63	2.43	85.08

Nine Element Microprobe Traverse of WC26A
Analyses calculated as weight percent oxide.

step	Fe	Ca	Al	Mn	K	Mg	Ti	Si	Na	Total
1	3.60	0.31	13.82	0.00	0.75	1.46	0.06	72.04	5.20	97.23
2	4.85	0.19	11.26	0.06	0.30	1.82	0.00	75.21	4.71	98.41
3	0.91	13.79	3.65	0.47	1.04	0.49	0.11	64.81	0.09	85.36
4	2.25	0.30	20.62	0.09	0.60	1.05	0.07	63.76	9.86	98.59
5	1.61	3.94	2.70	0.06	0.03	0.63	0.00	87.78	1.06	97.81
6	2.38	17.87	3.80	0.27	0.06	0.93	0.05	54.40	0.96	80.71
7	1.27	14.19	7.67	0.34	0.09	0.56	9.75	43.43	3.90	81.19
8	2.91	0.28	17.76	0.00	0.25	1.19	0.00	67.30	8.54	98.21
9	4.84	0.23	15.11	0.05	1.17	2.01	0.18	66.52	4.97	95.07
10	1.41	0.21	5.84	0.00	0.59	0.59	2.49	86.34	1.86	99.34
11	5.83	0.31	22.13	0.08	5.70	2.80	0.58	56.18	1.53	95.13
12	5.62	0.21	23.34	0.02	6.36	2.97	0.35	52.70	2.02	93.59
13	4.75	0.89	24.44	0.06	6.20	2.57	3.36	49.87	2.31	94.45
14	4.71	0.83	28.54	0.00	9.32	2.80	1.32	43.51	0.14	91.18
15	7.41	0.32	27.36	0.08	7.82	3.79	3.09	42.20	0.49	92.54
16	6.46	0.32	27.59	0.00	8.50	3.42	3.14	43.05	0.25	92.73
17	2.91	0.26	23.07	0.05	4.84	1.79	0.68	57.33	5.52	96.45
18	9.91	0.33	26.40	0.09	7.19	4.55	0.42	40.95	0.35	90.20
19	7.72	0.27	26.15	0.09	7.30	3.69	1.11	46.75	0.72	93.80
20	8.80	0.27	22.26	0.19	5.03	3.96	1.07	46.63	1.94	90.14
21	10.95	0.25	19.97	0.14	4.46	4.32	0.80	47.54	0.80	89.24
22	10.25	0.25	20.94	0.13	4.50	4.59	0.60	47.60	1.50	90.36
23	8.64	0.28	15.89	0.18	3.63	3.78	0.58	58.88	0.64	92.50
24	11.29	0.25	17.43	0.15	2.50	4.58	0.32	54.32	1.98	92.82
25	9.33	0.26	16.58	0.16	3.45	3.86	0.85	54.75	1.54	90.78
26	6.64	0.30	13.64	0.05	2.46	2.79	0.86	67.04	2.21	96.00
27	8.85	0.29	12.04	0.06	2.06	2.06	3.46	64.34	0.17	92.55
28	9.49	0.27	19.74	0.07	4.48	4.00	0.78	55.62	0.59	95.03
29	7.36	1.27	15.80	0.13	2.73	3.16	0.66	62.87	2.18	96.16
30	10.32	6.16	18.86	0.09	2.71	4.55	0.45	38.33	1.94	83.41
31	8.75	0.25	18.96	0.02	4.13	3.69	0.67	58.07	0.36	94.90
32	10.09	0.28	19.91	0.11	4.24	4.82	0.99	50.74	0.97	92.16
33	9.42	0.30	24.27	0.08	6.42	4.24	2.73	43.16	0.82	91.43
34	8.54	0.32	24.31	0.11	5.81	4.27	1.60	44.77	1.88	91.61
35	7.23	0.87	23.66	0.05	7.00	3.50	2.08	44.97	0.23	89.59
36	10.80	0.31	23.79	0.13	5.38	5.03	0.32	43.86	1.25	90.86
37	7.11	0.26	25.31	0.08	6.30	3.62	0.86	45.71	2.77	92.03
38	10.13	0.45	24.37	0.03	6.05	4.52	0.91	43.42	1.68	91.55
39	8.61	0.28	25.02	0.10	6.15	4.89	2.08	41.71	1.51	90.35
40	12.08	0.38	23.79	0.04	5.48	5.25	0.63	43.55	0.92	92.11
41	7.82	0.21	20.79	0.19	5.96	3.66	0.50	53.60	0.29	93.03
42	8.62	0.25	26.17	0.00	7.71	4.13	1.24	43.67	0.27	92.07
43	4.63	0.28	19.32	0.04	5.02	2.37	0.63	61.47	2.45	96.21
44	6.55	0.25	20.09	0.05	5.23	3.20	1.16	56.44	1.06	94.04
45	7.82	0.29	20.85	0.05	4.52	3.20	0.77	47.40	2.17	87.05
46	8.71	0.36	14.14	0.11	2.75	3.61	1.75	63.52	0.91	95.87
47	8.11	0.30	20.58	0.11	4.50	3.82	0.29	53.45	1.39	92.55
48	5.72	0.26	18.30	0.15	4.76	2.66	0.32	60.68	1.46	94.31
49	8.66	0.27	19.32	0.03	4.29	3.88	0.77	51.17	1.46	89.84
50	6.22	0.24	15.32	0.04	2.57	2.90	0.39	63.18	2.66	93.54
51	9.75	0.34	19.34	0.13	3.63	4.55	0.32	52.75	2.13	92.93
52	8.54	0.24	22.78	0.07	6.29	3.84	1.02	47.27	0.79	90.84

53	5.68	0.29	23.52	0.05	6.58	2.84	0.60	53.10	2.11	94.77
54	14.31	0.35	23.92	0.05	5.00	6.15	0.48	41.27	0.58	92.11
55	9.04	0.31	24.01	0.14	5.80	4.16	1.57	46.76	1.53	93.32
56	9.77	0.28	24.67	0.12	6.74	4.66	1.66	41.14	0.30	89.34
57	7.28	0.27	24.34	0.02	7.24	3.57	1.21	45.55	0.66	90.13
58	7.38	0.27	24.01	0.00	7.16	3.65	1.74	39.86	0.46	84.53
59	7.82	0.31	25.77	0.03	7.86	3.82	0.70	42.78	0.60	89.69
60	7.20	0.26	25.59	0.09	7.98	3.62	1.21	43.06	0.34	89.36
61	6.92	0.25	24.68	0.05	6.97	3.34	1.02	47.66	1.56	92.44
62	4.67	0.32	25.75	0.00	8.14	2.72	1.80	47.24	1.90	92.55
63	5.96	0.27	21.92	0.05	6.68	3.03	0.38	51.77	1.13	91.20
64	9.41	0.23	21.31	0.12	5.93	4.02	0.86	47.82	0.84	90.55
65	7.36	0.30	21.39	0.16	5.93	3.43	0.98	50.05	1.32	90.93
66	7.73	0.30	25.35	0.02	7.22	3.71	0.89	44.98	1.51	91.71
67	7.01	0.33	24.81	0.07	6.54	3.50	2.47	44.13	1.96	90.82
68	4.58	0.23	26.87	0.03	8.87	2.72	2.88	43.98	0.35	90.51
69	7.09	0.27	25.31	0.00	7.50	3.45	0.82	42.92	0.93	88.28
70	4.74	0.30	27.73	0.02	9.08	2.91	0.88	45.35	0.33	90.34
71	7.92	0.30	15.72	0.04	4.30	3.32	0.12	60.03	0.13	91.89
72	6.64	0.30	13.32	0.05	3.36	2.81	0.60	65.18	0.41	92.69
73	11.09	0.29	20.64	0.08	4.05	4.38	0.06	48.89	1.33	90.81
74	2.90	0.20	8.46	0.00	0.09	1.22	0.01	79.61	3.72	96.20
75	2.50	0.23	21.68	0.07	6.73	1.67	0.27	57.27	1.73	92.15
76	4.84	0.27	10.77	0.08	0.59	1.73	0.13	74.47	4.23	97.11
77	1.36	0.23	7.65	0.00	0.97	0.63	0.25	81.19	2.40	94.68
78	6.19	0.32	13.71	0.00	0.07	2.34	0.00	69.14	6.44	98.21
79	4.05	0.23	14.08	0.00	1.88	1.58	0.31	66.25	4.58	92.96
80	2.46	0.29	22.16	0.00	5.20	1.71	0.03	56.54	4.42	92.83

Nine Element Microprobe Traverse #2 of Sample WC26A
Analyses calculated as weight percent oxide.

step	Fe	Ca	Al	Mn	K	Mg	Ti	Si	Na	Total
1	5.38	0.32	17.74	0.07	3.72	2.18	1.02	61.30	3.19	94.92
2	4.51	0.28	15.65	0.05	3.36	1.89	0.66	67.28	2.71	96.38
3	6.41	0.23	16.23	0.05	2.86	2.50	0.73	63.61	3.58	96.21
4	6.73	0.32	18.84	0.02	3.07	2.69	0.35	59.87	4.55	96.44
5	6.37	0.31	16.00	0.11	2.99	2.65	0.68	64.38	2.82	96.32
6	4.03	0.35	15.92	0.04	3.41	1.74	0.52	66.20	2.97	95.17
7	6.04	0.25	18.58	0.04	2.95	2.58	0.35	60.55	4.38	95.72
8	6.19	0.34	14.30	0.02	2.91	2.23	0.45	68.26	2.11	96.80
9	2.45	1.97	15.72	0.14	1.45	0.91	0.29	67.47	6.68	97.08
10	6.12	0.41	14.41	0.02	3.45	2.45	0.57	68.17	1.13	96.73
11	5.69	0.34	22.59	0.16	4.55	2.38	0.75	55.61	4.77	96.84
12	10.36	0.56	25.70	0.18	6.56	4.49	1.27	44.25	1.00	94.37
13	10.14	0.38	24.79	0.05	5.61	3.99	1.52	44.87	2.23	93.58
14	7.81	0.26	19.23	0.09	5.41	3.27	1.42	57.00	0.75	95.24
15	8.93	0.32	22.11	0.26	4.86	3.66	1.21	51.94	2.19	95.46
16	8.52	0.40	22.32	0.17	5.79	3.67	1.05	51.08	1.11	94.11
17	7.59	0.42	21.89	0.10	5.69	3.21	0.66	53.97	1.65	95.18
18	9.04	0.63	21.38	0.19	5.26	3.62	1.91	50.97	1.32	94.32
19	8.35	0.38	22.43	0.20	5.02	3.65	0.84	50.51	2.41	93.80
20	6.83	1.13	19.93	0.13	4.93	3.06	1.14	55.21	2.05	94.42
21	7.45	0.32	17.89	0.02	4.21	3.12	0.90	58.49	1.54	93.93
22	8.50	0.32	20.09	0.12	3.38	3.30	0.62	54.66	4.07	95.06
23	6.77	0.66	16.76	0.02	3.64	2.72	0.77	59.28	2.21	92.83
24	8.36	0.29	15.26	0.04	2.98	3.08	0.94	61.78	1.36	94.10
25	7.66	0.34	19.57	0.11	3.14	3.03	0.39	57.63	4.13	96.00
26	6.75	0.32	16.90	0.08	2.65	2.61	0.84	62.04	3.58	95.77
27	8.23	0.35	20.51	0.08	4.71	3.25	1.07	54.56	2.24	95.01
28	6.80	0.36	24.05	0.05	6.72	3.20	2.07	48.91	1.69	93.85
29	3.29	0.32	15.43	0.00	3.00	1.49	2.88	63.82	3.03	93.25
30	7.80	0.31	24.01	0.12	6.09	3.32	1.27	48.89	2.72	94.53
31	8.39	0.30	22.61	0.16	5.20	3.66	0.97	50.80	2.06	94.13
32	10.66	0.30	21.62	0.13	4.77	4.00	1.54	51.36	1.52	95.89
33	7.26	0.32	21.40	0.04	3.99	2.95	1.13	53.38	3.78	94.24
34	7.17	0.25	17.93	0.05	3.40	2.96	1.09	59.18	2.93	94.97
35	6.12	0.32	15.95	0.15	2.72	2.38	0.84	64.58	3.59	96.65
36	4.02	0.46	15.13	0.00	2.38	1.58	0.96	67.92	3.70	96.16
37	2.55	14.49	10.98	0.39	0.89	0.97	0.14	50.35	4.30	85.07
38	6.68	0.28	12.85	0.00	2.34	2.43	0.81	70.07	1.71	97.17
39	4.48	0.28	16.16	0.00	2.03	1.76	0.65	67.59	4.97	97.92
40	7.91	0.32	14.61	0.08	2.70	3.04	0.58	63.65	1.88	94.76
41	6.32	0.32	12.11	0.12	1.97	2.18	0.63	69.81	2.02	95.47
42	8.27	0.34	16.30	0.09	2.77	3.05	1.32	60.58	3.04	95.77
43	9.23	0.31	16.75	0.15	2.53	3.67	0.81	58.29	2.55	94.30
44	7.63	1.42	16.38	0.04	2.89	2.93	0.61	60.95	2.68	95.53
45	5.08	0.30	13.09	0.00	2.21	2.13	0.49	69.11	3.01	95.42
46	8.25	0.30	14.56	0.07	2.82	2.95	0.66	63.85	2.07	95.53
47	6.07	0.25	14.10	0.15	2.89	2.40	0.71	67.59	2.07	96.23
48	11.11	0.30	18.10	0.13	2.81	4.09	1.33	53.53	2.48	93.08
49	8.80	0.80	17.85	0.05	3.87	3.51	1.08	56.53	1.54	94.03
50	9.43	0.25	23.57	0.05	5.82	3.96	1.38	48.46	1.38	94.31

Nine Element Microprobe Traverse #2 of Sample OG3
Analyses calculated as weight percent oxide.

step	Fe	Ca	Al	Mn	K	Mg	Ti	Si	Na	Total
1	1.50	2.48	6.78	0.00	0.35	0.76	0.07	80.13	3.34	95.39
2	3.23	5.37	10.13	0.14	0.67	1.62	0.00	66.43	4.58	92.16
3	8.96	15.68	0.11	0.82	0.04	4.96	0.00	46.61	0.00	77.18
4	5.92	6.11	10.24	0.25	0.36	2.67	0.00	55.84	4.61	86.01
5	1.11	0.21	13.25	0.00	0.17	0.28	0.15	71.60	7.22	93.99
6	4.19	0.26	15.66	0.00	1.75	1.29	0.25	67.24	4.20	94.84
7	3.13	0.34	29.02	0.00	8.82	1.52	3.45	40.89	0.56	87.73
8	5.32	0.31	28.80	0.00	8.38	1.95	3.57	39.91	0.46	88.70
9	4.47	0.29	28.90	0.00	8.41	1.77	2.91	39.82	0.32	86.89
10	4.05	0.34	28.43	0.00	8.53	1.72	0.64	41.27	0.89	85.87
11	4.04	0.31	29.00	0.00	8.79	1.70	1.38	40.21	0.33	85.75
12	4.35	0.25	29.31	0.00	8.86	1.92	0.79	40.29	0.26	86.04
13	5.75	0.30	27.89	0.00	8.00	2.25	1.98	39.29	0.28	85.74
14	4.43	0.28	27.02	0.00	8.04	1.93	1.33	40.16	0.69	83.89
15	5.61	0.24	18.29	0.00	2.27	1.82	0.04	56.94	5.89	91.10
16	9.42	1.81	24.18	0.00	6.07	3.27	0.38	38.05	0.40	83.59
17	5.60	0.28	21.45	0.00	4.45	2.29	0.15	42.44	2.79	79.44
18	0.35	0.02	1.54	0.00	0.23	0.22	0.02	3.81	0.64	91.14
19	4.20	0.27	11.44	0.00	1.59	1.34	0.01	67.93	3.08	89.86
20	2.96	0.25	15.10	0.00	0.32	0.91	0.64	64.95	7.58	92.71
21	3.78	3.45	10.84	0.00	0.95	1.46	0.01	67.31	3.29	91.09
22	2.99	0.35	12.36	0.00	1.70	0.96	0.29	70.39	3.50	92.55
23	4.29	0.30	24.38	0.00	6.00	1.83	1.18	48.43	2.18	88.59
24	11.84	2.50	22.01	0.14	4.52	4.31	0.97	35.23	0.23	81.75
25	7.71	0.30	25.57	0.00	4.98	2.73	0.69	44.51	2.58	89.07
26	6.31	0.32	22.65	0.00	4.89	2.15	0.58	50.26	2.51	89.67
27	5.39	0.27	24.78	0.00	6.63	2.11	0.97	45.82	0.93	86.89
28	6.88	0.29	24.23	0.00	5.86	2.37	1.14	39.80	1.37	81.95
29	3.50	0.29	8.54	0.00	1.10	1.05	0.00	71.57	2.11	88.15
30	2.16	1.43	7.77	0.00	1.93	0.92	1.23	76.86	0.19	92.50
31	3.55	0.34	23.76	0.00	6.78	1.54	5.25	43.61	0.90	85.73
32	6.16	2.83	5.06	0.06	0.59	2.21	0.05	69.31	0.18	86.46
33	3.13	0.28	6.57	0.00	0.93	1.04	0.00	80.71	1.08	93.72
34	6.55	0.32	22.33	0.00	5.52	2.44	1.20	45.58	1.93	85.86
35	4.17	0.31	14.80	0.00	3.07	1.40	1.24	59.71	2.44	87.14
36	5.68	0.32	19.51	0.00	3.93	1.84	0.22	51.23	2.99	85.71
37	1.76	0.37	9.66	0.00	0.17	0.63	0.00	77.11	5.09	94.80
38	2.72	0.28	22.04	0.00	4.93	1.31	1.46	51.47	3.58	87.79
39	4.80	0.30	19.64	0.00	4.29	1.82	0.95	53.86	2.54	88.19
40	3.20	0.66	11.23	0.00	1.68	1.12	0.59	69.57	2.90	90.95
41	4.79	6.00	14.98	0.15	0.96	2.70	0.00	43.80	6.96	80.34
42	11.56	19.14	1.85	0.82	0.14	7.02	0.00	21.02	1.17	62.72
43	9.80	17.24	3.92	0.69	0.07	6.20	0.00	27.71	3.07	68.72
44	11.45	19.94	4.08	0.91	0.03	7.35	0.00	15.27	3.29	62.32
45	2.83	4.77	14.02	0.15	0.02	1.45	0.00	53.13	8.67	85.04
46	4.13	3.96	15.54	0.09	1.04	1.97	0.00	52.23	7.86	86.84
47	2.67	1.12	21.20	0.00	5.19	1.23	2.19	50.86	3.79	88.24

48	6.88	9.96	2.98	0.43	0.22	3.58	0.70	51.27	1.11	77.15
49	3.85	2.64	11.92	0.00	0.71	1.81	0.06	59.97	5.34	86.31
50	2.47	0.28	11.61	0.00	2.07	0.83	0.18	68.82	3.14	89.39
51	3.23	2.48	2.31	0.00	0.30	1.29	0.00	79.94	0.28	89.94
52	9.68	17.21	4.28	0.71	0.04	5.91	0.09	29.01	2.85	69.76
53	6.01	8.27	10.06	0.39	0.73	3.25	1.32	45.33	4.09	79.45
54	1.43	0.19	4.96	0.00	0.38	0.48	0.05	81.39	2.09	90.96
55	1.02	0.27	11.42	0.00	1.09	0.41	0.23	72.71	4.53	91.68
56	2.86	0.38	14.76	0.00	2.17	0.92	1.16	63.54	5.07	90.87
57	4.86	0.35	14.18	0.00	3.14	1.60	0.11	62.98	1.34	88.55
58	12.62	15.40	8.68	0.68	1.55	6.56	0.07	21.80	0.54	67.91
59	13.92	23.52	0.11	1.09	0.05	9.42	0.01	3.73	0.00	51.84
60	2.27	1.79	15.31	0.05	1.17	0.92	0.36	58.21	8.02	88.10
61	5.12	4.02	12.77	0.07	2.61	2.11	0.09	55.51	3.15	85.46
62	13.57	21.15	2.96	0.90	0.60	8.71	0.61	6.66	0.12	55.12
63	3.38	0.30	8.08	0.00	0.45	1.02	0.19	75.71	3.24	92.37
64	3.24	0.33	16.61	0.00	1.39	1.17	0.09	61.87	6.26	90.95
65	5.57	0.32	7.35	0.00	1.42	1.82	0.21	69.88	0.52	87.08
66	5.19	0.30	14.95	0.00	2.08	1.60	0.18	59.00	3.80	87.10
67	6.39	0.30	24.42	0.00	5.49	2.35	0.00	46.05	2.25	87.25
68	3.95	0.32	10.57	0.00	2.75	1.28	0.52	70.23	0.28	89.89
69	4.98	0.26	17.09	0.00	3.39	1.82	0.28	58.34	2.33	88.51
70	6.61	0.26	25.75	0.00	6.82	2.42	0.14	35.52	0.27	77.79
71	4.36	0.29	15.43	0.00	4.21	1.60	0.19	60.59	0.26	86.92
72	2.51	0.33	23.90	0.00	4.90	1.16	1.43	50.29	4.18	88.70
73	4.48	0.32	20.38	0.00	5.00	1.61	1.00	56.02	1.84	90.66
74	1.64	0.33	16.14	0.00	2.05	0.61	0.05	64.64	6.35	91.81
75	1.56	1.39	26.33	0.00	7.68	1.13	0.68	47.71	1.34	87.84
76	3.84	0.34	22.19	0.00	5.07	1.38	0.19	52.38	3.52	88.91
77	2.74	0.32	27.70	0.00	8.84	1.46	0.82	41.98	0.54	84.40
78	0.93	0.58	5.84	0.00	0.70	0.42	0.07	80.55	2.81	91.90
79	1.64	0.44	4.30	0.00	0.45	0.48	0.00	84.79	1.33	93.42
80	1.68	0.38	8.81	0.00	1.24	0.53	0.06	77.44	2.99	93.13
81	3.88	0.28	18.17	0.00	3.54	1.27	2.29	55.11	4.38	88.91
82	2.71	0.34	16.58	0.00	1.72	0.95	1.05	60.72	7.16	91.24
83	6.24	0.80	21.35	0.00	3.68	2.37	0.17	46.73	4.28	85.62
84	4.96	1.05	17.74	0.00	3.65	1.86	1.13	55.34	2.68	88.41
85	2.96	0.27	10.84	0.00	0.17	0.84	0.42	69.57	6.32	91.40
86	3.48	2.38	10.68	0.00	1.85	1.64	0.07	62.97	2.59	85.66
87	2.35	0.30	10.63	0.00	0.89	0.76	0.12	71.44	4.82	91.32
88	7.92	0.34	11.69	0.00	0.30	2.63	0.01	59.48	4.34	86.73
89	5.56	8.48	5.64	0.29	0.59	2.62	0.39	54.70	3.72	81.98
90	8.41	13.02	3.62	0.63	0.52	4.31	0.26	43.57	0.73	75.07
91	4.95	0.27	21.40	0.00	5.12	1.84	4.88	46.74	2.34	87.54
92	7.39	0.30	23.07	0.00	5.97	2.78	0.43	40.63	0.76	81.33

Six Element Microprobe Traverse of Sample OG3
Analyses calculated in weight percent oxide.

step	Ti	K	Mg	Fe	Si	Al	Total
1	1.04	5.5	2.16	6.27	60.36	24.36	99.7
2	0.84	5.98	2.38	6.55	57.7	25.31	98.77
3	1.14	6.41	2.57	7.25	55.97	26.16	99.51
4	1.1	6.49	2.6	7.86	55.08	26.95	100.14
5	0.86	6.83	2.81	9.25	52.88	27.59	100.22
6	1.24	6.75	2.78	9.09	53.2	27.36	100.42
7	0.94	6.49	2.73	9.66	54.46	26.69	100.97
8	0.98	6.39	2.87	8.93	54.37	26.73	100.28
9	0.71	6.33	2.83	8.06	55.04	26.13	99.11
10	0.93	5.96	2.73	9.13	55.2	25.91	99.86
11	0.58	5.78	2.81	9.34	56.33	25.18	100.01
12	0.57	5.44	2.55	8.89	55.92	24.44	97.82
13	0.37	5.26	2.75	9.18	56.58	23.87	98
14	0.47	4.94	2.69	8.89	57.39	23.54	97.91
15	0.32	4.7	2.68	9.52	58.23	22.9	98.35
16	0.49	4.15	2.57	8.93	59.64	21.85	97.63
17	0.53	3.68	2.4	8.49	61.25	21.29	97.64
18	0.43	3.13	2.35	8.23	65.02	19.85	99
19	0.3	2.58	2.36	9	69.07	17.84	101.14
20	0.37	2.41	2.13	7.17	70.4	16.81	99.29
21	0.37	1.81	2.23	8.3	72.61	15.48	100.8
22	0.18	1.55	2.19	8.21	73.69	14.4	100.22
23	0.21	1.54	2.09	7.42	72.49	13.99	97.74
24	0.41	1.14	2.09	7.28	72.69	13.64	97.24
25	0.52	1.11	2.13	8	73.7	13.29	98.75
26	0.35	1.11	2.13	7.11	75.78	12.02	98.49
27	0.53	1.03	2.13	7.59	75.7	12.32	99.3
28	0.44	1.26	2.07	7.87	75.52	12.45	99.62
29	0.39	1.02	2.04	7.13	75.82	11.9	98.3
30	0.32	1.14	1.92	6.9	74.63	12.04	96.95
31	0.35	1.2	2.03	8.07	75.09	12.04	98.77
32	0.45	1.34	1.98	6.51	74.87	12.94	98.08
33	0.41	1.76	1.99	7.26	74.2	14.12	99.74
34	0.57	2.46	2.19	7.59	72.81	15.71	101.33
35	0.58	3.22	2.18	7.55	68.39	17.59	99.51
36	0.91	3.96	2.3	8.1	64.56	19.78	99.61
37	0.64	4.67	2.4	8.15	60.96	21.14	97.96
38	0.91	5.61	2.63	7.87	57.78	23.14	97.94
39	0.84	5.75	2.59	9.51	56.59	24.3	99.57
40	1.01	5.41	2.82	9.31	55.67	24.51	98.74
41	0.78	5.68	2.87	10.01	55.14	24.96	99.44
42	0.66	5.82	2.88	10.38	54.63	25.83	100.18
43	0.57	5.82	2.83	9.39	54.95	26.07	99.63
44	0.75	6.04	2.73	9.75	54.22	26.28	99.76
45	0.74	6.46	2.68	9.26	53.22	26.74	99.09
46	0.79	6.76	2.75	9.68	52.71	27.61	100.3
47	0.92	7.03	2.7	8.3	52.64	28.49	100.08
48	0.81	7.36	2.79	8.6	50.73	29.23	99.52
49	1.36	8.07	2.77	8.34	49.26	29.89	99.68
50	1.56	8.45	2.76	8.58	47.73	31.38	100.46

51	1.59	8.13	2.61	7.83	47.7	30.73	98.59
52	1.58	7.51	2.57	7.89	51.08	28.81	99.44
53	1.42	6.81	2.47	7.87	53	26.76	98.32
54	1.16	5.87	2.6	8.37	55.17	24.29	97.46
55	1.3	4.82	2.43	8.41	58.54	21.94	97.45
56	1.17	4.06	2.42	8.08	60.84	20.39	96.97
57	0.81	3.29	2.38	8.26	64.56	18.09	97.39
58	0.61	2.61	2.28	7.54	68.84	15.48	97.35
59	0.39	1.99	2.16	6.97	71.37	14.15	97.04
60	0.21	1.49	2.17	7.69	73.21	12.93	97.7
61	0.37	1.53	1.93	8.13	73.67	12.53	98.16
62	0.32	1.61	1.93	7.12	75.69	12.65	99.31
63	0.53	1.79	1.93	7.16	76.32	12.72	100.46
64	0.36	1.98	1.86	7.89	76.3	13.68	102.07
65	0.47	2.15	1.86	6.96	74.3	14.91	100.66
66	0.73	2.58	1.73	5.92	73.41	15.1	99.46
67	0.59	3.29	1.71	5.05	70.3	16.68	97.62
68	1.05	3.79	1.74	6.07	69.04	18.96	100.65
69	1.18	4.54	1.86	5.91	64.79	20.47	98.75
70	1.94	5.07	2.05	6.73	62.2	21.95	99.95
71	1.54	5.01	2.37	6.12	59.45	21.97	96.45
72	1.5	4.68	2.31	5.92	59.68	20.41	94.5
73	1.1	3.92	2.7	7.51	58.67	19.74	93.65
74	1.52	3.48	2.89	8.09	58.57	18.34	92.89
75	0.71	2.6	2.84	7.68	60.21	16.08	90.12
76	0.53	1.83	2.92	8.39	60.56	15.27	89.5
77	0.37	1.16	3.06	8.92	62.29	13.65	89.45
78	0.14	0.75	3.05	8.08	62.77	12	86.79
79	0.44	1.05	3	8.21	66.06	11.39	90.16
80	0.48	1.39	2.83	8.02	65.81	11.44	89.97
81	0.73	1.91	2.32	6.96	66.88	12.77	91.56
82	0.51	2.09	2.2	6.87	66.44	14.22	92.32
83	0.51	2.27	2.03	6.55	65.95	15.26	92.57
84	0.36	2.39	1.94	4.92	65.43	16.355	91.39
85	0.51	2.23	1.75	5.38	66.95	16.72	93.54
86	0.36	2.2	1.69	4.99	68.14	17.3	94.67
87	0.2	1.95	1.58	4.73	71.6	17.21	97.26
88	0.29	1.86	1.5	4.83	72.21	16.61	97.3
89	0	1.74	1.66	5.29	71.38	16.53	96.6
90	0.14	1.65	1.83	6.28	72.1	16.53	98.52
91	0.26	2.03	2.27	6.97	69.28	16.86	97.67
92	0.58	2.09	2.36	7.08	67.59	16.88	96.58
93	0.29	2.2	2.33	7.38	67.94	16.44	96.58
94	0.32	2.45	2.23	6.61	68.02	16.59	96.23
95	0.26	2.54	2.37	6.63	66.42	17.49	95.71
96	0.43	2.93	2.4	6.94	63.08	17.91	93.69
97	0.28	3.22	2.5	7.82	61.25	19.14	94.22
98	0.53	3.2	2.45	7.41	61.45	19	94.03
99	0.54	3.27	2.55	8	61.62	18.95	94.93
100	0.51	3.07	2.23	8.02	64.13	19.45	97.41
101	0.61	3.1	1.91	6.58	66.48	19.4	98.07
102	0.74	3.15	2	6.11	66.02	18.88	96.89
103	0.23	2.77	2.12	6.7	65.42	17.93	95.17
104	0.25	2.46	2.16	6.03	65.52	16.98	93.4

105	0.34	2.33	2.31	6.04	64.13	15.94	91.08
106	0.51	2.12	2.73	7.19	62.37	14.96	89.87
107	0.26	1.72	3.36	7.1	58.84	13.35	84.63
108	0.66	1.45	3.82	7.76	54.71	11.83	80.23
109	0.75	1.12	4.25	9.18	52.09	10.9	78.29
110	0.55	0.89	4.28	9.78	50.84	10.07	76.41
111	0.62	0.96	4.1	8.98	50.97	9.97	75.61
112	0.68	1.27	3.89	9.47	52.29	11.16	78.75
113	0.8	1.52	3.61	9.65	53.17	11.64	80.39
114	0.75	1.84	3.57	8.66	55.66	12.58	83.07
115	0.88	2.22	3.47	9.18	57.13	14.05	86.92
116	0.65	2.47	2.79	7.5	61.27	14.93	89.6
117	0.93	2.82	2.33	7.33	65.28	16.71	95.4
118	0.51	2.83	2.11	6.43	66.88	17.24	96
119	0.47	2.77	1.98	6.3	67.54	17.59	96.65
120	0.51	2.92	2.01	6.76	67.4	17.39	96.99
121	0.39	2.69	2.06	6.69	67.97	17.1	96.91
122	0.67	2.69	2.09	6.47	69.54	17.11	98.56
123	0.58	2.75	2	7.64	71.03	16.66	100.66
124	0.6	2.34	1.98	7.06	71.08	15.93	99
125	0.51	2.66	2.1	6.87	71.96	15.61	99.71
126	0.57	2.61	2.31	7.6	70.11	15.63	98.82
127	0.68	2.6	2.64	7.63	67.76	15.79	97.1
128	0.59	2.3	2.63	8.38	64.87	15.05	93.82
129	0.49	2.18	2.9	8.34	62.59	15.13	91.63
130	0.45	2.09	2.92	9.33	60.86	15.05	90.7
131	0.39	2.19	3.08	9.85	60.87	15.45	91.84
132	0.47	2.21	3.24	9.81	61.12	15.86	92.7

Three Element Probe Traverse of WC26B
Analyses calculated as weight percent oxide.

	Ti	K	Mg	Total
1.00	0.98	5.21	4.13	10.32
2.00	0.73	4.76	4.50	10.00
3.00	1.12	4.77	4.41	10.30
4.00	1.40	4.42	3.91	9.73
5.00	1.20	4.34	3.76	9.29
6.00	1.13	4.51	3.91	9.55
7.00	1.18	5.16	4.05	10.39
8.00	1.43	5.04	3.80	10.26
9.00	1.18	5.39	3.71	10.28
10.00	1.51	5.16	3.75	10.42
11.00	1.82	5.20	4.24	11.26
12.00	2.10	5.67	4.30	12.07
13.00	1.78	5.82	4.25	11.85
14.00	1.54	5.78	3.93	11.25
15.00	1.44	5.60	3.55	10.60
16.00	0.92	4.68	2.88	8.48
17.00	0.25	2.78	2.51	5.54
18.00	0.12	1.97	2.32	4.42
19.00	0.21	1.91	2.90	5.01
20.00	0.20	2.17	3.09	5.46
21.00	0.23	2.04	2.64	4.91
22.00	0.11	1.70	1.99	3.80
23.00	0.14	1.27	1.91	3.31
24.00	0.27	1.32	2.05	3.64
25.00	0.35	1.57	2.11	4.02
26.00	0.32	1.74	2.25	4.30
27.00	0.33	1.84	2.41	4.59
28.00	0.29	1.82	2.12	4.23
29.00	0.22	2.77	2.54	5.54
30.00	0.55	4.03	3.29	7.88
31.00	0.43	4.29	3.73	8.45
32.00	0.72	4.90	3.74	9.36
33.00	0.64	5.36	3.87	9.86
34.00	0.76	4.65	3.74	9.15
35.00	0.58	3.98	3.04	7.59
36.00	0.35	3.41	2.69	6.44
37.00	0.15	2.79	2.12	5.05
38.00	0.72	1.89	2.20	4.81
39.00	0.14	1.89	2.40	4.43
40.00	0.34	1.64	2.23	4.20
41.00	0.16	1.97	2.19	4.32
42.00	0.15	1.59	2.41	4.16
43.00	0.26	2.31	2.69	5.26
44.00	0.63	3.02	2.89	6.54
45.00	0.93	3.56	3.40	7.89
46.00	0.84	3.55	3.24	7.64
47.00	1.08	3.84	3.32	8.24
48.00	1.47	3.54	3.24	8.25
49.00	1.58	3.34	3.19	8.11

50.00	1.41	3.16	3.05	7.62
51.00	1.01	3.69	3.03	7.73
52.00	1.21	4.36	3.46	9.04
53.00	1.26	4.09	3.99	9.35
54.00	1.46	4.12	4.13	9.71
55.00	1.47	4.20	4.29	9.96
56.00	1.38	4.13	3.95	9.45
57.00	1.40	3.94	3.77	9.11
58.00	1.39	3.75	3.63	8.77
59.00	1.23	3.93	4.28	9.44
60.00	0.71	4.17	3.95	8.82
61.00	0.85	4.72	4.19	9.76
62.00	1.26	4.51	3.99	9.76
63.00	1.32	4.08	3.69	9.09
64.00	0.83	3.92	3.22	7.97
65.00	1.48	4.13	3.64	9.26
66.00	1.59	4.05	3.61	9.25
67.00	1.32	3.77	3.32	8.40
68.00	1.07	3.11	2.80	6.98
69.00	1.19	4.11	3.13	8.42
70.00	1.51	4.70	3.33	9.54
71.00	1.13	5.04	3.60	9.77
72.00	1.03	4.99	3.53	9.55
73.00	1.00	4.66	3.19	8.86
74.00	0.79	4.32	3.15	8.26
75.00	0.80	4.71	3.36	8.88
76.00	1.11	4.89	3.78	9.78
77.00	1.31	5.73	4.23	11.27
78.00	1.46	5.76	4.21	11.43
79.00	1.54	5.52	4.21	11.28
80.00	1.12	5.47	4.37	10.95
81.00	1.38	5.39	4.54	11.30
82.00	1.21	5.50	4.45	11.16
83.00	1.24	5.70	4.22	11.16
84.00	1.36	5.68	4.05	11.09
85.00	1.69	5.24	4.58	11.52
86.00	1.12	5.34	4.07	10.54
87.00	1.20	5.07	3.65	9.93
88.00	0.81	5.24	3.59	9.64
89.00	0.95	5.75	3.53	10.23
90.00	1.59	6.13	3.85	11.57
91.00	1.54	6.29	3.74	11.57
92.00	0.98	5.71	3.66	10.36
93.00	1.07	4.95	3.39	9.41
94.00	0.72	4.93	3.18	8.83
95.00	0.77	4.89	3.07	8.73
96.00	0.82	4.65	3.02	8.49
97.00	0.55	3.88	3.24	7.68
98.00	0.61	3.50	3.41	7.51
99.00	0.59	3.46	3.00	7.04
100.00	0.49	3.18	3.04	6.71
101.00	0.34	2.78	2.62	5.74

102.00	0.58	3.96	2.75	7.29
103.00	0.78	4.58	3.18	8.54
104.00	0.89	5.07	3.88	9.85
105.00	0.97	4.53	4.34	9.84
106.00	0.72	3.92	4.46	9.10
107.00	0.81	3.58	4.53	8.92

Three Element Traverse #1 of WC26A
Analyses calculated as weight percent oxide.

step	Ti	K	Mg	Total
1	0.05	0.73	1.39	2.16
2	0.02	1.16	1.69	2.88
3	0.19	2.09	2.	

Three Element Traverse #1 of WC26A
Analyses calculated as weight percent oxide.

step	Ti	K	Mg	Total
1	0.05	0.73	1.39	2.16
2	0.02	1.16	1.69	2.88
3	0.19	2.09	2.17	4.45
4	0.27	3.43	2.87	6.56
5	1.03	4.06	3.26	8.35
6	1.22	3.52	2.79	7.54
7	0.81	2.66	2.27	5.75
8	0.31	2.21	2.32	4.85
9	0.2	1.86	2.14	4.2
10	0.21	1.55	1.97	3.73
11	0.27	1.8	1.93	4
12	0.31	2.09	1.96	4.36
13	0.06	1.55	1.8	3.41
14	0	1.24	1.87	3.12
15	0.15	1.22	1.86	3.24
16	0.19	1.25	2.05	3.49
17	0.36	1.6	2.14	4.1
18	0.3	1.3	2.18	3.78
19	0.21	1.3	2.14	3.65
20	0.32	1.76	2.09	4.17
21	0.38	2.49	2.27	5.14
22	0.34	3.59	2.19	6.11
23	0.25	3.44	2.97	6.66
24	0.33	3.33	2.84	6.5
25	0.19	2.66	1.98	4.77
26	0.04	1.72	1.43	3.2
27	0.272	4.909	7.818	3.09
28	0.01	1.57	1.93	3.51
29	0.1	1.58	2.32	4
30	0.11	1.34	2.48	3.93
31	0.08	0.55	2.1	2.73
32	0.09	0.43	1.78	2.3
33	0.17	1.09	1.75	3.01
34	0.8	2.33	2.18	5.31
35	0.82	2.13	2.35	5.3
36	0.66	2.17	2.24	5.07
37	0.76	3.05	2.35	6.16
38	0.77	3.59	2.87	7.23
39	0.95	4.16	3.23	8.33
40	0.8	3.55	3.06	7.41
41	0.41	2.9	2.42	5.73
42	0.41	2.13	2.38	4.92
43	0.28	2.09	2.29	4.66
44	0.5	1.99	2.11	4.6
45	0.42	1.22	1.94	3.58
46	0.63	2.29	2.35	5.27
47	1.05	3.88	2.62	7.54
48	0.89	4.46	2.74	8.09
49	0.5	2.44	2.12	5.06

50	0.16	1.28	1.54	2.98
51	0.06	0.72	1.39	2.18
52	0.18	0.51	1.61	2.3
53	1.32	1.21	2.25	4.77
54	0.95	1.51	1.78	4.23
55	0.28	1.4	1.79	3.47
56	0.05	0.79	1.34	2.18
57	0	0.58	1.14	1.72
58	0.17	0.04	0.83	1.04
59	0	0.1	0.53	0.63
60	0.08	2.24	1.14	3.46
61	0.24	2.79	1.4	4.43
62	0	1.86	1.48	3.34
63	0	0.98	1.57	2.56
64	0	0.72	1.68	2.41
65	0	0.54	1.13	1.67
66	0	1.1	1.26	2.36
67	0.58	1.92	1.31	3.8
68	0.87	1.71	1.65	4.22
69	0	0.7	1.17	1.88
70	0	0.53	1.5	2.03
71	0	0.8	1.74	2.54
72	0.04	0.9	1.64	2.58
73	0.33	1.11	1.66	3.09
74	0.38	1.6	1.46	3.43
75	0.3	1.91	1.95	4.15
76	0.1	2.16	2.449	4.75
77	0	3.03	2.36	5.39
78	0.02	3.99	2.16	6.17
79	0.16	4.22	2.05	6.43
80	0.28	4.36	2.54	7.17
81	0.24	4.45	2.64	7.33
82	2	4.62	2.89	9.51
83	2.69	5.14	2.78	10.61
84	0.68	4.42	2.7	7.79
85	0.38	3.32	2.2	5.89
86	0.73	2.47	1.94	5.14
87	0.82	2.83	2.11	5.76
88	0.58	3.88	2.46	6.92
89	0.82	4.62	3	8.44
90	0.8	4.88	3.55	9.23
91	0.59	5.19	3.8	9.58
92	0.8	5.28	3.63	9.71
93	1.24	5.77	3.5	10.51
94	1.49	6.75	3.35	11.59
95	1.57	7.53	3.46	12.57
96	1.64	7.83	3.34	12.82
97	1.5	7.66	3.65	12.81
98	1.19	6.48	3.84	11.51
99	1.13	6.21	4.04	11.38
100	0.96	5.59	3.91	10.46
101	0.91	4.93	3.66	9.5

102	1.09	4.02	3.62	8.72
103	0.79	3.49	3.54	7.83
104	0.72	2.97	3.59	7.28
105	0.75	2.86	3.83	7.45
106	0.91	3.1	4.03	8.04
107	0.98	3.77	4	8.75
108	1.13	4.21	4.16	9.5
109	1.31	4.59	4.3	10.2
110	1.36	5.01	4.38	10.75
111	1.65	5.43	4.32	11.39
112	1.19	6.02	4.35	11.55
113	1.12	5.02	4.14	10.27
114	1.14	5.63	4.48	11.25
115	1.04	5.7	4.67	11.41
116	0.9	6.2	4.32	11.43
117	1.11	5.96	4.31	11.38
118	1.26	6.17	4.09	11.52
119	1.71	5.98	4.29	11.97
120	1.56	6.13	4.02	11.71
121	1.39	5.4	4	10.79
122	1.3	4.69	3.84	9.82
123	1.07	4.23	3.59	8.9
124	1	3.18	3.3	7.48
125	0.86	2.89	2.97	6.72
126	0.71	2.77	3.15	6.63
127	0.73	2.87	3.28	6.88
128	0.71	2.71	3.18	6.6
129	0.54	2.4	3.03	5.97
130	0.45	2.39	3.05	5.89
131	0.6	2.36	2.74	5.7
132	0.64	3.01	2.78	6.43
133	0.93	3.31	3.11	7.35
134	0.68	3.98	3.54	8.2
135	0.67	5.19	3.81	9.67
136	0.61	5.81	4.21	10.63
137	0.88	6.2	4.45	11.53
138	1.23	7	4.13	12.36
139	1.34	7.16	3.92	12.43
140	1.27	6.89	3.89	12.04
141	1.49	6.65	3.82	11.96
142	1.47	6.81	3.77	12.05
143	1.64	6.55	3.84	12.03
144	1.11	6.2	3.82	11.13

Three Element Traverse #2 of WC26A
Analyses calculated as weight percent oxid

Step	Ti	K	Mg	Total
1	0.41	1.63	1.34	3.38
2	0.38	1.66	1.51	3.55
3	0.5	2.17	1.91	4.59
4	0.27	2.01	2.09	4.36
5	0.03	0.95	1.44	2.43
6	0.16	1.26	1.36	2.79
7	0.17	1.71	1.37	3.25
8	0.46	3.38	1.77	5.61
9	0.48	4.7	1.08	7.05
10	0.43	6.12	2.54	9.09
11	0.39	5.8	2.71	8.91
12	1.41	3.68	2.79	7.89
13	2.99	3.82	2.8	9.61
14	4.8	3.53	2.88	11.21
15	5.41	2.89	2.34	10.64
16	2.45	2.55	2.16	7.16
17	0.75	3.7	2.25	6.69
18	0.36	4.48	2.46	7.3
19	0.77	4.66	2.86	8.28
20	0.93	4.66	3.2	8.8
21	1.42	5.04	3.96	10.42
22	0.98	6.82	3.86	11.66
23	1.25	7.45	3.36	12.05
24	2.34	7.46	3.4	13.21
25	2.12	7.63	3.47	13.22
26	2.02	7.5	3.78	13.3
27	1.49	7.32	3.73	12.54
28	1.25	6.56	4	11.8
29	1.27	6.14	3.94	11.36
30	1.18	4.97	3.77	9.93
31	0.97	4.52	3.45	8.93
32	0.79	3.77	3.77	8.34
33	0.8	3.14	3.46	7.42
34	0.63	3.18	3.63	7.44
35	1	3.61	3.93	8.55
36	0.98	4.02	4.15	9.14
37	1.29	4.36	4.23	9.87
38	1.21	5.28	4.25	10.73
39	1.36	6.13	4.18	11.67
40	1.5	6.23	4.27	12.01
41	1.47	6.2	4.19	11.86
42	1.22	6.21	4.22	11.65
43	1.8	6.29	3.92	12.01
44	2.4	6.48	4.07	12.95
45	2.6	6.52	3.95	13.06
46	2.54	6.41	4.12	13.06
47	1.54	6.43	4.02	11.99
48	1.94	5.84	4.04	11.82
49	1.668	5.56	4.04	11.28

50	0.8	4.59	3.52	8.91
51	0.74	3.64	3.34	7.71
52	0.84	3.59	3.7	8.13
53	0.75	3.11	3.32	7.18
54	0.71	2.88	3.19	6.78
55	0.67	3.06	2.88	6.61
56	0.59	2.9	2.94	6.43
57	0.79	2.44	2.69	5.92
58	0.69	2.02	2.54	5.24
59	0.52	2.41	2.52	5.45
60	0.73	3.7	2.88	7.3
61	0.7	4.91	3.22	8.83
62	0.75	5.79	3.16	9.7
63	1.66	7.2	3.38	12.24
64	2.11	8.2	3.29	13.59
65	1.7	8.11	3.22	13.03
66	1.52	8.15	3.12	12.79
67	1.04	6.72	2.88	10.64
68	1.06	3.95	2.43	7.44
69	0.85	1.65	1.93	4.43
70	1.22	0.38	1.42	3.02
71	0.54	0.5	1.19	2.23
72	0	0.51	0.93	1.44
73	0.34	0.84	1.04	2.22
74	0.39	1.29	1.13	2.8
75	0	1.76	1.36	3.12
76	0.06	1.38	1.24	2.69
77	0.07	1.12	1.03	2.22
78	0	0.41	0.86	1.27
79	0.07	0.32	0.92	1.31
80	0.06	0.11	0.89	1.06
81	0	0.14	0.93	1.07
82	0.13	0.8	1.16	2.09
83	0.23	0.43	0.83	1.49
84	0.14	0.23	0.8	1.18
85	0.15	0.06	0.64	0.85

Three Element Traverse of OG17
Analyses calculated as weight percent oxide.

Step	Ti	K	Mg	Total
1.00	0.06	0.21	0.56	0.83
2.00	0.08	0.11	0.60	0.79
3.00	0.06	0.54	0.81	1.41
4.00	0.43	1.34	2.09	3.87
5.00	0.52	1.74	2.29	4.55
6.00	0.85	3.54	3.12	7.50
7.00	1.22	4.35	3.56	9.13
8.00	0.81	2.82	2.98	6.61
9.00	2.59	2.22	3.15	7.96
10.00	0.23	1.71	2.66	4.60
11.00	0.54	2.03	2.79	5.35
12.00	0.88	3.97	4.90	9.75
13.00	1.37	5.51	3.61	10.49
14.00	0.74	3.00	2.67	6.41
15.00	0.66	5.82	4.31	10.80
16.00	1.26	7.51	2.97	11.74
17.00	1.42	7.29	3.69	12.39
18.00	1.71	5.68	2.79	10.19
19.00	1.70	5.11	2.98	9.78
20.00	0.69	6.07	2.75	9.51
21.00	0.73	5.94	2.93	9.60
22.00	1.35	8.29	3.23	12.88
23.00	4.11	8.40	3.36	15.87
24.00	2.85	5.55	2.63	11.03
25.00	1.94	6.21	2.52	10.68
26.00	0.72	5.76	3.30	9.78
27.00	0.63	6.15	3.56	10.34
28.00	1.50	7.16	3.93	12.59
29.00	1.19	5.97	3.68	10.84
30.00	1.05	6.03	2.98	10.06
31.00	0.16	3.43	2.05	5.64
32.00	0.00	2.71	1.58	4.29
33.00	0.13	3.94	4.01	8.08
34.00	0.22	2.74	2.21	5.18
35.00	0.66	3.89	3.47	8.03
36.00	0.16	3.84	3.65	7.65
37.00	0.89	5.46	3.33	9.68
38.00	1.32	5.30	3.16	9.77
39.00	0.97	5.34	3.82	10.13
40.00	1.48	4.53	3.14	9.15
41.00	0.30	2.81	3.10	6.21
42.00	0.51	2.77	4.31	7.59
43.00	0.39	4.02	3.35	7.76
44.00	7.97	3.68	3.73	15.38
45.00	2.59	5.38	3.90	11.87
46.00	1.30	3.70	4.15	9.16
47.00	1.41	3.66	3.76	8.83
48.00	0.97	2.73	2.55	6.25
49.00	0.54	2.96	2.27	5.77

50.00	0.77	3.66	1.89	6.32
51.00	1.32	5.07	3.05	9.44
52.00	2.18	3.91	3.10	9.19
53.00	1.45	4.82	2.80	9.08
54.00	1.13	4.51	2.97	8.61
55.00	1.06	4.77	3.85	9.68
56.00	0.81	4.08	2.94	7.83
57.00	0.51	3.38	3.07	6.96
58.00	0.96	3.95	3.54	8.45
59.00	0.91	4.21	4.19	9.31
60.00	2.86	3.11	3.78	9.75
62.00	3.32	3.99	3.02	10.32
62.00	1.55	4.52	2.89	8.96
63.00	1.07	3.37	2.96	7.39
64.00	0.52	2.98	2.18	5.68
65.00	0.52	3.51	3.25	7.28
66.00	0.32	3.25	2.70	6.27
67.00	0.81	5.35	3.69	9.85
68.00	2.98	5.03	2.98	10.99
69.00	1.01	5.55	4.23	10.79
70.00	1.87	5.16	3.67	10.70
71.00	0.72	4.64	2.24	7.60
72.00	0.99	4.86	3.20	9.05
73.00	0.93	5.67	4.41	11.00
74.00	2.45	6.82	3.92	13.20
75.00	1.59	7.16	3.80	12.55
76.00	1.98	6.36	3.80	12.16
77.00	1.49	6.61	4.07	12.17
78.00	1.18	6.98	3.72	11.88
79.00	1.99	7.05	3.67	12.70
80.00	1.84	7.19	3.72	12.76
81.00	0.49	5.18	2.96	8.64
82.00	0.09	4.10	2.97	7.16
83.00	0.85	4.38	4.44	9.66
84.00	0.91	4.70	3.79	9.39
85.00	0.21	3.68	2.77	6.64
86.00	0.71	4.97	3.87	9.55
87.00	0.29	2.44	3.00	5.73
88.00	0.27	3.06	3.07	6.41
89.00	0.36	5.64	2.44	8.45
90.00	2.17	5.57	3.81	11.55
91.00	0.17	2.89	4.63	7.69
92.00	0.27	4.58	3.78	8.63
93.00	0.16	2.18	2.80	5.14
94.00	0.30	4.08	3.43	7.81
95.00	0.17	1.91	2.88	4.96
96.00	0.20	2.59	3.61	6.41
97.00	0.14	2.75	1.88	4.77
98.00	0.20	3.75	3.29	7.24
99.00	0.33	5.14	3.03	8.50
100.00	1.07	4.38	3.18	8.65

Representative Probe Analyses of Dolomite
from Sandsuck Formation Phyllites and Siltstones

Weight percent:					Formula units:				
Ca	Mg	Fe	Mn	Total	Ca	Mg	Fe	Mn	Total
26.93	12.03	11.45	1.15	52.03	0.99	0.62	0.33	0.03	1.99
26.45	12.43	10.88	1.46	51.96	0.97	0.63	0.31	0.04	1.98
27.18	12.33	10.81	1.36	52.72	0.98	0.62	0.30	0.04	1.98
27.51	12.92	11.14	1.63	53.50	0.98	0.64	0.31	0.05	1.99
27.29	12.53	11.13	0.75	52.15	1.00	0.64	0.32	0.02	1.99
26.80	12.34	10.79	1.49	51.43	1.00	0.64	0.31	0.04	2.00
28.33	12.73	11.28	1.54	53.88	1.01	0.63	0.31	0.04	2.00
28.88	12.68	11.70	1.36	54.62	1.02	0.62	0.32	0.04	2.00
28.77	13.01	11.74	1.39	54.91	1.01	0.63	0.32	0.04	2.00
29.25	13.32	11.27	1.79	55.63	1.01	0.64	0.30	0.05	2.00
29.82	13.01	13.02	1.50	57.36	1.00	0.61	0.34	0.04	2.00
27.90	12.38	10.28	1.69	52.25	1.02	0.63	0.29	0.05	2.00
29.62	13.36	12.87	1.63	57.47	1.00	0.62	0.34	0.04	2.00
29.23	13.20	12.19	1.67	56.29	1.00	0.63	0.33	0.05	2.00
30.52	12.51	12.28	1.06	56.36	1.05	0.60	0.33	0.03	2.00
30.34	12.62	12.05	1.87	56.89	1.03	0.60	0.32	0.05	2.00
29.23	12.21	12.77	1.04	55.24	1.03	0.60	0.35	0.03	2.00
28.82	12.86	11.75	1.58	55.01	1.01	0.63	0.32	0.04	2.00
29.47	13.11	13.50	0.86	56.94	1.00	0.62	0.36	0.02	2.00
28.86	12.96	12.80	1.51	56.13	0.99	0.62	0.34	0.04	2.00
28.92	12.57	12.41	1.32	55.22	1.01	0.61	0.34	0.04	2.00
28.87	12.60	11.58	1.73	54.78	1.02	0.62	0.32	0.05	2.00
27.98	12.65	12.73	0.70	54.05	1.00	0.63	0.35	0.02	2.00
28.54	13.73	12.86	1.11	56.24	0.98	0.65	0.34	0.03	2.00
28.79	12.80	12.94	1.41	55.94	1.00	0.62	0.35	0.04	2.00
29.73	13.00	12.22	2.23	57.18	1.01	0.61	0.32	0.06	2.00
30.08	11.97	11.62	1.92	55.59	1.05	0.58	0.32	0.05	2.00
28.95	13.04	13.16	1.59	56.73	0.62	0.99	0.35	0.04	2.00
28.53	12.68	12.62	1.44	55.26	1.00	0.62	0.34	0.04	2.00
29.70	13.12	12.39	1.45	56.66	1.01	0.62	0.33	0.04	2.00
27.45	13.11	13.05	0.64	54.25	0.97	0.65	0.36	0.02	2.00
28.36	12.97	12.26	1.71	55.30	0.99	0.63	0.33	0.05	2.00
27.19	12.20	13.27	1.11	53.77	0.98	0.61	0.37	0.03	2.00
27.84	13.30	12.05	1.09	54.29	0.98	0.65	0.33	0.03	2.00
27.50	13.00	13.10	1.34	54.93	0.97	0.64	0.36	0.04	2.00
29.20	11.90	11.63	1.91	54.64	1.03	0.59	0.32	0.05	2.00

Traverse Normal to Bedding - WC26A
P domain in phyllite and siltstone.

step	Fe	Ca	Al	Mn	K	Mg	Ti	Si	Na	Total
1	6.52	0.25	25.6	0.11	7.41	3.07	0.39	47.4	1.92	92.8
2	4.55	0.27	27.8	0.05	8.55	2.75	0.59	47.8	1.25	93.7
3	8.21	0.23	24.9	0	7.46	3.91	0.18	47.0	0.72	92.7
4	7.82	0.27	26.3	0.09	8.3	3.95	1.15	44.2	0.58	92.6
5	4.82	0.24	28.3	0.08	9.46	2.79	0.22	46.4	0.13	92.5
6	5.54	0.28	27.1	0.12	9.07	2.8	0.44	46.5	0.9	92.8
7	6.25	0.43	26.3	0.04	8.46	3.11	0.71	45.4	1	91.8
8	4.9	0.32	28.1	0.07	9.11	2.84	0.54	48.0	0.12	94.0
9	3.13	3.72	27.3	0	9.25	2.38	1.54	43.0	0.26	90.6
10	4.48	0.32	28.7	0.02	9.4	2.71	2.05	45.1	0.25	93.0
11	3.18	0.24	26.3	0.03	8.86	2.24	1.84	41.0	0.09	83.8
12	2.99	0.24	29.5	0	10.1	2.05	0.76	47.6	0.34	93.6
13	4.29	0.23	24.2	0.01	8.48	2.2	0.41	47.5	0.12	87.5
14	4.2	0.28	25.0	0.07	7.89	2.55	2.33	44.9	0.66	87.9
15	8.21	0.26	27.3	0.09	7.91	4.04	0.5	41.6	0.22	90.1
16	6.7	0.28	28.5	0.09	8.59	3.55	1.24	44.5	0.33	93.7
17	4.98	1.56	26.2	0.04	9.16	2.77	1.34	44.0	0.17	90.3
18	5.38	0.34	28.4	0.1	9.47	3.06	1.18	44.9	0.21	93.1
19	1.36	0.23	17.8	0.01	0.07	0.56	0	68.3	10.3	98.7
20	0.99	0.57	17.0	0	2.15	0.63	0.18	66.3	7.59	95.4
21	1.77	0.25	13.2	0.04	1.46	0.73	1.64	74.5	4.86	98.5
22	5.48	0.21	11.9	0.03	0.69	2.14	0.1	72.9	5.39	98.9
23	2.22	0.27	17.0	0.05	0.38	1.09	0.15	66.6	9.29	97.2
24	2.8	0.19	5.28	0	0.05	1.08	0.04	86.9	2.37	98.7
25	8.97	0.29	18.0	0.09	2.83	3.86	0.38	49.8	3.53	87.8
26	1.51	0.16	9.12	0.12	2.03	0.79	0.14	82.2	2.5	98.5
27	1.77	0.3	19.7	0.02	4.94	1.1	0.22	61.8	4.79	94.7
28	0.93	0.23	18.4	0.06	0.47	0.44	0	65.8	10.9	97.4
29	2.04	0.23	11.9	0.05	0.39	0.91	0	76.3	6.86	98.7
30	0.63	0.21	5.6	0	0.42	0.34	0	86.8	3.21	97.2

49	1.04	0.22	56.69	11.8	1.54	71.28
50	1.07	0.1	56.62	11.88	1.7	71.37
51	0.82	0.11	57.53	11.66	1.57	71.7
52	0.77	0.71	57.65	10.42	1.35	70.89
53	0.71	0.93	56.71	10.69	1.34	70.38
54	0.66	1.03	56.85	10.76	1.68	70.98
55	0.8	0.44	58.17	10.84	1.71	71.96
56	0.6	0.03	59.95	10.64	1.82	73.04
57	0.65	0.01	57.78	10.93	1.65	71.01
58	0.75	0.03	57.4	11.69	1.68	71.55
59	0.7	0	55.6	10.83	1.61	68.74
60	0.84	0	55.61	9.93	0.99	67.37
61	0.95	0.25	57.64	10.86	1.28	70.96
62	0.93	0.05	56.53	10.18	1.18	68.87
63	0.96	0	57.05	10.8	1.53	70.34
64	0.93	0	57.96	11.41	1.83	72.14
65	0.76	0.02	56.84	12.5	1.82	71.95
66	0.95	0.09	55.3	14.11	2.04	72.48
67	0.89	0.03	52.35	12.9	1.85	68.02
68	1.1	0.25	52.84	13.46	2.07	69.72
69	1.72	0.21	53.31	14.02	1.49	70.75
70	1.93	0.5	48.79	15.17	1.52	67.91
71	2.18	0.89	45.87	15.79	1.55	66.29

Traverse Normal to Bedding - WC26A
Q domain in siltstone, bottom to top.

step	K	Ca	Si	Al	Na	Total
1	0.57	0.04	57.56	12.27	2.43	72.86
2	0.41	0.03	59.11	10.43	2.11	72.09
3	0.45	0.19	59.85	10.29	1.98	72.76
4	0.48	0.08	59.97	10.96	2.05	73.55
5	0.56	0.21	61.36	10.39	2.16	74.68
6	0.46	0.14	62	9.86	2.23	74.69
7	0.46	0.12	60.57	9.71	2.12	72.98
8	0.46	0.11	61.58	9.8	1.98	73.94
9	0.39	0.11	60.62	9.8	2.07	72.98
10	0.33	0.13	60.75	9.33	2.16	72.69
11	0.34	0.69	60.62	10.58	2.54	74.77
12	0.46	0.58	57.75	11.45	2.45	72.68
13	0.36	1.01	59.27	11.55	2.56	74.75
14	0.32	0.88	58.61	12.42	2.67	74.89
15	0.36	0.78	58.58	11.29	2.7	73.7
16	0.45	0.01	60.96	11.66	2.59	75.66
17	0.34	0	64.47	10.57	2.37	77.75
18	0.38	0.04	63.1	9.44	1.89	74.85
19	0.53	0	63.25	10.75	2.26	76.79
20	0.57	0.02	60.67	10.94	2.22	74.43
21	0.59	0.01	58.48	9.91	1.99	70.96
22	0.48	0	58.12	9.54	1.88	70.02
23	0.54	0.21	57.4	10.46	1.91	70.52
24	0.6	0.25	56.54	10.83	1.88	70.1
25	0.54	0.93	54.04	10.55	1.97	68.03
26	0.48	0.88	55.68	11.58	2.15	70.77
27	0.64	0.85	57.64	11	2.26	72.38
28	0.53	0.66	61	10.3	2.3	74.8
29	0.54	0.41	60.66	10.6	2.29	74.5
30	0.66	0.07	60.79	11.7	2.24	75.46
31	0.88	0.01	58.33	12.21	1.92	73.35
32	1.14	0	53.92	13.2	1.98	70.25
33	0.97	0	56.18	11.66	1.59	70.4
34	0.84	0	58.11	11.73	1.8	72.48
35	0.95	0	56.73	10.98	1.56	70.22
36	0.82	0.02	59.67	9.85	1.66	72.03
37	0.71	0	60.86	9.2	1.47	72.24
38	1.21	0	55.29	11.38	1.47	69.35
39	1.49	0.09	52.12	14.44	1.8	69.95
40	1.49	0	50.88	15.68	2.13	70.17
41	1.56	0	52.28	15.88	2.55	72.26
42	1.45	0.22	53.13	14.01	1.83	70.63
43	1.59	0.42	54.14	13.73	1.48	71.36
44	1.27	0.3	56.75	12.24	1.77	72.42
45	0.61	0.03	59.55	11.31	1.89	73.39
46	0.88	0.05	59.25	11.55	1.86	73.59
47	1.34	0.07	55.63	12.74	1.95	71.73
48	1.14	0.02	55.29	13.1	1.84	71.39